VOLUME 46, NUMBER 11

November, 1958

published monthly by The Institute of Radio Engineers, Inc.

Proceedings of the IRE®

contents

Poles and Zeros 1795

Ralph I. Cole, Director, 1958-1959 1796

Scanning the Issue 1797

PAPERS

Electronic Composites in Modern Television, *R. C. Kennedy and F. J. Gaskins* 1798

Transfluxor Controlled Electroluminescent Display Panels, *A. Rajchman, G. R. Briggs, and A. W. Lo* 1808

Incoherent Scattering of Radio Waves by Free Electrons with Applications to Space Exploration by Radar, *W. E. Gordon* 1824

Analysis of Millimicrosecond RF Pulse Transmission, *Max P. Forrer* 1830

A Quartz Servo Oscillator, *Norman Lea* 1835

Some Generalized Scattering Relationships in Transhorizon Propagation, *A. T. Waterman, Jr.* 1842

A Very-Wide-Band Balun Transformer for VHF and UHF, *T. R. O'Meara and R. L. Sydnor* 1848

Nomographs for Designing Elliptic-Function Filters, *Keith W. Henderson* 1860

The Annular Geometry Electron Gun, *James W. Schwartz* 1864

CORRESPONDENCE

Undersea and Subteranian "Atmospherics," *Ted Powell* 1870

On the Choice of Frequencies for Meteor-Burst Communication, *M. L. Meeks and J. C. James* 1871

The Superconductive Transition Radio-Frequency Mixer and the Problem of Cryotron Switching Time, *J. B. Woodford, Jr. and D. L. Feucht* 1871

Amplitude Scintillation of Extraterrestrial Radio Waves at Ultra-High Frequency, *H. C. Ko* .. 1872

Statistical Design and Analysis of Closed-Loop Control Systems with Error Sampling, *R. M. Stewart* 1873

On the Statistics of Filled Vessels, *John L. Stewart* 1873

Electron-Density Profiles in the Ionosphere During the IGY, *R. L. Smith-Rose* 1874

The Current Amplification of a Junction Transistor as a Function of Emitter Current and Junction Temperature, *W. W. Gärtner, R. Hanel, R. Stampfl, and F. Caruso* 1875

Alternative Detection of Co-Channel FM Signals, *H. W. Farris* 1876

A Series Expansion Method for Finding Approximate Laplace Transforms, *W. H. Lucke* 1877

Effective Collector Capacitance in Transistors, *R. Zuleeg* 1878

Maximum Utility in Government Contract Reports, *F. H. Warren and E. W. Herold* 1879

Proposal for a Maser-Amplifier System Without Nonreciprocal Elements, *S. H. Autler* 1880

WWV Standard Frequency Transmissions, *D. M. Kerns* 1881

A Communication Technique for Multipath Channels, *George D. Hulst* 1882

Magnetron Tuning Using a Ferrite Reciprocal Phase Shifter, *D. Bush* 1882

REVIEWS

Scanning the TRANSACTIONS 1885

Books:

"Faisceaux Hertziens et Systèmes de Modulation," by L. J. Libois, *Reviewed by J. B. Lair* 1886

"Programming for an Automatic Digital Calculator," by K. H. V. Booth, *Reviewed by Donn Combelic* 1886

NOVEMBER

published monthly by The Institute of Radio Engineers, Inc.

Proceedings of the IRE®

NOVEMBER

detail on the left.

"Switching Circuits and Logical Design," by S. H. Caldwell, *Reviewed by R. W. Stuart* .. 1887
"Missile Engineering Handbook," by C. W. Besserer, *Reviewed by Conrad H. Hoeppner* .. 1887

ABSTRACTS

Abstracts of IRE Transactions 1888
Abstracts and References 1892

IRE NEWS AND NOTES

Calendar of Coming Events and Authors' Deadlines 14A
Professional Group News 18A
Obituary 18A
Region 3 Technical Meeting 18A
Conference on Magnetism and Magnetic Materials 20A
Northeast Electronics Research and Engineering Meeting 24A
Annual Conference of the Professional Group on Vehicular Communications 26A
Eleventh Annual Conference on Electrical Techniques in Medicine and Biology 28A
1958 Eastern Joint Computer Conference 26A
Professional Groups 30A
Sections and Subsections 32A, 34A

DEPARTMENTS

Contributors 1883
IRE People 48A
Industrial Engineering Notes 146A
Meeting with Exhibits 8A
Membership 112A
News—New Products 38A
Positions Open 120A
Positions Wanted by Armed Forces Veterans 128A
Professional Group Meetings 152A
Section Meetings 106A
Advertising Index 189A

COVER

A new type of electroluminescent display panel is described on p. 1808 which can convert electrical signals into halftone images. An experimental model, developed by RCA Laboratories, employed a television signal modified for 30-line scan to produce the image on the right, and shown in enlarged *continued*

PROCEEDINGS OF THE IRE, published monthly by The Institute of Radio Engineers, Inc. at 1 East 79 Street, New York 21, N. Y. Manuscripts should be submitted in triplicate to the Editorial Department. Responsibility for contents of papers published rests upon the authors, and not the IRE or its members.

Fifteen days advance notice is required for change of address. Price per copy: members of the Institute of Radio Engineers, one additional copy $1.25; non-members $2.25. Yearly subscription price: to members $9.00, one additional subscription $13.50; to non-members in United States, Canada, and U. S. Possessions $18.00; to non-members in foreign countries $19.00. Second-class postage paid at Menasha, Wisconsin, under the act of March 3, 1879. Acceptance for mailing at a special rate of postage is provided for in the act of February 28, 1925, embodied in Paragraph 4, Section 412, P. L. and R., authorized October 26, 1927. Printed in U.S.A.

Airborne Instruments Laboratory Monograph on page 4A.

November, 1958
Vol. 46 No. 11

Proceedings of the IRE

Poles and Zeros

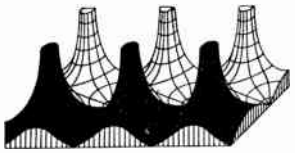

Once More, The Board. The September Board of Directors meeting in New York ran a thought provoking course over a great many topics, as is often the case when a new season begins. It acted on the major awards of the IRE for presentation next March, recognizing Dr. E. Leon Chaffee for the Medal of Honor for his contributions to our knowledge of the electron tube, and noting the forthcoming importance of the maser principle in the Liebmann award.

Dr. W. R. G. Baker and Dr. Alfred N. Goldsmith independently introduced proposals having to do with forward planning for IRE's future, both pointing out areas of future responsibility as electronics continues its growth into one of the world's largest business and professional areas. Dr. Goldsmith pinpointed some of the areas requiring future attention as being electrical education and curriculum studies, medical electronics, power generation by electronic means, methods of nonradio communication, remote control of processes, and the general area of navigation, astrogation and space electronics.

The Board also removed a restriction on the meetings of the IRE Representatives in the colleges, by no longer requiring these Regional assemblies to be held in connection with a Regional conference or symposium, thus permitting a freer choice of dates in keeping with academic calendars.

Reiterated was present IRE policy which restricts control and use of Section funds to usual areas of Section activity and operation. It was noted that the IRE Board delegates certain financial powers to the Sections and retains those powers not so delegated, in contrast to the U. S. Constitution which reserves all undelegated powers to the States. This seems logical—the central IRE authority established the Sections whereas the States established the U. S. federal government.

The attention of the Board was called to a small activity next spring: the National Convention, March 23–26.

Number One Hundred. Last month we greeted Anchorage, Alaska, as Section Ninety-Nine, and now we reach the one hundred mark by elevation of the Quebec Subsection to full Section status. Our greetings go to them as we pass a real milestone in IRE history. We must admit that there is as yet no truth to the rumor of the pending emergence of a French edition of the PROCEEDINGS, but we will say, *Nos amis du groupe Québec, soyez les bienvenus.*

Standards Is Standards. In 1946, after considerable polite discussion and with aid from the Department of Defense, a full juncture of electronic and power circuit symbols was achieved, now represented by ASA Standard Y32.2–1954. Major results of this action from the electronic viewpoint were the relegation into the discard of the old ladder-like resistor symbol and the inductor that was a resistor, and the introduction of a capacitor symbol involving the bowed lower plate to eliminate confusion of the old parallel-line symbol with the power symbol for a contactor.

The Editor feels that when one's field has a standard convention it is the duty of every practitioner to acquaint himself with and use these symbols, and is disheartened to find students, and yes, even professors, trying to tune circuits with contactors. In fact, the Editor is reported to have occasionally reminded some students of the impossibility of this operation.

But now our face is of a color approaching that of a parboiled Maine crustacean to find that our own STUDENT QUARTERLY has indeed published a paper including the now depreciated, disparaged, disapproved, denounced, and in fact decadent symbol for a capacitor—and compounded the felony by referring to the device as a condenser! O tempora! O mores!

Baby Kissing and All That. When you read this, one election will be over but the political maneuvering and planning for another should be well under way. This latter campaign should be so conducted as to discover the best fitted candidates for the positions of IRE Regional Director in Regions 1, 3, 5, and 7, nominees for which are to be chosen by the Regional Executive Committees next March.

Your Regional Director represents your Section and you, and should employ the ideas and wishes of the individuals and Sections in formulating IRE policies. He represents the electronic hinterlands as well as the macrocosm of our profession, must catalyze the activities of from four to sixteen Sections, earn a day-to-day living, and still become so well acquainted with the IRE in his two-year term as to intelligently contribute to the solution of its problems.

He must also spearhead his Region's conferences and symposia, and stimulate the activities of the IRE Student Branches. A candidate must therefore be a considerable person, one not idly selected over the post-Section-meeting mug, or by horse trading or prearrangement between Sections. Each Section should scrutinize its past officers, or other members with proven executive ability and knowledge of IRE operations, and honestly and forthrightly present their qualifications to the other Sections of their Region in advance of the March nominating meeting.

Protect us from the smoke-filled room in which Sections A, Q, and Z present favorite sons and all names are placed on the ballot to avoid mental wear and tear, or in which Section J insists that it is the "turn" for their candidate. Let us have forthright cogitation, cajoling, conflict, and cigars if it leads to nomination of our best possible candidates. Voters, arise!—J.D.R.

Ralph I. Cole

Director, 1958–1959

Ralph I. Cole (A'29–SM'46–F'58) was born in St. Louis, Mo., on August 17, 1905. He received the B.S. degree in electrical engineering from Washington University in St. Louis, and the M.S. degree in physics from Rutgers University in 1936. From 1929 to 1942, he was a civilian radio engineer with the Signal Corps Laboratories at Fort Monmouth, N. J. Projects assigned to his cognizance included direction finding systems and armored vehicle communication equipments and systems. Under his direction, the "Tank" radio communication set was developed using the first multiple wideband, integral superheterodyne (BC-312) receiver, and the first wideband crystal controlled radio transmitter (BC-223). He is the holder of several patents concerning improvements in radio direction finding systems and special radio component designs.

Commissioned as a Major in the Signal Corps in 1942, he was placed in charge of research and development of direction finding and intercept systems and of VHF fighter control systems required at that time by the Air Force. In 1945 he was transferred to the Air Force Watson Laboratories and assumed charge of the Engineering Division. He was awarded the Legion of Merit for his direction of research and development. When he returned to civilian life in 1947, he retained the rank of Colonel in the Air Force Reserve.

He was technical director of the Rome Air Development Center until 1952, when he became manager of military projects planning at Melpar, Inc.

Mr. Cole was the first Chairman of the Professional Group on Engineering Management, and is currently a member of its Administrative Committee. He was also Vice-Chairman of the Monmouth Subsection, and an organizer and Chairman of the Rome Subsection. In the Washington Section of IRE, he has held the offices of Secretary-Treasurer, Vice-Chairman, and Editor. He is currently Chairman of the IRE Ad Hoc Committee on Manpower.

He is Director of the Washington Society of Engineers and the Washington chapter of the Air Force Communications and Electronics Association, and a member of the Institute of Navigation, the Air Force Association, and the American Ordnance Association.

Scanning the Issue

Electronic Composites in Modern Television (Kennedy and Gaskins, p. 1798)—Those who watch the big color television programs, such as the Perry Como or Steve Allen shows, will have noticed recently the use of unusual composite pictures to achieve special effects. These trick shots are made possible by the Chroma-Key system described in this paper, a new technique which makes possible the artificial creation of a whole gamut of effects by electronic means, both in color and black and white. For example, with one camera trained on a small Buddha incense burner and another on two dancers, a realistic composite can be produced in which Buddha appears 40 feet high with the couple dancing at his feet. Not only will this development greatly enhance the artistry and entertainment value of television, but it will have important impact economically as well. Costly sets can now be replaced by miniatures, paintings, slides, film or tape recorded background scenes. As for the future, the electronic equipment itself may soon be able to create some backgrounds artificially. It is safe to say that Chroma-Key is the most important technical innovation in television since the advent of color.

Transfluxor Controlled Electroluminescent Display Panels (Rajchman, Briggs, and Lo, p. 1808)—Two important developments of recent years, the transfluxor and the electroluminescent cell, have been united to bring about a major step forward in the evolution of solid-state display devices of the type that are actuated by electrical signals rather than by X rays or light. In last month's issue one such device was proposed in which a ferroelectric material was used as the connecting and controlling link between the electrical input signal and each electroluminescent cell. In the present paper this function is performed by magnetic means. The transfluxor, a multi-hole ferrite core with unusual signal storage and control properties, is admirably suited to the demanding role of energizing a cell to a desired level for a desired length of time, without affecting the levels of adjacent cells. Since each cell level can be independently and rapidly controlled, it is technically feasible to display television images on the device, although it is by no means economically practicable as a substitute for a television picture tube. Nevertheless, it will undoubtedly find important use for giant size displays and as a read-out device for certain types of data handling systems.

Incoherent Scattering of Radio Waves by Free Electrons with Applications to Space Exploration by Radar (Gordon, p. 1824)—This paper offers as much in the way of exciting new prospects as any that has appeared in the PROCEEDINGS in recent years. The author first calls attention to the important fact that the extremely weak, and hence previously unconsidered, incoherent scattering of radio waves by free electrons in and above the earth's ionosphere can, in fact, produce a detectable radar echo if a powerful enough radar is used—and that the construction of such a radar now lies within our present capabilities. He then shows that this radar could probe the earth's surroundings out to a distance of 4000 miles, exploring several important phenomena such as electron density and temperature at various heights, streams of charged particles coming from outer space, and the ring current (if it exists) around the earth. Finally, he points out that this same equipment would be capable of obtaining radar echoes from the sun, Venus, and Mars, and possibly from Jupiter and Mercury, and could also detect radio emissions from previously undetected sources in remote reaches of the universe. To reach Mars the author figures on a one-megawatt radar operating at 200 mc with a 1000-foot dish antenna, a one-millisecond pulse, and a 2-kc receiver bandwidth. These timely and novel proposals are certain to excite a great deal of interest and discussion among the large body of scientists concerned with wave propagation, atmospheric physics, and radio astronomy.

Analysis of Millimicrosecond RF Pulse Transmission (Forrer, p. 1830)—This paper analyzes the distortion of short pulses due to the frequency dependency of the complex propagation constant of a transmission system. Due to the widening applications of millimicrosecond pulse techniques, the results and examples given will be of quite broad interest, especially to radar systems designers.

A Quartz Servo Oscillator (Lea, p. 1835)—Precise control of frequency has been of central interest to radio engineers for nearly 50 years. This paper describes a notable forward step in that long history—an oscillator that is potentially superior to any standard now available, short of an atomic device. The tube-dependent instabilities of conventional oscillators are completely avoided by using an RF bridge in which none of the arms has tube-related reactances. As a result, the oscillator is stable to 2 parts in 10^{10}, relative to the slight frequency drift of the crystal.

Some Generalized Scattering Relationships in Transhorizon Propagation (Waterman, p. 1842)—There is considerable controversy as to the physical mechanisms which cause microwaves to be propagated beyond the horizon. One of the principal explanations that has been offered and debated is that scattering is caused by atmospheric turbulence. This paper should help considerably to clarify matters by examining not the scattering mechanism itself, but rather what types of experimental measurements will be most useful in testing the validity of the turbulence hypothesis.

A Very-Wide-Band Balun Transformer for VHF and UHF (O'Meara and Sydnor, p. 1848)—A valuable development is reported in which ferrite is introduced in the construction of a transformer to achieve especially wide bandwidth. The transformer may be used as a phase inverter, a differential transformer, or a balun transformer. It is applicable in the frequency range of transition between lumped and distributed circuit techniques, where there is greatest need, and will greatly interest antenna people and those who need coupling devices at high frequencies.

Nomographs for Designing Elliptic-Function Filters (Henderson, p. 1860)—Considerable effort has been made in recent years to reduce the mathematical labor of filter design by means of graphs and tables. The elliptic-function filter is one of the most difficult types to design, and yet it offers important advantages over easier-to-design varieties. For these reasons, the labor-saving nomographs presented here will make a widely useful and valuable addition to the library of the filter design engineer.

The Annular Geometry Electron Gun (Schwartz, p. 1864)—Although considerable progress has been made in the design of electron guns, it has been mostly in connection with microwave tubes. Meanwhile, the guns employed in cathode-ray tubes and other beam-type display tubes have remained essentially unchanged over the past 20 years. In presenting a new type of kinescope gun, this paper makes a significant contribution in a field where even minor contributions are difficult to make. While of principal interest in electron optics, some unexpected features of this gun might be of interest for electron tubes with certain specifications of a related nature.

Scanning the Transactions appears on page 1885.

Electronic Composites in Modern Television*

R. C. KENNEDY† AND F. J. GASKINS‡, ASSOCIATE MEMBER, IRE

Summary—After a review of the various electronic techniques which have been used in television to simulate optical effects used in motion picture photography, a new process called "Chroma-Key" is described. "Chroma-Key" is an insetting or matting technique intended for color television which utilizes a highly saturated color background for the inset subject. Many of the problems normally associated with monochrome inset are nonexistent with the new approach. The apparatus required, methods of integration into a system, consideration of various influencing factors, and results of tests and on-the-air use are described.

INTRODUCTION

THE development of special effects generated electronically is a natural part of the progress and growth of the all electronic television broadcast system, first in monochrome and presently in full color. They are used for effecting smooth changes of scenes, transitions between different parts of a program, and providing interesting geometric patterns. More recently, NBC developed Chroma-Key electronic video inset technique has been utilized for increased flexibility in television program production.

Television was still in the monochrome flying disc era when a patent application was filed which described a means for producing fade-outs, fade-ins, and lap dissolves.[1] This made possible more artistry in changing scenes or mood in contrast to the sharp breaks which had previously been necessary.

A patent application filed in 1932[2] described a means of insetting the information from one television camera into information from another camera so as to produce a composite result. The term "inset" is used to describe the process whereby the brightness variation in the signal from a camera is used to delete a corresponding area from the picture from a second camera so that the first camera's picture will fit precisely in the "hole" thus created in the second camera's signal. Such a facility opened up many new possibilities. Since the background material could be any kind of art material, *e.g.*, stamps, post cards, magazine illustrations, transparencies, film, etc., the cost of sets could be vastly reduced and much greater freedom was offered the producer.

The basic technique involves placing the subject material to be inset in front of a black background. The camera output is at pedestal or black level except when scanning the subject. The presence of the black level output is used to generate a potential whose polarity is opposite to that of the potential produced while scanning the subject. These two potentials when shaped produce a pulse which is used as a switching mean choosing the output of the background source whe scanning black and choosing the output of the fore ground or inset camera when it is not scanning black The combination of the two video signals results in composite picture when viewed on a kinescope. Thi technique was first demonstrated at NBC around 1940 In the demonstration, a girl sitting in a chair in front of a black background in a studio was "inset" in a film showing a box seat at a race track.

Another patent application filed in 1937[3] described a more complex type of composite wherein three separate and distinct planes of depth were combined so as to have foreground inset into middle or intermediate ground material which in turn was inset into the background material.

To understand how such a technique might be used, the following explanation is offered. A film of the front of a sidewalk cafe in Paris showing people entering and leaving is the background. A group of actors seated at a table are placed in front of a black background in the studio. This middle ground subject matter is picked up by a studio camera and electronically inset into the background film. Finally, a film showing autos, bicycles, trucks, etc., moving along the street is inset into the composite formed of the previously described intermediate and background subject matter. The only requirements for proper constitution of the whole picture are: 1) that the scanning of any middleground subject matter must key out correspondingly scanned background material; 2) that the scanning of any foreground material must key out correspondingly scanned middle and background data; and 3) the timing of the middleground and foreground signals with reference respectively to the timing of the "hole" deleted in the background and middleground data must be proper to assure minimum demarcation or transition between the inset and the background. The timing of the inset to correspond to the "hole" deleted in the background utilizes well known television practices for timing of blanking, horizontal and vertical drive, and synchronizing signals in a television installation.

The most difficult condition to realize is to reduce to a minimum the line of demarcation between "inset" and the background. The switching action must be extremely fast, the transition symmetrical, and the shift of the dc axis between the two modes must be less than 1 per cent and retain that adjustment at least for the duration of a particular show.

* Original manuscript received by the IRE, April 16, 1958.
† Nat'l. Broadcasting Co., New York, N. Y.
‡ Nat'l. Broadcasting Co., Burbank, Calif.
[1] A. N. Goldsmith, U. S. Patent No. 2,043,997; June 16, 1936.
[2] A. N. Goldsmith, U. S. Patent No. 2,073,370; March 9, 1937.
[3] A. N. Goldsmith, U. S. Patent No. 2,172,936; September 12, 1939.

Numerous circuits had been tried, but it was not until 1952 that a satisfactory "switch" was described[4] which has made possible the various effects to be discussed. The switching amplifier is described in greater detail under the section on "Apparatus."

The switching amplifier responds in accordance with the kind of keying signal fed to it. Thus, a square wave whose duty cycle may be varied provides split screen and wipe effects. Other signal information in proper combination can produce diamonds, circles, squares, etc., in a wide variety of geometric forms. The waveform generator for this purpose is described under Apparatus.

The inset technique may be extended for a greater number of depths or planes of action. However, there are certain problems arising from the use of this type of effect. One is a matter of lighting. The amount of light required to illuminate the black set is quite low. However, the light necessary on the artists is quite high, causing some discomfort due to heat. One way to circumvent the problem is by letting red velvet be used instead of black for the background material. The artists then use green make-up and garments and green illumination is used. Green filters are used on the cameras to permit use of the so-called complementary black in contract to the true black.

The choice of black for gating or switching operation requires certain precautions to be exercised to prevent the appearance of background material in undesired portions of the picture. The artist cannot wear black clothing or have black hair. Neither may camera shots in closeups where the performer speaks be utilized as the background material may appear through his mouth.

Another consideration which requires very close attention to detail is that of perspective. The various depths or planes of action must be so proportioned in size that when the complete composite picture is viewed, all components, both scenery and subject alike, are able to create the critical impression of depth or perspective to the eye.

Two additional contributions which are pertinent to the present discussion are covered by patent applications filed in 1935[5] and 1939.[6] The first patent describes the use of geometric patterns, *e.g.*, circles, stars, diamonds, etc., on slides placed in a slide scanner (or viewed by a television camera) for generating keying information. The geometric figures may be white on black background or vice versa. In this arrangement two signals, either from cameras or other program sources, are fed into the switching amplifier. The signal from the slide scanner or a television camera then keys one program source into the other in accordance with the shape of the geometric design in the slide scanner.

The second patent covers the basic idea of using one camera to scan some geometric design for addition to a picture from some other source. The resultant picture would have the geometric design either black or white inset into the picture. However, the unique feature is that the inset figure might be a small arrow which may be moved about in the picture into which it is inset. With this facility, it is possible to point out an individual in a crowd such as is done when televising political conventions, etc.

Chroma-Key Electronic Video Inset

All of the methods discussed briefly thus far have been used primarily in monochrome television. The teachings are applicable equally to color television and many are presently in use today on color programs. It is obvious that the complementary black approach using red background material and green subject material cannot be used for color television, but the use of conventional black backgrounds with amplitude differentiation between inserted and background material has been used effectively.

The color signal is of such nature as to suggest two other methods for deriving the keying or switching data. As is well known, a color signal from the camera is actually in the form of three separate signals. In the colorplexer or encoder, these are combined in proper fashion together with the reference burst to form a single output signal. Either the signals at the input to the colorplexer or the waveform from its output may be used to generate a pulse suitable for switching.

The Chroma-Key electronic video inset technique differs from the technique employed in monochrome television in the broad sense in that differentiation between the foreground and background material is accomplished by differences in hue rather than differences in amplitude. A matrix and white balance circuit used to select the proper background hue, *e.g.*, blue, to generate a pulse followed by a high degree of nonlinear amplification, creates the switching signal when it is desired to derive it from the signals entering the colorplexer. The color signal analyzer or its equivalent is used to properly phase to and recover the necessary switching information from the colorplexer output signal.

Apparatus

Lap Dissolve Amplifiers

As is apparent from the above discussion, there are several pieces of apparatus needed to create all the various effects which have been described. Lap dissolves, fade-ins, fade-outs, and superimpositions are effects which can be produced by means of the lap dissolve amplifier. The circuitry of the lap dissolve amplifier presently in use is shown in Fig. 1.[7] Basically, the objective in these circuits is to provide a means whereby manual control is used to select the amount of signal from each of two cameras or sources of video informa-

[4] A. M. Spooner and T. Worswick, "Special effects for television studio productions," *Proc. IEE*, vol. 100, pt. 1, pp. 288–299; April, 1953.
[5] A. V. Bedford, U. S. Patent No. 2,164,297; June 27, 1939.
[6] A. V. Bedford, U. S. Patent No. 2,275,026; March 3, 1942.
[7] J. O. Schroeder, to be published in *Electronics*.

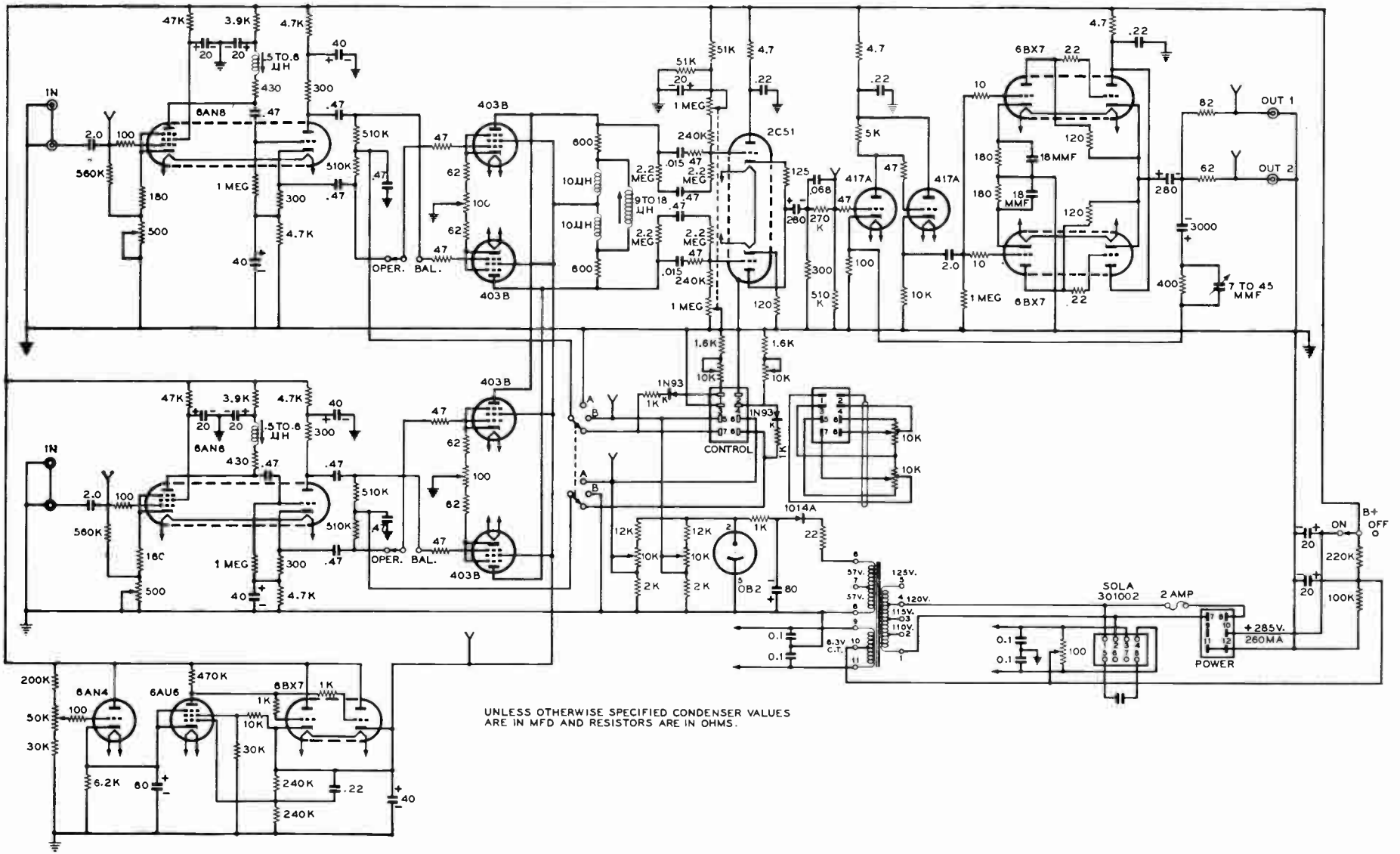

Fig. 1—Schematic diagram, electronic lap dissolve amplifier.

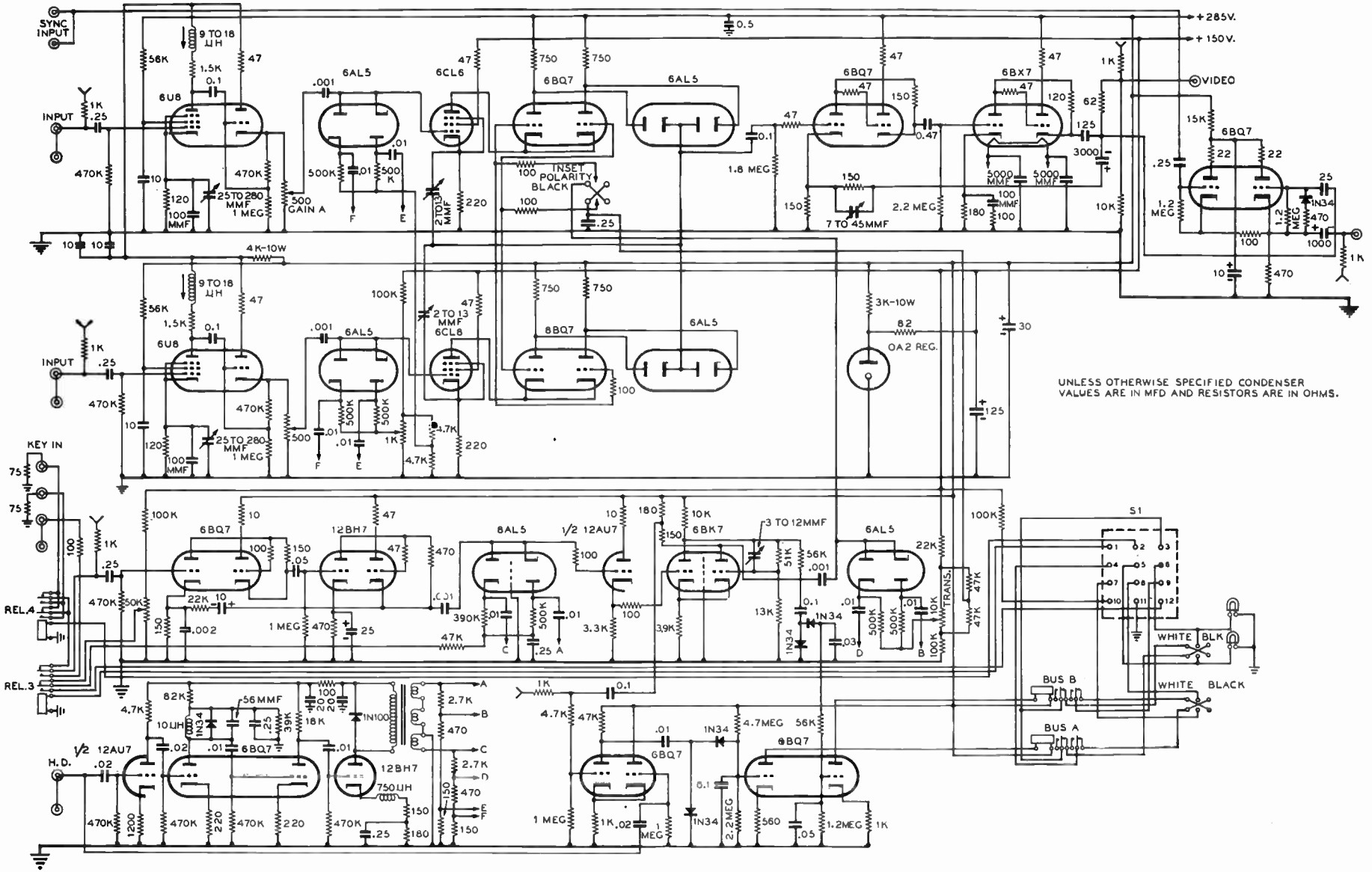

Fig. 2—Schematic diagram, special effects amplifier.

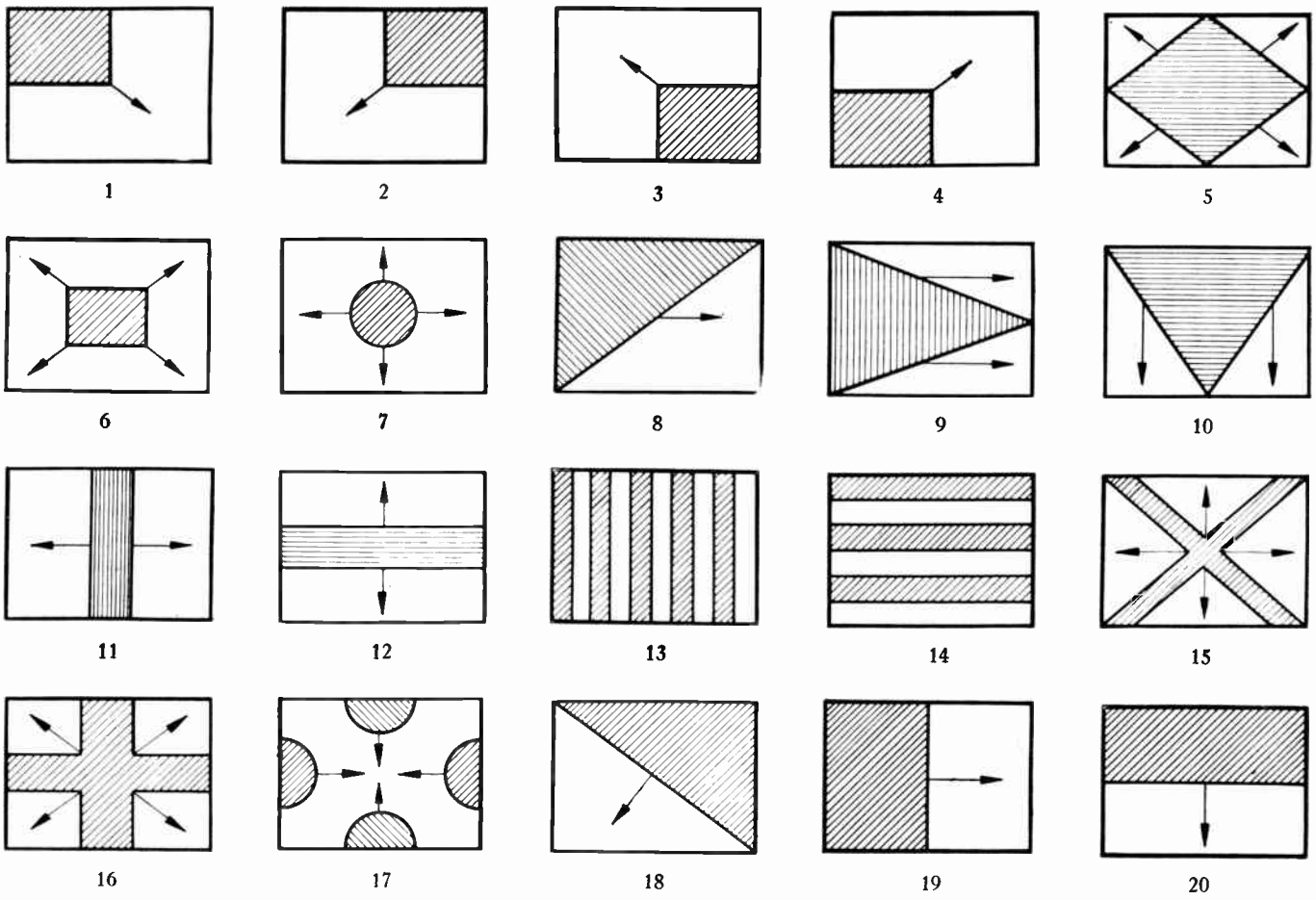

Fig. 3

tion prior to their being added in a common impedance. At one end of its travel, the manual control has effectively turned off one camera's output and turned on the other. The converse is true when the control is at the opposite end of its travel. For positions intermediate the output of each camera is contributing a fraction of its maximum and the resultant picture has the appearance of a double exposure. Placing the control in the middle of its travel permits half of each camera's output to be seen and a superposition is created. Operation of the control slowly from one extreme to the other produces a lap dissolve. If no video signal appears at one input of the amplifier, operating the control from this channel to the other produces a fade-in and the converse action produces a fade-out.

Special Effects Amplifier

Several circuits have been used for this type of operation but the most satisfactory one presently in use is shown in Fig. 2. As may be seen, the amplifier is capable of accepting two video signals and of being able to switch between them at a very fast rate.

In Fig. 2, one video input is through V4 and clamp diode V5 to the switch driver V6. The second video input is through V9 and clamp diode V10 to switch driver V11. The switch comprises tubes V7, V8, V12, V13, and V15. The output circuit is a feedback amplifier V2 and V3. Application of about 5 volts of short rise time step causes the switch to operate and the opposite sense step returns the switch to its original mode. The rise time of the applied step should be somewhat less than 0.1 μsec. The capacities in the switch are such as to limit its action to approximately 0.1 μsec and the drive signal should be of shorter duration so as to avoid increasing switching time.

The signal from the camera picking up the subject in front of the black background is used to operate the switching amplifier. This camera signal is fed into the KEY IN bus and is formed into a pulse suitable for driving the switch by means of V19, V20, V21, V22, and V18.

Special Effects Generator

The Special Effects Amplifier can be used not only for insets but for producing a wide variety of geometric effects provided proper types of keying signals are supplied to the switch.

A special piece of apparatus known as a Keying Generator has been developed for producing the requisite waveforms. Circuits are provided which produce sine

waves, saw teeth, and variable duty cycle rectangular waves of various multiples of field and line rate. These various waveforms permit generating split screens on vertical, horizontal, and diagonal bases, circles, venetian blinds, inset squares of adjustable size and location in the field, and many others are shown in Fig. 3.[8]

Chroma-Key Electronic Video Inset

In reflecting upon the limitations of monochrome inset it becomes apparent that the basic problems stem from lowlight areas resulting from low subject reflectance, shadows, surface contours, and subject lighting conditions in general. For proper switching operation, it is necessary that a large brightness difference be obtained between background and subject matter, and that this difference be translated into a large video signal increment. Thus, as has been pointed out earlier, extreme care is required in subject lighting.

If the situation is reversed wherein the unlighted subject is placed between an evenly lighted white backdrop and the camera, the silhouette formed could be easily utilized for deriving keying information for the switching amplifier, and shadows, subject reflectance, motion, etc., would no longer present a problem. This method would be excellent for creating silhouette effects but rather limited in application. It is this silhouette effect, however, which when used with a backdrop of a particular color that gives rise to the possibility of Chroma-Key. The subject is placed in front of a brightly lighted backdrop of a highly saturated hue. The subject may wear any colors other than is used in the background.

To understand how the background hue may be used to produce a keying signal, consider Fig. 4 which shows the vector representation of the chrominance subcarrier for primary and secondary colors in the color television system, together with the corresponding chrominance video levels for an encoder tuned to maximize the blue vector. Such a signal might be obtained by introducing the output of a color bar generator into the red, green, and blue terminals of a colorplexer or encoder. The encoder output is then demodulated in a circuit such as a color signal analyzer, the heart of which is a synchronous detector and calibrated delay line. By proper adjustment of the color signal analyzer, the amplitude of any particular color either primary or secondary may be maximized either positively or negatively. Thus the signals for all colors in the lower half of the vector polygon are negative. Furthermore, observe that black, gray, and white are all at zero amplitude. Hues above the zero line are sufficiently differentiated from blue to allow positive keying. This indicates that, assuming a highly saturated blue background, whites, grays, blacks, all hues in the lower half of the polygon of Fig. 4, as well as some low saturated colors in the magenta and cyan region may be used as subject material.

[8] E. P. Bertero, "Color video effects," presented at the NARTB Convention, Chicago, Ill.; April, 1956.

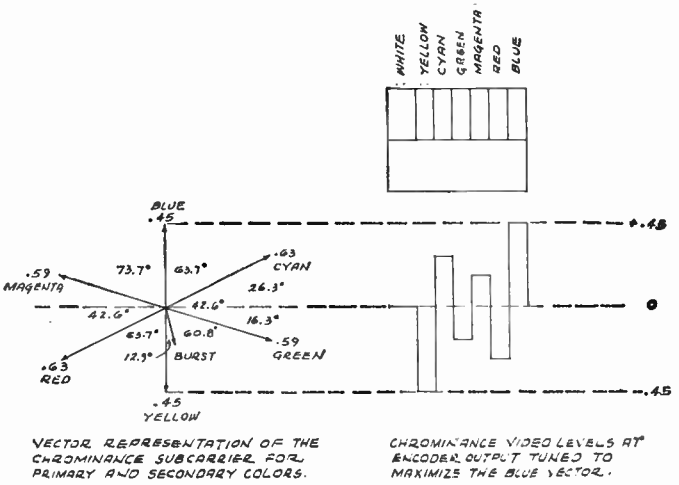

Fig. 4—Demodulated video signal.

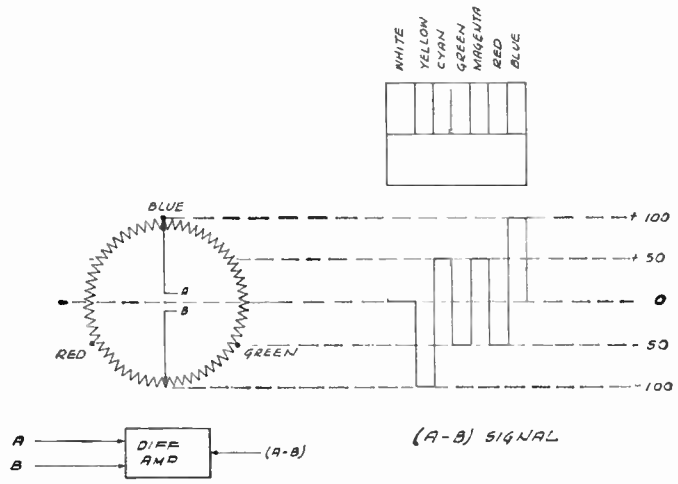

Fig. 5—"Hue-dial" signal.

It is apparent that excellent color differentiation is present in the video waveform for certain hues. Saturated blues and yellows, for example, yield positive and negative maximum signals, respectively, thus offering a very positive color difference signal for keying.

If it is desired to inset, for example, a yellow subject into some background picture, place the subject before an evenly lighted blue backdrop and use the camera signal after encoding to produce a positive blue waveform to key the special effects amplifier.

A second method, the "hue dial" shown in Fig. 5, consists of a three tap continuously wound potentiometer with two wiping contacts spaced 180 degrees apart. As indicated in Fig. 5 red, green, and blue primary signals from a low impedance driving source are applied to the three input terminals. The output signals from arms A and B are connected to the input terminals of a differential amplifier which combines these into an A-B output signal. This signal upon further processing becomes the keying signal to operate the switching amplifier. For equal R, G, and B input signals, *i.e.*, whites, grays, and blacks, there is no current flow in the arms

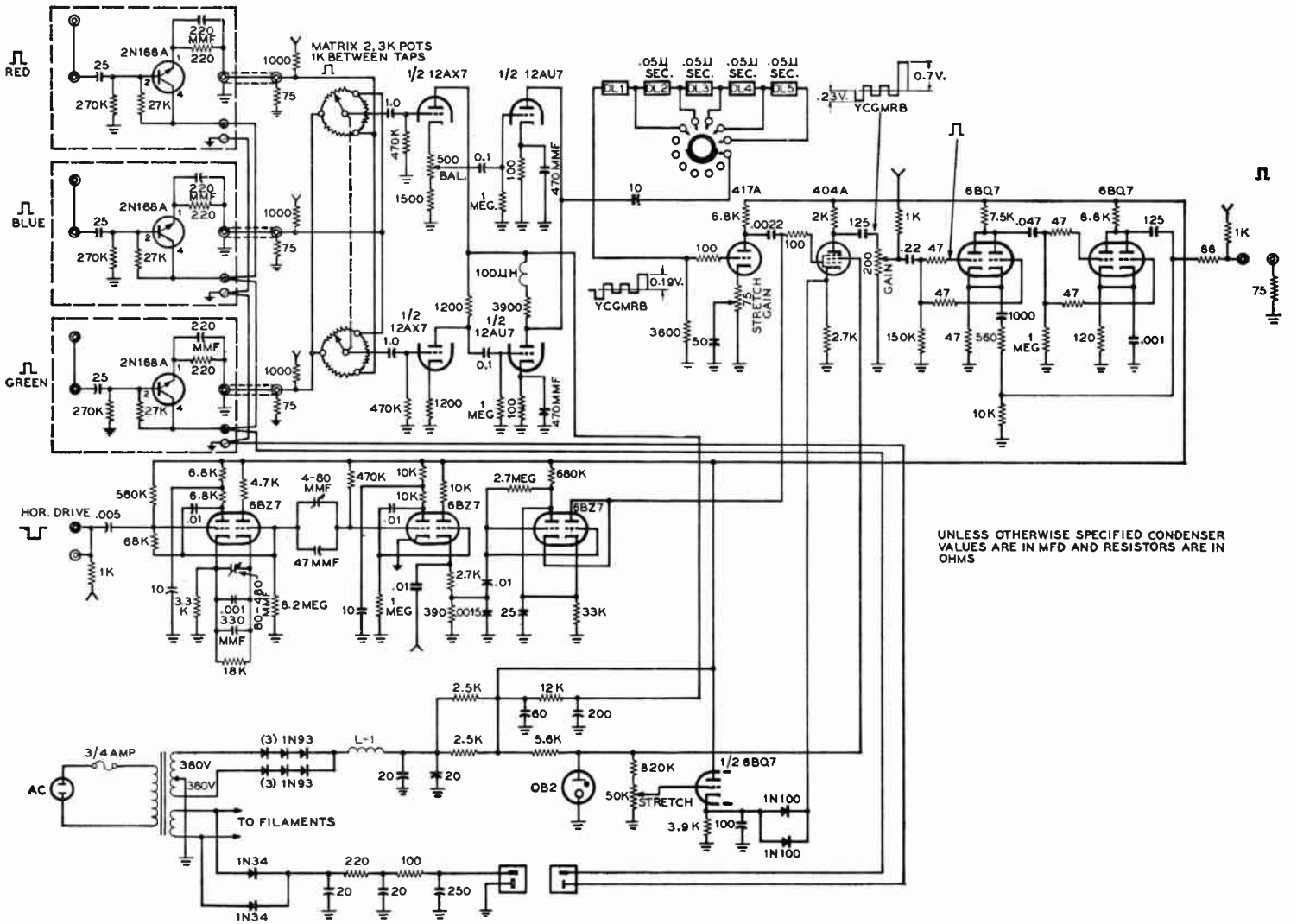

Fig. 6—Schematic diagram, chrominance background insertion gate pulse generator.

A and B, and the output is zero for all positions of A and B. However, when the camera is scanning, for example, a highly saturated blue area, the input to the potentiometer is R=0, G=0, and B=1. Proper positioning of arms A and B results in a maximum output signal of +1. The amplitude for other primaries and secondaries are listed below for blue maximized.

Red	R=1, G=0, and B=0	Signal Amplitude −0.5
Magenta	R=1, G=0, and B=1	Signal Amplitude +0.5
Green	R=0, G=1, and B=0	Signal Amplitude −0.5
Cyan	R=0, G=1, and B=1	Signal Amplitude +0.5
Yellow	R=1, G=1, and B=0	Signal Amplitude −1.0

This method of hue selection for developing the keying signal is much more desirable than using the encoded signal. The difficult delay problems associated with the latter are non-existent and the apparatus is simpler. At present, the "hue dial" is used in all NBC Chroma-Key equipment.

Processing of Matrixed Signal

In early versions of Chroma-Key apparatus, the matrixed signal was simply amplified, delayed, and applied directly to the switching amplifier. However, it has been found that in some instances this procedure has had to be modified in order to realize optimum performance. Since the switching amplifier must switch in intervals of 0.1 μsec, the signal causing it to operate must be a rectangular pulse having short rise time and a flat top. Experience showed that some camera tubes had landings which bowed and thus caused unreliable keying action on the edges of the picture. A tube having flat landing has constant output over all of a flatly lighted surface. It became apparent that additional signal processing was necessary to assure optimum operation. One technique which has been adopted is gamma stretching so as to raise the desired gating data as far above the remainder of the signal as possible. The desired signal is stretched 6 to 8 db above its normal value.

Chroma-Keyer

Fig. 6 is the circuit diagram of the Chroma-Keyer. Emitter followers are used at the input of the encoder to feed R, G, and B camera signals to the keyer proper. Two potentiometers form the matrix. At present, use is being made of a dual ganged, continuously rotatable potentiometer which allows much more flexibility for operational use. The two signals from the A and B arms of the matrix are amplified in an RCA 12AX7 amplifier, added in an RCA 12AU7 differential amplifier, and delayed. A WE 417A amplifier amplifies the signal and applies it to the clamped grid of a WE 404A amplifier used as a gamma stretch tube. Two RCA 6BQ7's form a feedback amplifier output circuit. Three RCA 6BZ7's are used to delay and control the width of the clamp pulses. Two Sylvania 1N34 diodes rectify a portion of the 6.3 volts filament current to provide 1.5 to 1.8 volts of dc at about 5.5 ma to energize the transistor emitter followers

The output of the Chroma-Keyer is approximately 0.7 volt peak for highly saturated color bars. The level is about 0.5 volt for the usual camera output for a highly saturated blue background. Fig. 7 shows the Chroma-Keyer waveforms for various adjustments.

Scenic and Lighting Requirements

Since so many factors tend to influence the over-all end result in a color composite, it is felt necessary to try to discuss the esthetic factors as well as the purely technical.

The success or failure of Chroma-Key depends to a large extent upon lighting. The set used for the inset portion of the composite picture, *i.e.*, the blue area before which the artist performs, must be very flatly lighted. If the full length of the artist is to be inset, the floor as well as the backdrop must be blue and very flatly lighted. This requirement must be met for all conditions. Full skirts on dancers cast shadows on the floor which may cause keying action with consequent loss of the legs of the dancer. It is for this reason that side lights and strip lights on the floor are highly desirable. It has been found that about 400 to 500 foot candles of light is necessary over the whole area to be inset.

It should be appreciated that the light on the subject itself should be completely independent of the background lighting requirements. The subject may be completely unlighted so that only a silhouette results, lighted on one side only, or any other way to meet the requirements for dramatic effect so long as it does not cast strong, hard shadows on the background.

With the above lighting requirements, it is obvious that the larger the set the greater the difficulty one must expect. This is especially true for dancing and other forms of rapid motion. The largest set which has been used thus far was 20 feet high and 56 feet long, but only one person was on the set walking slowly toward the camera. More flexibility is realized with a set about 12 feet high and 20 to 25 feet wide.

It should be realized that there is a very definite limitation on the size of a set which is a function of the television system itself. The larger the set, the further a camera must be from the subject. In other words, the larger the set the smaller will the subject appear. Since the transition interval between the background and inset material cannot be any less than approximately 0.1 μsec due to the bandwidth of the television system itself, the subject must be several times that interval in width at its narrowest part, *e.g.*, an arm or leg. In other words, the line of demarcation around the subject is of sufficient width to effectively limit the minimum size which a subject may approach.

The color of the paint used on the background and floor; and the care which it must be given are both very important. Only water soluble paints are used and these have low light reflectance. The color of the paint should be very highly saturated and should be as close to a primary color as possible. Since the subject to be inset

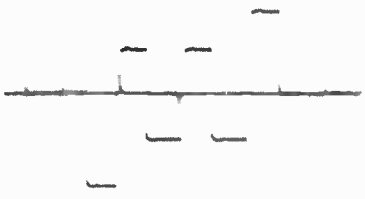

Properly adjusted unit showing cyan and magenta at ½ amplitude and blue at full amplitude. White balanced to zero.

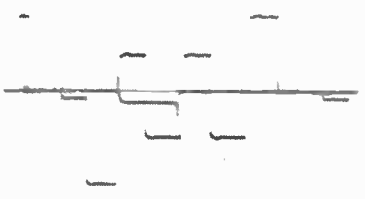

Matrix properly adjusted. White balance misadjusted.

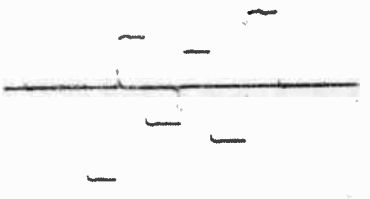

Matrix improperly adjusted. White balance to zero.

(a)

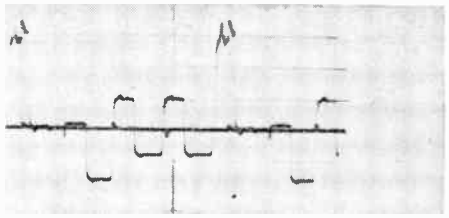

Insufficient blue stretch.

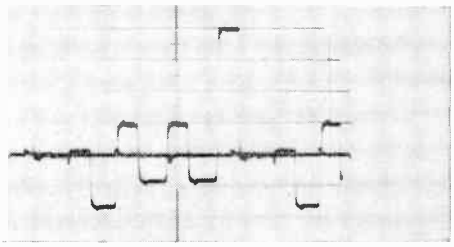

Properly adjusted blue stretch.

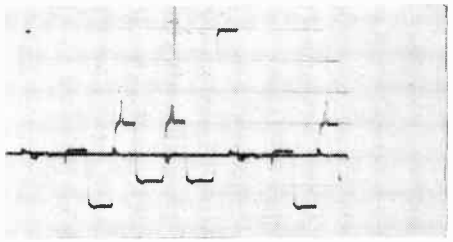

Excessive blue stretch.

(b)

Fig. 7—Chroma-Keyer wave forms.

is most generally a person, the color of the paint should be as unlike flesh as possible from the color television system point of view. This is the reason why blue has been discussed previously. The paint which has been used most successfully is Iddings-Ultra Marine Blue. It is used as it comes from the can with no foreign matter added. This means no other paint, thinner, nor pigment, even white, may be added. Experience has shown that even the addition of white paint can be disasterous.

The care of the painted surface is also very important. Actually, the painted surface is quite fragile since it is water soluble. Dust from shoes alters the color sufficiently to cause tearing of the inset. Shoe soles should be washed and the floor surface should be repainted after each rehearsal. If dancing or other excessive action is to occur, the surface should be dry mopped between numbers during the show.

Obviously blue cannot be used for all purposes. A product being advertised whose label has blue in it must be placed in front of some other color which does not occur in the label.

Graphic Art Considerations

The greatest use for the Chroma-Key technique is in the wide diversity of its application. No longer is it necessary to build a huge set of the Taj Mahal to produce the effect of its presence in the studio. A very small model, slide, or motion picture film can be used in lieu thereof and by proper proportioning of the camera angle widths, it is possible to make it appear that a person is walking in front of the building.

One such sequence was made using a small model of the pearly gate of Heaven about ten inches high. One camera was on the gate while another camera picked up the subject in front of the blue background. The effect produced as the subject walked forward was one of walking through the gate. The gamut of such possibilities is endless.

Films afford a tremendous variety of effects. Film of waves breaking on a shore has been used as background material with the inset subject walking on the beach. Another film of a stretch of road with curves, etc., has been used for background with the inset subject riding a bicycle along it. In addition to models and film, magazine illustrations, posters, post cards, transparencies, slides, stamps, etc., are all suitable for background material.

Artist's Effects

No discussion of the Chroma-Key technique would be complete without a consideration of the subject, artist, or performer, and his effects. Experience to date has shown that blue eyes are not a source of trouble even though the blue background is used for generating the keying signal.

Clothing can be a very difficult problem especially sequins and jewels. They tend to break white light into a continuous spectrum and the blue then causes keying.

Transfluxor Controlled Electroluminescent Display Panels*

J. A. RAJCHMAN†, FELLOW, IRE, G. R. BRIGGS†, ASSOCIATE MEMBER, IRE, AND A. W. LO†, SENIOR MEMBER, IRE

Summary—The feasibility of displaying images according to electrical signals using an array of electroluminescent cells magnetically controlled has been demonstrated by a working model. A transfluxor is associated with every electroluminescent cell. Each transfluxor is set by the coincidence of row and column current pulses to a level determined by the amplitude of the video signal, stores this level, and transmits energy continuously to the cell in proportion to the stored level. Both halftone and on-off control of brightness is possible. Scanning is accomplished by magnetically switching row and column conductors. The array has 1200 elements arranged in 30 rows of 40 each. The picture is uniform, exhibits good halftones, and has a maximum brightness of four foot lamberts.

To obtain sufficient voltage from the transfluxor to excite electroluminescence, drive by short, fast-rising pulses is used. Light output data for such pulses were obtained and it was found that a steeper dependence of light output upon voltage, a different color spectrum, and higher efficiency resulted than is obtained with sine-wave drive.

A modification using a linear transformer to couple the transfluxor and electroluminescent cell and driven by sine waves to operate as a transfluxor-tuned resonant circuit was demonstrated to be economical in driving and setting power.

For some applications, the full storage afforded by a transfluxor at each picture element is not necessary. A system was investigated which uses fewer transfluxors storing only a row of picture information at a time.

The demonstration panel has shown that it is possible to display pictures indefinitely, to store latent images without stand-by power, to use selective addressing through digital codes, and for the panel itself to provide much of its own switching. These unique properties can be obtained for alphanumeric, symbolic or pictorial information in displays ranging from a fraction of a square inch to many square feet in area.

Introduction

THE advent of electroluminescence opened the possibility of producing images by means of an array of discrete cells; each cell is subjected to an electrical excitation determining the intensity of light desired at that location. A display device of this sort used to produce images according to electrical video signals differs from the conventional cathode-ray tube in two main aspects: it is flat rather than conical and it operates by digital rather than analog scanning. Images measured in feet rather than in inches can be contemplated. Digital scanning is particularly useful to display quantized information.

Perhaps the simplest system consists of an array of electroluminescent (*EL*) cells, one terminal of each connected with like terminals of all cells of a row and the other terminal with the like terminals of all the cells of a column. Excitation of a given row and column impresses a greater voltage on the cell at the intersection than on any other cell in the array. The selected cell emits light almost at the exclusion of all others, because it is a characteristic of electroluminescence that the light output is a rapidly increasing function of the applied voltage. However, an examination of the properties of presently available *EL* cells indicates that such a simple system suffers from two basic difficulties. 1) In an array of a large number of cells (*e.g.*, 10^3 to 10^7) the maximum average light intensity, which is at most the peak intensity divided by the number of cells, is very small even for high voltage excitation close to the breakdown limit of the cells. 2) The image contrast suffers because the partial excitation of the cells on the row and column of the selected cell integrates over the period of the full frame scan to produce a relatively intense background. The contrast can be improved only moderately by resorting to the artifice of supplying appropriate compensating voltages to the unselected rows and columns. Adequate contrast can only be obtained with low voltages, yielding a very dim image.

In an ideal panel, to overcome the above difficulties, every element should emit light continuously at a level set by the scanning means until a new level is set, and the setting means should affect only the desired element and no other element. Under these conditions the average light level could be the same as the peak attainable from each cell and there would be no contrast limitation due to the scanning mechanism. In other words, for each element there should be a means 1) to store the level of display information, 2) to energize the *EL* cell according to the stored level, and 3) to establish the stored level by the coincidence of row and column excitations without affecting the stored level of any other element. This triple function can be performed by a transfluxor associated with each *EL* cell. The transfluxor is a magnetic gating device which can control, for an indefinitely long time, the transmission of ac power according to a level established by transient setting pulses acting in coincidence.

The possibility of making display panels of discrete *EL* cells, each cell controlled by a two-apertured transfluxor, was realized soon after the conception of the transfluxor. This was investigated by building an experimental display panel of 1200 elements. Reproduc-

* Original manuscript received by the IRE, May 29, 1958; revised manuscript received, August 8, 1958.
† RCA Labs., Princeton, N. J.

tion of television images was used to test the device. The first part of this paper is concerned with the principles of operation of this system, constructional details, and operating results. Also included in this part are some characteristics of excitation of electroluminescence by the short voltage pulses necessitated by the magnetic mode of driving.

The experimental panel has demonstrated that transfluxor driven electroluminescent displays have many desirable properties. Images of reasonable intensity, of excellent contrast, and good halftone quality are obtained. In addition, the inherent storage properties of the transfluxor permit one to freeze the picture and view it for as long as desired simply by arresting the scanning process. A latent picture can be stored indefinitely, without stand-by power.

The two main disadvantages of this display were found to be the complexity of construction and the poor power efficiency. Higher power efficiency can be obtained by using a transformer coupling between the *EL* cell and transfluxor, and by operating in a resonant mode. The addition of the transformer, paradoxically, also simplifies the construction because fewer winding turns are required on the transfluxor, which is the more difficult component to wind. This system is considered in a second part of this paper.

In a third part, additional methods of scanning the array are considered. Selective addressing of any element of the array in response to digital codes can be accomplished using magnetic switching techniques which are extensions of those used for the television-type scanning. Simpler systems of selection, suitable for alphanumerical display of information, are also described.

In the last part, another approach to the *EL* display problem is considered, which is based on the recognition that storage at every element of the array, while ideal, is not absolutely necessary. Acceptable brightness can be obtained with presently available *EL* phosphors by sharing storage elements between light cells so that only a portion, rather than all, of the light cells are energized at a time. The switching of the storing transfluxors to the appropriate *EL* cells is accomplished by voltage coincidence, as in the system first mentioned.

Transfluxor Control of Electroluminescent Cells

The principles of operation of a two-apertured transfluxor,[1,2] which will be shown to be suitable for display storage and *EL* cell control, can be explained with the aid of Fig. 1. The apertures are of unequal diameter and form three legs, numbered 1, 2, and 3. The core is

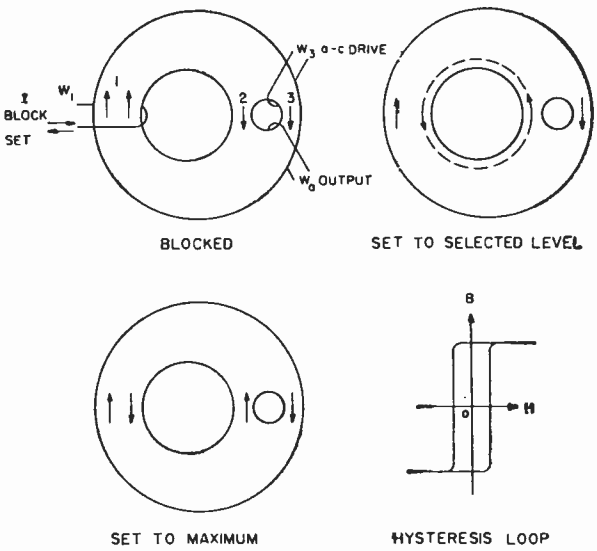

Fig. 1—Principle of two-apertured transfluxor.

made of a magnetic material exhibiting a nearly rectangular hysteresis loop, usually ferrite. Assume that at first a current pulse is passed through winding W_1 of sufficient intensity to saturate legs 2 and 3 in the direction indicated for the blocked state. The two legs will remain effectively saturated after the termination of the pulse since remanent and saturated inductions are nearly equal in square-loop materials. Consider now the effect of a sine wave alternating current in winding W_3 producing an oscillating magnetomotive force (mmf) along a path surrounding the smaller aperture. Depending upon its sense, this mmf tends to produce an increase in flux in either leg 2 or leg 3, but since neither increase is possible because these legs are saturated, there is no flux change. The transfluxor in this state is said to be "blocked" and little induced voltage appears across the output winding W_0. Consider now the effect of a "setting" pulse of current having a polarity opposite to that of the blocking pulse. This current applied to winding W_1 tends to reverse the flux direction of leg 1 of the blocked core. The magnetic field H produced decreases radially with distance measured from the center of the larger aperture according to Ampere's law $Hl=4\pi X$, where l is the circumference of the flux path and X the mmf. Because a critical value of H is required in square-loop materials to produce flux reversal, the flux will reverse from the radius of the aperture out to a critical radius only. The amplitude of the setting pulse determines this radius and can be prescribed so that any desired portion of the width of leg 2 will reverse its direction of saturation, while the rest of the leg, as well as the more distant leg 3, remains saturated in the original direction. After such a setting operation, the alternating current applied to winding W_3, at its first proper phase, will switch back the whole flux in leg 2 to its original direction of saturation and cause the flux in leg 3 to de-

[1] J. A. Rajchman and A. W. Lo, "The transfluxor—a magnetic gate with stored variable setting," *RCA Rev.*, vol. 16, pp. 303–314; June, 1955.
[2] J. A. Rajchman and A. W. Lo, "The transfluxor," Proc. IRE, vol. 44, pp. 321–332; March, 1956.

crease by the amount that the flux in leg 2 increased, which is precisely equal to that initially "set." On the next phase of the alternating current, the flux of leg 3 will be switched back to its original direction and the amount of set flux will be transferred back to leg 2. On successive excursions the amount of flux set in will be transferred back and forth between legs 2 and 3, and a voltage will be induced in the output winding, the magnitude of which is proportional to the set flux and is therefore seen to be determined by the amplitude of the single setting pulse. Although the transfluxor is made of material which is always saturated in one or the other direction, continuous or "halftone" control is possible because the output flux and voltage are determined by the critical radius, which can be varied continuously in a range.

The simplest method of using a transfluxor to control an *EL* cell is to connect the cell directly to the ac output of the transfluxor using an output winding of a few turns to obtain sufficient voltage. An array of such transfluxor *EL* elements is shown schematically in Fig. 2. Each *EL* cell is connected separately to each transfluxor. The output apertures of all the transfluxors are energized from a common ac source.

As mentioned in the Introduction, the transfluxor has an additional feature of great usefulness. It is possible to set any transfluxor in an array independently of the others by using a coincident-current method of selection. To accomplish this, two setting windings are provided for each transfluxor. Shown in Fig. 2, these windings (indicated as single turn) are connected in series in two sets. One set is connected in series in the row direction and the other set in the column direction of the array. Current pulses of the correct amplitude applied simultaneously to one row and one column winding group will set only the one transfluxor at the intersection of the row and column lines, and leave all the others unaffected. This can be understood with the aid of Fig. 3, which shows the setting characteristic for a typical transfluxor design. In obtaining this characteristic curve, a blocking pulse of 5 ampere-turns (AT) was applied prior to the application of each setting current pulse. If the setting current pulse applied is less than a threshold value I_0, insufficient H around the shortest flux path in the core will be produced to cause any flux reversal. Such pulses therefore will have no effect, no matter how often applied. For setting pulses exceeding the threshold value, the reversed flux increases nearly linearly with current to a maximum for a current I_1 corresponding to complete reversal of the flux of leg 2. For still larger pulses the output decreases because part of the flux of leg 3 is also reversed by the setting current, reducing the net flux available to be later transferred between legs 2 and 3. If the radial distance measured from the center of the setting aperture to the outer edge of leg 2 is less than twice the radius of the setting aperture, it follows from Ampere's Law that I_1 will be less than twice I_0. Such a condition is sufficient to permit the use of coincident-pulse setting. Either the row or the column current, or both, may be varied in amplitude to set different output levels. The row and column pulses can be generated by magnetic switches as described in a following section.

To utilize the setting characteristic exemplified by Fig. 3, it is necessary to first block the transfluxor before each setting operation. The pulses for this purpose can be applied simultaneously to all the transfluxors to clear

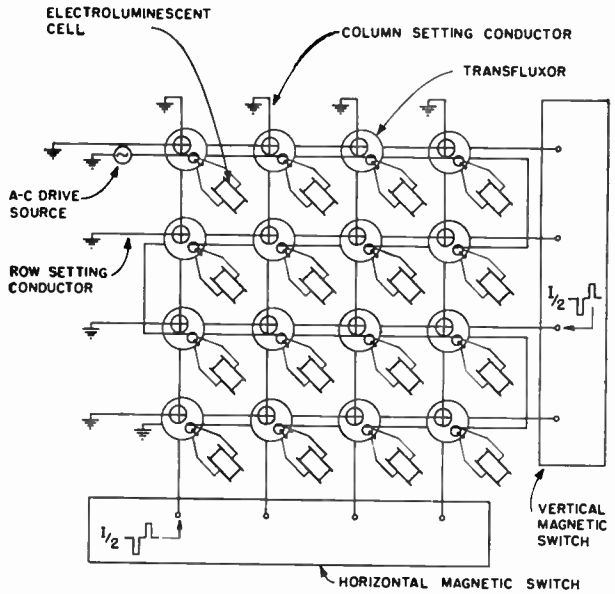

Fig. 2—Simplified diagram of a display device made up of an array of two-apertured transfluxors driving electroluminescent cells. The driving power is supplied to all the transfluxors connected in series from a single source. Transfluxor setting currents are supplied in coincidence by magnetic switches.

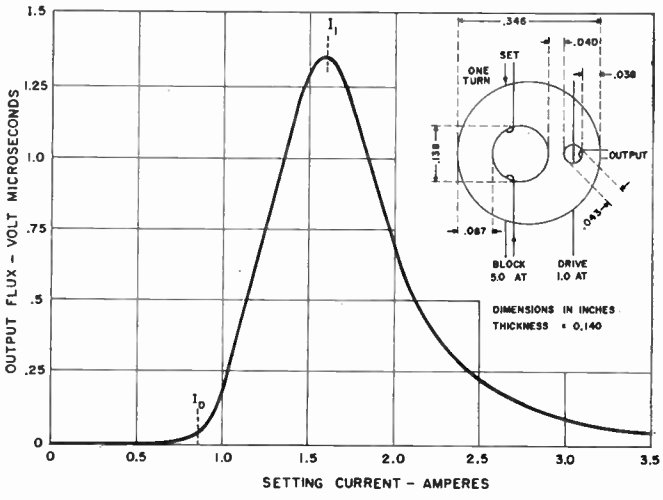

Fig. 3—Setting characteristic of transfluxor having dimensions indicated. The data were obtained for setting pulses of rectangular waveshape 2.0 μsec in duration. Currents less than I_0 produce little setting while currents greater than I_1 overset the core, reducing the output flux.

the whole array, or to a row at a time for row-by-row clearing. It was found that the blocking pulse must be considerably greater than I_1 to obtain a sharp threshold and reproducible setting characteristics. This is a result of the complex minor loop operation which can occur with practical magnetic materials of less-than-perfect hysteresis loop rectangularity. In principle, with perfect materials, the blocking operation should be merely the reverse of the setting operation, and blocking with pulses of amplitude I_1, and with pulses in coincidence, should be possible. With present materials, however, such operation is suitable only for on-off displays for which the reproducibility of setting is not critical.

Consideration must be given to the effect of the current flowing in an output load, such as an *EL* cell, upon the operation of the transfluxor. This current reflects a load mmf into the output magnetic circuit. The drive mmf must exceed the reflected load mmf. If the drive current is too large in the phase which tends to reverse upwards the flux of leg 3 (Fig. 1), the transfluxor in the blocked state may become spontaneously set because sufficient mmf may be available to switch leg 3 via the long path through leg 1. This "spurious unblocking" by the drive results in partial or full output when such an output level may not have been set into the device. To prevent this, it is necessary to limit the amplitude of this phase of the ac drive. On the other hand, the opposite phase can be of unlimited amplitude and most of the output voltage and power can be obtained from this phase. Therefore, it is best to energize the transfluxor unsymmetrically, with one "priming" phase sufficient only to produce flux transfer from the middle leg 2 to the outer leg 3, and a "driving" phase of larger amplitude to transfer energy efficiently to the load.

Light-Output Characteristic of an Electroluminescent Cell Under Pulse Excitation

Electroluminescent layers must be about 1 mil thick to contain sufficient phosphor to give reasonable brightness. Such layers require the order of 100 peak volts of ac excitation to give 10 foot lamberts of brightness at a frequency of 10 kc. Transfluxors having dimensions of fractions of an inch have only a few volt-microseconds of output flux. To obtain the necessary output voltage, *i.e.*, to match the transfluxor to the *EL* cell, the flux can be reversed rapidly and a number of output turns can be used. To keep the fabrication of an array of a multitude of cells simple, it is important to use as few turns as possible. This means that the flux reversal should be as fast as possible. For a reasonable number of turns, *e.g.*, 10 to 20, sine-wave drive at a frequency of several megacycles would be required. This would result in overheating of the ferrite. To avoid this, pulse drive is used. The rise of the pulse is made sufficiently fast to generate the required voltage, and the interval between pulses sufficiently long to avoid overheating. Pulse drive

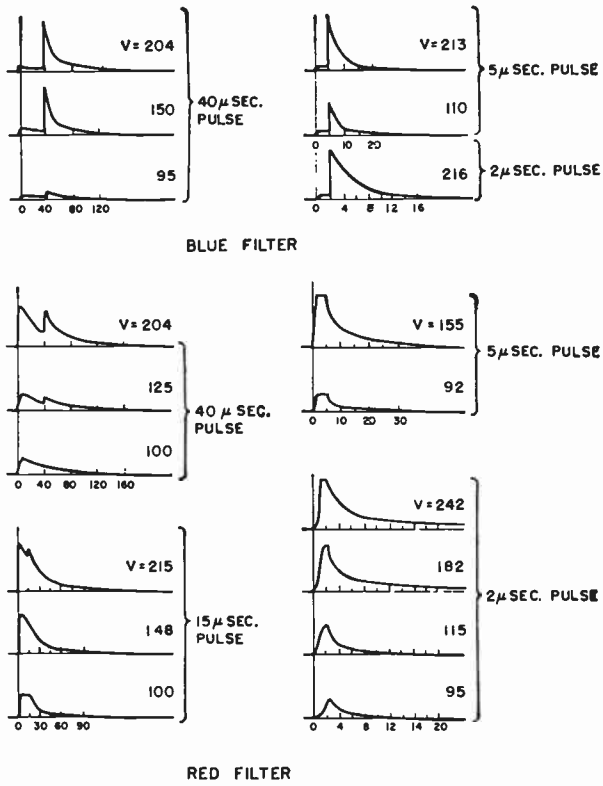

Fig. 4—Light-output waveforms for an electroluminescent cell excited by short rectangular voltage pulses. The waveforms were obtained for light transmitted through a red or a blue filter.

also provides a convenient way to obtain the unsymmetrical drive required for stable and efficient operation of the transfluxor.

Because of the limited transfluxor output flux, the output voltage pulses with pulse excitation will have durations of only a few microseconds at most. The behavior of an *EL* cell under such short-pulse excitation was studied,[3] as little published data were available. The results of this study are summarized here.

The phosphor tested had the composition 0.6 ZnS :0.4 ZnSe:Cu (0.1):Br[4] and was embedded in an epoxy plastic layer 1 mil in thickness. With sine-wave excitation, the color of the light generated is yellow at low frequencies, but shifts to green at high frequencies. The color components were studied separately using red, yellow and blue light filters. Light output waveforms for rectangular pulses are shown in Fig. 4. Most of the blue light is emitted after the pulse has terminated, and the decay of this light is faster the shorter the pulse. The waveform is nearly independent of excitation amplitude. The waveforms for the red light emitted are more complicated. A considerable portion of this light is emitted

[3] G. R. Briggs, "Light output of an electroluminescent cell excited by short voltage pulses," *Bull. Amer. Phys. Soc.*, ser. II, vol. 2, p. 155; March, 1957.

[4] I. J. Hegyi, S. Larach, and R. E. Shrader, presented at Luminescence Symp., Electrochemical Society, San Francisco, Calif., 1956.

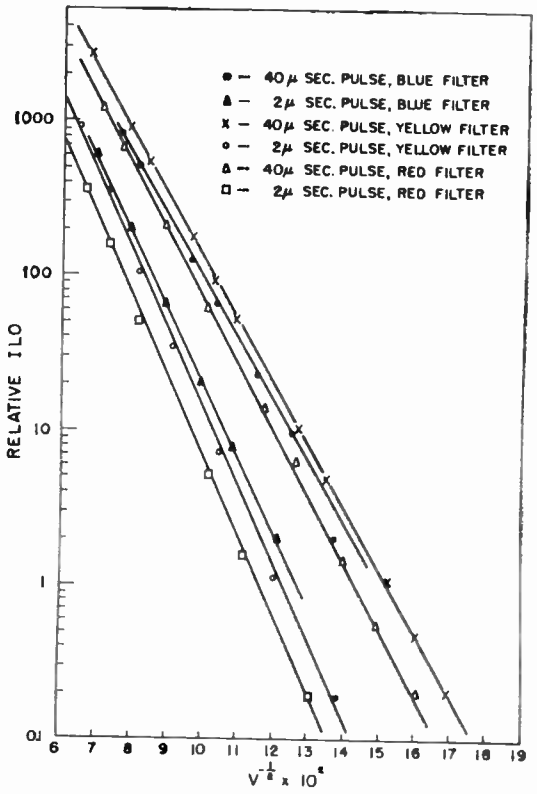

Fig. 5—Logarithm of electroluminescent cell integrated light output (*ILO*) vs $V^{-1/2}$ for rectangular pulses and red, yellow and blue light filters.

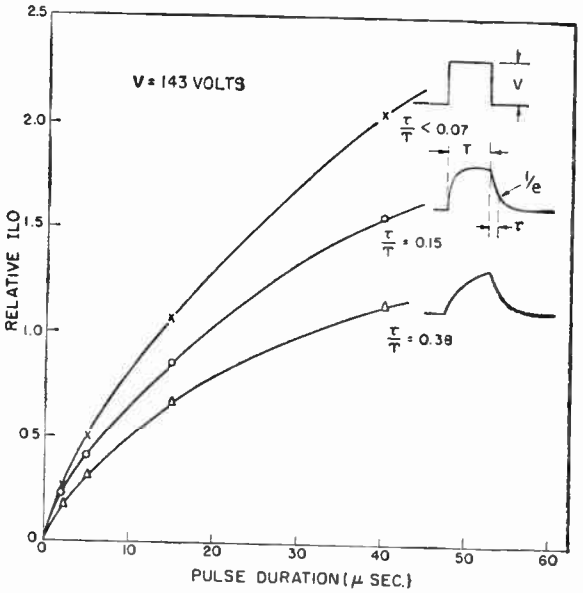

Fig. 6—*ILO* for pulses having exponentially rounded rising and falling edges vs pulse duration. *ILO* for rectangular pulses included for comparison. Data for red filter.

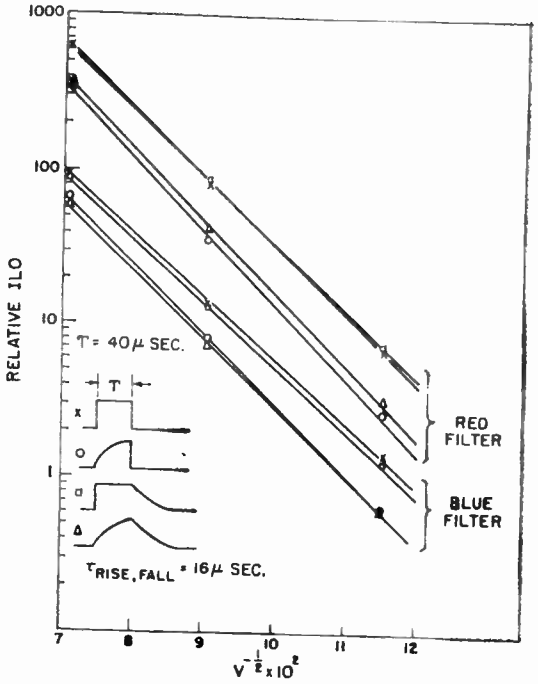

Fig. 7—Logarithm of *ILO* vs $V^{-1/2}$ for four different pulse shapes. Exponential portions of each pulse have the same time constant.

during the pulse, but for a given duration of pulse, the relative amount of light emitted after the pulse has terminated increases with pulse amplitude. As the pulse duration is increased, for a fixed pulse voltage, the trailing spike of light becomes more prominent, maintaining the same peak value with respect to the base line. For small pulses the trailing spike disappears.

It has been reported[5] that the total or integrated light output (*ILO*) for sine-wave excitation of electroluminescence obeys the relation

$$ILO = ae^{-b/V^{1/2}},$$

where V is the applied voltage and a and b are constants depending upon the phosphor used, the frequency, and the cell construction. The same law was found here to hold also for short-pulse excitation, as indicated by Figs. 5 and 7. The law seems to be obeyed regardless of pulse shape. Some values of the constant b for rectangular pulses are given in Table I. This constant, and hence the rate of increase of light with voltage, is greater the shorter the pulse.

Voltage pulses of waveshape other than rectangular were also investigated. Results for rounded pulses of practical interest are shown in Fig. 6. A fractional decrease of light results when the pulse is rounded which is nearly independent of pulse duration. Curves for the blue light component were found to be similar to those for the red fraction. The ratio of red to blue light for different degrees of pulse rounding was also measured; the results are listed in Table II. This ratio is nearly independent of the amount of rounding, but is very dependent upon pulse duration. This interesting result was

[5] P. Zalm, G. Diemer, and H. A. Klasens, "Some aspects of the voltage frequency dependence of electroluminescent zinc sulphide," *Phillips Res. Reps.*, vol. 10, pp. 205–215; February, 1955.

TABLE I

VALUES OF THE CONSTANT b FOR RECTANGULAR VOLTAGE PULSES

Pulse Length (μsec)	Filter	b
2	Red	119
	Yellow	117
	Blue	111
40	Red	99
	Yellow	94
	Blue	92

TABLE II

RATIO OF RED TO BLUE LIGHT FOR PULSES HAVING EXPONENTIALLY ROUNDED LEADING AND TRAILING EDGES. DATA FOR A PEAK VOLTAGE OF 143 VOLTS. FOR A GIVEN PULSE LENGTH THE RATIO IS NEARLY INDEPENDENT OF τ/T. SEE FIG. 6 FOR DEFINITION OF τ AND T

Pulse Length (μsec)	$\tau/T<0.07$	$\tau/T=0.15$	$\tau/T=0.38$
40	8.9	9.1	8.8
15	6.8	6.7	6.8
5	4.6	4.7	4.7
2	3.8	3.8	4.0

TABLE III

VALUES OF b AND RED/BLUE LIGHT RATIOS FOR PULSES OF DIFFERENT SHAPE HAVING THE SAME PEAK AMPLITUDES. COMPARED TO A RECTANGULAR PULSE, PULSE TYPE (2) GENERATES A GREATER FRACTION OF BLUE LIGHT AND HAS A GREATER b VALUE. PULSE TYPE (3) ALSO HAS A GREATER b VALUE BUT GENERATES RELATIVELY MORE RED LIGHT. PULSE TYPE (4) HAS ABOUT THE SAME RED/BLUE RATIO AS THE RECTANGULAR PULSE, BUT A GREATER b VALUE. DATA FOR 40-μSEC PULSES

Pulse Type	b		Ratio Red/Blue Light Output for Pulse Voltage		
	Red Filter	Blue Filter	$V=199$	$V=123$	$V=75.5$
Rectangular (1)	103	96	6.5	5.7	4.8
Exp. Rise Fast Fall (2)	111	106	5.1	4.5	4.1
Fast Rise Exp. Fall (3)	105	97	7.1	6.4	5.7
Exp. Rise And Fall (4)	108	103	6.3	5.7	5.4

investigated further, using pulses having one fast-rising or fast-falling edge and the other edge of exponential shape. The results are summarized in Table III from data given in Fig. 7. The slowly-rising portion of a rounded pulse was found to generate relatively more blue light and the slowly-falling portion relatively more red light than the corresponding parts of a rectangular pulse. The net color shift with the rounded pulse is therefore small.

Light-generation efficiency under short-pulse excitation was also investigated. Non-capacitive, *i.e.*, irreversible, *EL* cell charge flow per pulse was measured for rectangular pulses of several durations; the results are shown in Fig. 8. This charge flow multiplied by the pulse

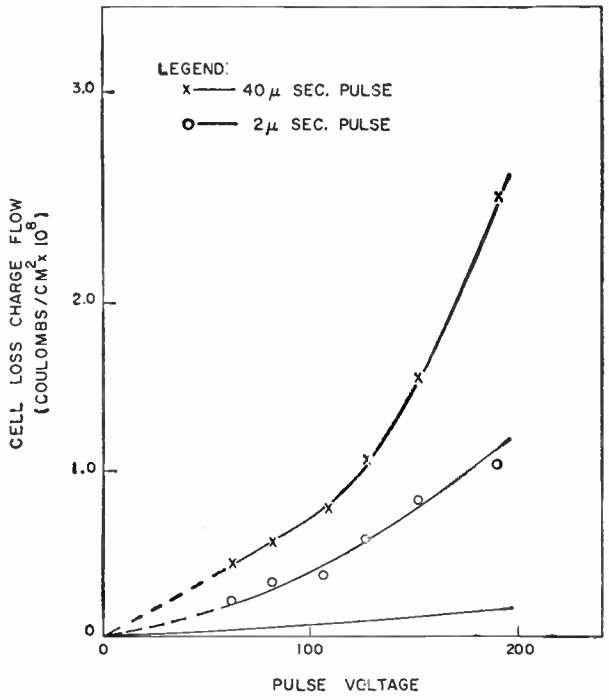

Fig. 8—Electroluminescent cell charge flow (minus capacitive component) vs pulse voltage, for rectangular pulses. This charge flow difference is proportional to cell energy loss per pulse, for a given voltage. Calculated charge flow for the plastic cell dielectric alone is indicated by the lowest curve.

voltage is the energy loss per pulse. The loss for a 40-μsec pulse is about twice that for a 2-μsec pulse of the same amplitude. The light output for the longer pulse is about eight times that of the shorter (Fig. 6), however, resulting in an efficiency for the longer pulse of four times that of the shorter. In addition, the energy loss decreases only slightly more rapidly than the square of the voltage, whereas the light decreases considerably more rapidly. For this reason a high pulse voltage should be used to obtain highest efficiency. For a 40-μsec rectangular pulse of 183 volts repeated 600 times per second to obtain an average brightness in the green region of the spectrum of 1.4-foot lamberts, the efficiency was found to be 0.55 lumen per watt.

OPERATION OF A TYPICAL TRANSFLUXOR-ELECTROLUMINESCENT ELEMENT

A typical current-drive waveform for a transfluxor driving an electroluminescent cell and the resulting voltage and light-pulse waveforms are shown in Fig. 9. The first, more intense pulse, of 5 AT is the drive pulse, and produces most of the light. The second pulse, of opposite polarity, is the prime pulse, limited to 1.5 AT in amplitude to prevent spurious unblocking of the transfluxor. This pulse is too small to generate any appreciable additional light. The output voltage waveform, having both positive and negative portions, differs greatly from any of the shapes considered in the study of the above section. In general, with this waveform the rate

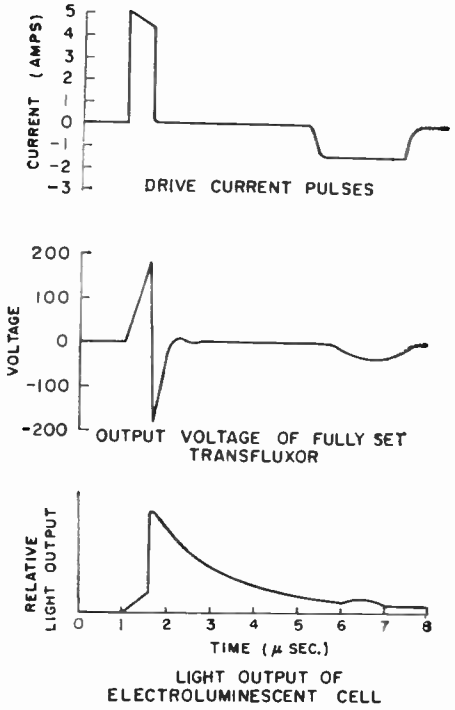

Fig. 9—Waveforms of transfluxor drive current, output voltage and electroluminescent cell light output for a typical transfluxor-*EL* cell combination. A one-turn drive and 17-turn output winding were used with two transfluxor cores, each having the dimensions shown in Fig. 3. The *EL* cell was 0.150 square inch in area and had a capacitance of 300 $\mu\mu$f.

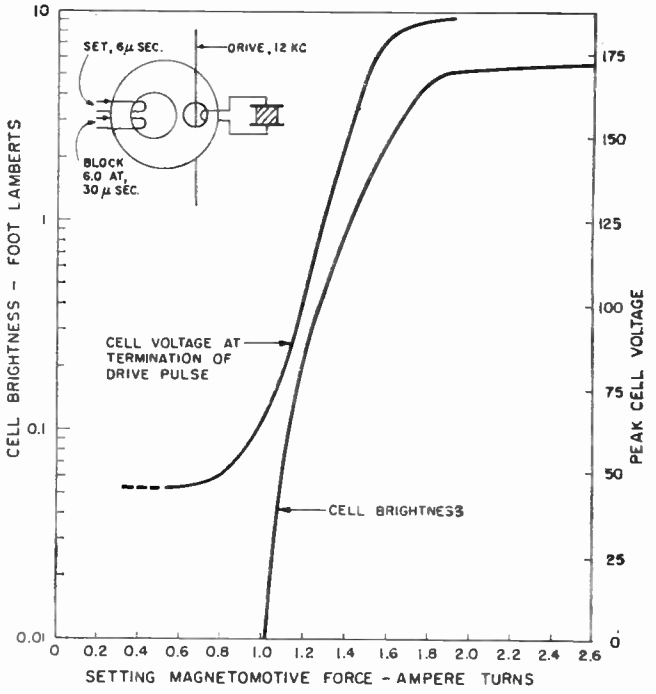

Fig. 10—Electroluminescent cell average brightness and peak voltage vs transfluxor setting magnetomotive force, for the unit described in the caption of Fig. 9.

of increase of light with voltage is about the same as for the 2-μsec rectangular pulse, whereas the absolute light output is considerably greater when compared on a peak voltage basis. The effective voltage is more nearly equal to the peak-to-peak value. Because of this high effective voltage, the *EL* cell efficiency, despite the small pulse duration, is also about the same as for the 2-μsec rectangular pulse of the same peak value, or about 0.15 lumen per watt at maximum voltage.

Fig. 10 shows curves of peak *EL* cell voltage and average brightness as a function of transfluxor setting magnetomotive force for a transfluxor-*EL* cell combination driven by the pulses seen in Fig. 9. A maximum brightness of 4 foot lamberts is obtained for drive pulses repeated at a rate of 12 kc. For this output, the drive-input power is 180 milliwatts and the power consumed by the *EL* cell, 28 mw. This represents an efficiency of 16 per cent in exciting the cell. As mentioned in the Introduction, a resonance method of improving the efficiency is discussed in a following section.

With the transfluxor blocked, some output voltage is still generated. Because of the steep light output-voltage characteristic of the *EL* cell, however, this produces almost zero light output, resulting in an excellent on-off contrast ratio. Because of its contrast and reasonable power consumption, this combination of *EL* cell and transfluxor, driven in the way indicated, was chosen as the basic building block for the 1200-element model.

Construction of the Display Array

Arrays of transfluxor-*EL* elements can be constructed by fabricating each element separately, by constructing groups of elements in units, or by some integral process making the whole array in one step. The first method appears to be very expensive even when the elements are manufactured using highly automatized techniques. The last method is difficult to implement because the microstructure of the elements which can be made by an integral process is restricted by that very process. Extreme perfection has to be assumed. Construction by groups, in particular by lines, appears to be most practical quite generally.

Constructional details of the 1200-element array are shown in Fig. 11. The elements were arranged in 30 rows of 40 elements each. The *EL* cells were fabricated a row at a time on glass bars of row width. The front surface of each bar was first coated with transparent tin oxide conductor, then silver contacting layers, overlapping the transparent conduction layer slightly, were sprayed along each side of the bar. These layers form low resistance common connections for the cells. They are required because the transparent conductor strip itself is not of sufficiently low resistance to form a satisfactory return path for the cell charging currents flowing under pulse conditions. These reinforcing conductors obstruct little of the area of the screen. A layer, 1 mil in thickness of *EL* phosphor in an epoxy resin plastic binder was next laid down over the transparent conductor. Finally, backing electrodes of sprayed silver were applied

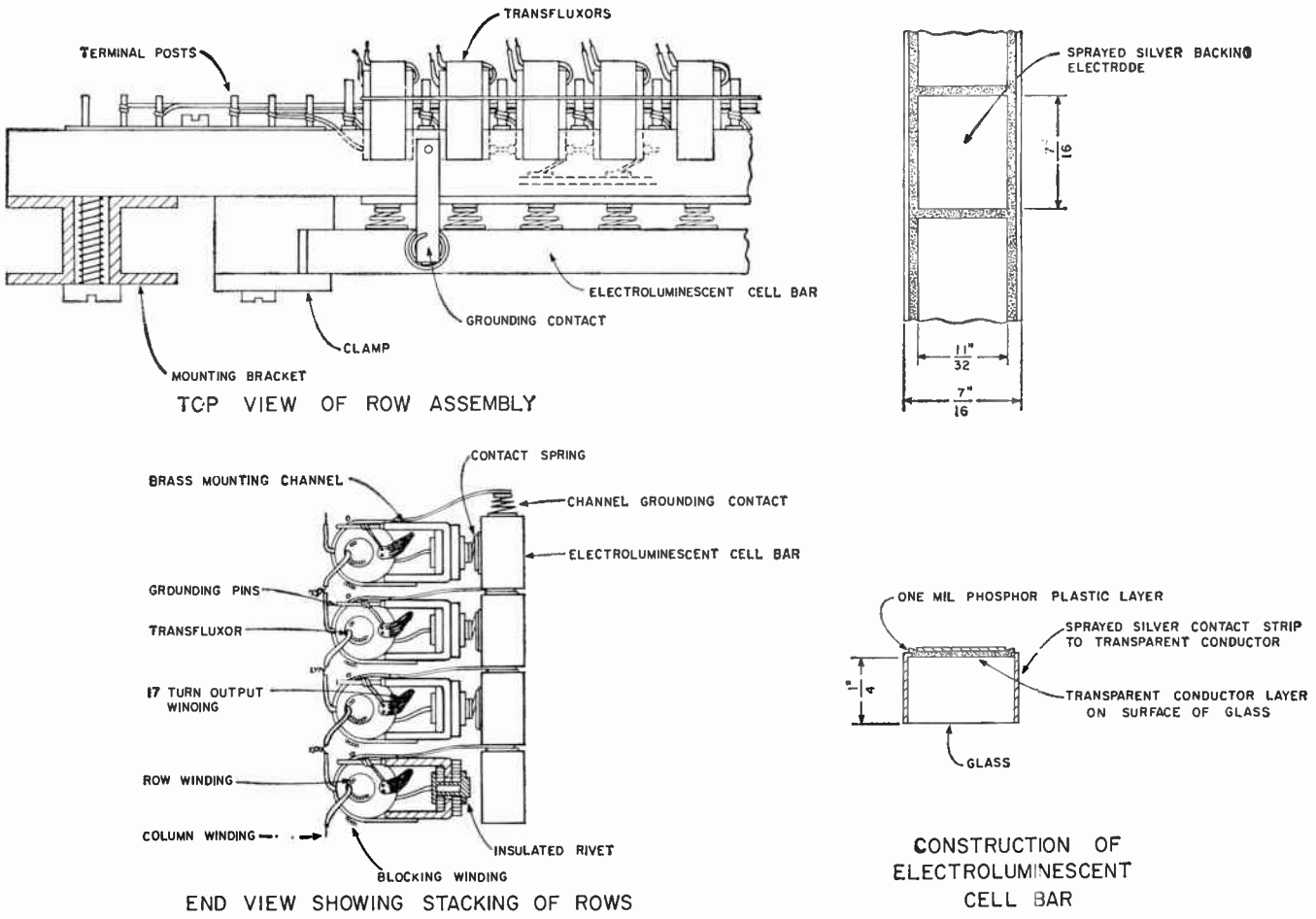

Fig. 11—Constructional details of the 1200-element array.

through a mask. The bars were mounted, by means of clamps, on brass *U* channels which also held the transfluxors and *EL* cell backing electrode contacting springs for the same row. The resulting row units, after being wired with all horizontal wiring, were stacked and clamped into a vertical frame to form the complete array. Phosphor-bronze leaves were forced between the *EL*-cell bars against the reinforcing conductors to ground each bar. The vertical columns were wired to complete the job.

Transfluxor output windings of 17 turns were wound using a special winding machine[6] which pulled the wire through the small aperture 17 times. The resulting turns had excess length and were twisted into a pigtail to reduce leakage inductance. All other windings, which were of one or two turns with the exception of a five-turn blocking winding, were wound around all the cores of a row at a time.

Views of the completed array, including scanners, are seen in Figs. 12 and 13. The array measures 13 by 17 inches and the over-all dimensions, including the scanners, are 24 by 32 inches with a depth of 1.5 inches. All pulses are supplied to the screen via a multiple-conductor cable one-half inch in diameter and several feet in length.

[6] A similar machine has been built at Stanford Research Institute. See "Pinhole coil winder," *Electronic Indus.*, vol. 17, p. 83; February, 1958.

Magnetic Scanning of the Display Array

To display halftone pictures, setting current pulses of variable, yet accurately controllable, amplitude must be supplied by the addressing devices. For this display, the decision was made to supply pulses of fixed amplitude, the threshold current I_0, to the column conductors, and to supply the pulses of variable amplitude to the row conductors. Magnetic switches based on the principle of current steering,[7,8] were developed for these purposes. These switches operate sequentially to scan the array in conventional television fashion.

The column or horizontal scanner for sending the current pulses I_0 is simpler and is described first. Referring to the schematic diagram shown in Fig. 14, the current

[7] M. Karnaugh, "Pulse-switching circuits using magnetic cores," Proc. IRE, vol. 43, pp. 570–584; May, 1955.

[8] J. A. Rajchman and H. D. Crane, "Current steering in magnetic circuits," IRE Trans. on Electronic Computers, vol. EC-6, pp. 21–30; March, 1957.

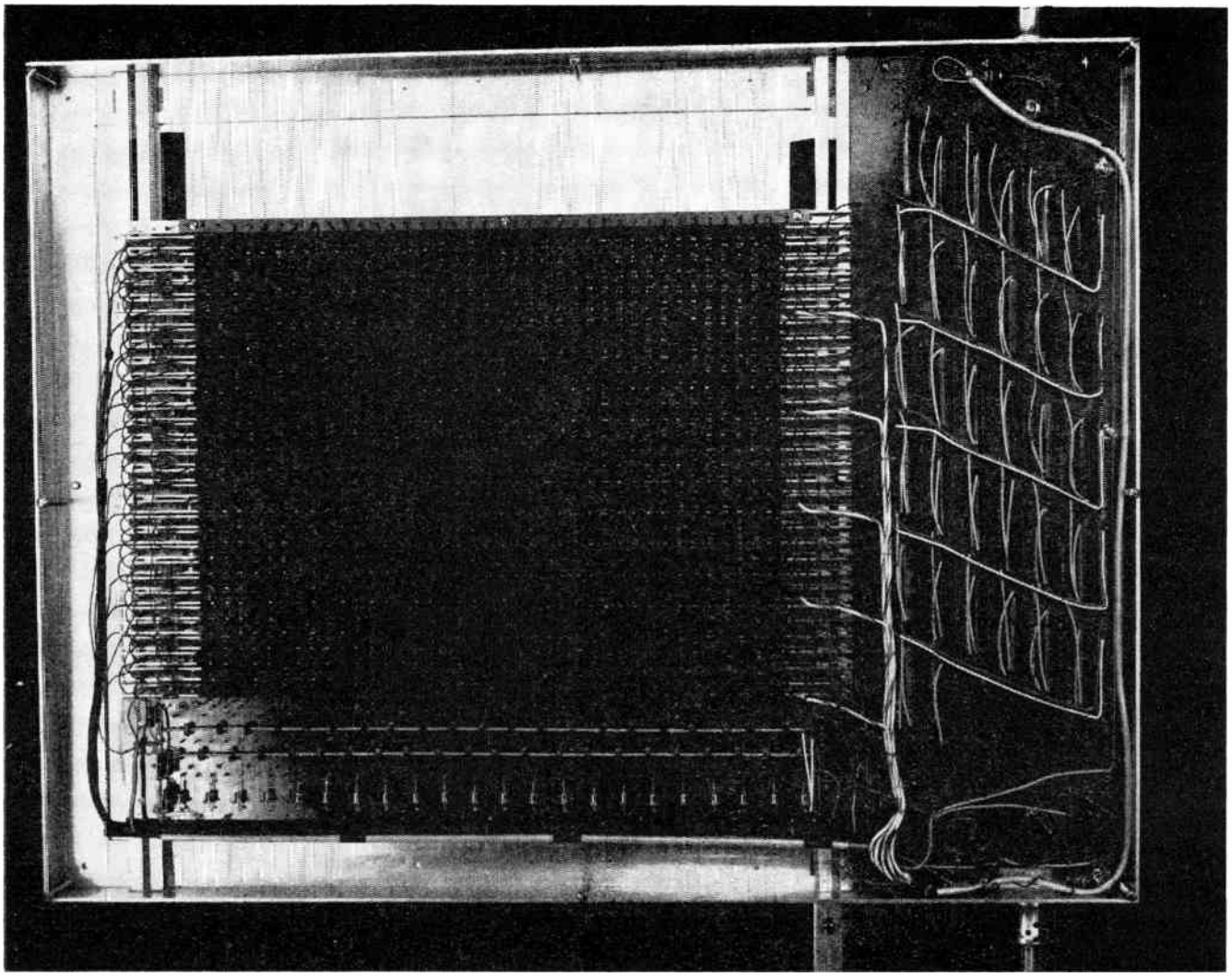

Fig. 12—Rear view of 1200-element display panel, showing the array transfluxors and magnetic scanners.

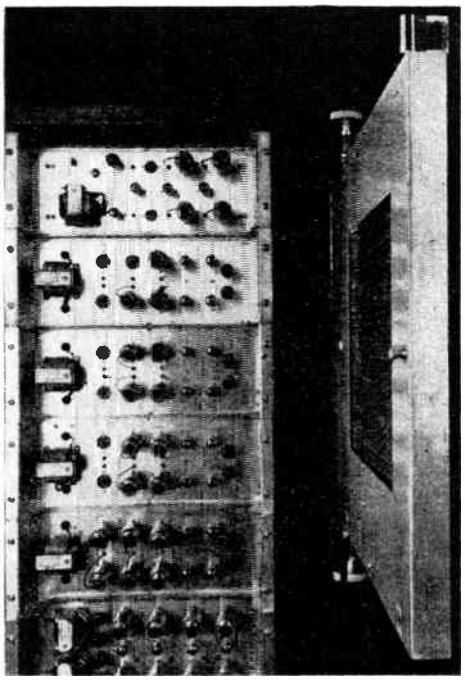

Fig. 13—Side view of display panel, showing the electroluminescent cell bars, part of the associated electronic circuitry, and the connecting cable.

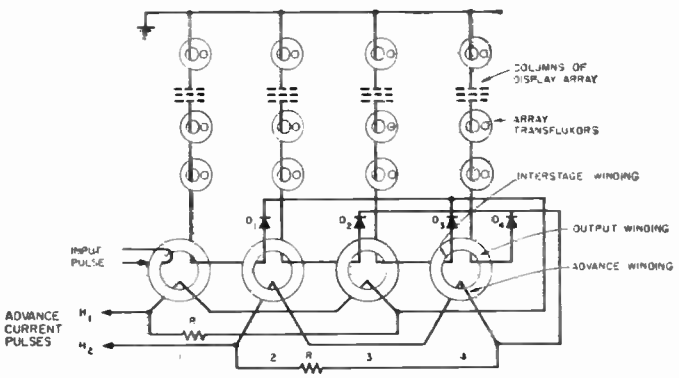

Fig. 14—Schematic diagram of magnetic core horizontal scanner. In this scanner the input advance current pulses are steered according to the flux states of the cores sequentially to the column conductors.

pulses H_1 and H_2, which are alternately applied, serve to advance an active core state as in an ordinary magnetic core shift register, but in addition are themselves steered by the active core to one of the output paths. The operation is as follows. The cores are all assumed to be initially in one of the two remanent states which will be designated N. Application of pulse H_1 or H_2 tends to hold the cores in the N state and only small and equal output voltages are generated by any core, so that the current pulse is distributed equally to all the columns via the diodes indicated. The current flow in any one column is sufficiently small, if the scanner is of reasonable length, that it can be neglected. Consider next what results when core 1 is switched to the other remanent state which will be designated P. If the pulse H_1 is applied now, this core will switch back to the N state. This will induce a voltage on its output winding greater than that of any of the other cores, forcing the voltage of the common diode bus sufficiently positive to disconnect the current paths via the diodes D_3, etc. Therefore, all the current will be driven or "steered" through diode D_1 into the output path of core 1. At the same time, this current will switch core 2 to the P state. If current pulse H_2 is now applied it will be switched in the same manner entirely to the output path of core 2, and at the same time it will activate core 3, *etc.*

The current steering property of this type of scanner means that the same current flows in both the advance and output windings of the active core. As a result, more turns must be wound on the advance winding than on the output winding to obtain a net switching mmf for the core.

Consideration must also be given to the array column voltage drop. Each scanner core must have sufficient flux and a large enough number of output turns to generate a voltage greater than the sum of the voltage drop in the column, the diode drop, and the voltage induced by a nonswitching core. This excess of voltage must be maintained for the duration of the advance pulse. Therefore the switching of the active core back to the N state cannot be quite complete when the advance pulse is terminated, for otherwise the shape of the trailing edge of this pulse, transmitted through the scanner, would not be preserved. On the other hand, if the core were not completely returned to the N state, spurious active states would be set up by subsequent advance pulses and would cause faulty operation of the scanner. To prevent this, resistances R are shunted across the advance-winding circuits. These resistances form a path which makes it possible for current to continue to flow in the advance windings after the pulse H_1 or H_2 has ceased, causing the active core to then complete switching. The energy source for this current is the magnetic energy of the reversible flux of the N-state cores, stored when the advance pulse is applied. When the pulse is terminated, the collapse of this flux generates voltages across the advance windings of the N-state cores, and the series effect of these forces current to flow in the loop consisting of the advance windings in series with R. Since no input advance pulse is being applied at this time, there is no counteracting current flow in the output winding and, therefore, a large net switching mmf on the active core results for only a moderate current flow in R. Because there are many cores storing energy, sufficient current to complete the switching can be obtained even with relatively large values of R. The shunting effect of R for the advance pulses thus can be neglected.

The horizontal scanner constructed for the model has 40 positions and furnishes pulses of 1.0 ampere for 6 μsec. The two advance pulses are generated by pentodes operating as constant-current generators. The diodes are of the junction-type 1N93. For each stage, an advance winding of 30 turns, an interstage winding of 5 turns, and an output winding of 25 turns are wound on the large aperture of a 0.140-inch-thick transfluxor of the same type used in the array. The smaller aperture is ignored. The scanner is mounted at the bottom of the array and has the same over-all depth as the array.

The row, or vertical, scanner is considered next. This scanner is more complicated than the column scanner because it must supply output pulses of variable amplitude repeatedly to a selected row conductor, during a horizontal scanning sequence, to set each of the 40-row transfluxors. A scanner using two-apertured transfluxors instead of simple cores was conceived for this purpose (see Fig. 15). Windings linking the large apertures of the transfluxors are connected in much the same manner as the windings of the horizontal scanner cores; the fully-set state of the transfluxor corresponds to the active or P state of the core. The output aperture of each transfluxor operates as a current-steering gate for the variable amplitude array setting current pulses supplied on line S. These pulses are steered to the output path associated with the fully set active transfluxor, but in being steered do not alter the state of this transfluxor. As a result, pulses will be repeatedly steered to the same channel until the active state is shifted to the next transfluxor, *etc.*

In Fig. 15 the circuits associated with the function of active-state transfer are drawn with double lines. Advance current pulses V_1 and V_2 serve the same purpose for this scanner as do H_1 and H_2 for the horizontal scanner, causing the active state to shift sequentially from the top to the bottom scanner transfluxor. The process is started by an input pulse applied to leg 2 of the first transfluxor, setting up the initial fully set state.

The transfer circuits also are utilized for a second purpose. It is necessary to first block a display transfluxor before setting to a new output level. This is done conveniently by using the interstage transfer currents to clear a row of the array at a time. The interstage output current pulse which, *e.g.*, causes the active state to shift from transfluxor 1 to transfluxor 2, blocks all the transfluxors of the first row of the array at the same time as it fully sets transfluxor 2. The setting pulses

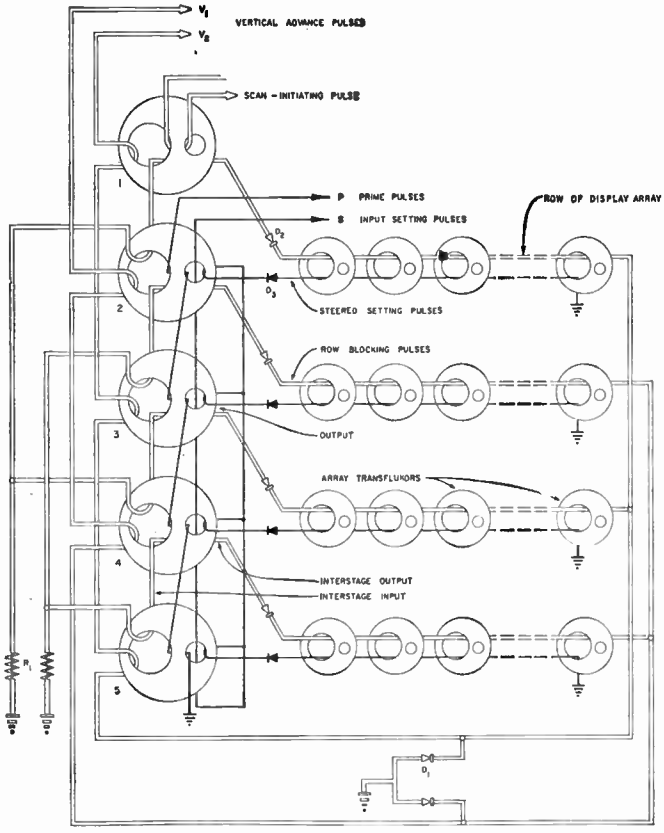

Fig. 15—Schematic diagram of magnetic vertical scanner. In this scanner transfluxors operate as gates for the setting pulses. Each gate is opened for one complete horizontal scanning period to transmit a row-setting burst of pulses to a selected row conductor. Setting pulses varying in amplitude over a range of ten to one can be steered through this device unaltered in shape.

TABLE IV
NUMERICAL DATA FOR THE VERTICAL SCANNER

Winding	Number of Turns	Current Pulse
Advance	10 (Large hole) 3 (Small hole)	6 amp, 30 μsec.
Interstage output	40	Triangular waveshape, 30 μsec. 0.75 amp for fully set array row, 1.5 amp for completely blocked array row
Interstage input	5	
Prime winding	4	0.3 amp, 5 μsec.
Setting current drive winding	5	
Setting current output winding	4	0.5 amp max., 8 μsec.

which follow are then steered via the output circuit of transfluxor 2 to set the elements of the first row to emit new levels of light.

The active state transfer circuits differ from those of the horizontal scanner because of the presence of diodes D_1 and resistances R_1. The diodes serve to shunt part of the vertical advance current away from the active interstage output circuit. The clamping action of these diodes makes the interstage coupling circuit appear to be closed. The resistances R_1 then are necessary to obtain a sufficiently small L/R time constant in the interstage circuit to allow the shift current to decay by the time the advance pulse is terminated, to insure complete switching of the active scanner transfluxor back to the inactive (N) state. It is necessary to use the shunting diodes because of the small advance-to-interstage output winding turns ratio chosen for the scanner transfluxors (see Table IV). It is possible to choose a turns ratio so as to eliminate these diodes and obtain purely current steered shift and blocking pulses.

The diodes D_2 in each interstage coupling loop serve to prevent spurious current flow in unselected coupling circuits. The negative voltage drop across one or the other resistance R_1 keeps all the diodes except that in the coupling circuit of the active transfluxor nonconducting while the advance pulses are applied.

The part of the circuit associated with steering the setting pulses S to the appropriate output path is schematically drawn using solid lines in Fig. 15. The setting pulses are applied as the drive pulses for the output apertures of the scanner transfluxors. On a separate line, prime pulses P, of opposite polarity and alternating with the setting pulses, are applied. These pulses are of constant, limited amplitude. In Fig. 15, the prime pulses are shown linking leg 2 of each transfluxor rather than the output aperture alone. This mode of connection is equivalent to the latter, but provides some additional protection against spurious unblocking. By priming on leg 2, the flux prefers to take the path via leg 3 rather than cause unblocking by taking the path via leg 1, because the former flux path is shorter. However, if the output path is too heavily loaded the priming flux may still be forced to go via leg 1, so that unblocking may still be possible.

To furnish setting pulses of variable amplitude, the current steering must function over a wide current range. For proper steering, the net magnetomotive force (driving mmf minus output mmf) applied to the output aperture must be sufficient to switch enough magnetic material to generate an output voltage exceeding the array row drop for the required duration of the setting pulse. The nature of the array drop is such that the flux required of the output of the scanner transfluxor varies linearly with setting current. As was pointed out in discussing the analog storage properties of the transfluxor, this type of variation is just what one observes in switching the flux around an aperture in a core of rectangular loop magnetic material of uniform thickness. To obtain proper steering, therefore, it is only necessary to provide a sufficiently large outside-to-inside diameter ratio for the material about the scanner transfluxor output aperture to handle the current range required. In practice, because of the lack of perfect hysteresis

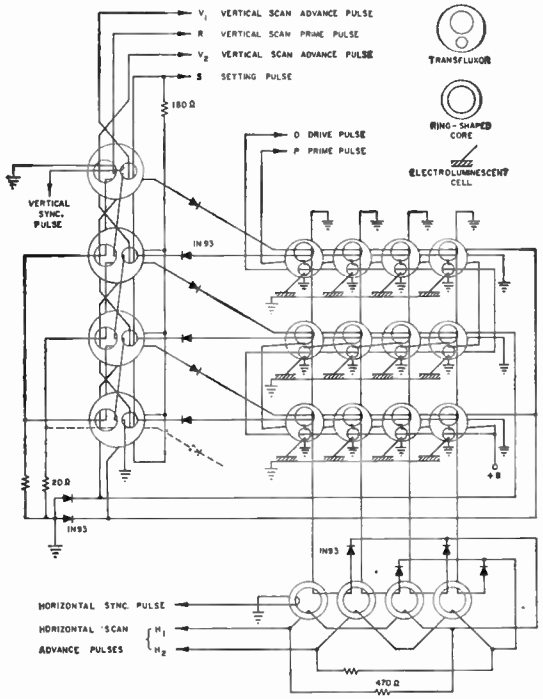

Fig. 16—Schematic diagram of display panel including scanners.

loop rectangularity, the range can be extended to smaller currents than expected. Using scanner transfluxors having the dimensions given in Fig. 3, a steering current range of ten to one is possible.

A 30-row vertical scanner was constructed for the 1200-element display. Like the horizontal scanner, it is mounted in the same frame and is the same depth as the array (see Fig. 12). Since a whole row of array transfluxors might be blocked at a time during a clearing operation, each scanner transfluxor must be provided with sufficient flux and number of interstage output turns to handle the back emf generated during this process. Accordingly, 17 of the same transfluxor cores (of 0.140-inch thickness) used in the array were used for each stage of the scanner. Numerical data regarding the number of winding turns, pulse amplitudes, and pulse shapes are given in Table IV.

A schematic diagram of the complete display system is given in Fig. 16. In this figure the array drive circuit is shown split into separate priming and driving circuits. This is convenient because all input pulses can then be of the same polarity, simplifying the pulser circuitry, and leg 2 priming, with improved protection against spurious unblocking, can be utilized. The vertical scanner schematic differs slightly from that in Fig. 15, in the use of "holding" windings linking the transfluxor-output apertures. On each transfluxor this winding is connected in series with the advance winding of the previous transfluxor. The application of an advance pulse, *e.g.*, V_1, then not only causes a current to flow in the coupling circuit of the active transfluxor, switching the following transfluxor to the active state, but also prevents this following transfluxor from being overset, by producing a mmf on leg 3 which "holds" the flux of this leg in the blocked direction.

Performance of the Array

The display device was tested by reproducing images from a television signal generated by a vidicon pickup camera modified for 30-line scan. The video signal was sampled 40 times per horizontal scan time interval to produce the level-setting pulses. Vertical and horizontal synchronizing pulses generated in the camera were used to initiate the scanners.

A photograph of a typical picture showing the half tone capabilities of the device is shown in Fig. 17. The resolution is limited, of course, because of the small number of elements used. The effect of this upon an image of a pattern can be seen from the photograph of Fig. 18.

The display has clearly demonstrated the performance to be expected from the ideal storage at every element provided by the transfluxor. Pictures with good contrast and adequate brightness are obtained. A low frame rate —15 per second—provides adequate illusion of continuous action and yet does not result in observable flicker as the picture is on nearly continuously. Each row emits light for 29/30 of each frame time and is off for only a maximum of 1/30 of this time while new levels are being set. In addition, only one row is off at a time. By interrupting the scanning process at the end of a frame, the last frame scanned can be viewed for as long a time as desired. The nonvolatile storage capability of the display permits storing a latent picture without stand-by power for any desired period of time. Pictures have been stored for several months after being set into the device.

The maximum brightness was 4 foot lamberts. It was limited by the power available from the energizing circuits, which were chosen to operate at a conservative rate of 12 kc. Using a greater pulse repetition rate, a brightness of 50 foot lamberts has been obtained.

The experimental model has shown that setting and blocking pulses as short as 1.5 μsec can be used with transfluxors fabricated of ferrite presently available in quantity. The possibility of shortening this time by an order of magnitude was investigated. Setting in 0.1 μsec was obtained with single elements consisting of three-hole transfluxors operated with a dc bias and intense setting pulses.[9]

The model has demonstrated also that making a number of uniform elements is not as serious a problem as

[9] J. A. Rajchman, "Principles of Core and Transfluxor Circuits," presented at International Symp. on Theory of Switching, Harvard University, Cambridge, Mass.; April, 1957. Also "Magnetic Switching," presented at Western Joint Computer Conf., Los Angeles, Calif.; May, 1958.

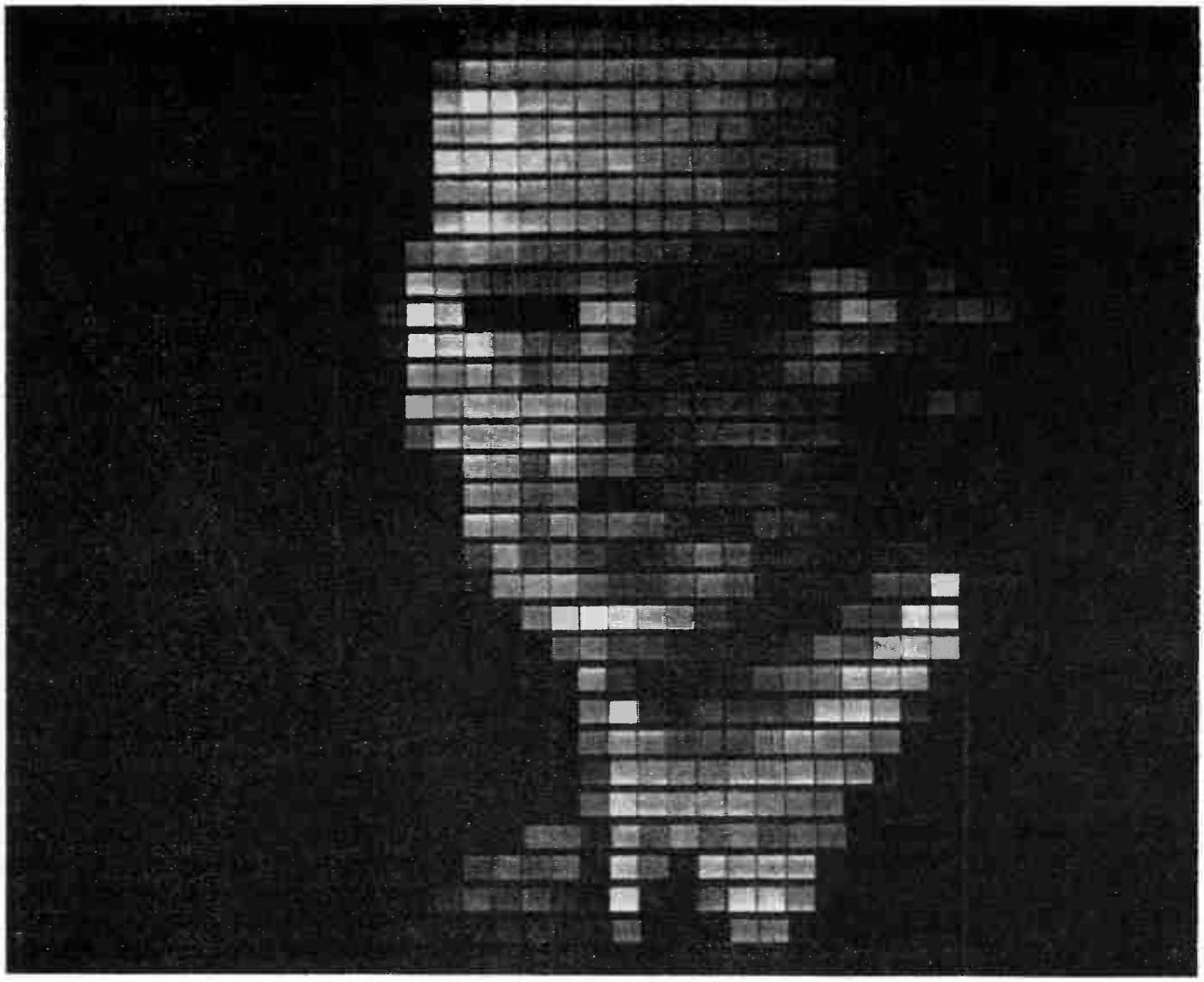

Fig. 17—Photograph of 30-line television image reproduced by the 1200-element display panel showing halftone capabilities.

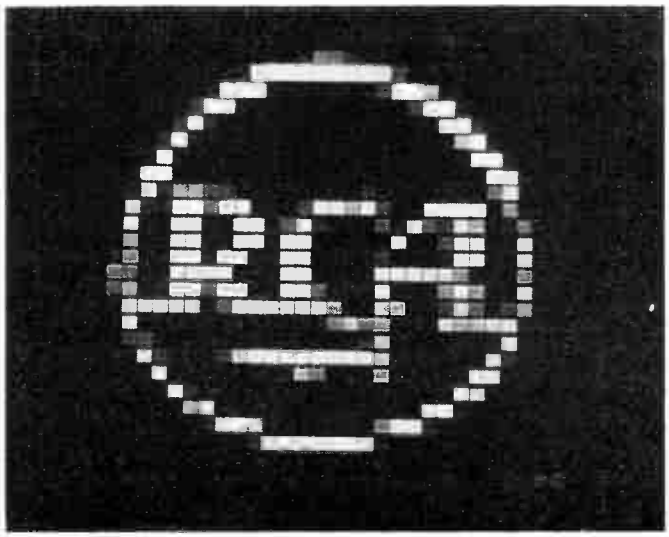

Fig. 18—Photograph of a pattern reproduced by the display panel.

could have been anticipated. Only simple pretesting and sorting of transfluxors and *EL*-cell bars sufficed to produce a satisfactorily uniform picture.

The working model has demonstrated the feasibility of producing a large picture with a flat device, comprising only solid state passive elements, by a method which provides nearly ideal performance. To the uniformity, good halftones and contrast, adequate brightness, lack of flicker, and versatile storage properties, should be added the possibilities of responding to coded electrical inputs, to be described below. However, these results are obtained at the price of a relatively complex fabrication technique. Also, the power consumption and associated electronic circuits are onerous.

Two means to overcome these difficulties—use of resonance and line-at-a-time storage—are discussed in following sections.

Resonant-Transformer Matching of Electroluminescent Cells

The relatively low driving efficiency which results when an electroluminescent cell is driven directly from the output winding of a controlling transfluxor is explained as follows. *EL* cells have, typically, power factors of less than 10 per cent and thus constitute, primarily,

capacitive impedances. Consequently, with short-pulse excitation, large capacitive cell current flows which reflects a large mmf into the transfluxor output flux path. The driving mmf must supply this mmf in addition to that required to reverse the output flux. The latter mmf cannot be too small a fraction of the former, for otherwise a relatively large output would be obtained when the transfluxor is blocked as a result of imperfect hysteresis loop rectangularity, and poor discrimination between blocked and set states would result. This means that relatively large transfluxors must be used which waste power in being driven. The drive current and output voltage also are considerably out of phase, and such drive is difficult to obtain efficiently from vacuum-tube or transistor current sources.

To improve the efficiency, the capacitive *EL*-cell current component can be resonated out with a low-loss inductor-transformer, as indicated in Fig. 19. A transformer having a core of low loss, low retentivity magnetic material is required for each transfluxor and *EL* cell. This transformer, although it is an additional component, actually simplifies the construction because only a single-turn link need be used to couple it to the transfluxor, eliminating the difficult-to-wind multiple turn output winding. The transformer can be of split-core construction, eliminating the need for toroidal windings. The *EL* cell in conjunction with the transformer and transfluxor, forms a resonant circuit which is tuned to the frequency of a sine-wave drive. The transfluxor reflects an inductance into the circuit which depends on its setting. This controllable inductance serves to tune the circuit in or out of resonance and adjust the *EL*-cell voltage.

In the most efficient mode of operation, there is resonance when the transfluxor is blocked. In this state, only small, reversible flux changes occur in the transfluxor and a small, but high-Q inductance is reflected into the circuit. In this condition of maximum *EL*-cell output the circuit operates at high efficiency. In the set state, some reversal of transfluxor output flux occurs and increases the reflected inductance as well as the power loss. The change in inductance detunes the resonant circuit, reducing the *EL*-cell output. The increased transfluxor loss compensates for the decreased power consumed by the *EL* cell, tending to maintain the input power constant. The drive source operates most efficiently under such constant-load conditions.

The resonant method of operation has an additional advantage. By using a large turns ratio on the transformer—one turn coupling the transfluxor and many turns driving the *EL* cell—a relatively small flux reversal in the transfluxor will control the output of the cell. A smaller transfluxor, dissipating less power and requiring less setting energy, can be used without greatly sacrificing on-off discrimination.

Experimental elements of the resonant type have been made which exhibit efficiencies better than 50 per cent. An element has also been made as small as

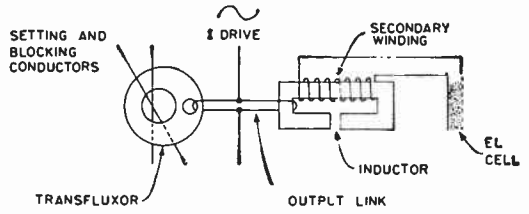

Fig. 19—Resonant transformer electroluminescent cell excitation circuit. The capacitance of the *EL* cell forms with the inductance of the transformer and transfluxor a resonant circuit which is tuned in or out of resonance with the ac driving frequency by the setting pulses. The transfluxor controls only real power components.

1/10×1/10×1/2 inch, for an *EL* cell measuring 1/10 inch square. The transformer for this element was constructed of coaxial cores of high-Q ferrite. The transfluxor was only 0.080 inch in outside diameter and had an output aperture of 0.008 inch.

Using resonance, the uniformity between elements must be good because each element is critically tuned. For this reason, the resonant type appears to be more suitable for on-off than for halftone displays.

Selective Addressing of the Array

Only sequential addressing, *i.e.*, scanning, has been considered thus far. For many applications, such as computer displays, it is desirable to select any element of the array from a coded address. Selective blocking as well as selective setting is desirable. As mentioned previously, selective blocking is most suitable for on-off displays, but most computer applications are of this type.

A coded input current steering magnetic switch to supply either a blocking or setting current pulse on the same conductor is shown in schematic form in Fig. 20. By causing clamp tube C to conduct and by energizing pulser A, a blocking current is generated in a selected line, whereas by energizing pulser D and causing clamp tube B to conduct, a setting pulse is generated on the same conductor. To operate the array by the coincidence of setting pulses, an identical switch is used for the other set of array conductors.

Binary coding is obtained by operating the current-steering cores in cascade.[8] As many cores are used in cascade as there are binary bits in the address; the cores are arranged in a conventional binary "tree" circuit. In operation, the current follows the one path through the tree for which none of the cores on that path have been set into P states by the coded input. On all other paths at least one core is set into a P state by the coded input and this core will be switched by the drive current, generating an output voltage which will cut off the series diode on that path. This type of operation is just the opposite of that described for the shift-register switches previously considered, for which only the core associated with the selected line was switched. This latter mode of operation is not possible with the cascaded binary switch, because in this switch half the

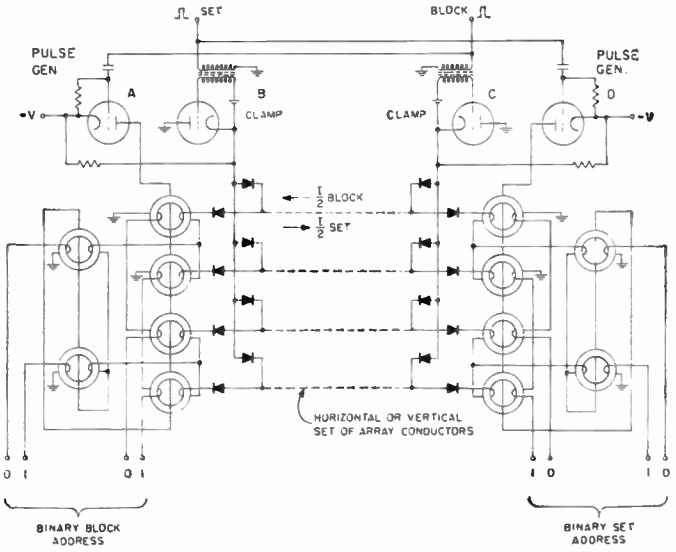

Fig. 20—Schematic diagram of a current steering magnetic switch with binary-coded input, for furnishing both coincident blocking and coincident setting pulses to an on-off type display.

cores are always set into P states by the coded input, and the switching of most of these would generate voltages which would force the current to split along spurious paths.

In the cascaded binary switch, each core must generate sufficient volt-second output to exceed the array conductor voltage drop for the time required to set an array transfluxor. This requirement arises because the switching of only a single core on an undesired path must generate sufficient voltage to hold the diode in that path cut off against the array conductor voltage drop, which is of the polarity to make this diode conduct. For this reason, and because so many cores are switched, this type of switch is not the most efficient.

Display of Fixed Patterns

A very simple transfluxor controlled display device can be made for displaying predetermined patterns such as alphanumeric characters (see Figs. 21 and 22). A separate setting winding is provided for each of the desired characters and each winding is wired through the array of transfluxors tracing out the desired pattern. A single current pulse on any of these windings will set the corresponding transfluxors and cause the selected character to be displayed. An experimental model having a 10×10 array of incandescent-lamp elements and supplied with 27 setting windings was built. The lamps were coupled to the transfluxors with single-turn windings. Because the low impedance light sources were well matched to the transfluxors, the efficiency was greater than 30 per cent. A photograph of the operating device is shown in Fig. 22.

The simplicity, versatility and efficiency of this device may make it useful for relatively large boards capable of displaying a number of characters.

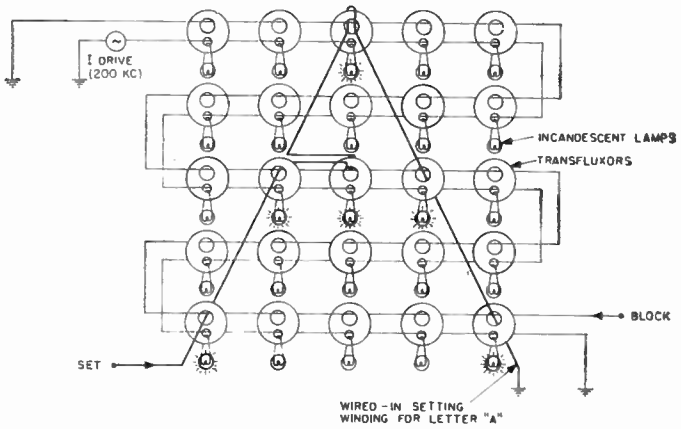

Fig. 21—Schematic diagram of a device which was built to display alphanumeric symbols. A separate wired-in setting winding is provided for each character. Incandescent lamp light sources coupled to transfluxors by single turn output windings are used.

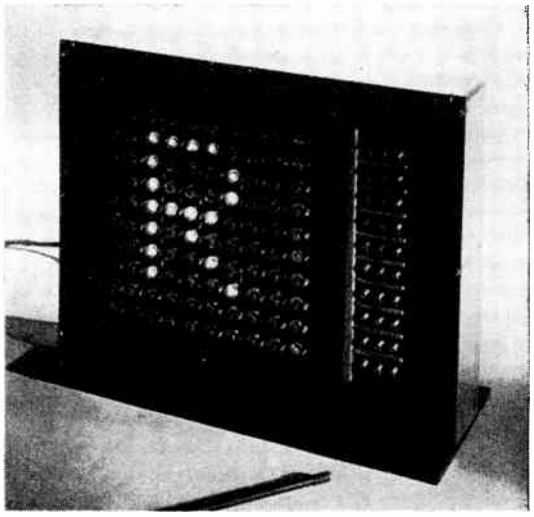

Fig. 22—Photograph of the alphanumeric display in operation.

Line-At-A-Time Storage and Excitation

As mentioned in the Introduction, storage is necessary with electroluminescent displays to obtain sufficient brightness and picture contrast. The use of a transfluxor with each element affords complete storage, but requires a large number of units. A method of sharing storage elements between EL cells to reduce the number of transfluxors required is to use a line-storage system such as that shown schematically in Fig. 23. In this system, only a single row of transfluxors is used. The display levels are stored for only one row of EL cells at a time. A particular row of cells is selected by the coincidence of output voltage pulses of various amplitudes supplied by the transfluxors driving column conductors and voltage pulses of constant amplitude applied to one selected row conductor. Every EL cell of the selected row is excited simultaneously, in accordance with the set levels, during one-row scanning period. This period

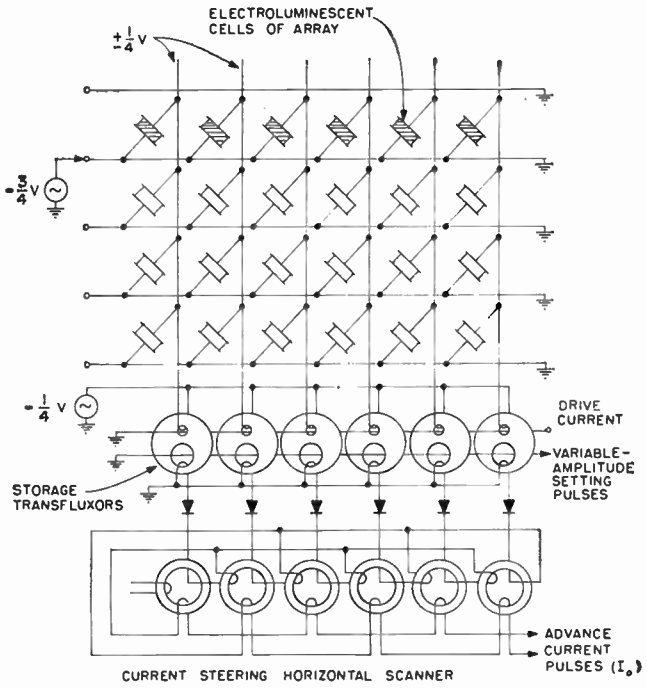

Fig. 23—Simplified schematic diagram of a line-at-a-time excitation system. Each electroluminescent cell of a preselected row is excited simultaneously by the coincidence of voltage pulses applied to the row with voltage pulses applied to all the columns simultaneously by transfluxor storage elements. A magnetic switch is used to scan the transfluxors.

may be sufficient to enable useful light output to be generated if it occurs sufficiently frequently, *i.e.*, if the number of rows in the frame is not too great. Typically, 200 to 300 rows can be excited in this manner to obtain a brightness of 1 or 2 foot lamberts.

Coincident *EL*-cell selection with fair picture contrast is possible with this system because a given cell is disturbed relatively less frequently by half-selecting voltage pulses than it is in a system without storage. The contrast can be improved further by arranging that each transfluxor supply output voltage pulses which range between $+\frac{1}{4}V$ and $-\frac{1}{4}V$, where V is the maximum *EL*-cell pulse voltage applied, and that the selected row conductor supply voltage pulses of $-\frac{3}{4}V$. With this system, voltage pulses applied to the cells of the selected row range between $V/2$ and V, which is sufficient to give almost complete on-off operation, yet the cells of unselected rows never are subjected to voltage pulses greater than $V/4$ in magnitude. Such small voltage pulses produce little light output, even when frequently applied. The contrast can be improved still further by inserting in series with each *EL* cell a nonlinear resistance. Resistances for which the current varies as the fourth to sixth or even higher power of the voltage can be made using powders of SiC or CdS embedded in epoxy plastic or ceramic materials.

Setting of the transfluxors can be accomplished by applying variable-amplitude setting pulses to the whole row of transfluxors in coincidence with pulses of constant amplitude applied to each transfluxor in succession. The latter pulses can be supplied by a current-steering switch, as indicated in Fig. 23.

In illustrating the basic principles of the system, only a single row of storage transfluxors has been considered. In actual practice it is not convenient to simultaneously set and derive the output from a single row of transfluxors, particularly when the input display levels are entering the system at a constant rate. Instead, two rows of transfluxors can be used. One row is set and the other excited during one line-scan period, while during the next period the roles of the rows are reversed. Blocking of the transfluxors can be done at the instant of reversal.

Conclusion

The working model has demonstrated for the first time that it is possible to display pictures by electroluminescence controlled in response to an electrical input signal. This demonstration of feasibility, and the various related studies which have been made, permit the following evaluation to be made of the principle of controlling arrays of discrete electroluminescent cells or other light sources by magnetic means.

The transfluxor ideally provides precisely the storage and switching functions that are required at every element of a display panel: it stores the level of display information, delivers power to the light source in accordance with that level, and acts as its own local switch in the process of scanning or selectively addressing the array. The addressing itself is performed very conveniently by cores and other transfluxors which make possible magnetic switching techniques of great versatility, useful for television-type scans with or without line or element interlace, selective or random addressing to any element, coded addressing, etc.

The main shortcoming of the system of transfluxor control of electroluminescent cells is the mismatch between the relatively low impedance of the magnetic device and the relatively high impedance of the cell. Drive by sharp pulses having high-frequency components solves the problem directly and leads to reliable operation without uniformity difficulties, but requires winding several turns through a small hole in each transfluxor and is somewhat wasteful of driving power. Drive through a resonant transformer permits easier winding and is more efficient in driving power, but presents problems of uniformity. The best solution would be provided by a new type of electroluminescent cell which would operate with a few volts, rather than hundreds of volts. There does not seem to be any fundamental barrier to forbid the hope for such a solid-state phenomenon.

In the present state of the art, there are a number of applications for magnetically controlled display panels.

Reproduction of television images of conventional resolution is technically possible, particularly with the compromise system using row storage, but would be very expensive and seems to be economically unjustifiable. On the other hand, by using this system very large displays, tens of feet in size, can be made relatively easier than by any other means. A large display, located in a central station, would be most useful for displaying information received from many distant locations. Transfluxor control can be applied also to small displays, particularly in systems requiring storage. An example is the board for displaying alphanumeric characters. For these displays, incandescent lamps can be used for locations having an ambient illumination too great for electroluminescence.

The inherent storage and switching properties of the display array also permit great flexibility in the choice of the system of gathering, transmitting, coding and decoding and displaying the information, either through alphanumeric or other symbolic or through actual pictorial representation. Element switching rates can be as high as several megacycles or, with the same elements, as low as needed for manual operation. There are many military and commercial applications for displays of this type, involving information gathered by radar, sonar, teletype or other means and transmitted by telephone or radio links. It is worth noting also that color can be added easily because of the inherent cellular structure of the display and the availability of electroluminescent materials emitting different colors.

Acknowledgment

The development of the techniques of electroluminescent cell fabrication was due to R. C. Ballard. Other members of the RCA Laboratories also assisted in the project. In particular, J. Walentine aided in the mechanical construction and J. Teza contributed to the circuit construction and testing.

Incoherent Scattering of Radio Waves by Free Electrons with Applications to Space Exploration by Radar*

W. E. GORDON†, MEMBER, IRE

Summary—**Free electrons in an ionized medium scatter radio waves weakly. Under certain conditions only incoherent scattering exists. A powerful radar can detect the incoherent backscatter from the free electrons in and above the earth's ionosphere. The received signal is spread in frequency by the Doppler shifts associated with the thermal motion of the electrons.**

On the basis of incoherent backscatter by free electrons a powerful radar, but one whose components are presently within the state of the art, is capable of:

1) measuring electron density and electron temperature as a function of height and time at all levels in the earth's ionosphere and to heights of one or more earth's radii;
2) measuring auroral ionization;
3) detecting transient streams of charged particles coming from outer space; and
4) exploring the existence of a ring current.

The instrument is capable of

1) obtaining radar echoes from the sun, Venus, and Mars and possibly from Jupiter and Mercury; and
2) receiving from certain parts of remote space hitherto-undetected sources of radiation at meter wavelengths.

* Original manuscript received by the IRE, June 11, 1958; revised manuscript received, August 25, 1958. The research reported in this paper was sponsored by Wright Air Dev. Ctr., Wright-Patterson Air Force Base, O., under Contract No. AF 33(616)-5547 with Cornell Univ.

† School of Elec. Eng., Cornell Univ., Ithaca, N. Y.

Introduction

FREE electrons in an ionized medium scatter radio waves incoherently so weakly that the power scattered has previously not been seriously considered. The calculations that follow show that this incoherent scattering, while weak, is detectable with a powerful radar. The radar, with components each representing the best of the present state of the art, is capable of:

1) measuring electron density and electron temperature as a function of height and time at all levels in the earth's ionosphere and to heights of one or more earth's radii;
2) measuring auroral ionization;
3) detecting transient streams of charged particles coming from outer space; and
4) exploring the existence of a ring current.

The capabilities listed above depend on the incoherent scattering of radio waves by free electrons. In addition the instrument is capable of:

1) obtaining radar echoes from the sun, Venus, and Mars and possibly from Jupiter and Mercury; and

2) receiving from certain parts of remote space hitherto-undetected sources of radiation at meter wavelengths.

The paper is divided into three parts:

1) radio wave scattering by free electrons,
2) applications of incoherent scattering to the exploration of the earth's upper atmosphere and surrounding space by radar, and
3) capabilities of the radar for additional exploration of space.

A single free electron scatters some of the energy associated with an incident radio wave, and the effect is described in terms of a scattering coefficient or cross section (Section I-*A*). Each free electron in an ionized medium containing many free electrons scatters some of the energy associated with a radio wave propagating through the medium. The scattered waves have coherence, limited coherence, or incoherence depending on certain conditions of wavelength and geometry. Coherent scattering is the standard problem of refraction of radio waves by an ionized medium. Limited coherence, which means that only the scattered waves from limited subvolumes of the ionized medium are coherent, is the problem propularly known as "ionospheric scatter." Complete incoherence of the waves scattered by free electrons, or simply incoherent scattering, and the conditions under which it is important are the subjects of principal interest in Section I-*B*. The incoherent scattering coefficient of free electrons in an ionized medium is derived in Section I-*C*. Due to the thermal motion of the electrons, the frequencies of the scattered waves are Doppler shifted from the incident wave frequency. The width of the spectrum of the scattered signal is therefore a measure of the electron temperature (Section I-*D*).

Incoherent scattering by free electrons is applied in Section II-*A* to the earth's upper atmosphere and surrounding space to show that electron density and electron temperature as functions of height and time can be measured with satisfactory resolutions in height and time by a powerful radar. The characteristics of the radar are given in Section II-*B*, along with its capability of measuring electron densities in and above the ionosphere, in aurora, in transient streams of charged particles in space, and in a ring current. Incoherent scattering at angles other than in the back direction is examined in Section II-*C*, and the characteristics are estimated of a system capable of producing detectable signals scattered in the F region of the ionosphere to distances of 3,000 kilometers.

The radar required to make the measurements described above has components selected for maximum sensitivity but uses techniques that are currently within the state of the art. The radar is capable of obtaining echoes from the sun and some planets (Section III-*A*). The receiving portion of the radar is capable of receiving from certain parts of remote space hitherto undetected sources of radiation at meter wavelengths (Section III-*B*).

I. Radio Wave Scattering by Free Electrons

A. Scattering Coefficient of a Single, Free Electron

The scattering coefficient of a single, free electron, is

$$\sigma_e = \left[\frac{\mu e^2}{4\pi m} \sin \psi\right]^2$$

$$\sigma_e = 8 \times 10^{-30} \sin^2 \psi \text{ (meters)}^2, \quad (1)$$

where all units are MKS; μ is the permeability of the medium ($4\pi \times 10^{-7}$); e and m are the charge and mass of the electron; ψ is the polarization angle—the angle between the direction of vibration of the incident field and the direction from the scatterer to the receiver; and σ_e is the power scattered into a unit solid angle per unit incident power density, per electron.

The scattering coefficient, it should be noted, does not depend on wavelength, but it does depend on aspect only in the usual dipole radiation sense as reflected in the polarization factor $\sin^2\psi$.

B. Scattering by Free Electrons in an Ionized Medium

To relate the problem of incoherent scattering by free electrons to other radio wave problems involving free electrons, consider first an ionized, but macroscopically neutral, medium. The criterion for distinguishing between the cases of incoherent and coherent scattering by free electrons can be stated in three interrelated ways, in terms of a Doppler shift of the radio frequency and the electron collision frequency, the spectrum of the irregularities of the medium, and a characteristic scale of the radio problem and the mean free path of the electrons. To emphasize the distinction, the three versions are presented below.

1) If the Doppler shift Δf of the radio frequency f due to scattering by a moving electron is larger than the collision frequency ν of the electrons ($\Delta f > \nu$), then the unshifted frequency and the Doppler shifted frequency will beat with one or more cycles, and the energy associated with an incident wave now appears in scattered waves that differ in frequency and are, therefore, incoherent. In terms of time rather than frequency, one says that the duration (time between collisions) of the scattered wavelets is long enough so that the difference in frequencies is apparent from one or more beats between the waves.

If the Doppler shift is smaller than the collision frequency ($\Delta f < \nu$), the duration of the wavelet at the Doppler shifted frequency is so short that it is substantially in phase (coherent) with an unshifted wave and the effect of the individual electron is best viewed macroscopically.

2) The scattering of radio waves in a medium containing irregularities is frequently discussed[1] in terms of the spectrum of the irregularities (mean square fluctua-

[1] R. Bolgiano, Jr., "The role of turbulent mixing in scatter propagation," IRE Trans. on Antennas and Propagation, vol. AP-6, pp. 161–168; April, 1958.

tions as a function of the size of the irregularity). The spectrum may have one or more subranges of sizes in which the spectrum has a characteristic shape. The spectrum of the fluctuations at the smallest sizes, as viewed macroscopically, decreases very rapidly with increasing wave number (decreasing size). This part of the spectrum, the viscous dissipation range, has previously represented the lower limit of sizes of interest. However, continuing toward larger wave numbers (smaller sizes) and replacing the macroscopic view by a microscopic view, one finds that the medium is discontinuous at a size of the order of the distance over which an electron is free to move (mean free path). The spectrum should be flat for a range of smaller sizes, suggesting no wavelength dependence of the scattering.

3) The problem of a radio wave propagating in a medium has associated with it a characteristic scale that indicates the element of length in the medium that is significant. The characteristic scale L depends on the wavelength λ, and the angle θ between the incident wave direction and the direction of the reradiated (scattered) wave.

$$L = \frac{\lambda}{2 \sin \theta/2} \tag{2}$$

If the characteristic scale is large compared to the mean free path ($L > l$), the effect of an individual electron is minimized by interaction (collisions); and the net effect of the electrons appears as a macroscopic change in the dielectric constant of the medium. If the characteristic scale is small compared to the mean free path ($L < l$), the macroscopic approach is replaced by a microscopic approach; and the effects of the individual electrons are considered.

The characteristic scale associated with the problem of refraction in an ionized medium is usually very large, since the angle θ is zero or very close to zero. The standard solutions of the refraction problem consider the effects of the electrons macroscopically, although refraction may be interpreted as all the individual electrons scattering coherently. The electron density N for the refraction problem is averaged over volumes whose dimensions are small compared to the scale L but, of course, large compared to the mean free path l.

In the "ionospheric scatter" problem[2] the characteristic scale is large compared to the mean free path of the electrons at, or just below, the E-region of the ionosphere. The macroscopic approach is employed in the solution, and the scattering coefficient depends on the spatial Fourier component of order L of the mean square fluctuation $\overline{(\Delta N)^2}$ of electron density. In terms of the effect of the individual electrons, this may be interpreted as coherent scattering by neighboring electrons, that is, electrons whose separations are limited to L. In this sense the scattered waves have limited coherence.

C. Incoherent Scattering Coefficient of Free Electrons

The free electrons in an ionized medium must be considered individually in a radio problem for which the characteristic scale is small compared to the mean free path of the electrons. The condition ($L < l$) is satisfied, for example, at a wavelength of 1.5 meters for backscatter ($\theta = \pi$ and $L = \lambda/2$) from the earth's ionosphere above 100 kilometers. Stated in terms of approach 1) above, the energy associated with the incident wave of frequency f is spread over a frequency band due to the Doppler shift produced by the thermal motion of the electrons. The Doppler shift Δf produced by an electron having a component v of velocity in the appropriate direction (in the plane containing transmitter, receiver, and scatterer and normal to the bisector of the scattering angle θ) is

$$\frac{\Delta f}{f} = \frac{2v}{c} \sin \theta/2, \tag{3}$$

or with 2)

$$\Delta f = \frac{v}{L}. \tag{4}$$

The scattered waves forming the spectrum over which the energy is spread are incoherent, since they have different frequencies.

If σ_e is the scattering coefficient of a single electron, then the scattering coefficient per unit volume of N electrons per cubic meter each radiating incoherently is found by adding the powers scattered by each electron. The incoherent scattering coefficient is

$$\sigma_N = \sigma_e N \text{ (meter)}^{-1}, \tag{5}$$

where σ_N is the power radiated into a unit solid angle per unit incident power density per unit volume.

D. Electron Temperature

Since the Doppler shifts described above result from the thermal motion of the electrons, it is possible to deduce the electron temperature by measuring the width of the spectrum of frequencies returned from a given volume. The spread of frequencies in backscatter from the ionosphere will be of the order of 100 kilocycles at an operating frequency of 200 megacycles.

II. Applications of Incoherent Scattering to the Exploration of the Earth's Upper Atmosphere and Surrounding Space by Radar

A. Electron Density Distribution with Height above the Earth

One can measure from the ground with suitable resolution in height and time the electron density and electron temperature in, between, and above the regular ionospheric layers of the earth's atmosphere, as well as

[2] D. K. Bailey, R. Bateman, and R. C. Kirby, "Radio transmission at VHF by scattering and other processes in the lower atmosphere," Proc IRE, vol. 43, pp. 1181–1231; October, 1955.

linearly, the signal-to-noise ratio of Fig. 1 can be linearly corrected for other values of these parameters.

Fig. 1 deserves study in detail. Before considering the detail, however, some general remarks are needed. The radar is powerful, but megawatt transmitters are available. The antenna is very large; but since the signal-to-noise does not depend on wavelength, the large area may be obtained with coarse mesh and moderate tolerances by selecting the longest wavelength (about 1.5 meters) consistent with cosmic noise limitations. The antenna may be fixed and pointed vertically.

E-Region of the Ionosphere: An electron density of 10^9 per cubic meter at a height of 100 kilometers is readily detected (signal-to-noise of 30) by the radar (Fig. 1) with a 0.1 millisecond pulse. While longer pulses produce higher signal-to-noise ratios (or permit smaller antenna areas, or transmitter powers), they suffer from poor height resolution. The 0.1 millisecond pulse averages over 15 kilometers of height, and larger intervals seem undesirable, especially at the lower ionospheric heights.

Electron densities as low as 10^8 per cubic meter may be detected below the E-region with the 0.1 millisecond pulse on the basis of incoherent scattering, but this may be masked by scattering of the limited coherence type. In the height interval 100 to 200 kilometers, electron densities greater than 10^8 per cubic meter will be detectable.

The height above which the macroscopic approach using limited coherence (coherent scattering by neighboring electrons) ceases to be important depends on the scale L as described in section I-*B*. For backscatter, $L=\lambda/2$, and the macroscopic approach can be neglected when the mean free path l is of the order of or greater than $\lambda/2$. For a frequency of 200 megacycles ($\lambda/2=\frac{3}{4}$ meter) this condition occurs for heights above 100 kilometers and one therefore expects only incoherent scattering above this height.

F-Region of the Ionosphere: A typical F-layer maximum electron density of 10^{12} per cubic meter will produce a signal-to-noise in excess of 1,000 with the 0.1 millisecond pulse at a height of 300 kilometers. Note that the F-layer maximum is detectable with a smaller antenna, say 30 meter diameter instead of 300 meter diameter, other parameters being the same.

In the lower F-region (200 to 300 kilometers) electron densities as low as 10^9 are detectable with the 0.1 millisecond pulse. Above 300 kilometers (but below 1,000 kilometers) 10^{10} electrons per cubic meter are detectable with the 0.1 millisecond pulse. Increasing the pulse to 1.0 millisecond, one is able to detect electron densities as low as 10^9 up to about 1,700 kilometers. The 1.0 millisecond pulse averages over a height interval of 150 kilometers, but this seems acceptable at these heights.

The Region $\frac{1}{6}$ to 1 Earth's Radii: The region of interest extends from about 1,000 to 6,000 kilometers above the ground. By lengthening the pulse to 10 milliseconds one can detect in this range of heights an electron density as low as 10^9 electrons per cubic meter.

Transient Streams of Charged Particles: Streams of charged particles originating in outer space and flowing near the earth may or may not be detected, depending on their range from the radar and electron density as detailed in Fig. 1. The prospects are exciting.

Stanford "Daytime Aurora Echoes":[3] Recent reports of Stanford Research Institute observers describe diffuse echoes from the auroral zone during the daytime at 400 and 800 megacycles with little wavelength dependence, in contrast to the aspect sensitive, high wavelength dependence nighttime auroral echoes. The radar, I understand, had approximately the following characteristics: transmitter power, 50 kilowatts; antenna diameter, 20 meters; pulse length, one millisecond; noise figure, 10 (estimated). Incoherent scattering (8) produces a signal-to-noise ratio of 10 for an echo from 10^{12} electrons per cubic meter at a range of 300 kilometers. Notice that (8) predicts no wavelength dependence of the incoherent scattering.

Ring Current: If the ring current exists and its characteristics (distance, electron density) are estimated, the possibility of detection by this radar can be determined from Fig. 1.

C. Scattering at Angles Other Than the Back Direction

Scattering by an electron has a dipole pattern as indicated by the factor $\sin^2\psi$. One therefore expects the same amount of power as that scattered in the back direction to be scattered in other directions for which the dipole factor is one. Hence separating the receiver from the transmitter does not affect the scattered power per unit volume. The scattering volume, however, now determined by the intersection of transmitting and receiving beams rather than pulse length and radar beam, is altered from

$$\frac{\pi}{4}\frac{\lambda^2 r^2}{A}h \text{ to } \left(\frac{\lambda r}{A^{1/2}}\right)^3 \frac{1}{\sin\theta},$$

where the transmitting and receiving antenna areas are each A; the volume is located symmetrically a distance r from transmitter and receiver; and the scattering angle is θ. With this volume filled with N electrons per cubic meter

$$P_R = \frac{P_T A^{1/2}\lambda}{r\sin\theta}\sigma_N. \tag{9}$$

The receiver noise power is given by (7), and the signal-to-noise ratio is

$$\frac{P_R}{N_R} = \frac{P_T A^{1/2}\lambda\sigma_N}{r\sin\theta FKTB}. \tag{10}$$

[3] R. I. Presnell, R. L. Leadabrand, R. B. Dyce, L. T. Dolphin, and A. M. Peterson, "398 mc auroral echoes obtained at College, Alaska," paper presented at URSI meeting, Washington, D. C.; April, 1958.

F-Region Scattering: A megawatt transmitter at $1\frac{1}{2}$ meter λ, 20 meter dishes, and a noise figure of 2 give a signal-to-noise ratio of one in a 100 kilocycle bandwidth at a separation ($2r$) between transmitter and receiver of 3,000 kilometers on the basis of incoherent scatter [$L=0$(meters) $<l=0$(kilometers)] in the F region of the ionosphere (300 kilometers height, 10^{12} electrons per cubic meter).

III. Capabilities of the Radar for Additional Exploration of Space

A. Solar System

If the radar described in Fig. 1 is modified by reducing the receiver bandwidth to two kilocycles (one millisecond pulse), it is capable of obtaining an echo from Venus and Mars and possibly from Mercury and Jupiter at their closest approach to the earth. Without pulse integration to improve the signal-to-noise ratio, the ratios are 50, 1, 0.3, and 0.1 for these planets, respectively, assuming that their radar cross sections are one-tenth of their actual cross sections. In the case of Jupiter the round-trip travel time of the pulse is about 70 minutes, during which time the earth rotates about 17.5 degrees. Feed motion in the fixed antenna does not provide 17.5 degrees of beam swinging, so the Jupiter observation, while possible from the standpoint of system sensitivity, is possible only with more beam mobility.

The same calculation applied to the sun gives a signal-to-noise ratio (without pulse integration) of 100, with proper allowance for the high level of solar noise. Although the mechanism[4] by which an echo might be obtained from the sun must be more complicated than that associated with the planets, it seems very likely that an echo will be obtained.

For a small meteor, taken as a sphere of radius $a<\lambda$ with finite conductivity, the ratio of the scattering cross section to the physical cross section is

$$\frac{\sigma}{\pi a^2} = 6.2\times 10^3\left(\frac{a}{\lambda}\right)^4. \tag{11}$$

The power received from a single meteor is

$$P_R = \frac{P_T A^2\sigma}{4\pi\lambda^2 r^4} \alpha \left(\frac{a}{\lambda}\right)^6. \tag{12}$$

A meteor at a range of 100 kilometers produces a signal-to-noise ratio of ten in a bandwidth of one kilocycle for the radar (Fig. 1) when the radius is

$$a \doteq 5 \text{ millimeters},$$

and meteors of this size will enter the beam very infrequently.

If the beam is filled with $n(a)$ meteors per unit volume of radius a, the received power is

$$P_R = \frac{P_T A h}{4\pi r^2}\int n(a)\sigma da \;\alpha \int n(a)a^6 da. \tag{13}$$

Present estimates[5] increase $n(a)$ by an order of magnitude every time the radius is halved. At this rate only the largest meteors contribute significantly, and the net effect of meteor echoes on the radar of Fig. 1 is negligibly small, although the ionization produced by the meteors at heights near 100 kilometers should be readily observed.

B. Further Radiation Detection

The collecting area of the radar antenna combined with a sensitive receiver provides a capability of detecting weak sources of radiation at meter wavelengths from limited parts of the sky. The limitation arises from the antenna beamwidth and the fact that the antenna reflector is fixed. Flux densities smaller by two or three orders of magnitude than those reported (10^{-25} watts meter^{-2} cycle^{-1}) in the Cambridge survey of radio stars[6] are observable. The Cambridge survey (at $\lambda=3.4$ meters) lists, for example, 82 sources in the declination range 18 to 24 degrees (about 2,000 square degrees of sky). Only four of these sources have flux densities in excess of 10^{-24} watts meter^{-2} cycle^{-1}. The antenna located at about north latitude 20 degrees and pointed vertically, but with some beam swinging available by moving the feed, could check the strength and position of many of the listed sources and add weaker sources to the list.

Acknowledgment

The discussion and suggestions of my colleagues, H. G. Booker, M. H. Cohen and B. Nichols, are gratefully acknowledged.

[4] F. J. Kerr, "On the possibility of obtaining radar echoes from the sun and planets," Proc. IRE, vol. 40, pp. 660–666; June, 1952.

[5] O. G. Villard, Jr., V. R. Eshleman, L. A. Manning, and A. M. Peterson, "The role of meteors in extended-range VHF propagation," Proc. IRE, vol. 43, pp. 1473–1481; October, 1955.

[6] J. R. Shakeshaft, M. Ryle, J. E. Baldwin, B. Elsmore, and J. H. Thomson, "A survey of radio sources between declinations $-38°$ and $+83°$," *Memoirs of the Royal Astron. Soc.*, vol. 67, p. 97; 1955.

Analysis of Millimicrosecond RF Pulse Transmission*

MAX P. FORRER†, SENIOR MEMBER, IRE

Summary—An analysis of millimicrosecond RF pulse transmission through uniform systems is presented. Quadratic approximations for the complex propagation constant are used, and a Gaussian pulse envelope is assumed. Employing Fourier transformation, the received waveforms are obtained for the general case of lossy, dispersive systems. The results are discussed and illustrated separately in terms of pulse distortions due to dispersion, due to losses and due to bandwidth limitations.

Introduction

With the increasing perfection of microwave broadband amplifiers and associated transmission components, practical applications of millimicrosecond RF pulse techniques are becoming more and more attractive. Among potential fields of application are short-pulse radar equipment and wide-band communication systems. Millimicrosecond pulse techniques have been successfully employed for waveguide testing.[1,2] The capability of generating and handling such pulses at high repetition rates of several hundred megacycles per second furthermore has opened up the possibility of designing logical circuitry for digital computers of exceedingly high speed. Several microwave circuits suitable for the generation of millimicrosecond RF pulses have been described in the literature.[3–5]

Analytical work in this field was recently published by Elliott,[6] who computes the degradation of an initially rectangular pulse envelope due to dispersion in a lossless waveguide. Gajewski[7] investigates the influence of skin effect on pulse propagation in waveguides. Wigington and Nahman[8] published a transient analysis, including experimental results, on coaxial cables with skin losses.

The present paper is characterized by the assumption of a transmitted pulse with Gaussian envelope. This is a realistic approximation of the pulse shapes actually realizable in the millimicrosecond range and has the additional advantage that the mathematical analysis yields results in closed form. The following theory is applicable to uniform microwave transmission systems and will relate pulse shapes (time functions) with the CW properties of the transmission system (frequency functions). A generalization of the theory for certain linear, two-port networks is possible.

General Analysis

A transmitted waveform $f(t)$, which may be taken to be proportional to voltage or electric field is assumed to be generated at the $z=0$ cross section of a uniform microwave transmission system. This system is infinitely long in the z-direction, and it is desired to calculate the received waveform $g(t, z)$ at a distance z. The transmitted waveform is expressed by an envelope function $f_1(t)$ and a carrier time function $f_2(t)=e^{j\omega_0 t}$, so that

$$f(t) = f_1(t)e^{j\omega_0 t}. \tag{1}$$

According to the Fourier theorem, the envelope function $f_1(t)$ is related to its spectrum $F_1(\omega)$ by

$$f_1(t) = \int_{-\infty}^{\infty} F_1(\omega)e^{j\omega t}d\omega, \tag{2}$$

so that (1) becomes

$$f(t) = \int_{-\infty}^{\infty} F_1(\omega)e^{j(\omega_0+\omega)t}d\omega. \tag{3}$$

Here, the transmitted waveform is expressed as a superposition of an infinite number of continuous sinusoidal oscillations, with amplitudes $F_1(\omega)$ and with frequencies $\omega_0+\omega$. The CW properties of microwave transmission systems are commonly described by a complex propagation constant

$$\gamma = \alpha + j\beta. \tag{4}$$

Each component oscillation of (3) thus gives rise to a wave propagating along z according to $e^{-\gamma z}$, so that the total received time function becomes

$$g(z, t) = \int_{-\infty}^{\infty} F_1(\omega)e^{j(\omega_0+\omega)t-\gamma z}d\omega. \tag{5}$$

The propagation constant γ may change with frequency in various ways depending upon the transmission system used. In order to obtain a general theory, the quantities α and β are expanded in Taylor series. Usually, the frequency variation of α and β are sufficiently smooth over the frequency range of interest so that they can be approximated by the first three terms of the Taylor series.

* Original manuscript received by the IRE, April 24, 1958; revised manuscript received, August 25, 1958. The analysis reported here was sponsored by the Info. Systems Branch of the Office of Nav. Res. under Contract NONR 2127(00).

† General Electric Microwave Lab., Palo Alto, Calif.

[1] A. C. Beck, "Microwave testing with millimicrosecond pulses," IRE TRANS. ON MICROWAVE THEORY AND TECHNIQUES, vol. MTT-2, pp. 93–100; April, 1954.

[2] A. C. Beck, "Measurement techniques for multimode waveguides," IRE TRANS. ON MICROWAVE THEORY AND TECHNIQUES, vol. MTT-3, pp. 35–42; April, 1955.

[3] C. C. Cutler, "The regenerative pulse generator," PROC. IRE, vol. 43, pp. 140–148; February, 1955.

[4] A. C. Beck and G. D. Mandeville, "Microwave traveling-wave tube millimicrosecond pulse generators," IRE TRANS. ON MICROWAVE THEORY AND TECHNIQUES, vol. MTT-3, pp. 48–51; December, 1955.

[5] C. A. Burrus, "Millimicrosecond pulses in the millimeter wave region," *Rev. Sci. Instr.*, vol. 28, pp. 1062–1065; December, 1957.

[6] R. S. Elliott, "Pulse waveform degradation due to dispersion in waveguide," IRE TRANS. ON MICROWAVE THEORY AND TECHNIQUES, vol. MTT-5, pp. 254–257; October, 1957.

[7] R. Gajewski, "Influence of wall losses on pulse propagation in waveguides," *J. Appl. Phys.*, vol. 29, pp. 22–24; January, 1958.

[8] R. W. Wigington and N. S. Nahman, "Transient analysis of coaxial cables considering skin effect," PROC. IRE, vol. 45, pp. 166–174; February, 1957.

$$\alpha(\omega_0 + \omega) = \alpha_0 + \alpha_1\omega + \alpha_2\omega^2 \quad (6)$$

$$\beta(\omega_0 + \omega) = \beta_0 + \beta_1\omega + \beta_2\omega^2. \quad (7)$$

Here, α_0 and β_0 are the values of attenuation and phase constant at the carrier frequency ω_0. α_1 and β_1 represent the linear slope at this frequency, and the quadratic coefficients are given by

$$\alpha_2 = \frac{1}{2}\frac{\partial^2\alpha}{\partial\omega^2}\bigg|_{\omega_0} \qquad \beta_2 = \frac{1}{2}\frac{\partial^2\beta}{\partial\omega^2}\bigg|_{\omega_0}. \quad (8)$$

These coefficients can be determined either through computation or by graphical means from an experimental plot of α and β vs frequency.

To illustrate the degree of approximation achieved by (7), a typical example is chosen, involving a X-band, $1\frac{1}{2}$ inch OD rectangular waveguide. A carrier frequency of $\omega_0/2\pi = 10$ kmc is assumed. The calculation of β at 8 and 12 kmc by (7) reveals errors of $+2.9$ per cent and -0.4 per cent, respectively, when compared with the accurate formula.

It is worthwhile noting that this method of Taylor series representation of α and β could not be advantageously employed for the analysis of base-band pulses ($\omega_0 = 0$), since α and β must be even and odd functions, respectively, of the frequency. In the case of carrier pulses, where the Taylor expansion centers around ω_0, no such restriction exists.

The Fourier integral, (5), can be solved as soon as the envelope of the transmitted pulse has been chosen. The assumption of a Gaussian envelope

$$f_1(t) = e^{-bt^2} \quad (9)$$

with spectrum

$$F_1(\omega) = \frac{e^{-\omega^2/4b}}{2\sqrt{\pi b}} \quad (10)$$

appears to be a good approximation to the waveforms actually realizable.[3-5] Theoretically, such a pulse lasts infinitely long; however, a practical pulse duration τ may be defined as the time elapsed between amplitude values that are a fraction $1/q$ of the maximum pulse amplitude at $t = 0$. The choice of q may depend on the sensitivity of the receiver, and on the noise in the system. Values of the order of $1/q = 1$ per cent (-40 db) or 10 per cent (-20 db) may be practical. The relation between b, τ and q is

$$b = \left(\frac{2}{\tau}\right)^2 \ln q. \quad (11)$$

It may be difficult to determine these pulse durations by oscillographic measurements. It is more convenient to measure pulse durations between "-3 db" points or between "$1/e$" points. Fig. 1 (next page), representing (11), serves to correlate these pulse durations through intersection of a horizontal line with the given curves.

The substitution of (6), (7) and (10) into (5) yields

$$g(z, t) = \frac{e^{j[\omega_0 t - \beta_0 z] - \alpha_0 z}}{2\sqrt{\pi b}} \cdot \int_{-\infty}^{+\infty} e^{-[(\alpha_2 z + 1/4b)\omega^2 + \alpha_1 z\omega] + j(-\beta_2 z\omega^2 + (t - \beta_1 z)\omega]} d\omega. \quad (12)$$

It is convenient to describe the received pulse in terms of a new time-scale, t', which is retarded with respect to t by the group delay $z/v_{gr} = \beta_1 z$. The integral in (12) may be solved in closed form.[9] Of interest is only the real part of the resulting expression, which represents the physically existing waveform.

$$\mathrm{Re}\, g(z, t') = \bar{g}(z, t') = g_1(z, t') \cos\{\Omega t' + \chi t'^2 + \delta\} \quad (13)$$

where

$$g_1(z, t') = \frac{\exp\left\{-\alpha_0 z + \dfrac{b(1 + 4b\alpha_2 z)[(\alpha_1 z)^2 - t'^2] - 8b^2\alpha_1\beta_2 z^2 t'}{(1 + 4b\alpha_2 z)^2 + (4b\beta_2 z)^2}\right\}}{\sqrt[4]{(1 + 4b\alpha_2 z)^2 + (4b\beta_2 z)^2}} \quad (14)$$

$$\Omega = \omega_0 - \frac{2b\alpha_1 z(1 + 4b\alpha_2 z)}{(1 + 4b\alpha_2 z)^2 + (4b\beta_2 z)^2} \quad (15)$$

$$\chi = \frac{4b^2\beta_2 z}{(1 + 4b\alpha_2 z)^2 + (4b\beta_2 z)^2} \quad (16)$$

$$\delta = (\omega_0\beta_1 - \beta_0)z - \frac{4b^2\beta_2\alpha_1^2 z^3}{(1 + 4b\alpha_2 z)^2 + (4b\beta_2 z)^2} - \frac{1}{2}\arg[1 + 4b\alpha_2 z + j4b\beta_2 z]. \quad (17)$$

Examination of this result for a lossless, nondispersive system immediately yields the undistorted transmitted waveform, $\bar{g}(z, t') = \mathrm{Re}\, f(t)$, confirming that the group delay $\beta_1 z$ is the correct propagation time for this case.

Inspection of (12) shows that convergence of the Fourier integral is guaranteed, provided

$$\alpha_2 z + \frac{1}{4b} > 0. \quad (18)$$

This imposes an upper limit upon z in case α_2 is negative (concave downward attenuation characteristic).

The following additional restrictions in the validity of the result are caused by the fact that (6), and there-

[9] D. Bierens de Haan, "Nouvelles Tables d'Intégrales Définies," G. E. Stechert and Co., New York, N. Y.; 1939. (Table 269.)

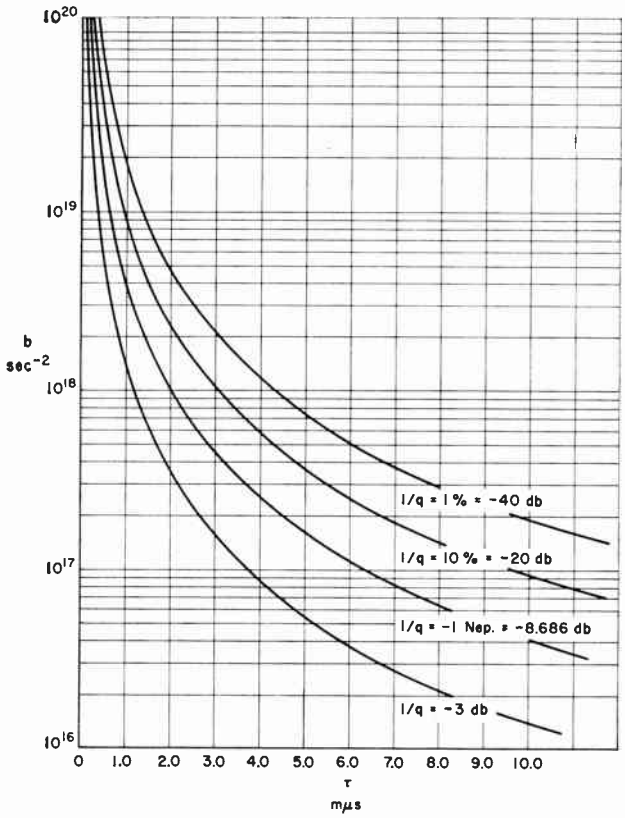

Fig. 1—Correlation of b, τ and q.

fore also (12) represent approximations. Eq. (6) shall be a valid approximation within a certain given frequency range. Consequently, the component waves being superposed by the integration, (12), must be confined to this frequency range. This is satisfied by requiring that

$$e^{-[(\alpha_2 z + 1/4b)\omega^2 + \alpha_1 z\omega]} \ll 1, \tag{19}$$

as ω exceeds the given frequency range. This assures that all component waves outside the given frequency range have amplitudes of negligible magnitude. In any given situation, (19) readily allows to estimate the maximum distance z up to which the analysis yields accurate results. In lossless systems z is not limited, and the same is true for lossy systems where both $\alpha_1 = 0$ and $\alpha_2 > 0$.

Eqs. (13) to (17) are useful for the general case of a system having both loss and dispersion. The received envelope $g_1(z, t')$ is still Gaussian, but appears flattened out and its peak is displaced from $t' = 0$. Eq. (16) reveals the existence of frequency modulation within the pulse, since the instantaneous carrier frequency is

$$\omega_0(t') = \frac{\partial}{\partial t'}(\Omega t' + \chi t'^2 + \delta) = \Omega + 2\chi t'.$$

The average carrier frequency (at $t' = 0$) appears shifted from ω_0 (15). Finally, RF phase at $t' = 0$ is given by (17).

It appears advantageous to discuss separately distortions due to dispersion, due to losses, and due to bandwidth limitation. Although, strictly speaking, there are no physical systems that give rise to distortions of only one of these categories, they nevertheless represent useful approximations.

Distortions due to Dispersion

Setting $\alpha = 0$, the solution (13) becomes

$$\bar{g}(z, t') = \frac{e^{-bt'^2/(1+(4b\beta_2 z)^2)}}{\sqrt[4]{1 + (4b\beta_2 z)^2}} \cos\left\{\omega_0 t' + \frac{4b^2\beta_2 z}{1 + (4b\beta_2 z)^2} t'^2 + (\omega_0\beta_1 - \beta_0)z - \frac{1}{2}\arctan(4b\beta_2 z)\right\}. \tag{20}$$

Of prime interest are the peak value of the envelope, the pulse duration, the frequency modulation of the carrier and the RF phase. The peak value of the envelope occurs at $t' = 0$, indicating that it has traveled with group velocity. The attenuation α_p of the peak pulse amplitude in decibels is

$$\alpha_p = 5 \log [1 + (4b\beta_2 z)^2]. \tag{21}$$

The pulse duration $\tau(z)$ is found to be

$$\tau(z) = 2\sqrt{\frac{1 + (4b\beta_2 z)^2}{b}} \ln q = \tau(o)\sqrt{1 + (4b\beta_2 z)^2}. \tag{22}$$

With the assumptions made, the instantaneous radian frequency of the carrier changes at a constant rate given by

$$\frac{\partial}{\partial t'}\omega_0(t') = 2\chi = \frac{8b^2\beta_2 z}{1 + (4b\beta_2 z)^2}. \tag{23}$$

The RF phase angle at $t' = 0$ is

$$\delta = (\omega_0\beta_1 - \beta_0)z - \tfrac{1}{2}\arctan(4b\beta_2 z) \tag{24}$$

where the second term is usually small compared to the first.

In the case of normal dispersion, β_2 is negative, meaning that the group velocity increases with frequency. Higher frequencies are therefore expected in the early part of the received pulse, while lower frequencies are expected at later times. Eq. (23) fully expresses this situation.

The above results are illustrated by a practical example, employing a X-band, $1 \times \frac{1}{2}$ inch OD rectangular waveguide. Again, a carrier frequency of $\omega_0/2\pi = 10$ kmc is chosen. One obtains

$$\beta_0 = (\omega_0^2 - \omega_c^2)^{1/2}/v = 1.58\ \text{cm}^{-1},$$
$$\beta_1 = \omega_0/(v^2\beta_0) = 4.41 \times 10^{-11}\ \text{sec cm}^{-1},$$
$$\beta_2 = -\omega_c^2/(2v^4\beta_0^3) = -0.266 \times 10^{-21}\ \text{sec}^2\ \text{cm}^{-1},$$

where

$\omega_c/2\pi$ is the cut-off frequency of the guide, and where $v = (\mu\epsilon)^{-1/2}$.

The attenuation of the peak value of the pulse envelope is shown in Fig. 2(a) for pulses of various lengths. Durations of these pulses are plotted in Fig. 2(b), where it is observed that the curves cross each other. Thus, there are locations where pulses of different initial length attain equal length. However, their carrier waveform still differs, determining their subsequent change of τ. The initially shorter pulse contains more frequency modula-

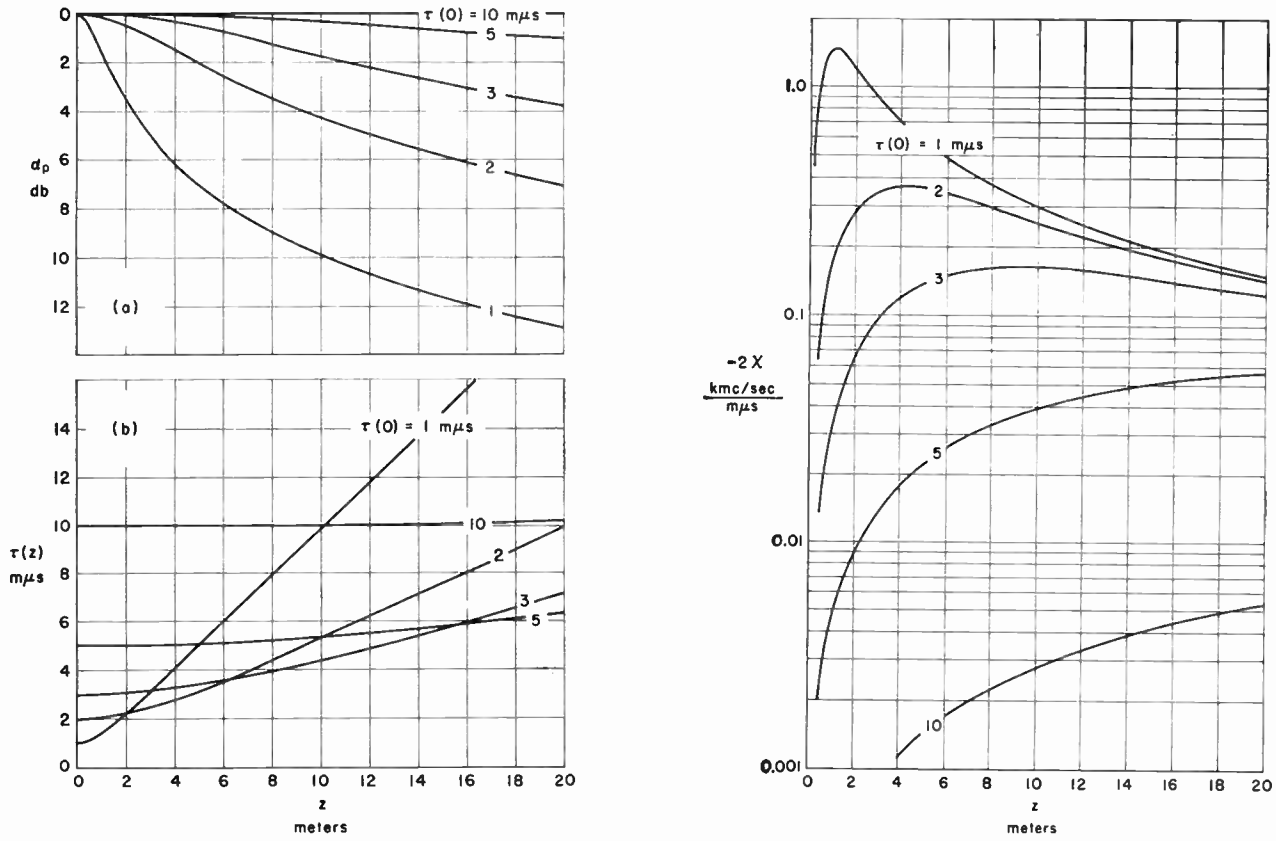

Fig. 2—Attenuation of envelope peak (a), pulse spreading (b), and rate of carrier frequency modulation (c) for pulses of various lengths. [$\tau(0)$ is measured between 10 per cent amplitude points.]

tion of the carrier than the initially longer pulse. The rate of change of instantaneous frequency is shown by Fig. 2(c), and the RF phase angle, as approximated by the first term of (24), becomes $\delta/z \approx 68$ degrees per centimeter.

These pulse deterioration effects could be reduced by decreasing β_2. In the case of the waveguide, this is accomplished by increasing the carrier frequency ω_0, however, an upper limit is set by the occurrence of the first higher-order waveguide mode. Relatively dispersion-free operation at a single mode may be achieved in suitably dimensioned ridged waveguides.

Distortions due to Losses

In a dispersionless system, the coefficient $\beta_2=0$, so that the solution (13) becomes

$$\bar{g}(z, t') = \frac{e^{-\alpha_0 z+(b[(\alpha_1 z)^2-t'^2])/(1+4b\alpha_2 z)}}{\sqrt{1+4b\alpha_2 z}} \cdot \cos\left\{\left(\omega_0 - \frac{2b\alpha_1 z}{1+4b\alpha_2 z}\right)t' + (\omega_0\beta_1 - \beta_0)z\right\}. \quad (25)$$

Of interest are again the behavior of the envelope and of the carrier as a function of z. In addition, the validity of the result must be tested in accordance with the discussion of (18) and (19) for every practical case.

The attenuation α_p of the peak pulse amplitude in decibels is

$$\alpha_p = 8.686\alpha_0 - \frac{8.686b(\alpha_1 z)^2}{1+4b\alpha_2 z} + 10\log(1+4b\alpha_2 z) \quad (26)$$

where the first term on the right equals the attenuation experienced by a CW signal at frequency ω_0. The pulse duration is

$$\tau(z) = 2\sqrt{(1+4b\alpha_2 z)\frac{\ln q}{b}} = \tau(o)\sqrt{1+4b\alpha_2 z} \quad (27)$$

and the shift in carrier frequency is given by

$$\Delta\omega_0 = \frac{-2b\alpha_1 z}{1+4b\alpha_2 z} \quad (28)$$

Positive slope of the attenuation characteristic thus decreases the carrier frequency, a situation which is intuitively expected, since the lower frequencies of the spectrum are enhanced with respect to the higher frequencies. This also explains the small gain term in (26) associated with α_1. In RG9A/U coaxial cable for instance, the carrier frequency shift would be expected to be -6.2 mc per meter for an X-band, 1-mμs pulse (between 10 per cent points).

Distortions due to Bandwidth Limitations

If a system is assumed whose transmission is strictly limited to the frequency band $\omega_0 \pm \omega_1$, the analysis may be resumed with (12), using the appropriate limits of integration, $\pm\omega_1$. Studying for example, a lossless and dispersionless system ($\alpha=\beta_2=0$), the integral in (12) becomes

$$I = \int_{-\omega_1}^{+\omega_1} e^{-\omega^2/4b+j\omega t'} d\omega. \quad (29)$$

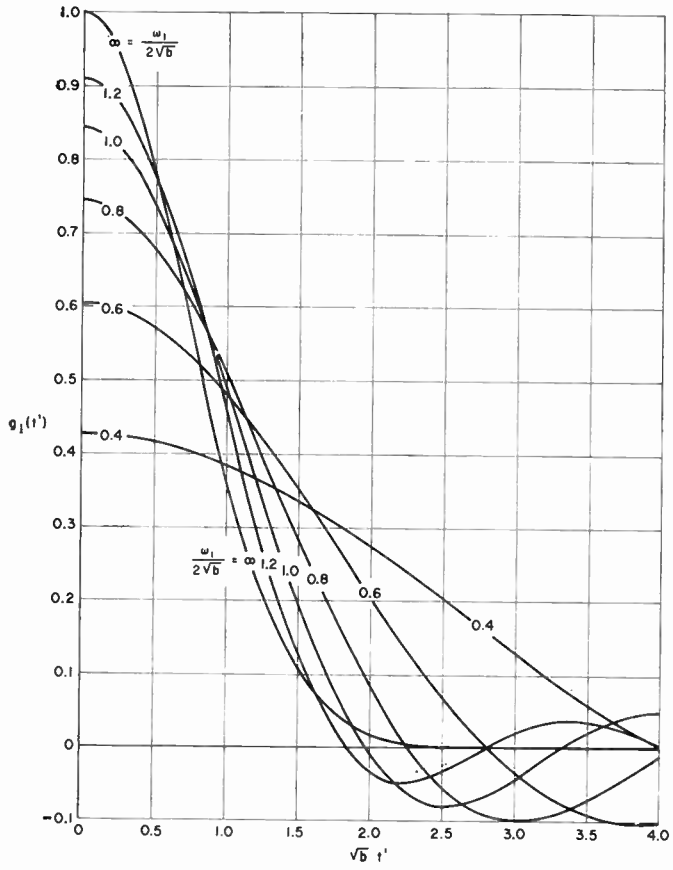

Fig. 3—Envelope functions $g_1(t')$ for various pulse lengths and bandwidths in systems with abrupt frequency-band limitation.

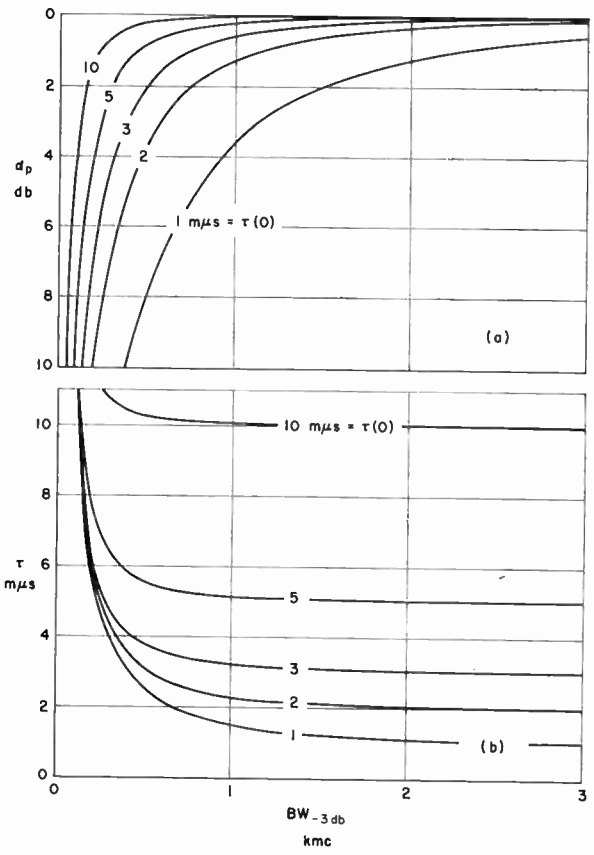

Fig. 4—Attenuation of envelope peak (a) and pulse spreading (b) due to Gaussian filter characteristic of variable half-power bandwidth. The pulse durations τ are those measured between 10 per cent amplitude points.

Rearranging the exponent to form a complete square and performing a variable transformation

$$\zeta = \frac{\omega}{2\sqrt{b}} - jt'\sqrt{b}$$

leads to

$$I = 2\sqrt{b}e^{-bt'^2}\int_{-\omega_1/(2\sqrt{b})-jt'\sqrt{b}}^{\omega_1/(2\sqrt{b})-jt'\sqrt{b}} e^{-\zeta^2}d\zeta \qquad (30)$$

where ζ is a complex variable. Eq. (30) cannot be integrated in closed form; however, it may be expressed in terms of the error function of a complex variable, defined by

$$\text{erf}\,(x+jy) = \frac{2}{\sqrt{\pi}}\int_0^{x+jy} e^{-\zeta^2}d\zeta = U(x,y) + jV(x,y) \qquad (31)$$

and having the properties

$$\text{erf}\,(-p) = -\text{erf}\,(p); \qquad \text{erf}\,(p^*) = \text{erf}^*\,(p). \qquad (32)$$

This function has been tabulated by Hastings and Marcum[10] and a mapping was originated by Laible.[11]

[10] C. Hastings and J. I. Marcum, "Tables of integrals associated with the error function of a complex variable," RAND Corporation, Santa Monica, Calif., Report RM-50; August 1, 1948.

[11] T. Laible, "Hoehenkarte des Fehlerintegrals," *Z. angew. Math. u. Phys.*, vol. 2, no. 6, pp. 484–487; 1951.

Eq. (30) now becomes

$$I = 2\sqrt{\pi b}e^{-bt'^2}U\left(\frac{\omega_1}{2\sqrt{b}},\ t'\sqrt{b}\right) \qquad (33)$$

so that the total solution, from (12), is

$$\bar{g}(z,t') = e^{-bt'^2}U\left(\frac{\omega_1}{2\sqrt{b}},\ t'\sqrt{b}\right) \cdot\cos\left\{\omega_0 t' + (\omega_0\beta_1 - \beta_0)z\right\}. \qquad (34)$$

The carrier waveform appears undistorted but the pulse envelope is no longer Gaussian. Since U is an even function of t' (32), the pulse envelope $g_1(t')$ has even symmetry with respect to $t'=0$, indicating that the center of the pulse travels with group velocity. The attenuation α_p of the pulse center is given by

$$(\alpha_p)^{-1} = U\left(\frac{\omega_1}{2\sqrt{b}},\ 0\right) = \frac{2}{\sqrt{\pi}}\int_0^{\omega_1/(2\sqrt{b})} e^{-x^2}dx$$

$$= \Phi\left(\frac{\omega_1}{2\sqrt{b}}\right) \quad \text{[voltage ratio]} \qquad (35)$$

which is the usual error function. Pulse envelopes are shown in Fig. 3, where the curve labeled $\omega_1/(2\sqrt{b}) = \infty$

s the undistorted Gaussian envelope obtained with in-inite bandwidth. All other envelopes are characterized oy small oscillations outside the major part of the pulse (overshoot). Considering for example a 3-mμsec pulse (between 10 per cent points) being transmitted through a filter with 750 mc total bandwidth one obtains $b = 10^{18}$ sec^{-2} (from Fig. 1) and,

$$\frac{\omega_1}{2\sqrt{b}} = \frac{\pi(BW)}{2\sqrt{b}} = 1.2$$

as the parameter of the received envelope. As seen from Fig. 3, the peak is 91 per cent of that transmitted, the 10 per cent points are spaced by 3.2 mμsec, and the overshoot does not exceed 5.5 per cent of the peak. Practically no distortions would be obtained for $\omega_1/2\sqrt{b} \geqq 2$.

For transmission systems, whose frequency band limitation is gradual rather than abrupt, a Gaussian filter characteristic with a transfer function

$$W(\omega_0 + \omega) = e^{-h\omega^2} \tag{36}$$

may be a good approximation. The pulse response of such a filter is immediately found from (25) by substituting $\alpha_0 = \alpha_1 = 0$ and $\alpha_2 z = h$. Fig. 4 illustrates the attenuation of the envelope peak and the pulse spreading as a function of the half-power bandwidth for pulses of various durations. Bandwidth requirements can thus be determined from a given tolerable attenuation and spreading.

Generalization of the Analysis

The present theory is applicable to certain linear, microwave two-port networks by introducing total attenuation a and total phase shift ϕ as measured between terminated reference planes. This is possible provided the frequency functions a and ϕ may be approximated similarly to (6) and (7). It then is merely necessary to substitute $a = \alpha z$ and $\phi = \beta z$ in the results.

Conclusion

Assuming a transmitted pulse with Gaussian envelope and a quadratic approximation to the complex propagation constant of a uniform transmission system, the RF pulse propagation problem is solved in closed form. While the received pulse envelope remains Gaussian, it appears flattened out. The carrier waveform is also changed. The effects due to dispersion (β_2) include pulse spreading and frequency modulation of the carrier within the pulse. A linear slope of attenuation (α_1) causes a shift of the carrier frequency towards lower attenuation. The quadratic term of the attenuation characteristic (α_2) usually causes pulse spreading. While all these pulse deterioration effects are very small for pulses equal to or longer than 10 mμsec, they increase extremely rapidly for pulses shorter than 3 mμsec.

The pulse transmission characteristics of a Gaussian filter is obtained as a special case of a lossy transmission system. In systems with abrupt frequency-band limitation, the pulse propagation problem leads to the error function of a complex variable. Here, the received pulse envelopes are no longer Gaussian but exhibit overshoot at the ends of the pulse.

Acknowledgment

Appreciation is due to the writer's colleague, Dr. S. V. Yadavalli, for helpful discussions.

A Quartz Servo Oscillator*

NORMAN LEA†

Summary—**The paper deals with a 5 mc oscillator whose frequency instabilities due to vacuum tube effects are at least 100 times less than those present in the best conventional oscillators which achieve stabilization by resonant vector balance. By using quartz crystals of low drift, it is therefore possible to reduce unpredictable frequency changes to one or two parts in 10^{10}. The tube-dependent instabilities in conventional oscillators are reviewed, the conclusion being that even with circuit Q values as high as 2 million it is not possible to guarantee frequency instabilities as low as 10^{-9}, much less 10^{-10}.**

A plan for dual stabilization by resonant-loop balance and bridge-operated servo to one part in 10^{10} is described. The development of an oscillator based on this plan and intended as a working frequency standard is explained with the aid of block diagrams and performance data.

* Original manuscript received by the IRE, April 11, 1958; revised manuscript received July 11, 1958. Published in 1958 IRE National Convention Record, pt. 5, pp. 234–242.

† Marconi's Wireless Telegraph Co., Ltd., Chelmsford, Eng.

Introduction

THE WORKS of Galileo and Huygens in the 17th century and of Nickelson and Cady from 1918 onwards were outstanding events in the art of frequency control.

During the whole of this time, it was well understood that a driving system introduces a frequency instabil-

ity which depends upon the uncertainty of phase of the driving force and upon the decrement of the resonator.

Quartz resonators having Q values of several million are now possible, and considerable improvements in phase stability have been made by the use of vacuum tubes and preferred coupling networks.

It will be shown, however, that these improvements are not sufficient to enable the present demands for oscillator stability to be met, if reliance is placed on the conventional method of stabilization by balance of vectors in a resonant loop.

Working frequency standards and control oscillators for navigational systems are now required with day-to-day instabilities no greater than one or two parts in 10^{10}. The quartz servo oscillator provides a solution.

Conventional Oscillators

Before considering any new approach to the problem, the tube-dependent instabilities in a conventional oscillator must be reviewed. Let it be assumed for the moment that the resonator and the components of the coupling network are perfectly stable, that there are no harmonics, and that there are no amplitude changes.

Vacuum Tube Imperfections

The well known instabilities are:

1) ΔC_g = Grid cathode capacitance;
2) ΔC_p = Plate cathode capacitance;
3) ΔC_{gp} = Grid plate capacitance;
4) ΔZ_k = Cathode interface impedance;
5) ΔT_t = Transit time;
6) ΔR_p = Plate resistance;
7) Δg_m = Mutual conductance.

These are all functions of supply voltages, temperature, time, and mechanical vibration; moreover, 1), 2), 3), and 5) are functions of g_m.

Fortunately, a complete review of the consequences of this complex state of affairs is unnecessary. It will be sufficient if one or two effects, known to be especially troublesome, are discussed.

Simplest Conventional Circuit

The simplest known low-loss network capable of providing the desired impedance transformations between resonator and tube system is the Colpitts arrangement of Fig. 1. The only network quantity which can be adjusted to minimize the total effect of tube instabilities is the ratio n of the mutual capacitances.

Capacitance Instabilities

It is easy to show that the total instability of frequency due to ΔC_g and ΔC_p is

$$\frac{\Delta\omega}{\omega} = \frac{\omega}{2g_mQ}\left(\frac{\Delta C_g}{n} + n\Delta C_p\right) \tag{1}$$

which has a minimum value of

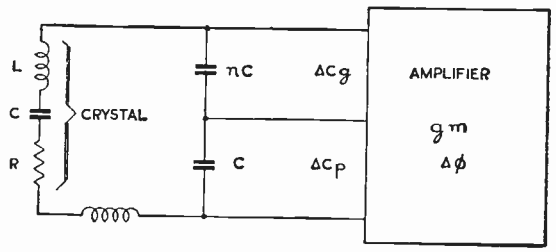

Fig. 1—Vector stabilization.

$$\frac{\Delta\omega}{\omega} = \frac{\omega}{g_mQ}\sqrt{\Delta C_g \cdot \Delta C_p} \tag{2}$$

when

$$n = \sqrt{\frac{\Delta C_g}{\Delta C_p}}.$$

For the case of a 5 mc crystal of $Q = 2$ million used in conjunction with a tube g_m of 2 ma/volt, we have an instability due to tube capacitance changes of

$$\frac{\Delta\omega}{\omega} = 7800\sqrt{\Delta C_g \cdot \Delta C_p}.$$

Experience suggests that in order to cover the tube changes that can occur in a mere 1000 hours operation, reasonable values are

$$C_g = 1 \quad \text{pF}$$
$$C_p = 0.1 \text{ pF};$$

hence, for the example suggested,

$$\frac{\Delta\omega}{\omega} = 2.4 \times 10^{-9}. \tag{3}$$

Phase Instabilities

If it be assumed that cathode interface impedance is the main cause of the phase instability of plate current, it is easily shown that phase instability is

$$\Delta\phi = \tan^{-1} g_m\Delta X_k \tag{4}$$

where ΔX_k is the instability of the reactive component of the cathode interface impedance.

The frequency instability due to this is

$$\frac{\Delta\omega}{\omega} = \frac{g_m\Delta X_k}{2Q}. \tag{5}$$

Values for ΔX_k are not predictable for specified changes of cathode temperature, but experience suggests that it is unsafe to assume operational variations much less than 10 ohms at 5 mc.

Assuming again that $Q = 2.10^6$ and $g_m = 2$ ma/volt the frequency instability due to phase effects is

$$\frac{\Delta\omega}{\omega} = 10 \times 10^{-9} \tag{6}$$

From the results (3) and (6), it is seen that the total instability due to capacitance and phase changes in an individual pentode may be

$$\frac{\Delta\omega}{\omega} = 12.4 \times 10^{-9}. \quad (7)$$

This suggests that the conventional oscillator cannot be expected to keep within 1 in 10^9 without most serious reservations.

Comparison with Meacham Circuit

In view of the wide publicity accorded to the Meacham Bridge Oscillator, its behavior in relation to the Colpitts circuit of Fig. 1 is worth noting. If the input and output transformers of a Meacham Bridge have their ratios chosen so that the combined effect of ΔC_a and ΔC_p is minimized, it is easy to show that

$$\frac{\Delta\omega}{\omega} = \frac{4\omega}{g_m Q}\sqrt{\Delta C_a \cdot \Delta C_p}. \quad (8)$$

This is four times as large as that given by the Colpitts type circuit.

The effect due to phase changes in the amplifier of a Meacham system is

$$\frac{\Delta\omega}{\omega} = \frac{2}{Q}\frac{\Delta\phi}{A}$$

where A is the voltage attenuation in the bridge or the voltage gain in the amplifier.

If the amplifier consists of a single pentode, the gain can be increased by using a higher g_m value, but as we have seen from (4) that $\Delta\phi$ is likely to be proportional to g_m, no advantage is gained. If the gain of the amplifier is increased by the use of more than one stage, it is not easy to obtain a worthwhile reduction of $\Delta\phi/A$ at 5 mc on account of the phase instabilities introduced by the electrode capacitances shunted across the interstage couplings, and by the instabilities of the interstage couplings themselves. For these reasons, the Meacham system at 5 mc has a performance inferior to that of the Colpitts circuit of Fig. 1.

Conventional Oscillator Conclusions

From the above discussions, the conclusions reached are:

1) It does not seem possible to devise a better basic oscillator system than that shown by Fig. 1.
2) If an oscillator of this type has a 5 mc crystal, the Q value of which is as high as 2 million, the instabilities arising from an individual vacuum tube may nevertheless exceed 1 in 10^8.
3) In cases where the effect of replacing an oscillator tube has to be regarded as an oscillator instability, the rating in respect to tube effects could be no better than about 3 in 10^8.
4) To obtain the performance of 1 or 2 in 10^{10} now required, a new approach is essential.

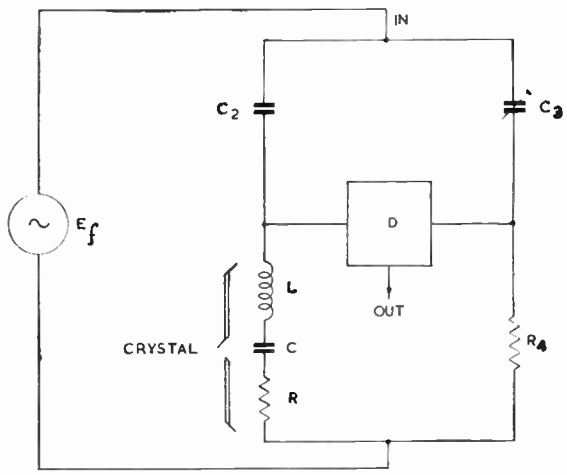

Fig. 2—Bridge stabilization.

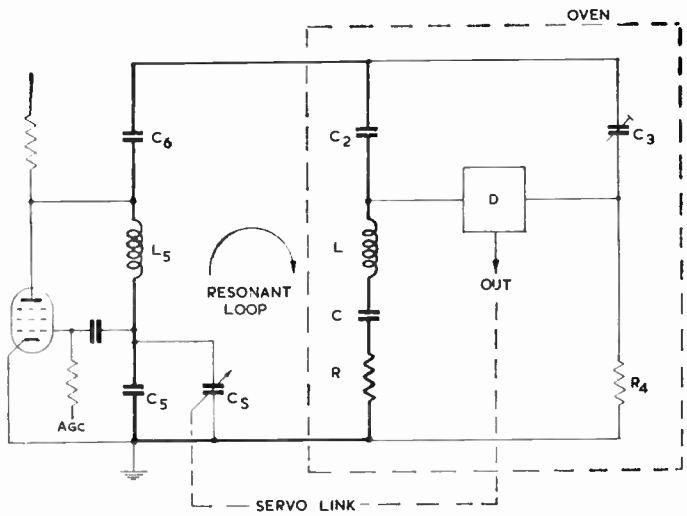

Fig. 3—Dual stabilization.

Plan for a Servo Oscillator

The tube-dependent instabilities of a conventional oscillator are completely avoided if frequency stabilization depends on the balance of an RF bridge in which none of the arms have tube-related reactances.

Such a bridge preferably takes the form shown in Fig. 2, the arms consisting of crystal LCR, a pure resistance R_4, and two loss-free capacitors C_2 and C_3. The bridge is fed from a convenient source E_f and has a sensitive detector D. Even with the low operating levels essential in precision crystals, such a bridge has an output above noise for a frequency departure of 1 in 10^{11} from reactance balance. It is therefore possible to use the detector output to adjust the frequency of the source E_f via a servo mechanism within one or two parts in 10^{11}.

The source E_f cannot be a simple LC oscillator, because its random FM would be prohibitive. To avoid the need for a separate crystal oscillator, the arrangement of Fig. 3 is a most welcome solution.

The RF bridge of Fig. 3 has arms designated as in Fig. 2 and has a resonant loop indicated by the heavy-lined rectangle. By making the impedances of the

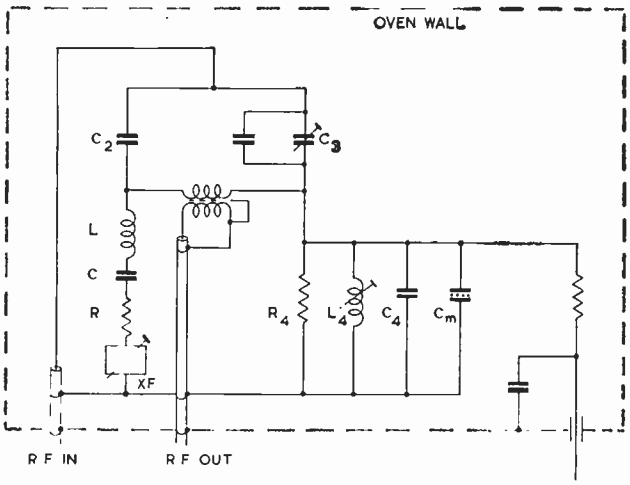

Fig. 4—The RF bridge.

bridge arms C_3 and R_4 large compared with those of C_2 and LCR, the resonant loop can operate independently of the bridge, to give stabilization by conventional vector balance. The Q value of the resonant loop is not much less than that of the crystal itself, so such stabilization is as good as in a conventional oscillator. (Note that the use of capacitance instead of resistance ratio arms avoids the reduction of Q value present in an earlier system.[1,2])

Simultaneously, the output of the bridge detector is made to control a reactance C_s located at a convenient point in the resonant loop, so that the frequency is continuously corrected within a few parts in 10^{11} of bridge balance.

The RF bridge is the only part of the system which need be held at constant temperature. All effects due to the instabilities of the oscillator tube and of C_5, C_6, and L_5, and of the coaxial input cable to the oven are eliminated by the servo control of C_s.

Fig. 4 illustrates more nearly the arrangement actually used. The components L_4 and C_4 enable the R_4 arm to be made nonreactive, C_m is a modulator to give sense-of-error information in the bridge output, and X_F provides a fine adjustment of datum frequency.

Fig. 5 shows the way in which the RF envelope of the bridge output changes with bridge unbalance.

Some early information about this plan has been given by the author,[1,3] and patents[4,5] are related.

Development

The first application of the plan described in the last section has been the development of an oscillator for use as a continuously working frequency standard. For this service there are no rigid size and weight restrictions, so it has been possible to include every feature which will permit adjustment for optimum performance. The oscillator is in cabinet form with 19″ slide-and-tilt panels for easy servicing without interrupting operation. "Preferred" easily obtained tubes are used. Fig. 6 indicates its external appearance and Fig. 7 is a simplified block diagram.

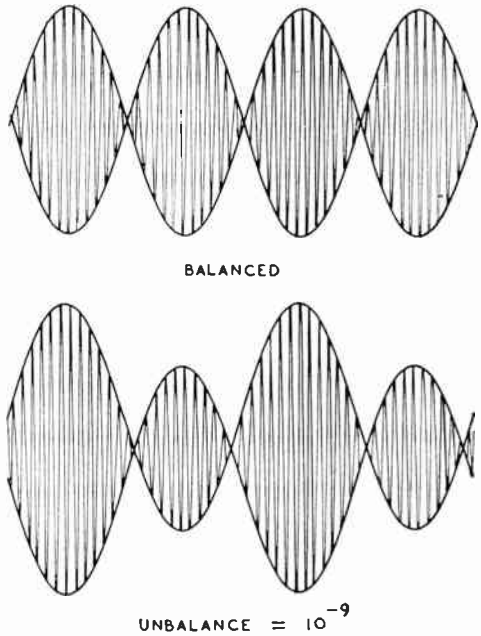

Fig. 5—Bridge ouput envelopes.

Crystal Bridge

The bridge follows Fig. 4 closely, all components being of the most stable types available. Construction is such that performance is cyclic over the range of 10° to 80°C. The output transformer has an unwanted signal in the secondary (due to the electric field of the primary) which is at least 70 db below the bridge input voltage. The secondary voltage is therefore always an accurate indication of bridge balance.

The method used for reactance modulation is important. The modulator must be regarded as an integral part of the bridge, both from an RF and thermal point of view—that is to say, it must be housed completely inside the metal wall of the oven. The modulator must be stable over a long life, not disturb oven temperature, not cause FM in the crystal resonant loop, and not introduce RF mutuals between the crystal bridge and outside circuits.

The requirements were not fully met by the rotary variable capacitor used in the early experiments,[1] and much less so by the chopper arrangement suggested by Sulzer[6] and copied by Behrend.[7] The best modulator

[1] N. Lea, "Quartz resonator servo—a new frequency standard," *Marconi Rev.*, vol. 17, pp. 65–73; 3rd quarter, 1954.
[2] F. D. Lewis, "Frequency and time standards," PROC. IRE, vol. 43, pp. 1046–1068; Sept, 1955.
[3] N. Lea, Discussion, Frequency Control Symposium, U. S. Signal Corps Eng. Labs., Asbury Park, N. J.; April, 1954.
[4] British Patent No. 741, 867.
[5] U. S. Patent No. 2,769,090.
[6] P. G. Sulzer, "High stability bridge balancing oscillator," PROC. IRE, vol. 43, pp. 701–707; June, 1955.
[7] W. L. Behrend, "Reduction of co-channel T.V. interference by precise frequency control of T.V. HF carriers," *RCA Rev.*, vol. 17, pp. 443–459; December, 1956.

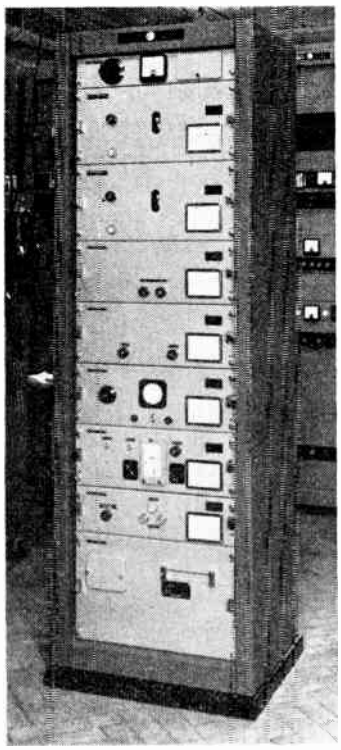

Fig. 6—Servo oscillator type RD101.

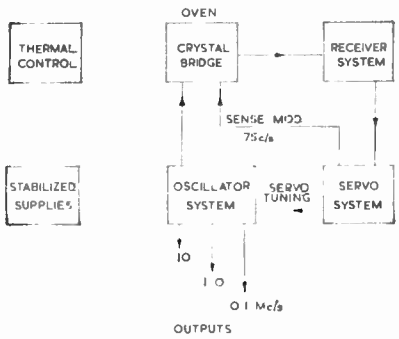

Fig. 7—Simplified block diagram.

so far found is a capacitor with variable permittivity dielectric, connected as already indicated by C_m in Fig. 4.

Tests over the last twelve months suggest that such a capacitor operated at constant temperature has a stable enough datum, if the LF modulating potential sweeps over most of the permittivity-voltage characteristic and if the peak reactance modulation corresponds to a frequency departure from bridge balance of no more than about 2 in 10^9.

It is found that such a peak modulation is quite satisfactory for obtaining rapid servo corrections of all frequency errors from 3 in 10^{11} up to 5 in 10^8. To minimize servo errors, the following precautions are taken:

1) Modulation is sinusoidal to escape the effect of harmonics and to facilitate R-balance adjustment.
2) The moduiation frequency is 75 cps to avoid conflict with supply frequencies and their harmonics.
3) The modulation source is a stable RC oscillator.

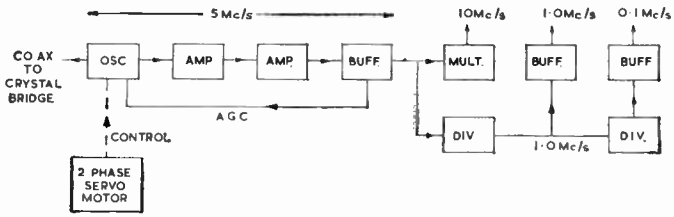

Fig. 8—Oscillator block diagram.

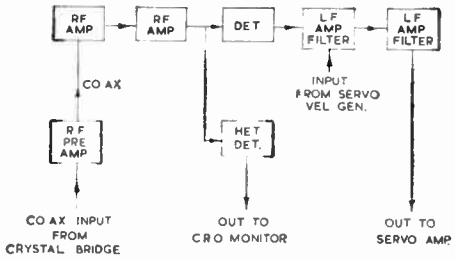

Fig. 9—Receiver block diagram.

4) Servo correction is by motor rather than by reactance tube, so that threshold boundaries are symmetrical with respect to the condition of perfect reactance balance.
5) The range of servo correction is sufficient to cover the effect of RF tube replacement.
6) The phase relation of "reference" to "control" signals is adjustable and monitored by CRO.

Thermal Control

In accordance with long established practice, thermal control is by resistance bridge with heat distribution to give a low ambient coefficient. The crystal temperature is stable to a few milli-degrees. A fine control enables the operating temperature to be aligned with the crystal characteristic. A relay contact for a remote alarm closes if the oven temperature becomes abnormal due to tube failures.

Oscillator System

The block diagram of Fig. 8 is self-explanatory. The circuitry is contained in a chassis separated from the oven unit by an 8 foot coaxial cable. The gain of the amplifier stages in the AGC system is stabilized to avoid changes in crystal operating level. A coaxial socket is mounted on the chassis to enable an RF millivoltmeter to be connected to the oscillator stage for measuring crystal operating level. To prevent signals from the high-level stages from reaching the receiver, the oscillator circuitry is very well screened and decoupled. The oscillator is fitted with a "test switch" to simulate errors of 10^{-8}, 10^{-9}, and 10^{-10}.

Receiver System

Fig. 9 shows a block diagram of the preamplifier and the receiver. The preamplifier is mounted on the oven chassis and avoids the danger of carrying the low-level 5 mc bridge output signal directly to the receiver chassis.

Most of the receiver selectivity is obtained by bridged-T networks in the LF stages. The heterodyne oscillator, offset from 5 mc, enables the RF envelope of the modulation cycle to be monitored for checking servo operation.

The circuitry of the receiver is specially screened and decoupled.

Servo Amplifier

This contains two separate 75 cps channels for the "control" and "reference" signals which feed the two-phase tuning motor on the oscillator. A stable RC oscillator provides the 75 cps "reference" signal and also a separate phase-adjusted output for exciting the modulator C_m of the RF bridge.

Monitoring

A CRO monitor is included in the cabinet to permit all salient voltages in the servo system to be checked without interrupting the high-precision service.

Metering of 60 voltages and currents in the various units is provided, together with a chart of normal readings on each panel.

Power Supplies

Two identical regulated supply units are used, the loads being apportioned in such a way as to minimize mutual effects in the event of partial tube failures. The "hum" of each unit is monitored by the CRO panel. The transformers cover the usual range of input voltages and frequencies from 40 to 60 cps. Circuit breakers are fitted which cannot be tripped by transformer surges set up by supply irregularities.

Operation

Crystal Bridge

R Balance: The R_4 arm of the bridge is easily made nonreactive when a setting of L_4 is found (Fig. 4) at which variations of C_3 cause no appreciable movement of the pointer on the servo correcting capacitor C_s. This is fortunate, because it is highly desirable that the operating frequency should be independent of exact R balance.

Adjustments: Tools which cause small thermal disturbance are provided for the adjustment of X_F, C_3, and L_4. The frequency control X_F covers a range of 2 in 10^7 and enables the operating frequency to be aligned with other sources to within a few parts of 10^{10}.

Oscillator Circuits (Fig. 8)

RF Level: Even in the best crystals, frequency is a function of operating level; therefore, the level is adjustable over a wide range, but stabilized as much as possible at the setting chosen.

To avoid an instability of level due to disturbance of the AGC voltage by even small oscillator tube grid currents, the oscillator tube is operated at a low mutual conductance.

In equipments now operating, levels of about 30 mv are used at the grid of the oscillator tube. This corresponds to about 2μw dissipation in the crystal.

Unwanted FM: The level of the first sideband relative to the 10 mc carrier output due to the 75 cps reactance modulation of the bridge is about -130 db. If the 10 mc output is multiplied to 10,000 mc, the first 75 cps sideband should have a level relative to the carrier no greater than -70 db, which is satisfactory for most microwave work.

As the modulation is of sine form, the second sideband is negligible.

Time of Servo Correction: The servo motor which drives the variable correcting capacitor C_s incorporates a 75 cps generator, the voltage output of which is proportional to velocity. This output is fed back to be added to the 75 cps control signal in the first LF stage of the receiver (Fig. 9).

With the normal setting of the amount of this feedback, the following times of error elimination to within 5 in 10^{11} are obtained.

Error introduced by test switch	Elimination time
10^{-8}	3 seconds
10^{-9}	1 second
10^{-10}	0.3 second

Output Loading: The frequency change due to loading any of the three coaxial outputs is less than 3 in 10^{11}.

Receiver System (Fig. 9)

Gain: The RF gain is adjustable over a wide range to facilitate initial RF bridge adjustments.

The gain is set to give rapid yet stable servo operation.

The gain of the receiver has no effect on the servo-controlled frequency other than a symmetrical change of the correction thresholds.

Heterodyne Oscillator: Adjustment of this has no effect on the outputs of the equipment.

LF Filtering: The phase stability of the 75 cps "control" output signal is adequate in spite of filtering in favor of 75 cps and rejection of 150 cps.

Saturation: The receiver system does not saturate sufficiently to inhibit servo correction, even if a frequency error of 10^{-7} is suddenly applied.

Servo Amplifier (Fig. 10)

The "reference" and "control" channels have fixed gain. The output level of the "reference" channel is incapable of driving the servo motor in the absence of a "control" signal. A balancing circuit eliminates unwanted output from the velocity generator at zero velocity.

The diode level-control in the 75 cps RC oscillator ensures that the frequency is stable to better than 1 in 1000. The modulator level is adjustable to provide proof of negligible frequency changes.

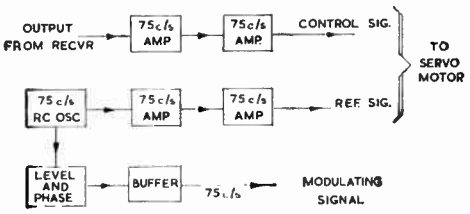

Fig. 10—Servo amplifier diagram.

Oscillator Frequency Comparisons

The method of comparison has been based on mechanical counting of beats over a period of 200 seconds at comparison frequencies of 100 and 1000 mc, to give recorder resolutions of 1 in 10^9 and 1 in 10^{10} per cm, respectively.

The count ambiguity of these recordings is one count in each case, that is to say, 0.5 in 10^{10} and 0.5 in 10^{11}, respectively.

The times of counting were controlled by a synchronous motor driven from a precision 100 cps source so the over-all recorder errors were no more than that due to the count ambiguity.

Three quartz servo oxcillators were operated in thermally separated rooms, each being fed from a different phase of the power supply. The RF outputs from the equipments were taken by coaxial cables to the recorder already indicated, the crosstalk between cables being insufficient to cause appreciable recording errors.

Fig. 11 is a typical 24-hour run at a resolution of 1 in 10^{10} per cm. It will be seen that the short-time scatter is no more than 5 in 10^{11} total, which is consistent with a servo threshold of about 3 in 10^{11} for each oscillator. There is a roughly sinusoidal change of about 3 in 10^{11} peak during the 24 hours, which is due to imperfection in the thermal control.

The relative drift between the two oscillators is about 1 in 10^{10} per day.

The recording of Fig. 12 shows a 36-hour comparison at a discrimination of 1 in 10^9 per cm.

This recording is of interest because it shows the effect of severe external vibration and the effect of replacing the oscillator tube in one equipment. At ten hours on the time scale, the oven chassis of the disturbed equipment was moved about 3 feet from a position it had occupied outside the cabinet for more than a week in connection with other tests.

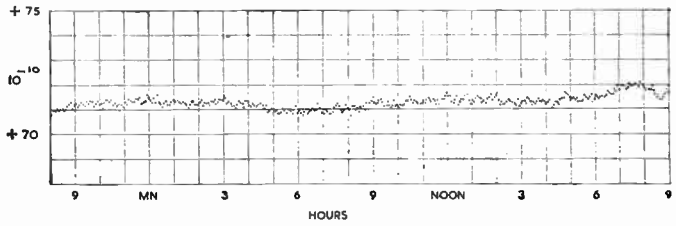

Fig. 11—24-hour recording at 10^{-10} per cm.

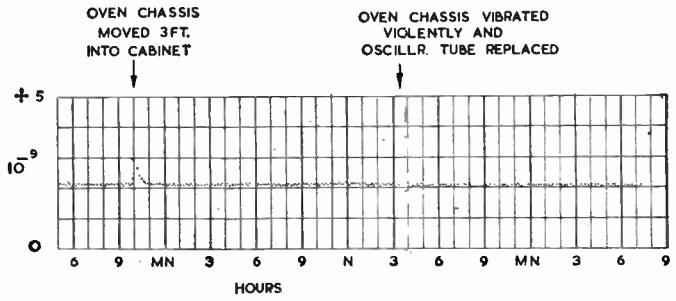

Fig. 12—36-hour recording at 10^{-9} per cm.

No special care was taken in placing the chassis on the runners and sliding it into the cabinet. The result of this operation was a frequency transient lasting less than an hour, the steady change being less than 1 in 10^{10}. At 3.30 hours on the next day, the oven chassis was vibrated violently in the presence of visitors.

At the same time, the oscillator tube was replaced by one chosen at random from a number of the same type. The combined effect of the vibration and tube replacement was a second transient of less than 1 in 10^9 peak and lasting less than one hour. Thereafter, for a period of 14 hours the record remained steady to within 1 in 10^{10} of the original datum.

Conclusion

The quartz servo oscillator avoids all the instabilities due to complex vacuum tube effects and circuit changes which are present even in the best conventional precision oscillator.

The servo oscillator in fact provides a continuously working frequency standard which is stable to 2 parts in 10^{10}, relative to a low linear crystal drift.

The equipment is generously engineered to facilitate adjustment to optimum performance.

Prime and operating costs are low for the performance achieved.

Some Generalized Scattering Relationships in Transhorizon Propagation*

A. T. WATERMAN, JR.†, SENIOR MEMBER, IRE

Summary—An analysis is made of the consequences to be derived from some fairly broad assumptions as to the nature of turbulent scattering and its effect on waves propagated through the troposphere. The intent is to provide a means for testing the general applicability of this model as an explanation for transhorizon propagation. General relationships for the variation of received power with distance are derived for various scatter-angle dependencies, and for various beamwidth configurations. These relationships are then extended to cover the phenomenon of aperture-medium coupling loss. The results are applied toward distinguishing those experiments which are definitive from those which are not.

I. Introduction

In experimental measurements on the propagation of microwaves to distances well beyond line of sight,[1–8] a substantial accumulation of evidence has been published indicating that the received wave consists of the sum of several components distributed over a small range of arrival angles. The model of pertinent atmospheric structure which has most abundantly been suggested as providing the mechanism for this form of propagation is that of turbulent scattering.[9–16] It is the purpose of this paper to point out some general consequences of the assumption that the pertinent mechanism is a single-scattering process distributed systematically throughout the atmosphere.

No attempt is made to investigate any basic turbulence mechanism. Rather, a generalized form for the conventional atmospheric scattering cross section[17] σ is assumed, and its consequences deduced. The intention is to reveal what types of empirical measurement are definitive in distinguishing appropriate scattering models.

In Section II, a generalized dependency of scattering cross section on scatter angle is taken as a starting point, and the variation of received power with distance is accurately derived for certain general cases when the transmitting and receiving antennas are broad beamed. Section III treats the cases that arise when the antenna beams are narrow compared with the angular path distance. This procedure is identical to that followed by Booker and deBettencourt[18] except that it employs the more generalized form of scattering cross section mentioned above. Then, combined cases are considered, in which a broad-beam antenna may be employed at one end of the path and a narrow-beam antenna at the other, as well as cases in which either or both of the beams may be broad in elevation but narrow in azimuth and vice versa. Expressions for the received power as a function of distance are given for each of these circumstances. In Section IV, this procedure is extended to apply to the concept of aperture-medium coupling loss, again using the generalized form of scatter-angle dependency, and applying it to a variety of antenna-beam configurations. Significant quantities to be observed in experimental measurements are discussed.

II. Power Received with Nondirective Antennas

For transmission between two points A and B on the earth's surface separated by a great-circle distance d, the usual geometry appropriate to the single-scattering concept in transhorizon propagation is shown in Fig. 1, which serves to define many of the quantities involved. The total power received at one terminus via a scattering process in the atmosphere depends on an

* Original manuscript received by the IRE, June 16, 1958. Presented at the URSI meeting, Washington, D. C., May 25, 1957. This work was supported by the U. S. Army Signal Corps under Signal Corps Contract DA36(039)SC-73151.

† Stanford Electronics Labs., Stanford University, Stanford, Calif.

[1] A. T. Waterman, Jr., N. H. Bryant, and R. E. Miller, "Some observations on antenna-beam distortion in transhorizon propagation," IRE TRANS. ON ANTENNAS AND PROPAGATION, vol. AP-5, pp. 260–266; July, 1957.

[2] J. H. Chisolm, A. T. Portmann, J. T. deBettencourt, and J. F. Roche, "Investigations of angular scattering and multipath properties of tropospheric propagation of short radio waves beyond the horizon," PROC. IRE, vol. 43, pp. 1317–1335; October, 1955.

[3] L. G. Trolese, "Characteristics of tropospheric scattered fields," PROC. IRE, vol. 43, pp. 1300–1305; October, 1955.

[4] Y. Kurihara, "Trans-horizon microwave propagation over hilly terrain," PROC. IRE, vol. 43, pp. 1362–1368; October, 1955.

[5] L. A. Ames, P. Newman, and T. F. Rogers, "VHF tropospheric overwater measurements far beyond the radio horizon," PROC. IRE, vol. 43, pp. 1369–1373; October, 1955.

[6] J. H. Chisholm, J. F. Roche, and W. J. Jones, "Experimental Investigations of the Angular Scattering and Multipath Delays for Transmissions Beyond the Horizon," presented at the URSI meeting, Washington, D. C.; May 23, 1957.

[7] W. H. Kummer and D. C. Hogg, "Characteristics of Signals Received on a Large Aperture Antenna in Propagation Beyond-The-Horizon," presented at the URSI meeting, Washington, D. C.; May 25, 1957.

[8] L. H. Doherty, "A 216-Mile 2700-MC/s Scatter Link," presented at the URSI meeting, Washington, D. C.; May 24, 1957.

[9] H. G. Booker and W. E. Gordon, "A theory of radio scattering in the troposphere," PROC. IRE, vol. 38, pp. 401–412; April, 1950.

[10] F. Villars and V. F. Weisskopf, "The scattering of electromagnetic waves by turbulent atmospheric fluctuations," *Phys. Rev.*, vol. 94, pp. 232–240; April, 1954.

[11] F. Villars and V. F. Weisskopf, "On the scattering of radio waves by turbulent fluctuations of the atmosphere," PROC. IRE, vol. 43, pp. 1232–1239; October, 1955.

[12] A. D. Wheelon, "Note on scatter propagation with a modified exponential correlation," PROC. IRE, vol. 43, pp. 1381–1383; October, 1955.

[13] R. A. Silverman, "Turbulent mixing theory applied to radio scattering," *J. Appl. Phys.*, vol. 27, pp. 699–705; July, 1956.

[14] E. C. S. Megaw, "Fundamental radio scatter propagation theory," *Proc. IEE*, vol. 104C, pp. 441–455; May, 1957.

[15] H. Staras, "Forward scattering of radio waves by anisotropic turbulence," PROC. IRE, vol. 43, pp. 1374–1380; October, 1955.

[16] K. A. Norton, P. L. Rice, and L. E. Vogler, "The use of angular distance in estimating transmission loss and fading range for propagation through a turbulent atmosphere over irregular terrain," PROC. IRE, vol. 43, pp. 1488–1526; October, 1955.

[17] Power scattered per unit solid angle per unit volume per unit incident power density.

[18] H. G. Booker and J. T. deBettencourt, "Theory of radio transmission by tropospheric scattering using very narrow beams," PROC. IRE, vol. 43, pp. 281–290; March, 1955.

integration over the volume of space above the earth's surface. As long as the scattering falls off sharply with increasing scatter angle θ, it is an easy matter to approximate the integral. However, since the volume over which the integral is to be taken is semi-infinite in extent, while the value of the integral itself is finite, an assessment of the accuracy involved in using an approximation is not immediately apparent. Consequently, there is some merit to performing the integration exactly in those cases where that is possible.

The imposed conditions for this treatment follow.

1) The scattering cross section σ can be expressed in the form

$$\sigma(\theta) = \frac{b}{\sin^m\left(\frac{\theta}{2}\right)}. \tag{1}$$

2) The turbulent structure of the atmosphere is constant throughout the volume over which the integration is taken (b = constant).
3) The gain functions of the transmitting and receiving antennas (including the effects of earth reflections) are similarly constant.
4) Polarization effects are neglected.

With these restrictions, the scattered power (in watts) received by an antenna beyond line of sight from the transmitter can be written as

$$P_R = \frac{P_T G_T G_R \lambda^2 b}{16\pi^2 a \sin\left(\frac{d}{2a}\right)} \int_{-\pi/2}^{\pi/2} \int_{\cot^{-1}[\cos\beta \cdot \cot(d/2a)]}^{\theta - \cot^{-1}[\cos\beta \cdot \cot(d/2a)]} \frac{d\gamma \cdot d\left(\frac{\theta}{2}\right) \cdot d\beta}{\sin^m\left(\frac{\theta}{2}\right)} \tag{2}$$

a form somewhat similar to that given by LaGrone[19] and by Herbstreit *et al.*[20] In the above,

P_T = transmitted power (W)
$G_{T,R}$ = gain of transmitting and receiving antennas
λ = wavelength (m)
a = modified earth's radius (m)
d = distance between transmitter and receiver (m)
b = constant (of dimensions m^{-1}) relating scattering cross section to scattering angle as seen in (1)
θ = scattering angle
γ = angle between the straight line joining transmitter and receiver and the line from transmitter (or receiver) to a volume element
β = angle between the vertical plane through transmitter and receiver and the plane containing transmitter, receiver and volume element.

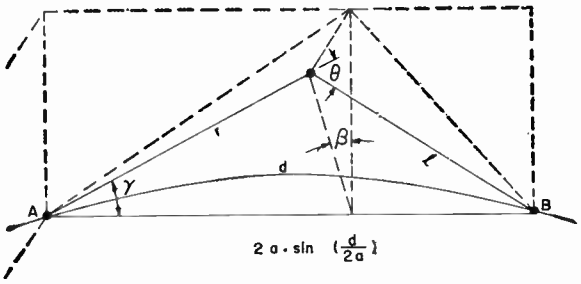

Fig. 1—Scatter-propagation geometry.

The integration extends over the space above both the tangent plane at the transmitter and that at the receiver.

When m is an even integer, the integration is readily performed.[21] Exact solutions are listed below, as are also the leading terms in their expansions (which are valid when the argument $d/2a$ is very small).

$m = 2$:

$$P_R = \frac{P_T G_T G_R \lambda^2 b}{32\pi a \sin\left(\frac{d}{2a}\right)} \left\{ 4 \log \left[\frac{1 + \csc \frac{d}{2a}}{2} \right] \right\} \tag{3}$$

$$\approx \frac{P_T G_T G_R \lambda^2 b}{16\pi d} \left\{ 2 \log \left(\frac{a}{d} \right)^2 \right\} \tag{3a}$$

$m = 4$:

$$P_R = \frac{P_T G_T G_R \lambda^2 b}{32\pi a \sin\left(\frac{d}{2a}\right)} \left\{ \frac{1}{3} \cot^2\left(\frac{d}{2a}\right) + \frac{8}{3} \log \left[\frac{1 + \csc\left(\frac{d}{2a}\right)}{2} \right] \right\} \tag{4}$$

$$\approx \frac{P_T G_T G_R \lambda^2 b}{16\pi} \left\{ \frac{4a^2}{3d^3} \right\} \tag{4a}$$

$m = 6$:

$$P_R = \frac{P_T G_T G_R \lambda^2 b}{32\pi a \sin\left(\frac{d}{2a}\right)} \left\{ \frac{3}{40} \cot^4\left(\frac{d}{2a}\right) + \frac{7}{15} \cot^2\left(\frac{d}{2a}\right) + \frac{32}{15} \log \left[\frac{1 + \csc\left(\frac{d}{2a}\right)}{2} \right] \right\} \tag{5}$$

$$\approx \frac{P_T G_T G_R \lambda^2 b}{16\pi} \left\{ \frac{6a^4}{5d^5} \right\} \tag{5a}$$

[19] A. H. LaGrone, "Volume integration of scattered radio waves," PROC. IRE, vol. 40, p. 54; January, 1952.
[20] J. W. Herbstreit, *et al.*, "Radio Wave Scattering in Tropospheric Propagation," Natl. Bureau of Standards, Washington, D. C., Rep. No. 2459; April 15, 1953.
[21] A. T. Waterman, Jr., "Radio Power Received via Tropospheric Scattering," Applied Electronics Lab., Stanford University, Stanford, Calif., Tech. Rep. No. 461-1; July 18, 1955.

$m = 8$:

$$P_R = \frac{P_T G_T G_R \lambda^2 b}{32\pi a \sin\left(\frac{d}{2a}\right)} \left\{ \frac{5}{168}\cot^6\left(\frac{d}{2a}\right) + \frac{6}{35}\cot^4\left(\frac{d}{2a}\right) + \frac{19}{35}\cot^2\left(\frac{d}{2a}\right) + \frac{64}{35}\log\left[\frac{1+\csc\left(\frac{d}{2a}\right)}{2}\right]\right\} \quad (6)$$

$$\approx \frac{P_T G_T G_R \lambda^2 b}{16\pi}\left\{\frac{40a^6}{21d^7}\right\}. \quad (6a)$$

If one observes the progression in the above expressions for received power, as the scatter-angle exponent m varies, it is possible to write a general formula:

$$P_R \approx \frac{P_T G_T G_R \lambda^2 b}{4\pi^2} \cdot A_m \cdot \frac{a^{m-2}}{d^{m-1}} \quad (7)$$

in which the coefficient A_m is

$$A_m = \frac{\pi 2^m}{(m-1)(m-2)} \cdot \frac{1\cdot 3\cdot 5\cdot\cdots(m-3)}{2\cdot 4\cdot 6\cdot\cdots(m-2)}, \quad (8)$$

where m is an even integer greater than 2. Here the variation of the distance dependence on m is evident.

The above expressions, both the exact and the approximate, apply only to an isotropic volume-type single scattering in which the meteorological coefficient b, defined in (1), is constant throughout the scattering volume. Under these conditions the above general results are in close agreement with those obtained by Gordon[22] in the special case of $m = 4$.

If the quantity b were not constant but were considered as varying inversely with some power n of height above the earth's surface ($b\alpha 1/h^n$), then the distance dependence of received power would be

$$P_R \alpha \frac{1}{d^{m-1+2n}}, \quad (9)$$

a result which is again consistent with Gordon's.[22]

For currently practical cases, the distance d is small relative to the effective earth radius a, so that the approximate expressions [(3a), (4a), etc.] differ hardly at all from the exact [(3), (4), etc.]. It is at least academically comforting, then, to note that previous approximate evaluations of the integral in (2) are in close agreement with the more rigorous treatment here.

III. Power Received with Narrow-Beam Antennas

The procedure here is first to develop a crude expression for the broad-beam case which is in agreement with (7), and then to utilize it in the narrow-beam treatment.

Those who have been concerned with the development of theories of turbulent scattering have generally deduced a scatter-angle exponent m lying somewhere in the vicinity of 4 to 6.[9-16] In this range, the coefficient A_m appearing in the general expression (7) for received power is very nearly constant. We may define an effective volume in the atmosphere from which all of the scattering can be considered as originating. The volume is demarcated by surfaces on which the scattered power has dropped to some fraction (about $\frac{1}{5}$) of its maximum value. It has dimensions along the path, across it vertically, and across it horizontally given respectively by

$$\Delta x \doteq \frac{d}{2}(5^{1/m} - 1)$$

$$\Delta y \doteq \frac{d^2}{4a}(5^{1/m} - 1)$$

$$\Delta z \doteq \frac{d^2}{2a}\sqrt{5^{2/m} - 1}. \quad (10)$$

If we then utilize this effective volume, we can derive an expression for the received power as a function of distance, which is of the same form as (7). It differs only in the nature of the coefficient, but this coefficient has nearly the same value.[23]

$$P_R \doteq \frac{P_T G_T G_R \lambda^2 b}{4\pi^2}\left[2^m(5^{1/m} - 1)^2\sqrt{5^{2/m} - 1}\right]\frac{a^{m-2}}{d^{m-1}}. \quad (11)$$

The merit of employing this artifice will be seen when we deal with antenna beams of asymmetrical shape. In such cases the effective volume of the atmosphere will be in part delineated by the narow dimension of the beam employed and in part by the atmospheric scattering, as specified in (10). However, the above expressions (7) and (11) apply to the case of broad-beam antennas.

If we consider now the other extreme in which both antennas have beamwidths between half-power points, (ϕ, horizontally, and ψ, vertically), which are small compared with the angular path length d/a (*i.e.*, $\phi \ll d/a$ and $\psi \ll d/a$), then the effective scattering volume is limited by the antenna beams alone. In this event, a procedure similar to that given by Booker and de-Bettencourt[18] yields

$$P_R \doteq P_T \frac{G_T G_R \lambda^2 b 2^m}{4\pi^2}\left[\tfrac{1}{2}\phi\psi_1\psi_2\right]\frac{a^{m+1}}{d^{m+2}} \quad (12)$$

in which subscripts 1 and 2 refer to the two antennas and ϕ applies to that antenna having the narrower azimuthal beamwidth. Here the expression in square brackets depends on the beamwidths, which of course are related to the gains (the G's). Also note that the distance dependence is different from that in the broad-beam case in (11).

[22] W. E. Gordon, "Radio scattering in the troposphere," Proc. IRE, vol. 43, pp. 23–28; January, 1955.

[23] Actually (7) differs from (11) by a factor of 4, since a perfectly reflecting foreground was assumed for the latter and subsequent equations, in order to facilitate comparison with the Booker-deBettencourt treatment in reference 18.

Next consider a hybrid case, in which antenna no. 1 is narrow beam, in both dimensions, and antenna no. 2 is broad beam. In this case the y and z dimensions of the effective scattering volume are limited by no. 1's narrow beam, ψ_1 and ϕ_1, while the x dimension is given by the expression in (10). The received power then becomes

$$P_R \doteq P_T \frac{G_T G_R \lambda^2 b 2^m}{4\pi^2} [(5^{1/m} - 1)\psi_1\phi_1] \frac{a^m}{d^{m+1}} \cdot \quad (13)$$

Note again that both the coefficient in brackets and the distance dependence have changed.

Other combinations may be considered. However, rather than discuss each possible configuration separately, it is simpler to note the general form of the expressions

$$P_R = \frac{P_T G_T G_R \lambda^2 b 2_m}{4\pi^2} B_m \frac{a^{q-1}}{d^q} \quad (14)$$

and then to list the coefficient B_m and the exponent q which will occur in each particular case. This scheme is presented in Table I. No attempt has been made here

TABLE I*

Antenna No. 1 beamwidth		Antenna No. 2 beamwidth		Coefficient, B_m	Exponent, q
Azimuth	Elevation	Azimuth	Elevation		
B	B	B	B	$(5^{1/m}-1)^2\sqrt{5^{2/m}-1}$	$m-1$
B	N	B	B	$(5^{1/m}-1)\sqrt{5^{2/m}-1}\psi_1$	m
N	B	B	B	$(5^{1/m}-1)^2\phi_1$	m
N	B	N	B	$(5^{1/m}-1)^2\phi$	m
B	N	B	N	$\frac{1}{2}\sqrt{5^{2/m}-1}\psi_1\psi_2$	$m+1$
N	N	B	B	$(5^{1/m}-1)\psi_1\phi_1$	$m+1$
B	N	N	B	$(5^{1/m}-1)\psi_1\phi_2$	$m+1$
N	N	N	B	$(5^{1/m}-1)\psi_1\phi$	$m+1$
N	N	B	N	$\frac{1}{2}\psi_1\phi_1\psi_2$	$m+2$
N	N	N	N	$\frac{1}{2}\psi_1\phi\psi_2$	$m+2$

* Scheme for ascertaining the coefficient B_m and the exponent q in formula for received power (14), for various configurations of antenna beamwidths (N refers to "narrow," B to "broad").

to combine antenna gain (G) and beamwidth (ϕ or ψ), since the normal, though misleading, procedure is to adjust received power to compensate for plane-wave antenna gain.

With regard to the dependence on distance d in these expressions (*i.e.*, with regard to the exponent q), some generalizations can be made. Consider the four beamwidths involved: the vertical and horizontal beamwidths of each antenna, transmitting and receiving. If all four beams are broad (in the sense discussed above), the received signal falls off as the inverse $(m-1)$st power of the distance. If any one of the four beamwidths is narrow, the distance dependence is inverse mth power. If any two of the four are narrow, the distance dependence is inverse $(m+1)$st power—unless the two narrow widths are the azimuthal widths of the two antenna beams, in which case the dependence is inverse mth. No more than one narrow azimuthal beamwidth may be counted, in this general rule. Again, if three of the four beamwidths are narrow (remembering that azimuthal width may be counted only once), then the distance dependence is inverse $(m+2)$nd power. Finally, if all four beamwidths are narrow, the distance dependence is inverse $(m+2)$nd. These rules can be seen more readily by a glance at Table I than by a lengthy verbal description.

To write them down explicitly, let r be the number of narrow beamwidths involved, with the above qualifications (*i.e.*, r may be 1, 2 or 3); then the distance dependence is

$$P_R \alpha \frac{1}{d^{m-1+r}} \cdot \quad (15)$$

In short, the more the beamwidths are narrowed, the more rapidly the received signal decreases with distance. Also, of course, the greater the value of scattering-dependency exponent m, the greater the decrease of signal with increasing distance.

If a decrease of scattering parameter b with height is taken into account, then (9), when modified to fit the narrow-beam case, gives a distance dependence of

$$P_R \alpha \frac{1}{d^{m-1+r+2n}} \cdot \quad (16)$$

Although the derivations (11) to (16) are admittedly crude, their general form is a consequence of assuming a turbulent volume scattering, and where applicable they are in agreement with previous theoretical results derived for specific cases. An important point to note, however, is the number of adjustable parameters available for obtaining agreement with experiment. m depends on the turbulence model employed and is still in dispute among theorists; b and n depend partly on the turbulence model and partly on meteorological measurements which are not entirely satisfactory; the effective earth's radius, a, depends on average refracting conditions and so is also adjustable. In addition there is the question of anisotropic turbulence as has been discussed by Staras.[24] Finally, the effects related to terrain and siting of the antennas provide additional complications.

In consequence, critical experiments for ascertaining the correct scattering model are not those which depend merely on absolute measurement of received power or its variation with distance.

[24] H. Staras, "Antenna-to-medium coupling loss," IRE Trans. on Antennas and Propagation, vol. AP-5, pp. 228–231; April, 1957.

TABLE II*

Antenna No. 1 beamwidth		Antenna No. 2 beamwidth		Coefficient C_m	Geometric mean of narrow beamwidths α	Exponent r
Azimuth	Elevation	Azimuth	Elevation			
B	N	B	B	$(5^{1/m}-1)$	ψ_1	1
N	B	B	B	$\sqrt{5^{2/m}-1}$	ϕ_1	1
N	B	N	B	$\sqrt{5^{2/m}-1}$	ϕ	1
B	N	B	N	$2(5^{1/m}-1)^2$	$\sqrt{\psi_1\psi_2}$	2
N	N	B	B	$(5^{1/m}-1)\sqrt{5^{2/m}-1}$	$\sqrt{\psi_1\phi_1}$	2
B	N	N	B	$(5^{1/m}-1)\sqrt{5^{2/m}-1}$	$\sqrt{\psi_1\phi_2}$	2
N	N	N	B	$(5^{1/m}-1)\sqrt{5^{2/m}-1}$	$\sqrt{\psi_1\phi}$	2
N	N	B	N	$2(5^{1/m}-1)^2\sqrt{5^{2/m}-1}$	$\sqrt[3]{\psi_1\phi_1\psi_2}$	3
N	N	N	N	$2(5^{1/m}-1)^2\sqrt{5^{2/m}-1}$	$\sqrt[3]{\psi_1\phi\psi_2}$	3

* Scheme for ascertaining the coefficient C_m, the geometric mean of the narrow beamwidths α and the exponent r in the formula for the aperture-medium coupling loss, (19), for various configurations of antenna beamwidths (N refers to "narrow," B to "broad").

IV. Aperture-Medium Coupling Loss

We may continue to follow the procedure developed by Booker and deBettencourt,[18] but now in a more generalized manner. The next step is to evaluate the aperture-medium coupling loss, which is defined as the ratio of the power which would be received if the plane-wave gain of each antenna were realized to the power which is received when antenna beamwidths are sufficiently narrow to exclude some of the scattered power from contributing to the received signal. If antenna gains are fully realized, that is, if all of the pertinent volume of the atmosphere is illuminated by the antennas, (7) and (11) apply. In other cases, equations such as (12) and (13) may apply. The appropriate equation can be found from (14) and Table I. Thus, to find the the aperture-medium coupling loss for two narrow-beam antennas, we take the ratio of (11) and (12), and obtain

$$L_c = [2(5^{1/m}-1)^2\sqrt{5^{2/m}-1}]\frac{(d/a)^3}{\psi_1\phi_1\psi_2}. \qquad (17)$$

This result is close to that obtained by Booker and deBettencourt[18] for the special case in which the scattering exponent m is equal to 4 and the narrow antenna beams are symmetrical and equal. The quantity in square brackets in (17) then becomes roughly 0.5, while their value was 0.43.

Other cases are similarly obtained. When one antenna beam is narrow in both dimensions, the other being broad, the ratio of (11) to (13) yields a coupling loss of

$$L_c = [(5^{1/m}-1)\sqrt{5^{2/m}-1}]\frac{(d/a)^2}{\phi_1\psi_1}. \qquad (18)$$

Again, rather than list each case individually, it is simpler to construct a general scheme. Let the aperture-medium coupling loss be expressed generally as

$$L_c = C_m\left(\frac{d/a}{\alpha}\right)^r. \qquad (19)$$

Then the coefficient C_m, the geometric mean of the narrow beamwidths α and the exponent r, can be found from Table II, for the appropriate combination of antenna beamwidths (which are categorized in the same manner as in Table I).

It will be recognized that these general results are similar in form to the more specific relations derived by Staras[24] (which also take into account the transition region between narrow and broad beams). There is a small quantitative difference arising partly from his more precise treatment and partly from his inclusion of anisotropy considerations.

As in the case of the variations of signal level with distance, it is possible here also to make some generalizations with regard to aperture-medium coupling loss. The coupling loss varies directly as a power r of the angular distance (d/a). This power is equal to the number of narrow beamwidths in the four widths involved (azimuth and elevation beamwidth of each antenna, transmitting and receiving), with the exception that only one of the two azimuthal beamwidths may be counted. This exception is of practical importance in the following respect: if in a particular situation one antenna already has a beamwidth which is narrow in azimuth, then in narrowing the other down to the same azimuthal width there will be no increase in coupling loss, that is, the increased gain obtained by so narrowing the beam will be fully realized. The gist of these

remarks was pointed out by Staras[24] in his statement that the coupling loss is not shared equally between the two antennas.

It is important to note, however, that the aperture-medium coupling loss, by virtue of its being a ratio of two expressions of the form given in (14), does not contain some of the controversial parameters: the scattering coefficient b and height dependence n. Two characteristics—the power dependence of the coupling loss on angular distance, and an inverse dependence on the product of the narrow beamwidths involved—are consequences of the assumption of a volume scattering *per se*, not of its detailed aspects. Only the coefficients C_m depend on the particular scattering dependencies assumed.

Consequently, if (19) is plotted logarithmically, so that the coupling loss varies linearly with the ratio of the angular distance d/a to the geometrical mean of the narrow beamwidths, as in Figs. 2–4, then the slope of the lines should be equal to r, the number of narrow beamwidths involved, regardless of the details of the volume scattering. Such details will affect the displacement of the lines (on a logarithmic plot) but not the slope. Thus a direct measurement of aperture-medium coupling loss over an appreciable range of antenna sizes should provide a basis for testing the broad concept of single-scattering throughout a volume.

In Figs. 2–4 (19) is plotted in decibels using the appropriate constants obtained in Table II. These curves are accurate, at least in slope, in the right-hand portion of each figure; in the left-hand portion all curves have to approach zero asymptotically; in between, the transition has merely been estimated by eye. The three figures correspond to three beamwidth configurations, as labeled. The effect of varying the scatter-angle exponent m, which is evident in the spacing of the curves, probably has at least some relative accuracy.

Experimental data are entered on these figures. In Fig. 2 data taken at 2.29 kmc by the Lincoln Laboratory of Massachusetts Institute of Technology[6] are entered as crosses (+). These points, while clearly indicating the increase in coupling loss with narrowing beamwidth, are not quite sufficient to check the slope of the curves in the coupling-loss region. One other point, taken at 9.36 kmc by Trolese,[3] is also entered (⊙). It is distinctly at odds with the scattering-model derivations.

Fig. 3, applicable when only one antenna beam is narrow, contains three isolated experimental data. One obtained by Trolese[3] (⊙) is in disagreement with this scattering model. The other two, obtained by Lincoln Laboratories[6] and by Kummer and Hogg,[7] are consistent with a value of scatter-angle exponent m of about 5 or 6. If taken together, they appear to substantiate the slope of the theoretical curve, though it is doubtful if such a conclusion should be drawn, since

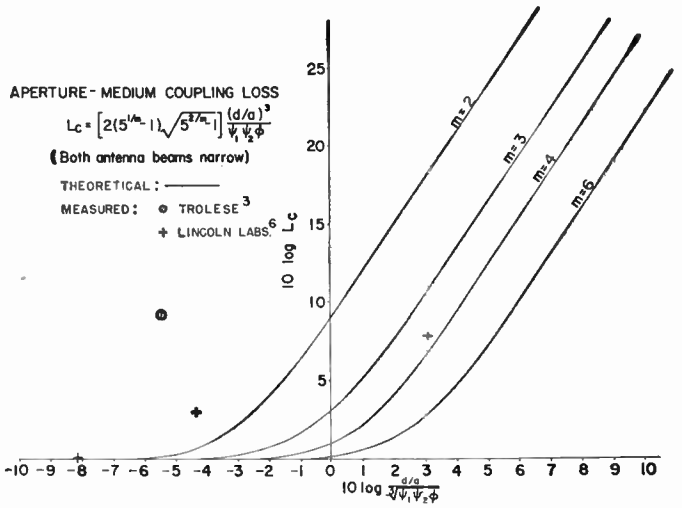

Fig. 2—Aperture-medium coupling loss (L_c) vs ratio of angular distance (d/a) to beamwidth ($\alpha=3\sqrt{\psi_1\psi_1\phi}$), when both antenna beams are narrow.

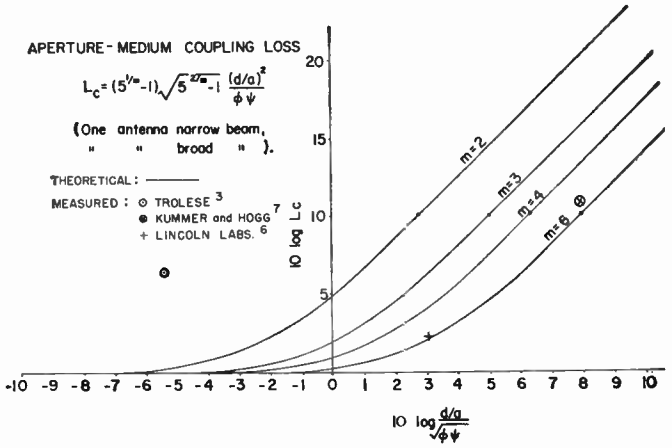

Fig. 3—Aperture-medium coupling loss (L_c) vs ratio of angular distance (d/a) to beamwidth ($\alpha=\sqrt{\phi\psi}$), when one antenna is a narrow beam.

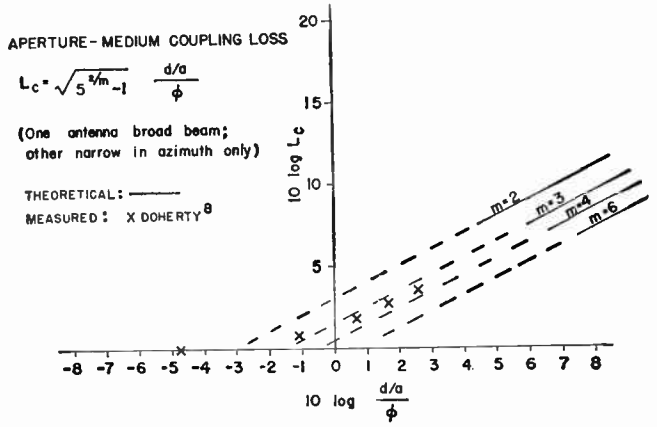

Fig. 4—Aperture-medium coupling loss (L_c) vs ratio of angular distance (d/a) to beamwidth (ϕ), when one antenna is a narrow beam in azimuth only.

the data were taken on different paths at different frequencies.

In Fig. 4 only one antenna beam is narrow, and it in azimuth only. Four experimental points measured by Doherty[8] are entered. They are in general agreement with the theoretical curves. However, the accuracy of the present treatment is scarcely adequate for distinguishing the most appropriate value of exponent m in this case.

V. Conclusion

Insofar as a single-scattering process distributed throughout a volume of the atmosphere is to be considered the mechanism for transhorizon propagation, this paper has deduced several consequences of that general hypothesis. First, a general form of the received power has been accurately deduced; for practical purposes, in the simplest cases, it is summarized by (7). When one or both of the antenna beams are narrow in one or both dimensions, the received power is obtained from (14) and Table I. The discussion indicates why experiments measuring such quantities are likely to be indecisive.

However, the ratio of powers received when only the beamwidth (or only the path length) is varied, and the consequent aperture-medium coupling loss, furnishes a far better means for experimentally testing the applicability of this type of scattering. Eq. (19) and Table II provide appropriate formulas, and the subsequent discussion indicates the pertinent relationships to be sought. The extent to which some existing data fit into this picture is illustrated.

Finally, it should be pointed out that many of the data which have been used to support arguments favoring specific turbulent-scattering hypotheses will in fact support a variety of scattering models. Therefore, it is important to distinguish the consequences of these various models.

A Very-Wide-Band Balun Transformer for VHF and UHF*

T. R. O'MEARA† and R. L. SYDNOR‡

Summary—**A transformer is described which may be used as a phase inverter, a differential transformer, or as a balun transformer. Practical models have been built which operate over more than two decades of frequency range with bandwidths approaching 1 kmc. Insertion loss in a typical transformer fluctuates between 1 and 2 db over the range of frequencies from 5 to 1000 mc.**

For successful operation the transformer depends upon the magnetic properties of a suitable ferrite core material and not upon the usual resonant lines or cavities commonly utilized with such devices [1]–[3].

The ferrites used are not of the low loss, UHF variety but rather are selected on the (approximate) criterion of yielding a high absolute value of permeability over the entire frequency range, and are typically of a class intended for use at much lower frequencies.

List of Symbols

C = capacitance across the faces of a cavity-transition transformer; terminal capacitance.

C_{ca} = complex capacitance per unit length of a coaxial-cylindrical cavity-line filled with lossy dielectric (magnetic) material.

$F_a = \ln r_3/r_2 / \ln r_4/r_1$ = magnetic material filling factor for a coaxial-cylindrical cavity-line.

F_b = magnetic-material filling-factor for a biconical coaxial line.

F_0 = an optimum value for F_a or F_b.

l = length of a transmission line.

L_{ca} = complex inductance per unit length of a coaxial-cylindrical cavity-line filled with lossy magnetic material.

L_1, L_2, L_3 = inductance of the cross-connecting rods in a cavity-transition transformer.

r_1, r_4 = inner and outer radius of the conducting surfaces of a coaxial-cylindrical cavity-line.

r_2, r_3 = inner and outer radius of a magnetic (ferrite) insert in a coaxial cylindrical cavity.

Z_{in} = input impedance of a coaxial-cylindrical cavity-line.

* Original manuscript received by the IRE, June 20, 1958; revised manuscript received, August 14, 1958. The experimental work described in this paper was undertaken at the University of Illinois, Urbana, Ill. (see [14]), and supported by the Office of Naval Research and the Bureau of Ships.

† Hughes Research Labs., Culver City, Calif.

‡ University of Illinois, Urbana, Ill.

$\bar{Z}_{in}$ = normalized input impedance of a coaxial cylindrical cavity-line.

Z_0 = characteristic impedance of the input or output transmission lines of a cavity-transition transformer.

$Z_{ca} = \sqrt{L_{ca}/C_{ca}}$ = characteristic impedance of a coaxial-cylindrical cavity-line which is filled or partially filled with magnetic material.

Z_{cb} = characteristic impedance of a conical-coaxial cavity-line which is filled or partially filled with magnetic material.

$Z_c = \sqrt{\mu_e/\epsilon_e}$ = ratio of the characteristic impedance of a coaxial-cylindrical cavity-line filled or partially filled with magnetic material, to the same cavity-line with a free space filler.

$\Gamma = \omega\sqrt{L_{ca}C_{ca}}$

ϵ_r = complex permittivity of a dielectric material relative to that of free space $= \epsilon_r' - j\epsilon_r''$.

μ_r = complex permeability of a dielectric (or magnetic material) relative to that of free space $= \mu_r' - j\mu_r''$.

ϵ_v = permittivity of free space.

μ_v = permeability of free space.

$\eta = \sqrt{\mu_v/\epsilon_v}$.

ϵ_e = an effective value of complex normalized permittivity for a cavity-line only partially filled with a dielectric material.

μ_e = an effective value of complex normalized permeability for a cavity-line only partially filled with a dielectric (or magnetic) material.

ω = angular frequency.

λ = wavelength in free space.

Introduction

THE essential problem in a wide-band balun transformer design is to accomplish a phase inversion over a wide band of frequencies. Once the inverted output is made available, the uninverted output is achieved by line splitting techniques or by the artifices to be explained later.

An obvious type of phase inversion (using coaxial transmission lines) is shown in Fig. 1(a). However, the transformer which is the subject of this paper was not originally conceived in terms of the transmission line inversion technique of Fig. 1, but rather evolved from a more conventional transformer in a manner resembling that shown in Appendix 1. In Fig. 1(a), the inner and outer conductors are simply cross connected. A problem arises when one attempts to preserve the shielding by connecting the two outer conductors together [4]. This difficulty may be overcome, for a relatively narrow band of frequencies, by the use of a quarter-wavelength reso-

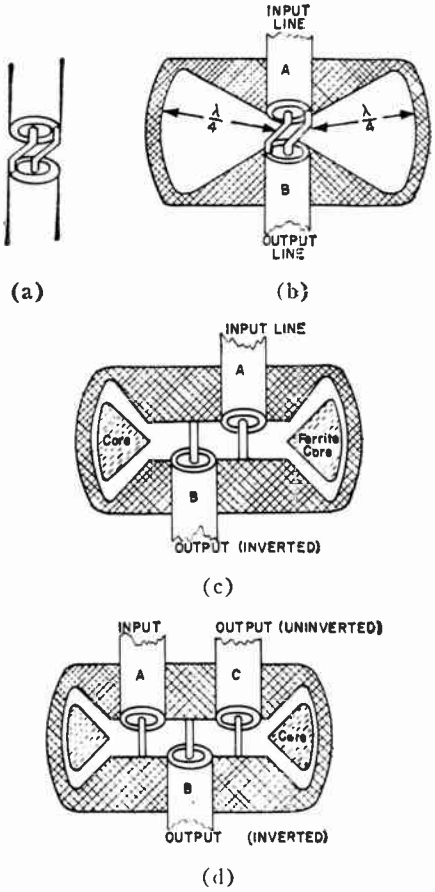

Fig. 1—Development of balun transformer from a transmission line transition. (a) Transmission line transition. (b) Phase inversion tuned "transformer." (c) Phase inversion transformer (cross section). (d) Balun transformer (cross section).

nant (air-filled) cavity, shown as a biconical transmission line in Fig. 1(b). Because of size limitations, such a structure is only practical at UHF.

Such structures do lend themselves to some pulse work, however, if the length of the shield is adjusted to eliminate distortion of the original pulse, with the reflected pulse occurring at a later time [3], [4]. For this purpose, at least one previous investigator [4] has suggested filling the shield with a lossy medium with low permittivity and high permeability, the technique used in this paper.

As the emphasis is to be placed on very-wide-band devices, consider the ferrite-filled structure of Fig. 1(c). At low frequencies it is possible to regard the case as a single turn coil, wound on a magnetic core, which shunts the coaxial transmission line transition. As in all magnetic cored transformers, this shunting effect increases with decreasing frequency and determines a low-frequency limit for the transformer. At high frequencies, however, it is best to regard the core and its cavity as a transmission line long in wavelengths. If the core material is too good (that is, loss free), then, at a frequency such that the cavity transmission line has the

dimensions of a half wavelength, the cavity will short circuit the coaxial lines. If a very "lossy" core material is used, the cavity input impedance will be approximately equal to the characteristic impedance of the cavity for all frequencies where the cavity is sufficiently large in wavelengths; this characteristic impedance may be made moderately high and wide band by careful design.

It is instructive to compare the cavity-transition transformer circuit parameters with those of a more conventional transformer. As mentioned, cavity impedance is analogous to core impedance of a conventional transformer. However, the usual *winding* leakage inductance and capacitance is nonexistent in the new transformer. There is a certain amount of *terminal* capacitance and inductance but these can be made very small. Further, these parameters can be balanced against one another, as shown later. The low-frequency response can be independently extended downward as far as is desired, subject only to the limitations of the core size and the available magnetic materials.

Therefore, there is no direct interrelation between the high and the low-frequency cutoff factors, as occurs in more conventional transformers. The unavoidable terminal capacitances and inductances are the deciding factors in bandwidth, if the core cavity maintains its characteristic impedance.

When the transformer is designed as a balun transformer, the noninverted output may be taken directly from the input. However, better output balance is obtainable if the construction shown in Fig. 1(d) is used. A somewhat more detailed drawing of a balun transformer is given in Fig. 2. Note that the cross connectors are arranged at the vertices of an equilateral triangle to preserve the symmetry between the two outputs C and B.

It is possible also to extend the concept to yield a "four-winding," or hybrid, balance-to-balance transformer. One simply adds another input line on the same side as the B line of Fig. 1(d).

Terminal Leakage Inductance and Capacitance

The cross-connector lead lengths can be made quite short as shown in Figs. 1 and 2. Thus, the inductance of the cross connections will be quite small (on the order of thousandths of a microhenry), while the capacitance across the faces may be on the order of a few micro-microfarads. Equivalent circuits of the phase inverter transformer, together with the terminal capacitance and inductance, may be represented (to a first approximation) by the lumped circuit elements shown in Fig. 3(a). Analogous parameters for the balun transformer are shown in Fig. 3(b). In both of these circuits, the core impedance has been omitted for simplicity. It also is possible to conceive of transition schemes which endeavor to match cable impedances—as a distributed

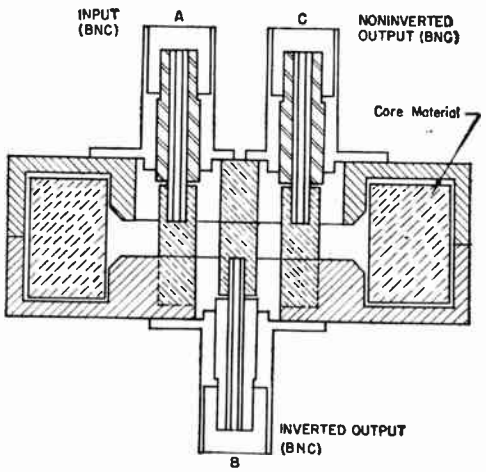

(a)

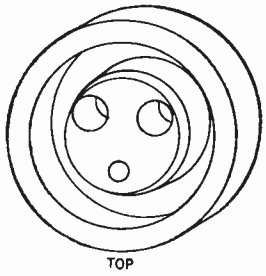

(b)

Fig. 2—Details of balun transformer construction. (a) Assembled cut-away. (b) Inside view (cross-connecting rods and coaxial connectors removed).

parameter network. However, these are not considered in this paper.

The cross-connector inductances L are diminished if the gap is made smaller, but in so doing the capacitance across the faces, C, becomes larger. An optimum situation exists when the gap is the correct width to establish an L/C ratio according to the low-pass filter design relationship:

$$Z_0^2 = \frac{L}{C}, \tag{1}$$

where Z_0 is the characteristic impedance of the coaxial transmission lines to be cross connected. The LC product sets an upper frequency limit which is typically in the high kilomegacycle region.

For the balun transformer, there is a four-to-one impedance transformation, and the design criterion of (1) must be modified. Specifically, in terms of the parameters shown in Fig. 3(b), there results

$$L_3 = L_2 = 2L_1, \tag{2}$$

$$Z_0^2 = \frac{L_1}{C}. \tag{3}$$

Therefore, the cross-connecting rods shown in Fig. 1 to

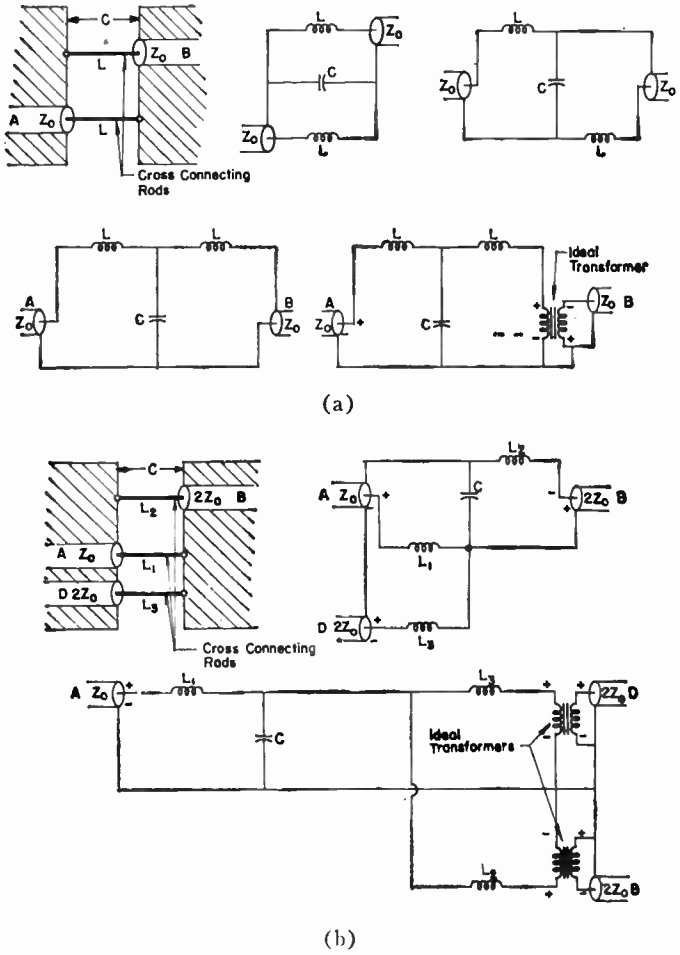

Fig. 3—Terminal leakage inductance and capacitance parameters. (a) Phase inverter parameters (arranged as a low-pass filter). (b) Balun transformer parameters (arranged as a low-pass filter).

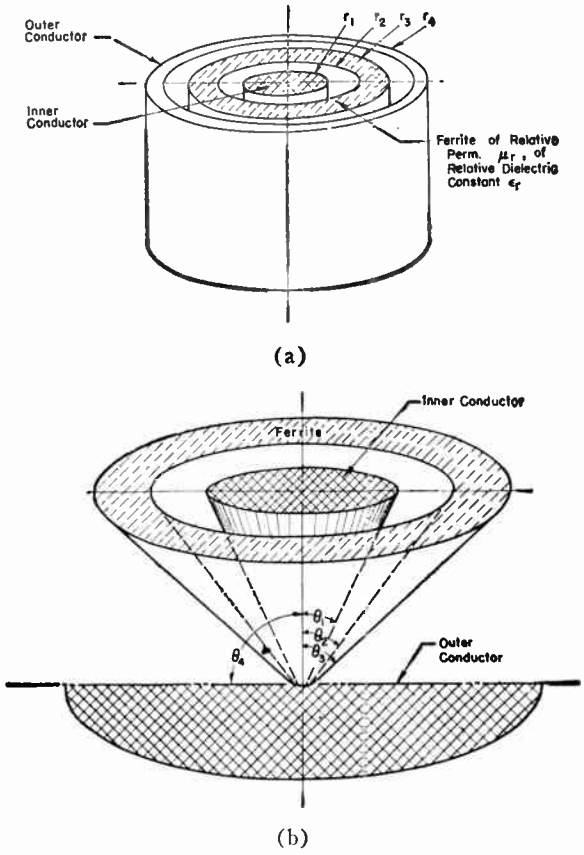

Fig. 4—Partially filled ferrite cavities with uniform characteristic impedance. (a) Coaxial, circular-cylindrical cavity. (b) Conical cavity.

Fig. 3 should not be of the same diameter. The output terminals B and C should be connected by sufficiently smaller rods (L_2 and L_3) to double their inductance relative to that of the rod of A (L_1).

Core Impedance

As mentioned, if the core consists of sufficiently lossy material, the input impedance to the core cavity becomes simply its characteristic impedance, for sufficiently high frequencies. It is not an easy matter to make this characteristic impedance very much higher than the characteristic impedance of the coaxial transmission lines which are shunted by the core. The reason for this stems from the fact that the transmission line transitions must be accomplished within the cavity. Thus, the length of the path in which the magnetic energy of the cavity is stored must be relatively large, and it is difficult to obtain a high ratio of stored-magnetic to stored-electric energy. The ferrite may be of some help as its relative permeability μ_r may exceed its relative dielectric constant ϵ_r over a large frequency range. Even in the instances where the cavity does not have a (uniform) characteristic impedance, it is reasonably clear that the objective of obtaining a high ratio of stored magnetic to stored electric energies is still desirable.

It is possible to analyze easily any type of cavity which has a uniform characteristic impedance; this will be done for two special cases: the coaxial cylindrical cavity and the biconical cavity. As is shown, the highest input impedances are obtained by only partially filling the cavities with ferrite, and so this more general condition is assumed from the beginning.

The Coaxial Cylindrical Cavity

It may be shown by consideration of the stored electric energies involved in the structure of Fig. 4(a) that the complex capacitance per unit length, C_{ca}, is given by

$$C_{ca} = \frac{2\pi\epsilon_v}{\ln\left(\frac{r_4}{r_1}\right) + \left(\frac{1}{\epsilon_r} - 1\right)\ln\left(\frac{r_3}{r_2}\right)}, \qquad (4)$$

where ϵ_v is the permittivity of free space. Note that ϵ_r is a complex number for most ferrites [5], consequently, C_{ca} is also a complex number, and only the real part of C_{ca} represents the true capacitance, while the imaginary part represents a loss term.

In a similar fashion, by considering the stored magnetic energies involved in the structure of Fig. 4(a), it may be shown that the complex inductance per unit length L_{ca} is given by

$$L_{ca} = \frac{\mu_v}{2\pi}\left[\ln\left(\frac{r_4}{r_1}\right) + (\mu_r - 1)\ln\left(\frac{r_3}{r_2}\right)\right], \tag{5}$$

where μ_v is the permeability of free space. Again it must be remembered that μ_r and hence L_{ca} are, in general, complex numbers [5] and that only the real part of L_{ca} represents the true inductance.

The following equations are based on the assumptions of a simple TEM type wave propagation. The assumption is not strictly consistent with proper consideration of the boundary conditions unless the line (or cavity) is entirely filled with ferrite. However, it is a basis for an approximate analysis, valid for sufficiently low frequencies. The same equations (for the coaxial cylindrical line) are derived on a more rigorous basis in a previous report by the authors [14]. All the work which follows is therefore a good approximation only when the spacing r_4 to r_1 is small in wavelengths.

The characteristic impedance of the uniform cavity-line is found to be

$$Z_{ca} = \sqrt{\frac{L_{ca}}{C_{ca}}} = \left\{\frac{\eta}{2\pi}\ln\left(\frac{r_4}{r_1}\right)\right\} \cdot \left\{[1 + (\mu_r - 1)F_a]\left[1 + \left(\frac{1}{\epsilon_r} - 1\right)F_a\right]\right\}^{1/2}, \tag{6a}$$

where

$$F_a = \frac{\ln\left(\frac{r_3}{r_2}\right)}{\ln\left(\frac{r_4}{r_1}\right)}. \tag{6b}$$

It is convenient to regard F_a as a filling factor that is unity when the cavity is completely filled and zero when the ferrite is not present. The form of (6a) makes it desirable to consider the last factor as the root of the product of an effective normalized permittivity, ϵ_e, and an effective normalized permeability, μ_e; thus,

$$\mu_e = 1 + (\mu_r - 1)F_a, \tag{7a}$$

$$\epsilon_e = \frac{1}{1 + \left(\frac{1}{\epsilon_r} - 1\right)F_a}. \tag{7b}$$

It is convenient to work with an impedance, Z_c, which is normalized in terms of a free space line; thus,

$$Z_c = \left(\frac{\mu_e}{\epsilon_e}\right)^{1/2} = \{[1 + (\mu_r - 1)F_a] \cdot \left[1 + \left(\frac{1}{\epsilon_r} - 1\right)F_a\right]\}^{1/2}. \tag{8}$$

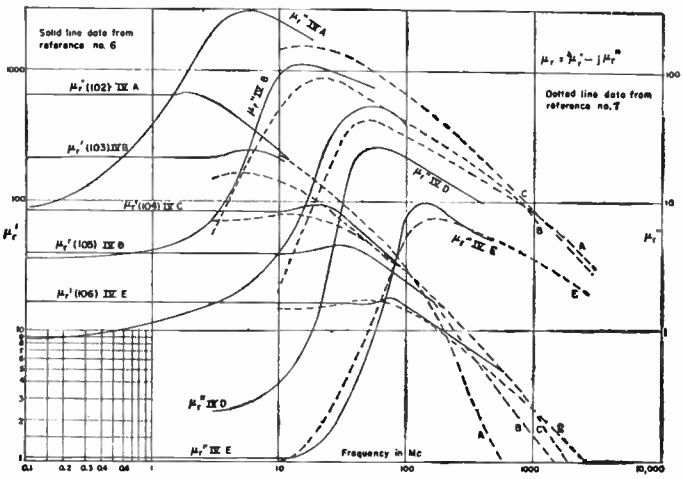

Fig. 5—μ_r' and μ_r'' for various Ferroxcube ferrite materials.

The problem thus becomes that of selecting F_a to maximize $|Z_c|$. A maximum $|Z_c|$ does not necessarily result in a minimum insertion loss, but the correlation is usually close enough to justify this simplifying assumption. If F_a must be large, then (7b) suggests selecting a ferrite with a low value of ϵ_r.

However, if F_a is perhaps 0.8 or less, then even a material like Ferroxcube III [6] ($\epsilon_r = 5 \times 10_4$) is a possibility. In order to progress with this problem, it is required that further simplifications be made regarding Z_c. This is done using two sets of assumptions: 1) μ_r and ϵ_r are both real, *i.e.*, the ferrite material is lossless, and 2) μ_r is complex, but

$$\epsilon_r \gg \frac{1}{1 - F_a}$$

so that $1/\epsilon_r$ terms may be dropped at the beginning.

In the first case, it is shown in Appendix II that a maximum Z_c is obtained for a particular F, F_0, such that

$$F_0 = \frac{\mu_r - 2 + \frac{1}{\epsilon_r}}{2\left(1 - \frac{1}{\epsilon_r}\right)(\mu_r - 1)}. \tag{9a}$$

If it is assumed that ϵ_r is very much greater than unity (see Fig. 5), then (8) becomes

$$F_0 \doteq \frac{\mu_r - 2}{2(\mu_r - 1)}. \tag{9b}$$

If it is further assumed that μ_r is very large compared to two (as it is over most of the frequency range) then to another approximation,

$$F_0 \doteq \frac{1}{2}. \tag{10}$$

Next, the second set of assumptions is used as a starting

point. In this case, the magnitude of Z_c is given by

$$Z_c = \{ | 1 + (\mu_r' - j\mu_r'' - 1)F_a | (1 - F_a) \}^{1/2}, \quad (11)$$

where the real and imaginary components μ_r' and μ_r'' have been substituted for complex μ_r. It is shown in Appendix III that a maximum Z_c is obtained for $F = F_0$, where:

$$F_0 = \frac{|\mu_r|^2 - 5\mu_r' + 4 \pm \sqrt{|\mu_r|^4 + 9(\mu_r')^2 - 8|\mu_r|^2 - 2|\mu_r|^2\mu_r'}}{4[|\mu_r|^2 - 2\mu_r' + 1]}. \quad (12)$$

This equation is a bit too unwieldy for application, but it is interesting to note that if μ_r is assumed entirely real then (12) becomes

$$F_0 = \frac{\mu_r' - 2}{2[\mu_r' - 1]}, \quad (13)$$

$$F_0 = \frac{-1}{\mu_r' - 1}. \quad (14)$$

The first of these solutions would be expected from (9a), and the second is unimportant.

On the other hand, if μ_r is assumed entirely imaginary —a good approximation for most ferrites at VHF and UHF (see Fig. 5)—(12) becomes

$$F_0 = \frac{(\mu_r'')^2 + 4 \pm \mu_r''\sqrt{(\mu_r'')^2 - 8}}{4[(\mu_r'')^2 + 1]}. \quad (15)$$

A maximum exists only if $\mu_r'' \geq \sqrt{8}$, but this includes most of the cases of practical interest. If μ_r'' is larger than ten (see Fig. 5), then to a fair approximation, either

$$F_0 \doteq \frac{(\mu_r'')^2 + 2}{2(\mu_r'')^2} \doteq \frac{1}{2}, \quad (16)$$

or

$$F_0 \doteq \frac{1}{(\mu_r'')^2}. \quad (17)$$

Only the first case (16) includes enough core material to give good low-frequency response. Thus, it is fairly safe to conclude from (16) and (10) that a maximum $|Z_c|$, circular cylindrical core is about half filled ($F = 0.5$), provided that either μ_r or μ_r'', and ϵ_r are reasonably large.

The Biconical Coaxial Cavity

It may be shown that by the substitution of variable

$$r = \tan\frac{\theta}{2}, \quad (18)$$

the equation for the characteristic impedance, Z_{cb}, of the conical cavity [Fig. 4(b)] may be written at once by reference to (6a) and (6b) as

$$Z_{cb} = \left\{ \frac{\eta}{2\pi} \ln \left[\frac{\tan\frac{\theta_4}{2}}{\tan\frac{\theta_1}{2}} \right] \right\} \left\{ [1 + (\mu_r - 1)F_b] \left[1 + \left(\frac{1}{\epsilon_r} - 1 \right) F_b \right] \right\}^{1/2}, \quad (19)$$

where

$$F_b = \left[\ln \left[\frac{\tan\frac{\theta_3}{2}}{\tan\frac{\theta_2}{2}} \right] \right] \left[\ln \left[\frac{\tan\frac{\theta_4}{2}}{\tan\frac{\theta_1}{2}} \right] \right]^{-1}. \quad (20)$$

Reference to Fig. 4 shows that $\theta_4/2$ is $\pi/4$ for this figure. The usual case of interest will be the biconical cavity [see Fig. 1(c) or 1(d)] whose characteristic impedance $\bar{Z}_{cb}$ is given by the relationship

$$\bar{Z}_{cb} = 2Z_{cb}. \quad (21)$$

If Z_{cb} is normalized in terms of the characteristic impedance of a free space filled line, one obtains the same equation as previously (with F_b instead of F_a), and all the arguments which have preceded pertain equally well here. In similar fashion this same argument would pertain to any uniform cavity (assuming only a TEM mode), with the appropriate modification of the filling factor F.

Calculations on Core Impedance

To calculate core impedances over the wide frequency range which these transformers are capable of achieving, it is required to know both the complex permeability μ_r and the complex permittivity ϵ_r over larger frequency ranges than published to date for most ferrite materials. Possibly the widest range of information is available for Ferroxcube 102 material [7], [8] (also designated as IVA). Fortunately, this material appears to be a good ferrite for balun transformer application.[1] The values of μ_r', and μ_r'' for this material (and others) are shown plotted in Fig. 5. Values of $|\mu_r|$ and $|\epsilon_r|$ for 102 are shown plotted in Fig. 6. The available data on μ_r extended from 10^{-1} to 3000 mc [7], [8], but the data on ϵ_r extended only up to 100 mc [7]. The variation of ϵ_r with frequency is slow and regular, so it was felt justified to extrapolate the ϵ_r curves by two decades, as was done in Figs. 6 and 7. One may represent μ_r and ϵ_r by

$$\mu_r = |\mu_r| \angle -\delta_\mu, \quad (22a)$$

[1] This is true even though the manufacturer recommends this material for general use at frequencies *below* 500 kc.

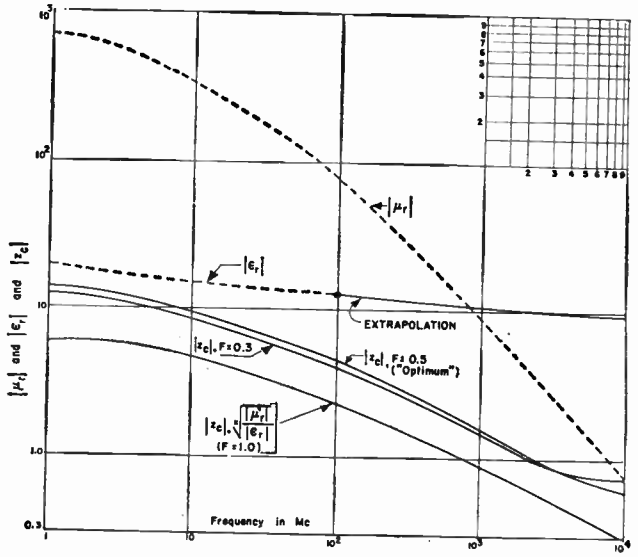

Fig. 6—$|\mu_r|$, $|\epsilon_r|$, and $|Z_c|$ for Ferroxcube 102 (IVA) as a function of frequency.

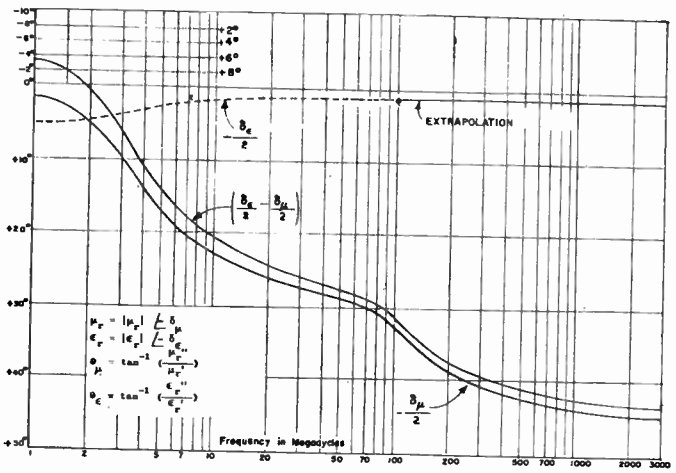

Fig. 7—$\delta_\mu/2$ and $\delta_\epsilon/2$ for Ferroxcube 102 (IVA) as a function of frequency.

and

$$\epsilon_r = |\epsilon_r| \angle -\delta_\epsilon . \tag{22b}$$

The loss angles δ_μ and δ_ϵ are shown plotted in Fig. 7 for 102 material.

One may now derive the input impedance to a cavity transmission line using these parameters. This input impedance is given by

$$Z_{\text{in}} = Z_{ca} \tanh \Gamma l, \tag{23}$$

where Z_{ca} is the characteristic impedance of the cavity (as discussed previously), l is the length of the line (or depth of the cavity), and Γ is the complex propagation constant. In terms of the complex inductance and capacity per unit length, Γ may be expressed as

$$\Gamma = \omega\sqrt{L_{ca}C_{ca}}, \tag{24}$$

where L_{ca} and C_{ca} may be expressed in terms of (4) and (5) to become

$$\Gamma = \omega[\mu_r\epsilon_r]^{1/2}\left[\frac{1 + (\mu_r - 1)F}{1 + \left(\frac{1}{\epsilon_r} - 1\right)F}\right]^{1/2}, \tag{25a}$$

or using the definitions 7(a) and 7(b),

$$\Gamma = \frac{2\pi}{\lambda}[\mu_e\epsilon_e]^{1/2}. \tag{25b}$$

Substituting (25b) and (6a) in (23), the equation for the input impedance (23) becomes (for the coaxial cylindrical cavity)

$$Z_{\text{in}} = \left[\frac{\eta}{2\pi}\ln\frac{r_4}{r_1}\right]\left[\frac{\mu_e}{\epsilon_e}\right]^{1/2}\tanh\left[\frac{2\pi l}{\lambda}(\mu_e\epsilon_e)^{1/2}\right]. \tag{26}$$

The form of (26) makes it convenient to plot the half-loss angle of μ_r and ϵ_r, as was done in Fig. 7. The second and third factors are considered one at a time. The second factor has been defined as normalized characteristic impedance, Z_c, in the previous section, and its magnitude is shown plotted in Fig. 6 for 102 material and various values of F. It is seen that above approximately 800 mc the ferrite material *diminishes* the characteristic impedance of the line, if the line is entirely filled with ferrite. On the other hand, if the filling factor is 0.5 (the optimum over most of the frequency range), the ferrite enhances the characteristic impedance of the line up to a much higher frequency—2.5 kmc—as may be seen from Fig. 6. Note that over most of the frequency range the $F=0.5$ line will have nearly double the characteristic impedance of the $F=1.0$ line. At frequencies above perhaps 3.0 kmc, the assumptions of the foregoing section (large μ_r or μ_r'') no longer pertain, and higher values of characteristic impedance are obtained by going to smaller values of F. As an example, the $F=0.3$ curve is also plotted in Fig. 6.

The importance of the characteristic impedance is dominant only if the cavity-line is large in wavelengths; diminishing the filling factor raises the frequencies for which this is true. Thus, at the lower end of the frequency range it is required to examine the effect of the third factor of (26). In order to tie this factor down to specific frequencies, it was necessary to decide upon a specific length of line. One inch was chosen because a number of commercial ferrite toroids were available in this height. The factor Γl for this one-inch cavity-line is shown plotted (on a Smith Chart) in Fig. 8 for the same three values of filling factor previously considered ($F=0.3$, 0.5, 1.0), again assuming 102 ferrite material. Also, $\tanh \Gamma l$ for a free space filled line ($F=0$) is shown plotted (on the periphery of the Smith Chart) for comparison of the relative "wrap around." Note that as F becomes small ($F=0.3$), $\tanh \Gamma l$ approaches more and

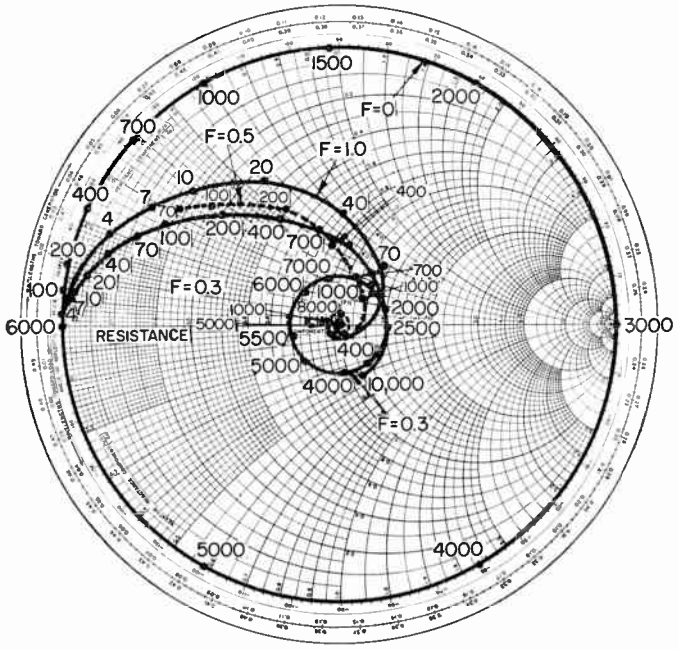

Fig. 8—Tanh Γl for a one inch long (102) ferrite-filled cavity-line.

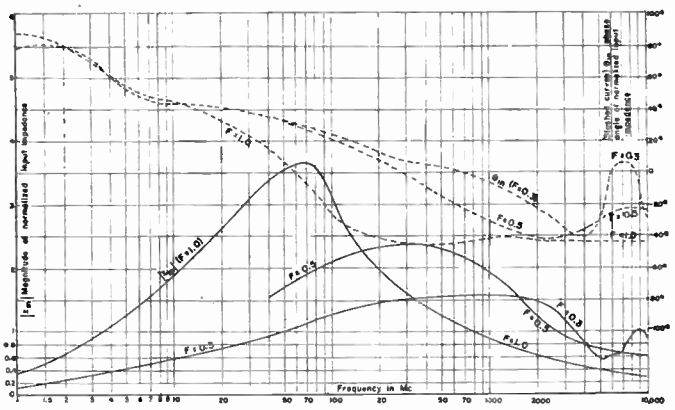

Fig. 9—Normalized input impedance to a one inch long ferrite-filled cavity-line.

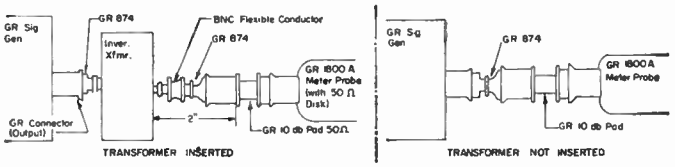

Fig. 10—Measurement circuits for insertion loss.

more closely the behavior of an air-filled line. It is clear that if operation must be extended to low frequencies, then decreasing F will eventually hurt more by decreasing tanh Γl than it aids by increasing Z_c.

Unfortunately, there is no way to compare the relative importance of these effects other than to work out specific examples; this was done. Let the product of the second two factors of (26) be defined as the normalized input impedance, $\overline{Z}_{in}$, of the cavity-line, where

$$Z_{in} = Z_c \tanh \Gamma l = \sqrt{\frac{\mu_e}{\epsilon_e}} \tanh \left[\frac{2\pi l}{\lambda} \sqrt{\mu_e \epsilon_e} \right]. \quad (27)$$

Both magnitude, $|\overline{Z}_{in}|$, and phase angle, θ_{in}, of $\overline{Z}_{in}$ are shown plotted in Fig. 9, for the same values of F as previously, by using the data of Fig. 6 to Fig. 8. Each value of F is clearly superior in certain frequency ranges, but on the whole, smaller values of F tend to give flatter curves and hence broader band transformers. Reference to Fig. 8 shows that this tendency cannot continue much beyond $F=0.3$, as resonance effects become increasingly more evident as F decreases further. Note that the ferrite does not greatly enhance the characteristic impedance of the corresponding free space filled cavity-line; its chief value is in increasing the electrical length of the line and in damping out the resonance effects which would otherwise cause short circuits of the transformer at the resonant frequencies.

If only moderately wide bandwidths are required, it would appear feasible to use a quite low value of filling factor and to make the line just long enough to be antiresonant at the center of the band. It should be possible to obtain relatively large values of $\overline{Z}_{in}$ by this technique, compared to the curves of Fig. 9, and to reduce transformer insertion loss accordingly. The curves of Fig. 9 make it clear how one must pay for increased bandwidth with increased insertion loss.

Various Types of Experimental Transformer Configurations and Insertion Loss Measurements

Four experimental transformers were built and checked for frequency response. Only the last of these is described here in detail.

The measurement circuit used is shown in Fig. 10. This circuit is not capable of giving insertion loss measurements with a very high order of accuracy, but is justified since it made possible a very large number of measurements, over a very wide frequency range, with a reasonable amount of effort. Note that the measurements were actually made on a phase inverter transformer, not a balun, and that the cross-connecting rod for the noninverted output terminal was removed. The lack of a suitable 400-ohm balanced load or generator necessitated this procedure. There is every reason to believe, however, that the insertion loss for equivalent phase inverter and balun transformers would be the same.

The GR 1800A VTVM probe (with its 50-ohm disk) does not present a resistive termination to the line at the high frequencies involved, nor are the absolute readings of the meter of any significance at the high end of the frequency range. However, it is felt that by using the resistive pad attenuator and relying only on the relative meter readings (of nearly the same value) that the measurements are meaningful.

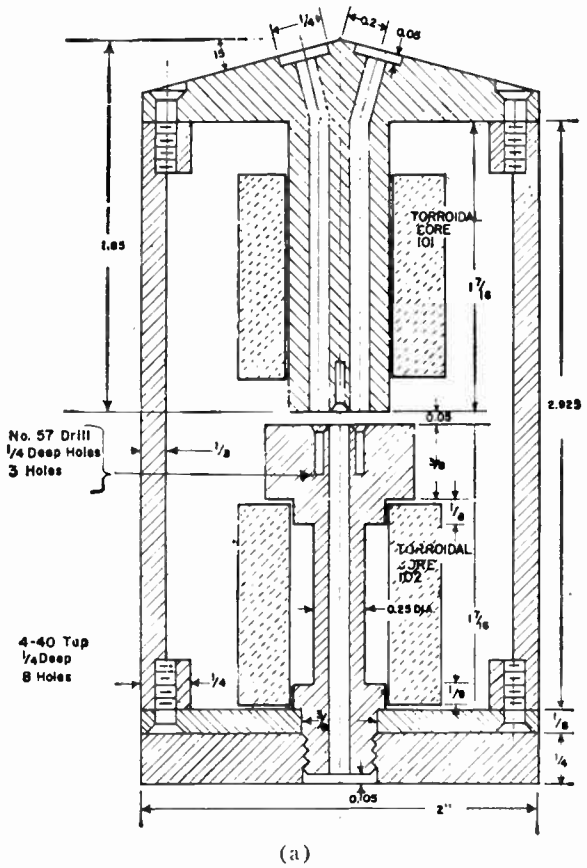

(a)

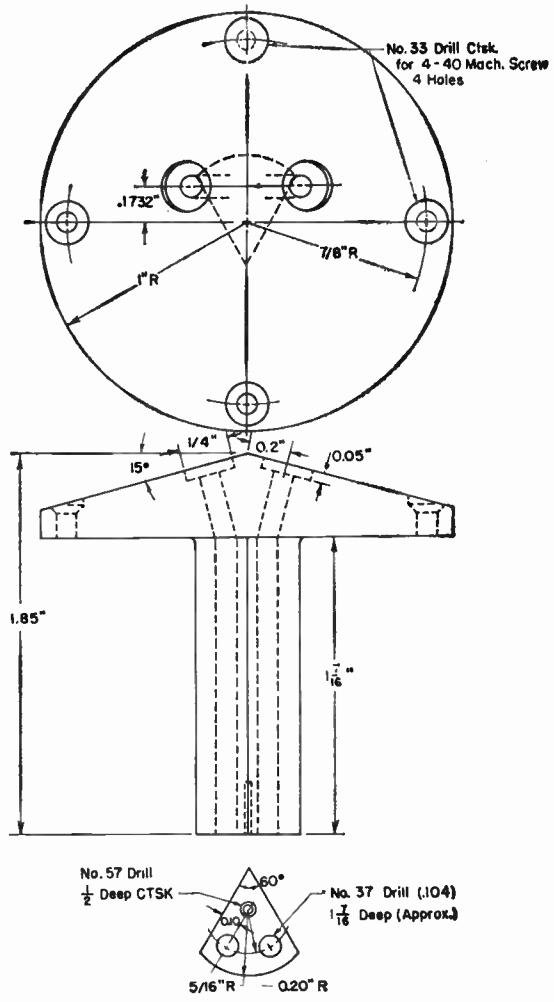

(b)

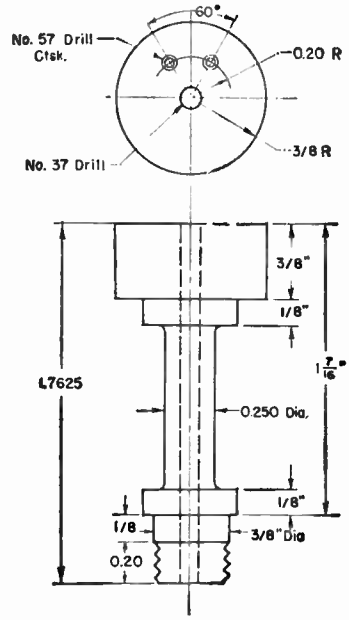

(c)

Fig. 11—Balun transformer (Mark IV).

The transformer to be described (Mark IV) is the most complicated of the four and probably the best, since it is smaller, has less weight, and has a wider bandwidth than the others [14]. Reference to Fig. 11(a) shows that the Mark IV cavity design incorporates two coaxial cylindrical cavities of the type previously shown in Fig. 4(a). The top cavity was partially filled with Ferroxcube 101 ferrite, which has an appreciably higher $|\mu_r|$ than 102 at frequencies up to 30 mc, while the bottom cavity was filled with 102 ferrite. The wedge-cylindrical shaped center conductor of the upper cavity of Fig. 11(b) made it difficult to calculate a filling factor, but this factor is estimated to be about 0.45, while the free-space characteristic impedance is estimated to be 92 ohms. The filling factor for the mid-section of the bottom cavity is 0.356, while its free-space characteristic impedance is 117 ohms. Note that the internal coaxial lines were quite small in this unit. This served to make the effective radii of the inner conductors of both cavity lines small, raising their characteristic impedance. In order to leave room to affix two BNC connectors, side by side, it was required to bring the two upper internal transmission lines out in the Y shape shown in Fig. 11(a) to meet these connectors.

The insertion loss measurements which were made on this transformer are shown in Fig. 12, together with

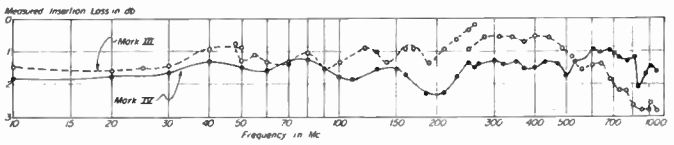

Fig. 12—Insertion loss for Mark III and Mark IV transformers.

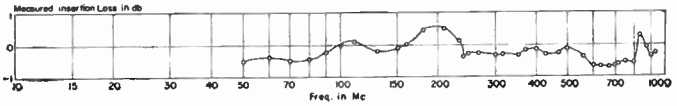

(a)

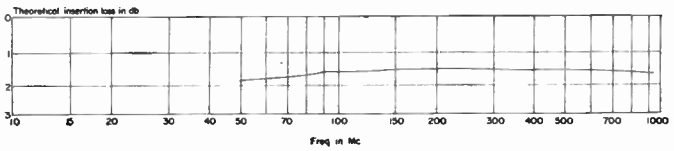

(b)

Fig. 13—(a) Difference between theoretical and experimental values, Mark IV. (b) Insertion loss for Mark IV, theoretical values.

those of another transformer (Mark III) unit for comparison. The general tendency predicted by the curves of Fig. 9 is in evidence here; namely, that the Mark IV unit, for which F is relatively small, gives improved performance at the high-frequency end (UHF) but tends to be somewhat more lossy over the low end (VHF) than the Mark III unit, with a larger value of F. Also shown [Fig. 13(b)] is a curve of insertion loss calculated from Fig. 8 and Fig. 3. Good agreement is obtained, inasmuch as the range of values in concerned. The variance in the shape of the curves points out the errors inherent in the lumped constant circuit approximation and the measuring technique.

Balance-to-Unbalance Measurements (Balun Efficiency) and Input Impedance Measurements

Fig. 14 presents the data obtained on balance-to-unbalance ratio for the Mark IV Balun transformer, and the methods used to obtain this data.

For the low-frequency range, no difficulty was observed in measuring the balance-to-unbalance ratio directly, as shown in Fig. 14.

The data for the middle frequency range were obtained in a similar manner to that of the low-frequency range. However, much more care was required in such matters as matching of cable lengths, termination of the cables in their characteristic impedance, etc. Also, different signal generators and voltmeters were required because of the difficulty in obtaining a single set of signal generators and meters to cover the entire frequency range.

The high-frequency [12], [13] range data were obtained by the use of an entirely different procedure, as is demonstrated by Fig. 14(c). In this frequency range,

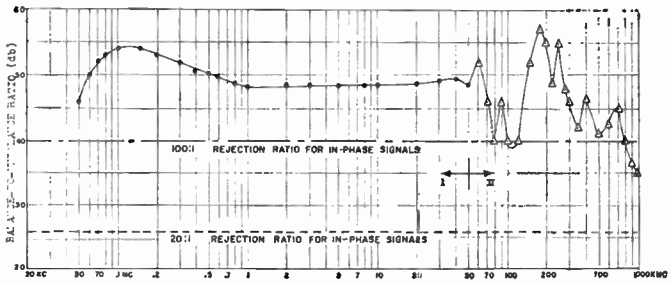

(a)

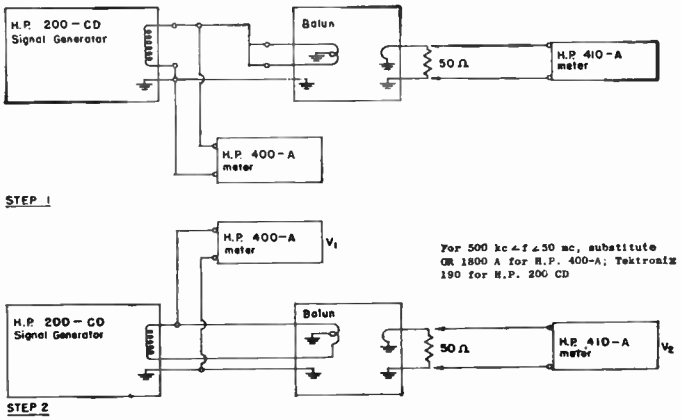

(b)

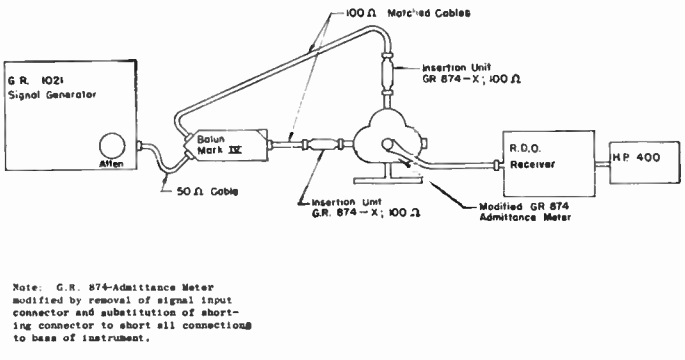

(c)

Fig. 14—(a) Mark IV balance-to-unbalance measurements (balun efficiency). (b) Circuit used for measuring balance-to-unbalance ratio (50 kc $< f <$ 50 mc). (c) Circuit used for measuring balance-to-unbalance ratio (50mc $< f <$ 1000 mc).

any departure from matched conditions, either in the electrical lengths of the cables or in the termination of these cables in their characteristic impedance, results in quite large errors in the data obtained. By the use of a General Radio Type 1602A Admittance Meter, modified to measure the currents in the transmission lines on the balance side of the balun (both the in-phase and the out-of-phase components of the line currents can be measured by moving the "susceptance" lever through 180 degrees) and to terminate the cables in their characteristic impedance (100 ohms), data were taken of the balance-to-unbalance ratio over the upper end of the frequency range.

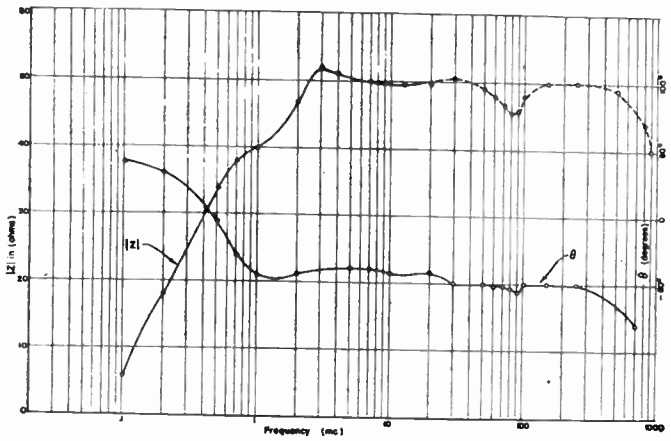

Fig. 15—Input impedance of balun transformer, Mark IV.

As can be seen from Fig. 14, the balance-to-unbalance ratio is well above 20:1 over the entire frequency range of 50 kc to 1000 mc and well above 100:1 from 50 kc to 800 mc. The erratic behavior of the curve near the upper end of the frequency range is most likely due, at least in part, to the rather imperfect measuring techniques which were used. Even then, the rejection of in-phase signals is at worst quite adequate for many uses.

Fig. 15 shows the input impedance of the Mark IV Balun Transformer as a function of frequency. Although the balance-to-unbalance ratio is good over the lower frequency range, it is evident that the input impedance drops quite rapidly below 2 mc. While it is true that the problem of standing waves on transmission lines is not as acute at the lower frequencies, maximum power transfer is important, nevertheless. In order to improve the input impedance at the low frequencies, the insertion of a washer-shaped piece of laminated permalloy would be applicable, possibly extending the range of usable input impedance to the audio range.

Conclusions

Some of the more important conclusions reached in the course of this work were as follows.

1) It is possible to employ gainfully closed magnetic cores in transformers at frequencies from ten to one hundred times greater than is commonly thought possible.
2) One may obtain enormous extensions of bandwidth with the sacrifice of a few db in insertion loss, compared to more conventional resonant structure balun transformers.
3) The transition structures used for balance-to-unbalance transformation do indeed have very-wide-band properties.

It was felt that the limitations on the measured balance-to-unbalance and insertion loss performance were in many cases (over the frequency range), set by the measuring technique rather than by the device itself.

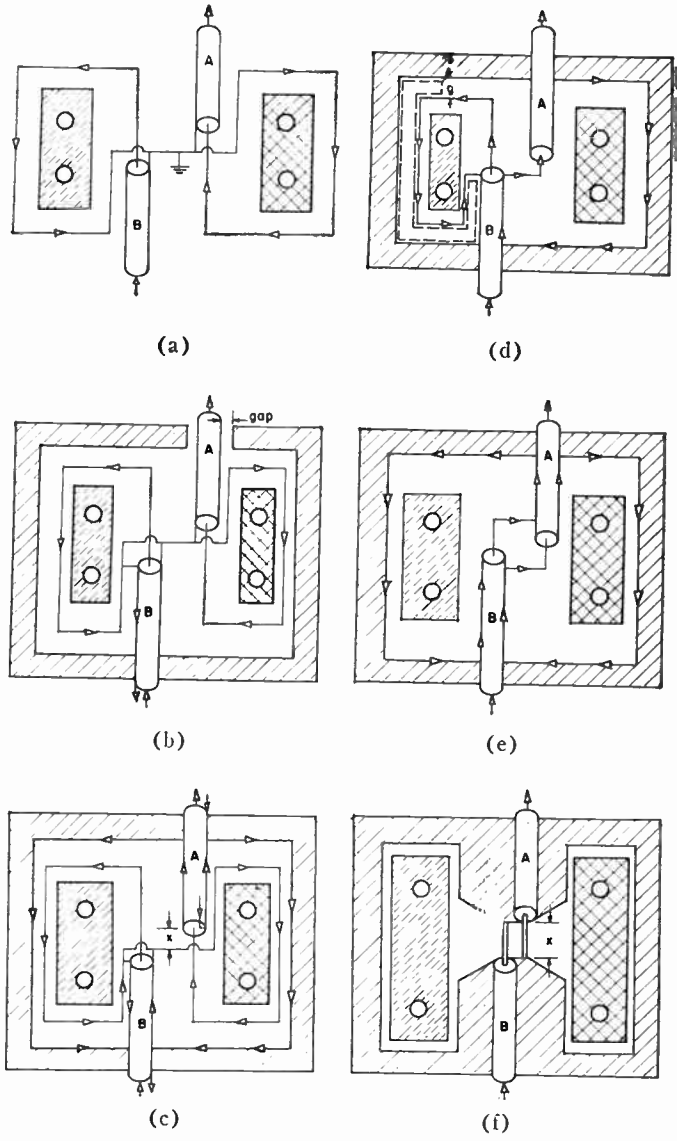

Fig. 16—Development of phase inverter (or balun) transformer from a conventional transformer.

Appendix I

Development of Phase Inverter (or Balun) Transformer from a Conventional Transformer

One way of showing the development of this transformer from a conventional two-turn phase inverter transformer is presented in Fig. 16. Fig. 16(a) shows two transmission lines coupled to a two-turn phase inverter transformer of rather conventional construction. The center tap is connected to the outer casing of both transmission lines. The turns are wound on a magnetic toroid (shown in cross section) and for the moment may be considered as thin copper tape. Fig. 16(b) illustrates an attempt to encase the unit in a conducting housing. It is seen that a nonconducting gap must be introduced in order to prevent the housing and the outer conductors of the transmission lines from completing a conducting path around the core, *i.e.*, acting as a shorted turn. This

gap, at this location, presents several disadvantages; among these is poor shielding action.

In Fig. 16(c), the original gap has been closed and instead an open circuit has been introduced internally at point X to prevent the shorted turn action. This is a "split screen" transformer such as has been described in more conventional forms [10], [11]. Shielding is now complete; however, a new phenomenon has been introduced. It can be seen by tracing a line integral path from the outer conductor of transmission line B into the inner conductor of this same line that, in effect, the core has been encircled twice, *i.e.*, the transformer now has a one-to-two turns ratio. One of these turns (for line A) can be eliminated by the expedient of the connections shown in Fig. 16(d). In this figure, it is seen that the case itself has been made to replace a winding.

Similarly, it is shown that the case itself can be made to replace the left-hand winding for the transmission line B. If the line integral of the electric field is evaluated around the path shown by the dotted lines in Fig. 16(d), it is seen that the voltage across a typical gap g is proportional to only the leakage flux enclosed; *i.e.*, it is small. By pushing the winding even closer to the case, the leakage flux which is enclosed grows even smaller, as does the gap voltage. In the limit then, the winding can be made coincident with the case without any short circuit phenomenon occurring. The transformer then appears as shown in Fig. 16(e). There is now no *winding* leakage inductance or capacitance whatever.

The lead lengths can be made still shorter by adopting the mode of construction shown in Fig. 16(f), where the only leakage inductance of the transformer is in the connecting leads across the gap, X, and the only significant capacitance is that existing across the gap.

The extension to a balun transformer follows the technique already shown in Fig. 1(c) and 1(d).

Appendix II

Maximization of the Core Impedance, μ_r and ϵ_r Assumed Real

The square of the normalized core impedance is given, from (8), as

$$Z_c^2 = [1 + (\mu_r - 1)F]\left[1 + \left(\frac{1}{\epsilon_r} - 1\right)F\right]. \tag{28}$$

Differentiating with respect to F and equating to zero gives

$$\frac{dZ_c^2}{dF} = (\mu_r - 1)\left[1 + \left(\frac{1}{\epsilon_r} - 1\right)F\right] + [1 + (\mu_r - 1)F]\left[\frac{1}{\epsilon_r} - 1\right] = 0. \tag{29}$$

Collecting terms and solving for F gives F_0, where

$$F_0 = \frac{\mu_r - 2 + \frac{1}{\epsilon_r}}{2\left(1 - \frac{1}{\epsilon_r}\right)(\mu_r - 1)}. \tag{30}$$

The second derivative of Z_c^2 is always negative since $\epsilon_r > 1$, $\mu_r > 1$ for any value of F, so F_0 must be a maximum.

Appendix III

Maximization of the Core Impedance, μ_r Assumed Complex and ϵ_r Assumed Large

Under these assumptions, the fourth power of the core impedance magnitude [using (11)] becomes

$$|Z_c|^4 = [(1 - F + F\mu_r')^2 + (\mu_r'')^2F^2][1 - F]^2. \tag{31}$$

Differentiating with respect to F and equating to zero gives

$$[(1 - F + F\mu_r')(\mu_r' - 1) + (\mu_r'')^2F][1 - F] - [(1 - F + F\mu_r')^2 + (\mu_r'')^2F^2] = 0. \tag{32}$$

Simplifying and collecting terms gives

$$[(1 - F)(\mu_r' - 1) - F\mu_r' + F|\mu_r|^2][1 - F] - [(1 - F)^2 + 2(1 - F)F\mu_r' + F^2|\mu_r|^2] = 0. \tag{33}$$

After collecting terms in descending powers of F, there results

$$2[-|\mu_r|^2 + 2\mu_r' - 1]F^2 + [|\mu_r|^2 - 5\mu_r' + 4]F + \mu_r' - 2 = 0. \tag{34}$$

Solving for F gives F_0,

$$F_0 = \frac{|\mu_r|^2 - 5\mu_r' + 4 \pm \sqrt{|\mu_r|^4 + 9(\mu_r')^2 - 8|\mu_r|^2 - 2|\mu_r|^2\mu_r'}}{4[|\mu_r|^2 - 2\mu_r' + 1]}.$$

Acknowledgment

The authors wish to give acknowledgment to Robert W. Walton, of the Ground Systems Laboratories, Hughes Aircraft Company, who worked out many of the construction details involved in the experimental transformers while he was at the University of Illinois.

Bibliography

[1] E. G. Fubini and P. J. Sutro, "A wide-band transformer from an unbalanced to a balanced line," Proc. IRE, vol. 35, pp. 1153–1155; October, 1947.

[2] R. D. Bogner, "Balun for UHF television," *Radio and Telev. News*, vol. 51, pp. 5–7; January, 1954.

[3] I. A. D. Lewis, "A transmission line pulse inverter," *Rev. Sci. Instr.*, vol. 23, p. 769; December, 1952.

[4] R. W. Rochelle, "A transmission line pulse inverter," *Rev. Sci. Instr.*, vol. 23, pp. 298–300; June, 1952.

[5] J. Smit and H. P. J. Wijn, "Physical properties of ferrites," in "Advances in Electronics," Academic Press, Inc., New York, N. Y., pp. 69–136; 1954.
[6] F. G. Brockman, P. H. Dowling, and W. G. Steneck, "Dimensional effects resulting from a high dielectric constant found in a ferromagnetic ferrite," *Phys. Rev.*, vol. 77, pp. 85–93; January, 1950.
[7] J. J. Went and E. W. Gorter, "The magnetic and electrical properties of Ferroxcube material," *Phillips Tech. Rev.*, vol. 13, pp. 181–193; January, 1952.
[8] H. P. J. Wijn, M. Givers, and C. M. Van der Burgt, "Note on the high frequency dispersion in nickel zinc ferrites," *Rev. Mod. Phys.*, vol. 25, p. 91; January, 1953.
[9] A. Fairweather, F. F. Roberts, and A. J. E. Welch, "Ferrites," *Reps. Progr. in Phys.*, vol. 15, pp. 142–172; 1952.
[10] D. Maurice and R. H. Minns, "Very-wide band radio frequency transformers," *Wireless Eng.*, vol. 24, pp. 168–177; June, 1947, and pp. 209–217; July, 1947.
[11] T. R. O'Meara, "A wide band high frequency transformer using a ferrite core," *Proc. Natl. Electronics Conf.*, vol. 10, pp. 778–790; 1954.
[12] A. C. Sim, "Balance measurements on balun transformers," *Electronics*, vol. 26, pp. 188–191; September, 1953.
[13] A. C. Sim, "Balance Measurements on Balun Transformers," RCA, Rep. No. LB-872; July 22, 1952.
[14] R. L. Sydnor and T. R. O'Meara, "A very wide-band balun transformer for VHF and UHF," University of Illinois, Urbana, Ill., Tech. Rep. No. 9, NONR 1834(02); July, 1957.
[15] W. K. Roberts, "A new wide-band balun," PROC. IRE, vol. 45, vol. 45, pp. 1628–1631; December, 1957.
[16] A. I. Talkin and J. V. Cuneo, "Wide-band balun transformer," *Rev. Sci. Instr.*, vol. 28, pp. 808–815; October, 1957.

Nomographs for Designing Elliptic-Function Filters*

KEITH W. HENDERSON†, MEMBER, IRE

Summary—**The elliptic-function filter is of considerable importance because of its ability to provide simultaneously small pass band ripple, large stop band attenuation, and very sharp cutoff, with equal-ripple behavior in both the pass band and the stop band.**

The fundamental design parameters are the pass band ripple, the stop band attenuation, the transition bandwidth, and the number of poles required. They are interrelated in a rather complicated way involving certain elliptic functions, so that determination of a compatible set of parameters is both tedious and difficult.

Two nomographs relating these parameters have been devised, by means of which suitable values can be determined easily and quickly. The ranges covered are: pass band ripple, from less than 0.05 up to 3 db; stop band attenuation, from 3 to 40 db (extendable to any value above 40 db simply by renumbering certain scales); transition bandwidth, 0.001 to 1 times the cutoff frequency, and number of poles, 1 to 20.

Once a compatible set of parameters has been determined, the approximation function can be obtained in a straightforward manner. The necessary formulas are given, and the procedure for evaluating them is described briefly.

Characteristics of Elliptic-Function Filters

THE elliptic-function filter is of considerable importance because of its ability to provide simultaneously small pass band ripple, large stop band attenuation, and sharper cutoff than can be obtained with other conventional types, with equal-ripple behavior in both the pass band and the stop band. The price paid for these advantages, from the designer's viewpoint, is considerably more work in obtaining a suitable approximation function—partly because of the greater number of fundamental design parameters to be specified or determined and partly because of certain computational difficulties, such as inadequate tables of the elliptic functions and the necessity of resorting to infinite series.

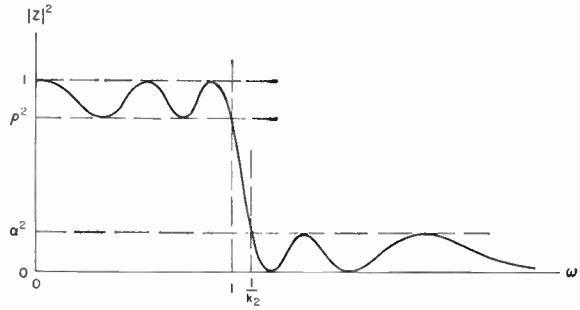

Fig. 1—Typical transmission characteristics of normalized low-pass elliptic-function filter ($n=5$).

The transmission characteristics of a normalized low-pass elliptic-function filter are defined in Fig. 1. The pass-band ripple and stop-band attenuation in decibels, $\bar{\rho}$ and $\bar{\alpha}$, are related to these transmission characteristics in the following way. Considering ρ^2 and α^2 with respect to unity,

$$\bar{\rho} = -10 \log \rho^2 \tag{1}$$

$$\bar{\alpha} = -10 \log \alpha^2. \tag{2}$$

Thus, if $\bar{\rho}$ and $\bar{\alpha}$ are specified (in db),

$$\rho^2 = 10^{-0.1\bar{\rho}} \tag{3}$$

$$\alpha^2 = 10^{-0.1\bar{\alpha}}. \tag{4}$$

The number of ripples in the pass band and the num-

* Original manuscript received by the IRE, May 12, 1958; revised manuscript received, August 11, 1958.
† Lockheed Aircraft Corp., Palo Alto, Calif.; formerly with Stanford Res. Inst., Menlo Park, Calif.

ber in the stop band are equal, and are determined by the number of poles n. Obviously k_2 is the parameter that defines the sharpness of cutoff or selectivity of the filter.

(Although it has been modified somewhat for simplicity, the notation used here is based on a report by Fano,[1] which differs in certain unessential details from that of other authors. Fano defines the limits of the transition band as 1 and $1/k_2$ on a frequency scale ω, while some authors define them as $\sqrt{k_2}$ and $1/\sqrt{k_2}$ on a frequency scale $\omega'=\omega/\omega_0=\omega/\sqrt{\omega_1\omega_2}$, with $\omega_0^2=\omega_1\omega_2=1/k_2$ and $\omega_1/\omega_2=k_2$. It is easily verified that the definitions are identical.)

In the application of elliptic functions, it turns out that ρ and α determine a constant[2]

$$k_1=\left[\frac{\frac{1}{\rho^2}-1}{\frac{1}{\alpha^2}-1}\right]^{1/2}, \tag{5}$$

which is then related to k_2 by

$$q(k_1)=|q(k_2)|^n. \tag{6}$$

where q is a certain elliptic function called the "nome" or "modular constant" of k_1 or k_2, whose exact nature is not of importance at this point.

Broadly, the task of obtaining the desired approximation function may be divided into two parts. The first part consists of obtaining suitable values of ρ, α, n, and k_2 which satisfy (5) and (6). The second part consists of using these data to obtain the poles and zeros by means of other elliptic functions and elliptic integrals. Because of the complicated way in which the parameters are related, it is generally not a simple problem to determine one from the others, and considerable time can be spent in juggling them in order to obtain compatible values. In studying the relations among them, it became evident to the author that a valuable addition to the tools of the designer would be a pair of nomographs by means of which suitable values could be determined easily and quickly.

Use of Nomographs

The nomographs are given in Figs. 2 and 3. The typical use of Fig. 2 is illustrated in Fig. 4. If $\bar{\rho}$ and $\bar{\alpha}$ are specified (in db) it is necessary to start from A and B. Vertical lines from these points and horizontal lines through their intersection with the appropriate curves at C and D locate the corresponding points E and F on the vertical scales. If ρ^2 and α^2 are specified (as percentages, for example), the quantities $[(1/\rho^2)-1]$ and $[(1/\alpha^2)-1]$ can be computed easily and the points E and F found directly. A line through E and F then gives the correct value of k_1 at G.

If desired, the scale of $\bar{\alpha}$ can easily be extended by the addition of any multiple m of 40 db since the relation between $\bar{\alpha}$ and $[(1/\alpha^2)-1]$ is very nearly linear for $\bar{\alpha}>40$ db. All that is necessary to change the $\bar{\alpha}$ scale to one extending from $40m$ to $40(m+1)$ db is to multiply the $[(1/\alpha^2)-1]$ scale by 10^{4m} and the k_1 scale by 10^{-2m}. Such a scale extension is not possible with $\bar{\rho}$ and $[(1/\rho^2)-1]$, because the relation between them is not linear, but the range of values of $\bar{\rho}$ covered should be adequate for most cases.

Typical uses of Fig. 3 are illustrated in Fig. 5. If k_1 and n are specified, k_1 is located at A in Fig. 5(a), and a horizontal line is drawn intersecting the k_1 curve at B, from which point a vertical line is drawn to the specified n line at C. A horizontal line through this point intersects the $[(1/k_2)-1]$ curve at D. Finally, a vertical line from this point locates a value of $[(1/k_2)-1]$ at E, from which k_2 can be easily computed.

If k_2 and n are specified, the procedure is the same in reverse, first locating $[(1/k_2)-1]$ at E, then proceeding from E to D, to C, to B, to A, thus determining k_1.

Fig. 5(b) shows a different situation, in which k_1 and k_2 are tentatively specified with n to be determined. The vertical line through C and the horizontal line through D will intersect at E, which will generally lie somewhere between two n lines. In this case it will be necessary to decide which of the nearest n values to use, and either k_1 or k_2 or both must be adjusted slightly so that the intersection at E will fall on the n line chosen.

(See the following section regarding the scales involving q_1 and q_2.)

Construction of Nomographs

The construction of Fig. 2, which relates $\bar{\rho}$, ρ^2, $\bar{\alpha}$, α^2, and k_1 by (1)–(5) above, deserves no explanation here, for it is straightforward and well covered by numerous textbooks on nomography. The construction of Fig. 3, relating k_1 to k_2 and n in accordance with (6), is considerably more complicated because of the nature of the nome q.

The nome is defined as

$$q(k)=\exp-\pi\left[\frac{K(k')}{K(k)}\right] \tag{7}$$

where K is the complete elliptic integral of the first kind.[3-5] Its "modulus" k and the "complementary modulus" k' are related by

$$k^2+k'^2=1. \tag{8}$$

[1] R. M. Fano, "A Note on the Solution of Certain Approximation Problems in Network Synthesis," Res. Lab. of Electronics, Mass. Inst. Tech., Cambridge, Mass., Tech. Rep. No. 62; April 16, 1948.

[2] A. J. Grossman, "Synthesis of Tchebycheff parameter symmetrical filters," Proc. IRE, vol. 45, pp. 454–473; April, 1957.

[3] F. S. Woods, "Advanced Calculus," Ginn and Co., New York, N. Y., ch. 16; 1934.

[4] P. F. Byrd and M. D. Friedman, "Handbook of Elliptic Integrals for Engineers and Physicists," Lange, Maxwell and Springer, Ltd., New York, N. Y., pp. 8–18; 1954.

[5] E. Jahnke and F. Emde, "Tables of Functions," Dover Publications, New York, N. Y., 4th ed., ch. 5; 1945.

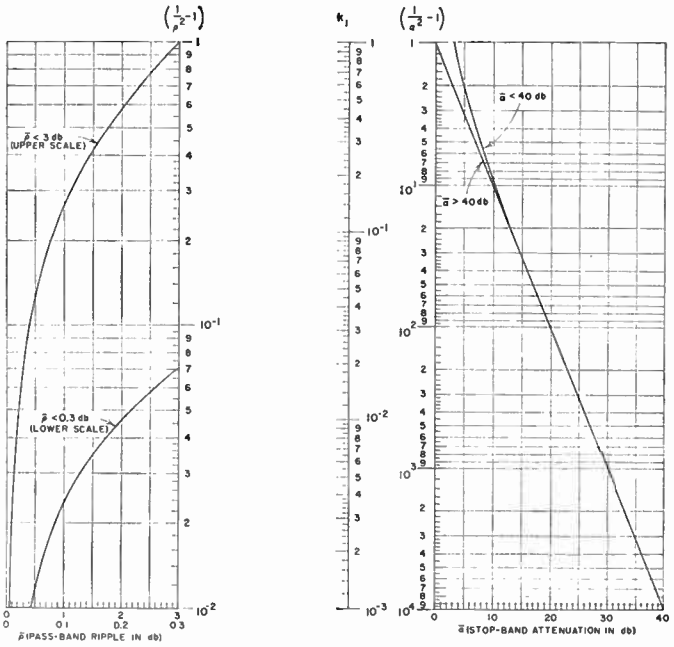

Fig. 2—Nomograph relating $\bar{\rho}$, ρ^2, $\bar{\alpha}$, α^2, and k_1.

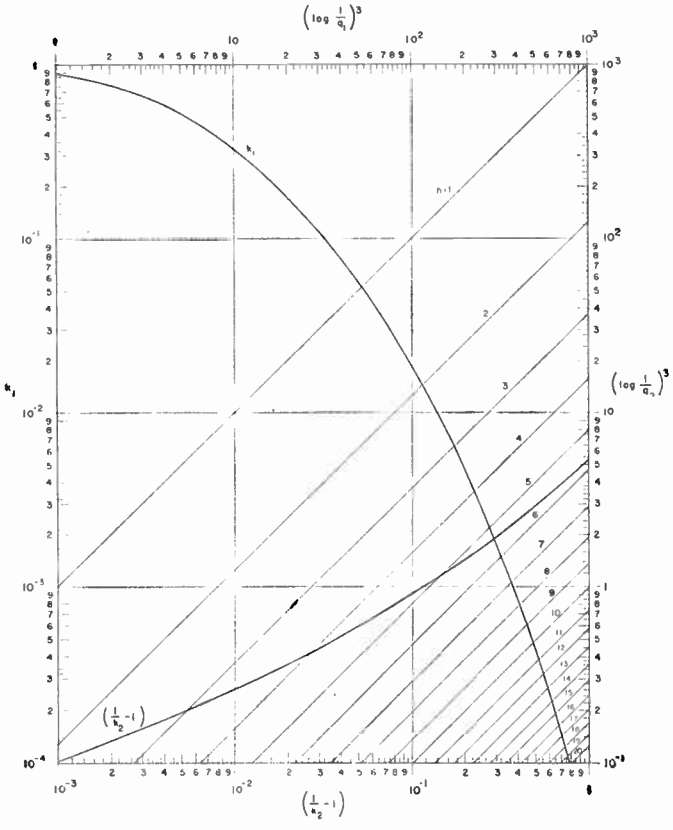

Fig. 3—Nomograph relating k_1, k_2, and n.

In accordance with (6) the modulus may be either k_1 or k_2. For brevity, it is convenient to employ the commonly used abbreviations $q_1=q(k_1)$, $q_2=q(k_2)$, $K_1=K(k_1)$, $K_2=K(k_2)$, $K_1'=K(k_1')$, and $K_2'=K(k_2')$.

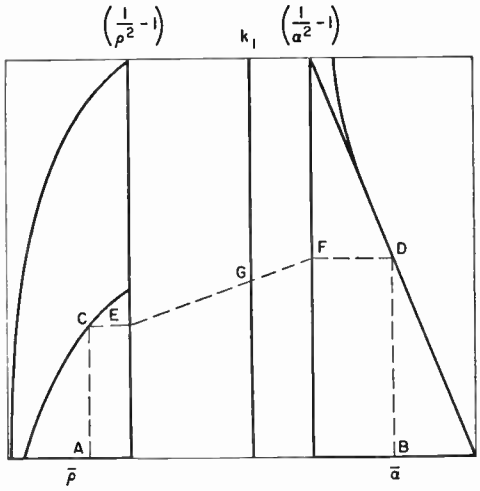

Fig. 4—Typical use of nomograph in Fig. 2.

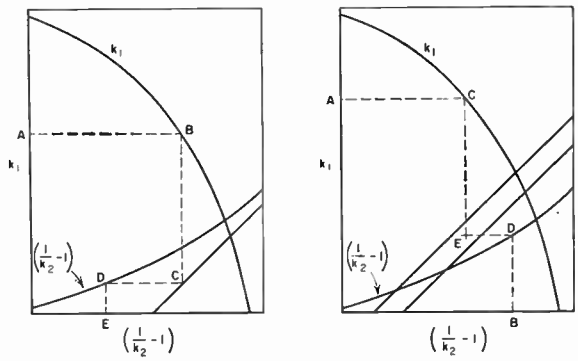

Fig. 5—Typical use of nomograph in Fig. 3. (a) k_1 and n specified, k_2 unknown; (b) k_1 and k_2 specified, n unknown.

The functions q, K, and K' have all been tabulated.[6,7] It will be noticed from the tables that as k_1 becomes small q_1 decreases so rapidly that accurate interpolation becomes impossible, but for $k_1<0.1$ it is entirely satisfactory to use the approximation[8]

$$q_1 \approx \frac{k_1^2}{16}. \tag{9}$$

On the other hand, for sharp cutoff k_2 is near unity and it becomes necessary to resort to an infinite series in order to obtain q_2 accurately.[9,10] Fortunately, some of the series for q converge very rapidly.

If (6) is written in logarithmic form and plotted on log-log coordinates, q_1 and q_2 are related by a set of straight lines corresponding to the values of n. For computational convenience the members of (6) were first inverted. For purposes of scale-length adjustment the logarithms were then raised to an arbitrary (inte-

[6] Byrd and Friedman, *op. cit.*, pp. 322–323.
[7] Jahnke and Emde, *op. cit.*, ch. 4 and 5.
[8] Byrd and Friedman, *op. cit.*, p. 11, item 112.04.
[9] *Ibid.*, p. 299, items 901.00, 901.01.
[10] Jahnke and Emde, *op. cit.*, ch. 4, p. 43, item 6.

gral) power a. The straight lines in the nomograph of Fig. 3 are therefore defined by

$$\left(\log \frac{1}{q_1}\right)^a = n^a \left(\log \frac{1}{q_2}\right)^a \tag{10}$$

for log-log coordinates, corresponding to

$$a \log \log \frac{1}{q_1} = a \log n + a \log \log \frac{1}{q_2} \tag{11}$$

for linear coordinates.

It was found more convenient to work with $[(1/k_2)-1]$, which is the width of the transition band, instead of k_2 itself. Thus, Fig. 3 is essentially a superposition of k_1 vs $[\log (1/q_1)]^a$, $[\log (1/q_2)]^a$ vs $[(1/k_2)-1]$, and (10) for different values of n, plotted on compatible scales with $a=3$. Once k_1, k_2, and n have thus been related, the scales for $[\log (1/q_1)]^a$ and $[\log (1/q_2)]^a$ are no longer needed. They have been included in Fig. 3 merely for reference, but may be completely ignored in the use of the nomographs.

Approximation Function

In order to obtain the behavior expected from this type of filter, it generally is necessary to specify the poles and zeros quite precisely. The nomographs enable one to choose a tentative set of parameter values, but the values thus obtained are not sufficiently accurate for the actual filter design. Therefore, it is essential that the designer establish them accurately by means of tables and/or series, and to make sure that they are compatible in accordance with (5) and (6), before evaluating the formulas leading to the approximation function. Once he has done that, he can proceed in a straightforward manner to obtain the approximation function. Except for the slight adjustment in some of the parameter values that may be necessary at this point, the nomographs eliminate the extensive trial-and-error procedure previously necessary in obtaining a compatible set of values.

For the approximation function it is necessary to distinguish between the cases of n even and n odd. In both cases the zeros are on the $j\omega$ axis of the p plane (where $p=\sigma+j\omega$), and the poles occur in conjugate pairs in the left half plane, with an additional pole on the negative real axis (hence a zero at infinity) in the case of n odd. The approximation function is written conveniently as[11]

$$Z(p) = \begin{cases} M \prod_{i=1}^{n/2} \left[\dfrac{\left(p+j\dfrac{1}{\eta_i}\right)\left(p-j\dfrac{1}{\eta_i}\right)}{\left(p+\dfrac{\mu_i}{\xi_i}+j\dfrac{\nu_i}{\xi_i}\right)\left(p+\dfrac{\mu_i}{\xi_i}-j\dfrac{\nu_i}{\xi_i}\right)} \right] & (n \text{ even}) \\ \dfrac{M}{\left(p+\dfrac{\mu_{(n+1)/2}}{\xi_{(n+1)/2}}\right)} \prod_{i=1}^{(n-1)/2} \left[\dfrac{\left(p+j\dfrac{1}{\eta_i}\right)\left(p-j\dfrac{1}{\eta_i}\right)}{\left(p+\dfrac{\mu_i}{\xi_i}+j\dfrac{\nu_i}{\xi_i}\right)\left(p+\dfrac{\mu_i}{\xi_i}-j\dfrac{\nu_i}{\xi_i}\right)} \right] & (n \text{ odd}) \end{cases} \tag{12}$$

where

$$\eta_i = k_2 \operatorname{sn} (\beta_i, k_2) \tag{13}$$

$$\mu_i = \operatorname{cn} (\beta_i, k_2) \operatorname{dn} (\beta_i, k_2) \operatorname{sn} (\gamma, k_2') \operatorname{cn} (\gamma, k_2') \tag{14}$$

$$\nu_i = \operatorname{sn} (\beta_i, k_2) \operatorname{dn} (\gamma, k_2') \tag{15}$$

$$\xi_i = 1 - \operatorname{dn}^2 (\beta_i, k_2) \operatorname{sn}^2 (\gamma, k_2'). \tag{16}$$

In these equations sn, cn, and dn are the Jacobian elliptic functions.[2,3,12] The modulus k_2 is, of course, one of the design parameters, and k_2' can be determined by means of (8).

The argument

$$\beta_i = \left(\frac{2i-1}{n} - 1\right) K_2 \quad (n \text{ even or odd}) \tag{17}$$

and the argument

$$\gamma = \frac{K_2 F(\phi, k_1')}{n K_1} \quad (n \text{ even or odd}), \tag{18}$$

where K_1 and K_2 are complete elliptic integrals of the first kind, as previously defined. The factor $F(\phi, k_1')$, in which

$$\phi = \sin^{-1} \rho, \tag{19}$$

is the incomplete elliptic integral of the first kind.[2,3,5] If k_1 is sufficiently small,[13]

$$\gamma \approx \frac{2K_2 F(\phi, k_1')}{n\pi}. \tag{20}$$

Finally, the constant multiplier

[11] For n even this expression might be written more compactly by dispensing with the conjugate factors and letting the index i range from 1 to n, but in the case of n odd $\eta_i=0$ for $i=(n+1)/2$ and the numerator would be improper.

[12] Byrd and Friedman, *op. cit.*, pp. 18–29.

[13] *Ibid.*, p. 10, item 111.02.

$$M = \begin{cases} \alpha & (n \text{ even}) \\ \dfrac{K_1'}{\left(\dfrac{1}{\rho^2} - 1\right)^{1/2} K_2'} \cdot & (n \text{ odd}) \end{cases}. \quad (21)$$

The complete and incomplete elliptic integrals and the Jacobian elliptic functions have all been tabulated.[5,14–17] Unfortunately, the tables are often inadequate for sufficiently accurate interpolation and one must use a series.[18–20] If the modulus is sufficiently near zero or unity, the Jacobian elliptic functions may be computed from approximation formulas in closed form involving trigonometric or hyperbolic functions.[21]

[14] *Ibid.*, pp. 321–329.
[15] H. B. Dwight, "Tables of Integrals and Other Mathematical Data," The Macmillan Co., New York, N. Y., revised ed., pp. 234–235; 1947.
[16] G. W. Spenceley and R. M. Spenceley, "Smithsonian Elliptic Functions Tables," Smithsonian Miscellaneous Collections, Smithsonian Institution, Washington, D. C., vol. 109; 1947.
[17] L. M. Milne-Thomson, "Jacobian Elliptic Function Tables," Dover Publications, New York, N. Y.; 1950.

Acknowledgment

The author is indebted to Dr. William H. Kautz of the Stanford Research Institute for his encouragement and valuable suggestions in the development of this paper.

[18] Byrd and Friedman, *op. cit.*, pp. 297–299, 302–305.
[19] Jahnke and Emde, *op. cit.*, ch. 5 and 6.
[20] Dwight, *op. cit.*, pp. 169–172.
[21] Byrd and Friedman, *op. cit.*, pp. 24–25, items 127.01, 127.02.

The Annular Geometry Electron Gun*

JAMES W. SCHWARTZ†, ASSOCIATE MEMBER, IRE

Summary—**The annular geometry gun represents a distinct departure in electron gun design and operation. The modulator section contains an annular cathode, annular control grids and accelerating grids, a beam bending probe and an electron object electrode. Very high modulation sensitivity, inverted modulation characteristics, internal electronic video signal amplification, and automatic "white noise" inversion are among the unique performance features of the annular geometry gun. Beam control is produced by a focus modulation process. The final spot is formed by imaging a geometrical aperture in the object plate. This results in very high resolution capabilities and an optimum focus condition and spot size which are practically independent of beam current.**

Introduction

THE electron guns now employed in kinescopes, cathode-ray tubes, and other beam-type display devices differ only superficially from types employed twenty years ago. Electron gun research, on the other hand, has been active and fruitful during this period.[1] Most of the effort, however, has been directed toward problems associated with various types of microwave tubes.

The basic requirements of a kinescope gun are that it produce a high-perveance narrow-angle electron beam which can be converged to a very small spot, and that the beam intensity be readily modulated over several orders of magnitude with a minimum effect on spot focus. There usually are other considerations which influence design such as gun size, cost, and life. Quantitatively these requirements have been sufficiently different from those of the microwave tube field for none of the modern developments to be applied commercially in kinescopes and other display tubes.

This paper deals with a new type of kinescope gun employing an annular geometry in the modulator section. It is capable of producing very high resolution pictures and exhibits some unique modulation characteristics.

Annular Geometry

A cross-sectional view of the modulator region of an annular geometry gun is shown in Fig. 1. The active cathode emission area is the inside surface of a right circular cylinder. The cathode is surrounded internally by two control grid annuli. Two acceleration grid annuli in turn surround the control grid. An axial probe electrode is placed on one side of the grid opening and an object electrode on the other. A series of conventional electron lenses are employed beyond the object electrode to form the final focused beam.

Normally the two control grid annuli are operated at the same potential. Since no distinction is ordinarily necessary when reference is made to these electrodes, they are simply designated the control grid, G_1. The acceleration grid annuli are often operated at different potentials and collect markedly different currents. It is convenient to call the acceleration grid annuli nearest the probe G_{2A}, and the other acceleration electrode G_{2B}.

* Original manuscript received by the IRE, April 25, 1958; revised manuscript received, July 28, 1958. Published in 1958 IRE National Convention Record, pt. 3, pp. 13–20.
† Kaiser Aircraft and Electronics, Div. of Kaiser Industries Corp., Oakland, Calif.; formerly with RCA Labs., Princeton, N. J.
[1] C. Susskind, "Electron guns and focusing for high-density electron beams," in "Advances in Electronics and Electron Physics," Academic Press, New York, N. Y., vol. 8; 1956.

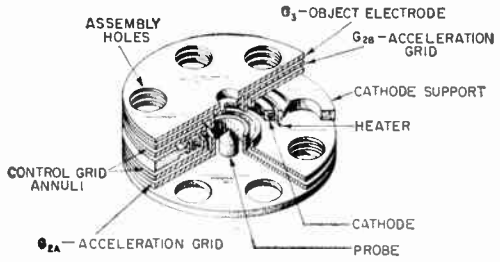

Fig. 1—Cross-sectional view of the modulator region of the annular geometry gun.

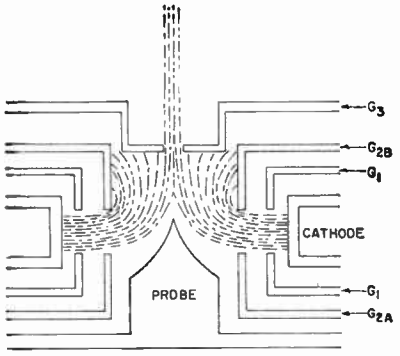

Fig. 2—Schematic picture of electron flow in annular geometry gun.

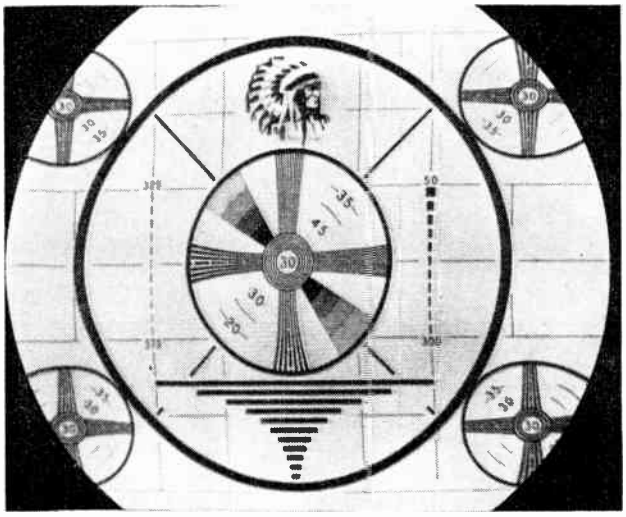

Fig. 3—Resolution pattern shown on 70° 16-inch kinescope.

Electron Object Formation

In a conventional kinescope gun electrons are accelerated axially from the cathode to form a small crossover.[2,3] This minimum beam cross section is subsequently imaged at the screen by means of electron lenses. The crossover is not an ideal object for several reasons. The current distribution invariably is of an ill-defined Gaussian nature,[4] and is limited in density more by lens aberrations or other effects than by fundamental considerations.[5,6] In addition, near zero grid bias the crossover grows very rapidly, causing spot "blooming." Furthermore, the virtual crossover position is usually dependent upon beam intensity, and hence the optimum focus condition varies with beam modulation.

In the annular geometry gun electrons are accelerated in the cathode region due to the field produced by the positively biased acceleration grid rings. Subsequently they pass into the inner region bounded axially by the probe and object electrodes. Axial and radial field components exist in this region and cause the electrons to be directed toward the object electrode.

Fig. 2 shows a schematic plot of the electron trajectories. The electrons tend to uniformly illuminate the aperture in the object electrode forming the electron object.

Since the position and size of the electron object are determined by the physical aperture in the object electrode, one would expect the final spot size and optimum focus requirement to be nearly independent of beam intensity, subject only to space charge perturbation. Experimental guns of this type do exhibit a constant spot size and focus requirement. In the particular geometry employed, very little perturbation effect could be detected.

The uniformly illuminated aperture produces a spot of very nearly uniform intensity and with sharply defined edges. In most of the experimental guns a 0.007-inch diameter object hole was employed. Fifty volts is a typical operating potential for the object electrode. In the experimental 16-inch tubes, electron optical magnifications of between 1 and 2.5 existed. Magnifications even lower than this are readily possible even in relatively short guns if one takes full advantage of the low object voltage.

Fig. 3 is a photograph of a standard resolution pattern produced by an annular geometry gun in a 16-inch 70° kinescope. The limiting resolution is about 1000 lines.

Beam Modulation

The two control grid annuli are normally connected together electrically and are biased negatively with respect to the cathode. The cathode current control grid characteristic is quite similar to that of a conventional electron gun except that the annular cathode currents are larger.

Current from the cathode is collected by each of the acceleration grid annuli and on the object electrode. Some of the current directed at the object electrode

[2] I. G. Maloff and D. W. Epstein, "Electron Optics in Television," McGraw-Hill Book Co., Inc., New York, N. Y.; 1938.

[3] M. Ploke, "Elementary theory of production of electron beams with triode systems," *Z. Angew. Phys.*, pt. I, vol. 3, December, 1951; pt. II, vol. 4, January, 1952.

[4] R. R. Law, "High current electron gun for projection kinescopes," PROC. IRE, vol. 25, pp. 954–976; April, 1937.

[5] M. E. Haine, "A contribution on the triode system of the cathode ray tube electron gun," *J. Brit. IRE*, vol. 17, pp. 211–216; April, 1957.

[6] G. W. Preston, "Effect of cathode roughness on the maximum current density in an electron beam," *J. Appl. Phys.*, vol. 27, pp. 627–630; June, 1956.

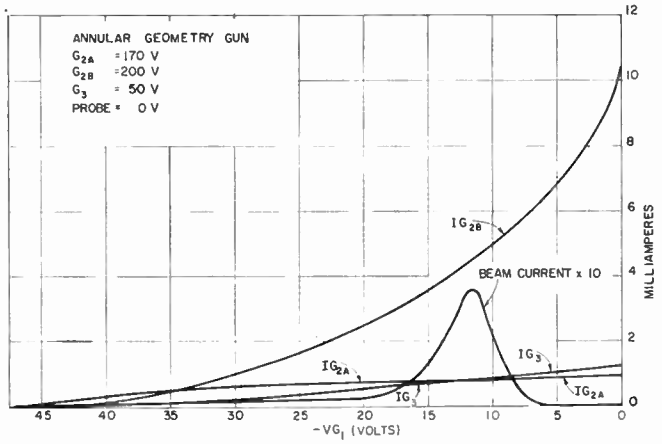

Fig. 4—Grid control characteristics

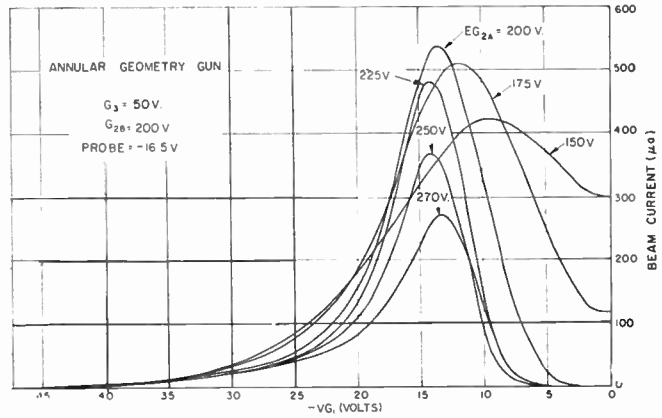

Fig. 5—Variations in grid control characteristics (EG_{2A} A parameter).

passes through the aperture in it forming the beam. The amount entering the beam depends not only upon the magnitude of the current directed at the object electrode, but also on the spatial distribution of the electron flow. Certain operating conditions exist which can cause the axial current density at the object electrode to fall to zero. When this happens over an area equal to that of the aperture no current enters the beam.

Fig. 4 shows a plot of beam current, acceleration grid currents, and object electrode current vs control grid voltage. It is taken for the particular set of operating voltages listed on the graph. Under these conditions the beam current rises slowly when the control grid is raised from a remote cutoff of about -50 volts; at -17 volts the current begins a sharp rise and then peaks at about -11.5 volts. The beam current then falls rapidly reaching zero at about -5.5 volts.

Several features of this unique operating characteristic are of interest. If the gun is modulated on the -5.5 to -11.5 volt portion of the grid characteristic only 6 volts of drive signal are required for full beam modulation. The direction of modulation is reversed from that of conventional grid characteristics. "Whiter than white" signals cause reduction in beam current. This constitutes a form of automatic noise inversion.

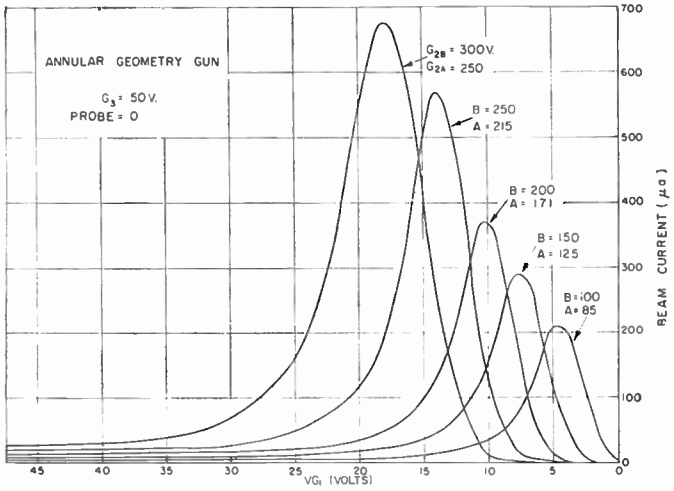

Fig. 6—Grid control characteristics with EG_{2B} A parameter and optimized EG_{2A}.

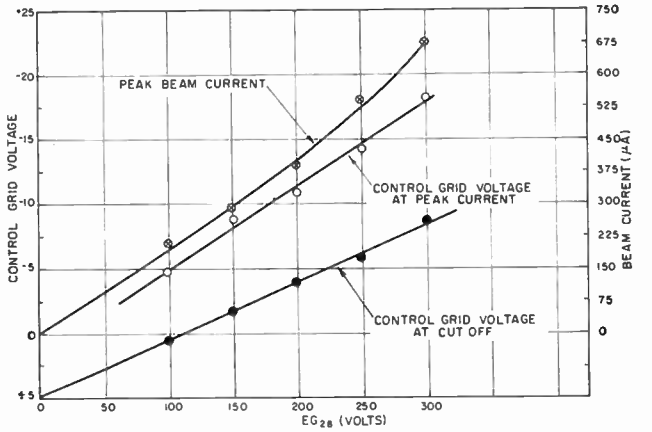

Fig. 7—The influence of G_{2B} voltage on optimized characteristics.

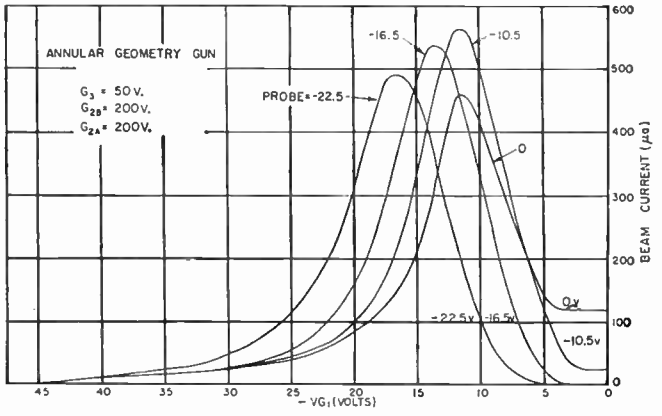

Fig. 8—The influence of the probe voltage on the control characteristics.

Fig. 5 shows the effect of variation in control characteristic obtained when the acceleration grid annulus nearest the probe, G_{2A}, is operated at various potentials. For television picture reproduction an optimum voltage exists which produces a sharp modulation characteristic but does not greatly attenuate the peak beam current.

The family of characteristics obtained for various values of optimized acceleration annuli voltages are shown in Fig. 6. The peak current varies almost in direct proportion to the acceleration voltage. The control grid voltage at which the peak current occurs and the value at which it falls essentially to zero both vary almost linearly with acceleration voltage. These relationships are shown in Fig. 7.

Probe electrode voltages also affect the control characteristics. The most significant effect regarding modulation is probably the influence the probe voltage has on the background current beyond cutoff. This effect is illustrated in Fig. 8.

Amplification Within the Kinescope

Fig. 4 reveals that an appreciable current flows to the acceleration grid annuli nearest the object electrode. If a load resistor is placed in series with the voltage supply to this electrode, video signal amplification will be obtained. Since the current increases rapidly beyond beam cutoff, sync signal stretching is affected.

Fig. 9 shows a circuit diagram of an annular geometry gun used to reproduce television pictures and to supply sync and sound IF gain. The amplified signal is shown in Fig. 10.

It is possible to reapply the amplified signal to the probe or object electrode, thereby obtaining some interesting effects. Among them is the possibility of further increase in the modulation sensitivity of the gun. With the particular gun designs tested this effect was fairly small, but other geometries might produce an appreciable effect. It should be recognized that reapplying signal to the probe or object electrodes does not constitute a closed loop circuit but rather produces a cascade action. This is because signal applied to the probe or object electrode has little effect on acceleration grid current.

Cathode Considerations

The emission area of the annular cathode is about ten times greater than that of a conventional kinescope gun. If efficient use is made of the emission current in forming the beam, it is possible to reduce the current density loading at the cathode below that of conventional guns. The extent to which this may be accomplished depends upon the object electrode aperture size and upon the fraction of the cathode current that is collected by the acceleration grid. In general, spot size and signal amplification ability may be traded against higher efficiency. The details of the best compromise would depend upon the requirements of the particular application.

A spiral stainless steel heat shield is used to support and shield the outer surface of the cathode annulus. The construction details are shown in Fig. 11. Despite the larger area of the annular cathode, the heater power requirement (3.4 watts) is about the same as that of most commercial kinescopes (3.7 watts).

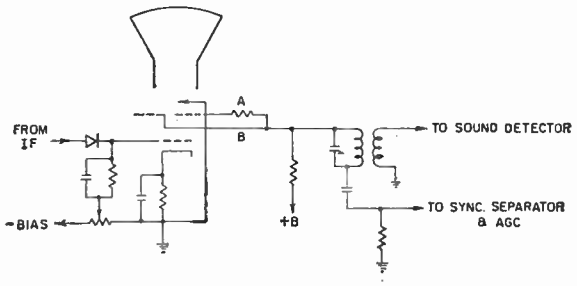

Fig. 9—Circuit for operating annular geometry gun as an amplifier and picture reproducer.

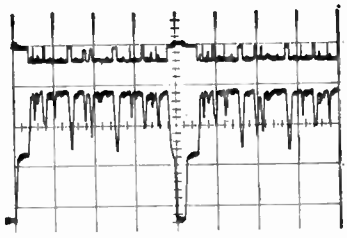

Fig. 10—Sync amplification and stretching. Top—input; bottom—output; scale—20 v/cm.

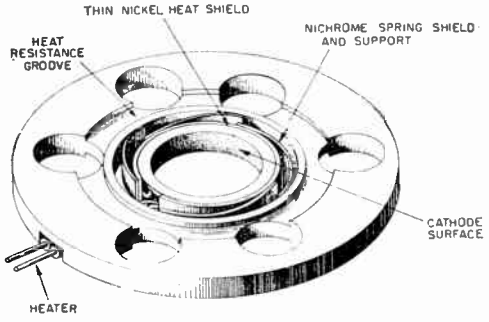

Fig. 11—Cathode assembly construction.

The dependence of the life of a cathode on emission current density is a subject of considerable controversy. There is, however, no question about the deleterious effects of positive ion bombardment. Since the annular geometry gun employs a geometry that shields the cathode surface from back-streaming positive ions, this cause of emission failure is eliminated.

Electron Optics

An analytical treatment of the annular geometry gun is restricted by the fact that closed-form solutions to the potential equation are not known for configurations of this type.

Certain general characteristics, however, can be deduced analytically and others investigated by means of numerical techniques.

Space Charge Free Trajectories

If the effect of the presence of the beam is neglected, Laplace's equation for the potential applies. Numerical values of the space charge free potential may be determined by the use of an electrolytic tank or resistor board

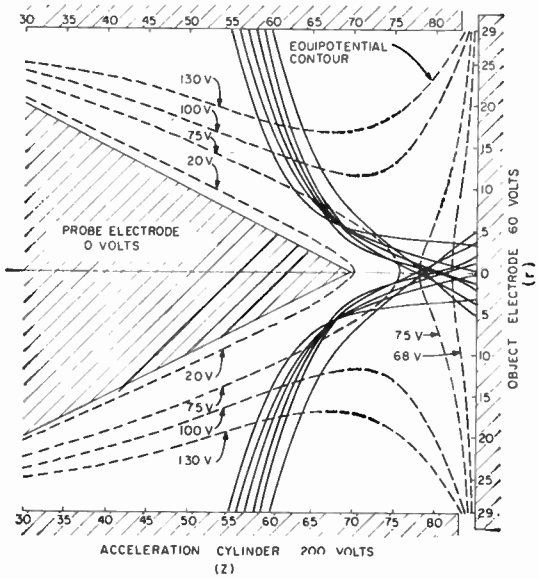

Fig. 12—Trajectories for 75° injection angle.

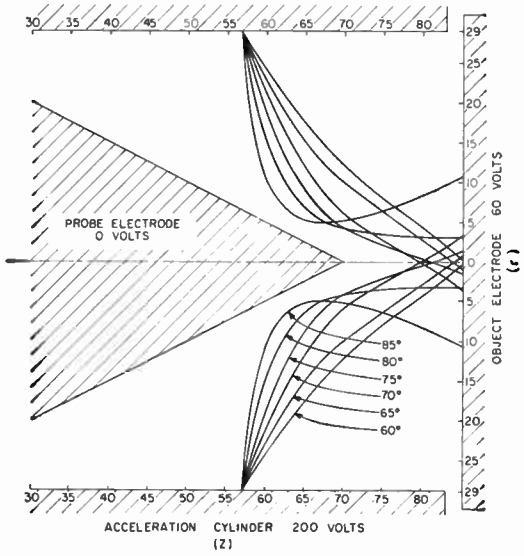

Fig. 13—Trajectories for various injection angles.

analog.[7] Electron trajectories may then be computed by hand or on an automatic calculator.

Fig. 12 shows an idealized geometry that has been used to study the space charge free trajectories. The beam is assumed to start at a cylindrical surface equivalent to some equipotential surface whose radius is slightly smaller than the acceleration grid radius. An initial angle, which is produced by a voltage or geometric asymmetry of the acceleration grid annuli, is also assumed at the idealized starting surface. The object electrode is approximated by an equipotential disk with no aperture. Trajectories for a starting angle of 75° are shown together with the equipotentials for the voltage conditions employed.

Fig. 13 shows the trajectories of electrons which start at the same axial position, but with various initial angles.

Since the trajectories which terminate within a small area near the axis can originate at any azimuthal position, the current density at the object electrode may be many times that at the injection cylinder. A small spread in initial angle has very little influence on the density.

Consider electrons which are emitted from a given axial coordinate at the cathode with a finite axial emission velocity, v_{oz}, and are then accelerated to the "starting" surface. Let the axial and radial velocity of an electron at the starting surface emitted with $v_{oz}=0$ be given by v_{Rz} and v_{Rr}, respectively. Then the angle at the starting plane is

$$\theta_{Ro} = \operatorname{ctn}^{-1}\frac{v_{Rz}}{v_{Rr}} \tag{1}$$

[7] G. Liebmann, "Solution of partial differential equations with a resistance network analogue," *Brit. J. Appl. Phys.*, vol. 1, pp. 92–103; April, 1950.

and the starting angle of an electron which possesses a small axial emission velocity is approximately

$$\theta_R = \operatorname{ctn}^{-1}\frac{v_{oz}+v_{Rz}}{v_{Rr}}. \tag{2}$$

The angular spread is

$$\Delta\theta_R = \frac{d\theta_R}{dv_{oz}}v_{oz} = \frac{-v_{oz}}{1+\operatorname{ctn}^2\theta_R}\frac{1}{v_{Rr}}$$

$$\Delta\theta_R = \frac{-v_{oz}}{v_{Rr}}\sin^2\theta. \tag{3}$$

If the potential at $r=R$ is V_R, than $v_{Rr}=\sin\theta\sqrt{2\eta V_R}$. The equivalent emission potential corresponding to v_{oz} is $V_{ez}=v_{oz}^2/2\eta$. Using these relationships (3) takes the form

$$\Delta\theta_R = \sqrt{\frac{V_{ez}}{V_R}}\sin\theta. \tag{4}$$

For the value $V_R=200$ v, $V_{ez}=0.1$ v and $\theta=75°$. $\Delta\theta_R$ equals only 1.2°. From this it may be concluded that axial emission velocities at the cathode only slightly reduce the current density at the object electrode. Radial emission velocities have also been found to have only a small influence on the current density at the object electrode.

Angular Momentum

Unfortunately, azimuthal emission velocities have a very profound effect on the current density at the object electrode. Since the annular geometry gun possesses cylindrical symmetry, angular momentum with respect to the gun axis is conserved. If we designate the cathode radius by R_o and the azimuthal velocity at the cathode by $v_{o\phi}$, then at any radius, r, the azimuthal velocity $v_{r\phi}$ is given by

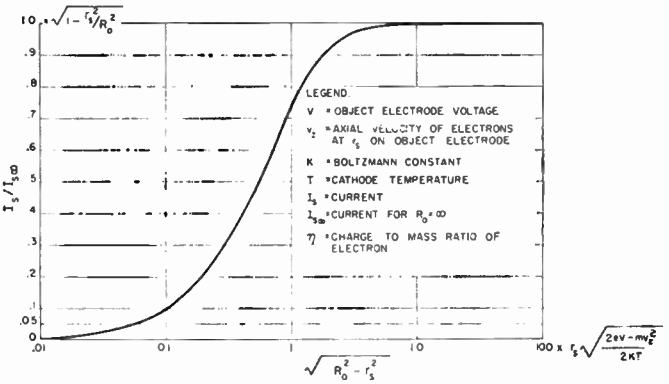

Fig. 14—Current arriving within radius r_s at the object electrode vs cathode radius R_o.

$$v_{r\phi} = \frac{R_o v_{o\phi}}{r}. \tag{5}$$

The azimuthal velocity has associated with it a radial outward force F_ϕ which prevents electrons with any angular momentum from reaching the axis. F_ϕ is given by

$$F_\phi = \frac{m v_{r\phi}^2}{r} = \frac{m(R_o v_{o\phi})^2}{r^3} \tag{6}$$

where m is the electron mass. A synthetic potential, V_ϕ, which would give rise to F_ϕ if the electron were confined to a nonrotating plane takes the form

$$V_\phi = \frac{1}{e}\int_\infty^r F_\phi dr = -\frac{R_o^2 v_{o\phi}^2}{2\eta r^2}. \tag{7}$$

Here e is the electronic charge and η the electronic charge to mass ratio, e/m.

The smallest radius r_s that the electron can reach is obtained by including V_ϕ and the axial velocity $v_z(r)$ in the energy equation. This results in (8) and (9).

$$r_s = \frac{R_o v_{o\phi}}{\sqrt{2\eta V(r_s, z) - v_z^2(r_s, z) + v_{o\phi}^2}} \tag{8}$$

$$v_{o\phi} = r_s\sqrt{\frac{2\eta V - v_z^2}{R_o^2 - r_s^2}}. \tag{9}$$

If J_c is the emission current density at the cathode, and L is the axial length of the emission area, then for a Maxwellian azimuthal emission velocity distribution the current, I_s, falling within a radius, r_s, at the object electrode cannot exceed

$$I_s = \frac{J_c 2\pi R_0 L}{\sqrt{2\pi kT/m}}\int_{u=-v_\phi}^{+v_{o\phi}} e^{-(u^2 m/2kT)}du \tag{10}$$

$$I_s = 2J_c R_o L \operatorname{erf}\left[\frac{r_s}{R_o}\sqrt{\frac{2eV - mv_z^2}{2kl\left(1 - \frac{r_s^2}{R_o^2}\right)}}\right]. \tag{11}$$

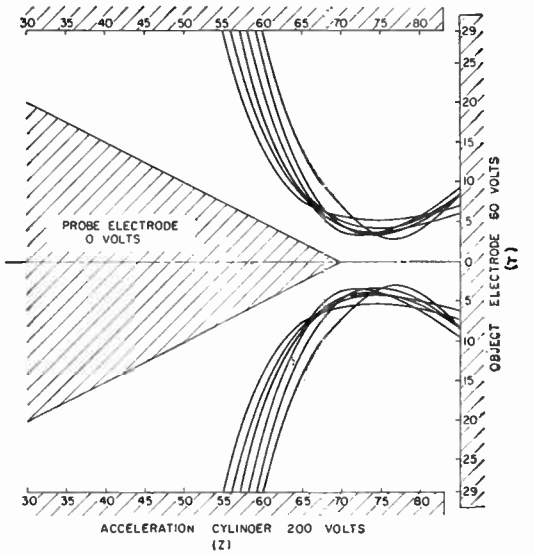

Fig. 15—Trajectories for 75° injection angle and 0.025 ev azimuthal emission energy.

Here v_z is the axial velocity of electrons at radius r_s as they reach the object electrode and V the potential of the object electrode. T is the absolute temperature of the cathode and k the Maxwell-Boltzmann constant.

In the limit as R_o, the cathode radius, goes to infinity the maximum current within r_s at the object electrode goes to

$$I_s = 4\sqrt{\pi} J_c L r_s\sqrt{\frac{2eV - mv_z^2}{2kT}}. \tag{12}$$

Fig. 14 is a plot of I_s vs cathode radius, R_o. It should be noted that the current that can be obtained within r_s increases with increasing cathode radius R_o, but that very little is gained in making $\sqrt{R_o^2 - r_s^2}$ more than about three times

$$r_s\sqrt{\frac{2eV - mv_z^2}{2kT}}.$$

The value of the quantity

$$\sqrt{\frac{2eV - mv_z^2}{2kT}}$$

varies with gun design and operation but normally would fall within the range 5 to 20.

Referring to (9) it is obvious that only small values of $v_{o\phi}$ are needed to prevent current from reaching a small radius r_s if R_o is large. It is therefore possible to control the current reaching any given value of r_s by purposely controlling $v_{o\phi}$ by using a nonaxially symmetric geometry. This could lead to a very sensitive form of modulation.

Fig. 15 shows the trajectories in r, z space (rotating coordinate plane) for electrons which start off with about 0.025 ev azimuthal energy at the cathode.

Space Charge Effects

The modulation process in the annular geometry gun depends directly on space charge effects. It is not readily feasible to analytically investigate such effects for the annular cathode geometry. An approximation to the behavior may, however, be obtained by considering the flow of electrons inward from the surface of a long cylinder. The solutions of Langmuir and Blodgett[8] to the inverse case where electrons flow outward from an internal cathode may be applied directly to compute the smallest radius, r_s, to which the electrons may propagate as a function of injected current per unit length, I, injected voltage, V_R, and the injection surface radius, R. The Langmuir-Blodgett expression is

$$V_R = I^{2/3}R^{2/3}\left(\frac{81}{8}\right)^{+1/3}\eta^{-1/3}B^{4/3}. \qquad (13)$$

B is given as a tabulated function of R/r_s. Fig. 16 is a plot of r_s vs I. The curve has a most perplexing form showing that any current less than $13.4\times10^{-6}V_R^{3/2}/R$ amperes per unit length can propagate all the way into the axis. As this value is reached, however, the minimum radius, r_s, abruptly changes from zero to a value of $R/44.0$. Furthermore, the Langmuir-Blodgett expression indicates that in the current range $13.4\times10^{-6}V_R^{3/2}/R$ to $14.8\times10^{-6}V_R^{3/2}/R$ there are an infinite number of possible values of r_s.[9]

For an emission length of 0.015 inch, an injection radius of 0.075 inch, and an injection voltage of 200 volts, about 8 ma of current are required to prevent electrons from propagating to a radius of 0.0035 inch. Even though the Langmuir-Blodgett geometry is somewhat different from that of the annular geometry gun, this corresponds almost precisely with the observed performance of an annular geometry gun of these dimensions.

No effects such as might be expected from a multivalued r_s have been observed.

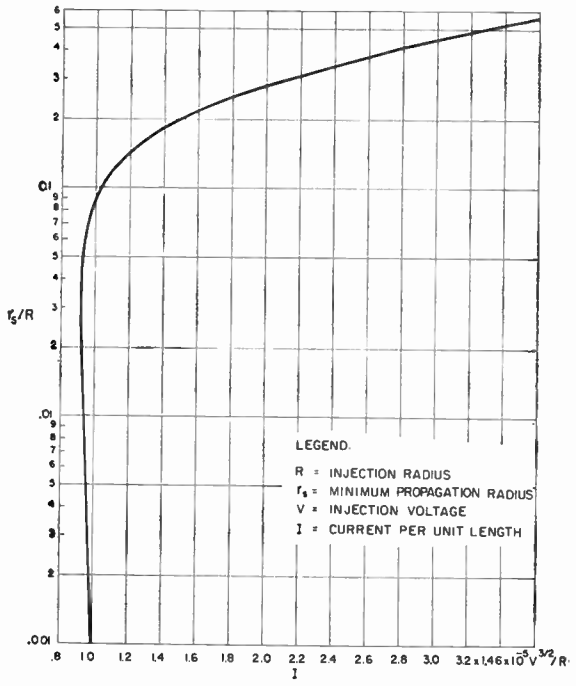

Fig. 16—Minimum radius vs current per unit length for space charge limited currents in cylindrically symmetric flow.

[8] I. Langmuir and K. B. Blodgett, "Currents limited by space charge between coaxial cylinders," *Phys. Rev.*, vol. 22, pp. 347–356; October, 1923.

[9] H. F. Ivey, "Space charge limited currents," in "Advances in Electronics and Electron Physics," Academic Press, New York, N. Y., vol. 6; 1954.

Correspondence

Undersea and Subterranean "Satellites"*

The rather paradoxical and ironical fact appears to develop that before long man will probably become more familiar with the characteristics of the terrain of other planets than with those of the interior regions of his own home planet. The Pacific's undersea "canyons" and the plastic and semi-molten layers in the earth's outer shell may turn out to be more remote and inaccessible than the Martian ice-caps.

Radiosonde balloon and satellite techniques might be applied to probe the earth's interiors. A self-contained and self-powered shell might be lowered several miles into the sea, particularly into deep gorges. Long insulated probes with bared electrode tips could feed high-gain, low-noise, dc amplifiers inside the sphere to detect any current streams. The amplifier could then code a small sonar which could relay the information via a vertical-beam transducer to the mother ship above. This would avoid long cable runs with their induction noise, attenuation, and leakage problems. Magnetometers and radiation counters could also be used. In the case of deep oil-well shafts, similar techniques might work with miniaturized and transistorized equipment, particularly where water is being pumped down into underground caverns to drive the oil crude to the surface.

Such "satellite" detectors, used in conjunction with earth magnetic-field and radio-noise observations immediately following sun-spot storms, might possibly provide some useful meteorological and geophysical data. This may also be true in the case of terrestrial electrical storms.

TED POWELL
Glen Oaks, L. I.
New York, N. Y.

* Received by the IRE, April 8, 1958. This letter antedates two recent articles on oceanography in *Sci. Amer.* which discuss the new deep-sea bathyscaph and the ultrasonic float.

On the Choice of Frequencies for Meteor-Burst Communication*

The peak power of echoes from most meteor trails varies as λ^3, where λ is the radio wavelength. Furthermore, the average duration of individual meteor echoes varies approximately as λ^2. Both of these factors favor the choice of long wavelengths for meteor-burst communication. A detailed analysis by Eshleman[1] has shown that the wavelength dependence of the duty cycle is approximately $\lambda^{2.4}$, if one takes into account these factors plus the cosmic background noise which also depends on wavelength.

TABLE I

A Comparison of Duty Cycles Measured at 10 db above Average Peak-Background-Signal.

Time		Duty cycle (per cent)		Duty cycle ratio (49 mc: 74 mc)	Median ionospheric scatter on 49 mc (relative to 1 μv into 50-ohm receiver)	Time interval analyzed (minutes)
Hour	Date	49 mc	74 mc			
0100	4/18/58	7.5	2.8	2.7	−23 db	15
0500	5/23/58	10.7	4.5	2.4	−25 db	10
0600	4/ 3/58	7.2	5.8	1.2	−17 db	22
0900	4/18/58	7.8	6.3	1.2	−14 db	15
1130	10/ 4/57	4.0	3.9	1.0	−12 db	15
1600	4/ 3/58	5.1	2.5	2.0	−17 db	19
1800	4/ 3/58	4.1	1.4	2.9	−20 db	27

Recent experiments which we have conducted, however, show an additional factor which should be taken into account and which favors the choice of shorter wavelengths.

Our experiments have been performed over a 1250-km path from Boston, Mass., to Columbia, S. C. Transmissions[2] from Boston on 49 mc (5-kw output) and on 74 mc (3-kw output) were monitored simultaneously at Columbia. Five-element Yagi antennas were used in all cases, and the receiver outputs were recorded on an Edin multichannel recorder. In addition to the meteor bursts, an ionospheric-scatter background signal was observed on 49 mc, while negligible ionospheric scatter was observed on 74 mc.

The ionospheric-scatter component in these measurements appeared as a kind of variable background noise with which the meteoric component would have to compete in a 49-mc burst communication system.

The threshold for measuring the duty cycle of meteor bursts must be set, therefore, with respect to the ionospheric-scatter background rather than cosmic noise whenever ionospheric scatter is present. Table I shows the results of a series of duty-cycle measurements made simultaneously on 49 mc and 74 mc at various times during a six-month period. These results represent a random sampling of the data arranged in order of increasing local time. The duty cycle was measured 10 db above the average peak-background-signal, including ionospheric scatter as background on 49 mc. Table I shows that the duty cycle during the night is two or three times greater at the lower frequency as compared with a predicted duty cycle ratio of 3.4, based on Eshleman's analysis. During the day, and particularly near noon, when the ionospheric component is strong, the duty cycles become about equal on the two frequencies. Furthermore, if one considers ionospheric scatter signals as noise, then the signal-to-noise ratio is independent of the transmitter power, while the signal-to-noise ratio for cosmic noise may be increased by increasing transmitter power.

Thus it would be possible to increase the duty cycle at 74 mc by increasing the transmitter power, but on 49 mc an increase in power would increase the duty cycle only at those times of day when ionospheric-scatter background is not the limiting factor.

It is believed that these observations constitute a strong argument for the use of higher frequencies for meteor-burst communications.

M. L. Meeks
J. C. James
Eng. Experiment Station
Georgia Inst. Tech.
Atlanta, Ga.

* Received by the IRE, August 11, 1958. This work was supported by the AF Cambridge Res. Center under Contract No. AF 19(604)—1593.

[1] V. R. Eshleman, "On the wavelength dependence of the information capacity of meteor-burst propagation," Proc. IRE, vol. 45, pp. 1710–1714; December, 1957.

[2] The transmitters were operated under another contract by Pickard and Burns, Inc., Needham, Mass.

The Superconductive Transition Radio-Frequency Mixer and the Problem of Cryotron Switching Time*

In a recent communication[1] Aharoni, *et al.*, have discussed the dependence of the switching time of the cryotron[2] on the L/R time constant of the circuit. There is another problem of more general interest in the switching time of the cryotron and other superconductive transition devices.[3] Regardless of the L/R time constant to be achieved in circuit design, it is commonly considered that there is an absolute limitation on the switching time, imposed by the time duration required for the transition from the superconductive to the normal conductive state or vice versa, depending on the switching mode. It is suspected on physical grounds that this inherent switching time limits computer operation to the kilomegacycle range. However, in the present state of the instrumentation art and the development of the switching element, it has proved difficult to measure directly the switching time in devices for very rapid switching. Moreover the preparation of suitable thin-film elements with reliable mechanical characteristics over the extreme temperature range involved has also proved most difficult.

The authors have approached the problem of the determination of the inherent switching time through measurements on the superconductive transition radio-frequency mixer. In the present form of this device, a thin film of suitable material, such as high-purity tin, serves as a flux shield between input and output-coupling loops. A radio-frequency local oscillator energizes a field coil surrounding the loop-shield assembly and functions to switch the shield material in and out of the superconducting state at a rate equal to twice the oscillator frequency. A signal fed to an input loop is thus mixed with a signal of twice the local-oscillator frequency, and the difference or sum frequency is retrieved in an output loop. Ambient temperature is adjusted for maximum mixer output by controlling the vapor pressure in a liquid-helium chamber in which the mixer assembler is immersed.

The configuration used is elementary, and measurements are relatively easy, dealing with simple sinusoidal radio-frequency signals. Consequently, it is expected that the approach outlined will yield information very rapidly on the perplexing problem of determining fundamental physical limitations on switching rate.

Efficient mixing at any particular local-oscillator frequency indicates that an appreciable portion of the superconducting film has undergone a transition of some kind in a time interval of roughly one quarter the local-oscillator period. Experiments to date have resulted in well-defined mixing operation in time intervals as short as 1.2×10^{-9} seconds. This is appreciably faster than the shortest time interval obtained elsewhere in direct measurements of switching time. There is no indication that the time interval measured is the shortest possible. Higher-frequency tests will be undertaken shortly following a current series of tests on mixing efficiency.

J. B. Woodford, Jr.
D. L. Feucht
Dept. of Elec. Eng.
Carnegie Inst. Tech.
Schenley Park
Pittsburgh 13, Pa.

* Received by the IRE, April 28, 1958. This work is part of a program of low-temperature electronic studies supported in part by the Office of Naval Res. and the IBM Corp.

[1] A. Aharoni, E. H. Frei, and S. Shtrikman, "The switching time of the cryotron," Proc. IRE, vol. 46, p. 780; April, 1958.

[2] D. A. Buck, "The cryotron—a superconductive computer element," Proc. IRE, vol. 44, pp. 482–493; April, 1956.

[3] J. W. Crowe, "Trapped-flux superconducting memory," *IBM J. Res. Dev.*, vol. 1, pp. 294–303; October, 1957.

Amplitude Scintillation of Extra-terrestrial Radio Waves at Ultra-High Frequency*

The intensity of radio stars, as received at ground level on meter wavelengths, is known to exhibit fluctuations. This phenomenon was first discovered by Hey, Parsons, and Phillips[1] at a frequency of 64 mc. Subsequent work by Smith, Little, and Lovell[2] showed that the fluctuations are not inherent in the radio star itself, but are produced in the earth's ionosphere. These fluctuations are analogous to the twinkling of optical stars on optical wavelengths and are often referred as "radio-star scintillation." More extensive work was later carried out at VHF by various workers, notably in England and Australia. The results of this work have been recently reviewed by Booker[3] and Little, *et al.*[4]

It is now believed that radio-star scintillation is caused by the irregularities in the earth's ionosphere. The irregularities have different radio-frequency refractive indexes and thus present important effects on the propagation of radio waves. The refractive index of an ionized medium which contains N electrons per cm^3, each of charge e and mass m, can be expressed as

$$\eta = \sqrt{1 - \frac{4\pi Ne^2}{m(2\pi f)^2}}$$

where f is the frequency in cycles per second. The deviation of the refractive index from unity decreases with increasing frequency. This suggests that the amplitude of the flutuations would decrease as the frequency increases. The existing observational evidence shows that scintillation is weak at the high-frequency end of the VHF band and becomes stronger as the frequency decreases through the VHF band. It was generally considered that ionospheric scintillation would be negligible at frequencies above 300 mc. The purpose of this communication is to present results of scintillation measurements made at UHF. It is found that at 40 degrees north latitude, the ionospheric effects upon radio-star scintillation are still significant at a frequency of 915 mc when the radio star is near the northern horizon.

The observations were made at the Ohio State University Radio Observatory (latitude 40°1′ north and longitude 83°03′ west). The equipment consists of a 40-foot diameter, polar-mounted parabolic reflector antenna, and a crystal superheterodyne receiver. The antenna has a beam width of 1.7 degrees between half-power points at 915 mc. The gain of the antenna is about 39 db over an isotropic radiator. The receiver is operated at a frequency of 915 mc. The dc output of the second detector is followed by an automatic pen recorder. The time constant of the system is approximately 2 seconds. The radio star Cygnus A (IAU19N4A; right ascension 19^h 58^m, declination +40°37′) was chosen for scintillation measurements because of its small angular size, strong intensity and wide range of altitude angles (horizon to zenith). Cygnus A rises from approximately 32 degrees east of north of Columbus, reaches the zenith at its meridian transit, and sets at 32 degrees west of north. It is significant to note that at low elevation angles, Cygnus A is in a northerly direction and is therefore observed through the disturbed auroral F regions.

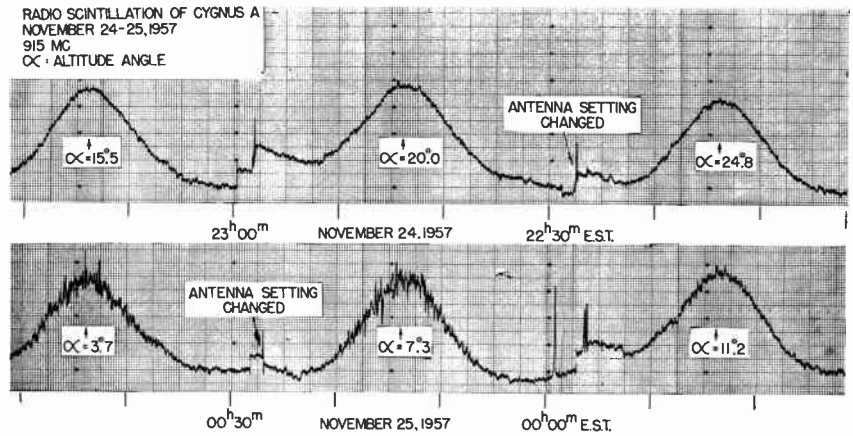

Fig. 1—Drift curves of the radio star Cygnus A at its setting on November 25, 1957, taken with a 40-foot-diameter parabolic reflector antenna at 915 mc.

The observations were made by setting the antenna beam slightly west of Cygnus A in hour angle (about 7.5 degrees) and the receiver output recorded as the radio star drifted through the antenna beam. This procedure was repeated at various angles of altitude, so that about 18 drift curves were obtained daily between the altitude angles of 90 degrees to 0 degree. Fig. 1 shows typical drift curves of Cygnus A recorded at various elevation angles as the radio star sets in the northwest. The amplitude of the fluctuation is strongest near the horizon, and decreases very rapidly as the elevation angle is increased. At elevation angles above 10 degrees, scintillation was seldom observed except during the periods when strong auroras were reported.

The amplitude and rate of the scintillation at low elevation angles have been observed to change from day to day. Fig. 2 shows drift curves obtained at the same elevation angle of 3.7 degrees on different nights. The amplitude of scintillation ranges from less than few per cent to over 50 per cent of the steady component of the flux density of Cygnus A, while the rate of scintillation varies from ½ to 6 peaks per minute. The mean amplitude fluctuation index is 20 per cent and the mean fluctuation rate is 2.6 peaks per minute during the past four months (November, 1957, through February, 1958). The scintillation was observed more frequently during the months of November and December, 1957, than in January and February, 1958. Thus, the percentage of days during the month on which the amplitude fluctuation index exceeds 10 per cent was 87 per cent in November and 91 per cent in December, and dropped to 82 per cent in January and to 73 per cent in February. This suggests that the scintillation characteristics at 915 mc may have diurnal and/or seasonal variations.

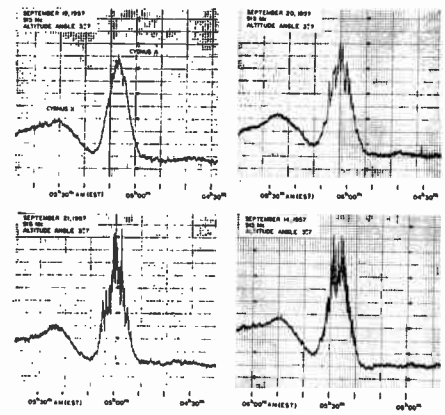

Fig. 2—Scintillation records from the Cygnus A radio star taken at altitude angle of 3.7 degrees on different nights. The records illustrate quiet (upper left), average (upper right), and highly disturbed conditions (lower).

A comparison of the scintillation data and the 3-hour geomagnetic K index has also been made. It was found that the fluctuation rate is roughly proportional to the K index, as shown in Fig. 3. The correlation coefficient of the two is 0.6. The probability of the observed correlation occurring by chance is less then one in 1000. The amplitude fluctuation index is, however, relatively unaffected by the change of the K index.

It has also been observed that the scintillation characteristics are markedly affected by the presence of auroras. During the periods of auroral displays, scintillation was observed at both lower and higher angles of elevation and was always characterized by a larger fluctuation index and a higher fluctuation rate. This indicates that the effects of auroras on radio-wave propagation are still pronounced at 915 mc. It is therefore very probable that auroras may be detectable by radar technique at frequencies up to 900 mc. Work on the detection

* Received by the IRE, April 16, 1958. This work has been supported by the U. S. Air Force Cambridge Res. Center, Electronics Res. Directorate, Contract No. AF 19(604)1591 through the Ohio State Univ. Res. Foundation.

[1] J. S. Hey, S. J. Parsons, and J. W. Phillips, "Fluctuations in cosmic radiation at radio-frequencies," *Nature, London*, vol. 158, p. 234; August 17, 1946.

[2] F. G. Smith, C. G. Little, and A. C. B. Lovell, "Origin of the fluctuations in the intensity of radio waves from galactic sources," *Nature, London*, vol. 165, pp. 422–424; March 18, 1950.

[3] H. G. Booker, "The use of radio stars to study irregular refraction of radio waves in the ionosphere," PROC. IRE, vol. 46, pp. 298–341; January, 1958.

[4] C. G. Little, W. M. Rayton, and R. B. Roof, "Review of ionospheric effects at VHF and UHF," PROC. IRE, vol. 44, pp. 992–1018; August, 1956.

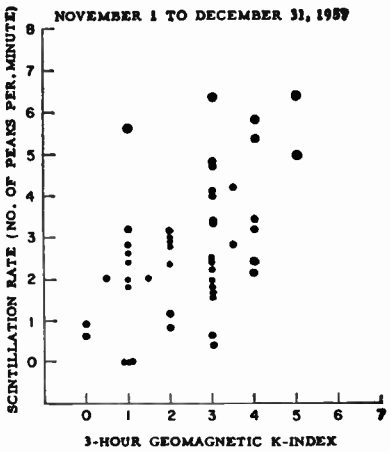

Fig. 3—Comparison of the fluctuation rate with the 3-hour geomagnetic K index.

of the auroras echoes using radar has so far been limited to lower frequencies.

The work described here is continuing and plans are made for simultaneous observations of scintillation at two other frequencies in the UHF region.

The writer is grateful to Prof. John D. Kraus for his valuable discussions.

H. C. Ko
Radio Observatory
Dept. of Elec. Eng.
The Ohio State University
Columbus 10, Ohio

Statistical Design and Analysis of Closed-Loop Control Systems with Error Sampling*

A previous paper[1] by the writer describes a statistical technique applicable to the problem of restoring sampled data and some interesting general results which have been obtained. The method used was essentially an amalgamation of Lindval's representation of sampled data as a time function, synthesized by superposition of δ functions, with Wiener's methods of generalized harmonic analysis.

This technique may also be applied to closed-loop control systems. The means of doing this comprise part of a paper,[2] which, when it is published, will evidently receive only limited distribution. It was therefore felt that this letter to the editor of PROCEEDINGS might be in order.

It might be well to mention here that the method of the author's previous paper[1] and this note treats the error at *all times* directly, rather than at just the sample times as has been done by several authors.

Consider the closed-loop control system indicated by Fig. 1. By methods similar to

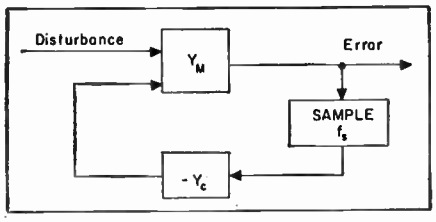

Fig. 1—Sampled error control system.

those already described,[1] it is easily shown that the Fourier transforms of error ϵ and disturbance D (assumed to be stationary random time series) over a long but finite time $-T \to +T$ are related approximately[3] by

$$\epsilon_T(f) = Y_m(f) \cdot \left[D_T(f) - f_s Y_c(f) \sum_{-\infty}^{+\infty} \epsilon_T(f - nf_s) \right]. \quad (1)$$

This relationship may be inverted to obtain an expression for the error in terms of the disturbance in the following way. Substitute for f,

$$f' = f - mf_s. \quad (2)$$

Then, for every integral m,

$$\epsilon_T(f - mf_s) = Y_M(f - mf_s) \times \left\{ D_T(f - mf_s) - f_s Y_c(f - mf_s) \sum_{-\infty}^{+\infty} \epsilon_T[f - (n + m)f_s] \right\}. \quad (3)$$

But

$$\sum_{n=-\infty}^{+\infty} \epsilon_T[f - (n + m)f_s] = \sum_{n=-\infty}^{+\infty} \epsilon_T(f - nf_s). \quad (4)$$

Thus, if we write an infinite set of equations, using every integral value of m in the expression above once, and then sum,

$$\sum_{-\infty}^{+\infty} \epsilon_T(f - nf_s) = \sum_{-\infty}^{+\infty} Y_M(f - nf_s) D_T(f - nf_s) - f_s \left[\sum_{-\infty}^{+\infty} Y_M(f - nf_s) Y_C(f - nf_s) \right] \cdot \sum_{-\infty}^{+\infty} \epsilon_T(f - nf_s). \quad (5)$$

Hence,

$$\sum_{-\infty}^{+\infty} \epsilon_T(f - nf_s) = \frac{\sum_{-\infty}^{+\infty} Y_M(f - nf_s) D_T(f - nf_s)}{1 - f_s \sum_{-\infty}^{+\infty} Y_M(f - nf_s) Y_C(f - nf_s)} \quad (6)$$

and then from (1)

$$\epsilon_T(f) = [1 - X(f)] Y_M(f) D_T(f) + [X(f)] \sum_{1}^{\infty} [Y_M(f - nf_s) D_T(f - nf_s) + Y_M(f + nf_s) D_T(f + nf_s)] \quad (7)$$

where

$$X(f) = \frac{f_s Y_c(f) Y_M(f)}{1 + f_s \sum_{-\infty}^{+\infty} Y_M(f - nf_s) Y_c(f - nf_s)}. \quad (8)$$

Using the methods outlined,[1] it follows from (7) that, if D is a stationary random time series having a spectral density function $\Phi_D(f)$, the spectral density of the error is given by

$$\Phi_\epsilon(f) = |1 - X(f)|^2 \{ |Y_M(f)|^2 \Phi_D(f) \} + |X(f)|^2 \left\{ \sum_{1}^{\infty} |Y_M(f - nf_s)|^2 \Phi_D(f - nf_s) + |Y_M(f + nf_s)|^2 \Phi_D(f + nf_s) \right\}. \quad (9)$$

The integral of this function over all frequencies gives the mean-square error and may be so used to evaluate an existing or contemplated system. It is also obviously of the same form as the expression for error spectral density in the case of filtering independent signal and noise and, hence, Wiener's method for this case may be used directly to find the best X, given $Y_m(f)$, and $\Phi_D(f)$. In this case, (8) must be inverted to find $Y_c(f)$, the required optimum feedback-frequency function. This can be done by the same technique used above to obtain (7) from (1). The result is

$$Y_c(f) = \frac{1}{f_s Y_M(f)} \left\{ \frac{X(f)}{1 - \sum_{-\infty}^{+\infty} X(f - nf_s)} \right\}.$$

One interesting (and somewhat unfortunate for the analyst) property of this closed-loop system, not shared by the data restorer, is that if we consider a hypothetical "unrealizable" filter in the loop, the minimum error attainable is always zero. The proof and/or interpretation is left to the reader. Thus, in estimating minimum mean-square error attainable, it is *essential* that the "realizability" condition be preserved.

R. M. STEWART
Ramo-Wooldridge Corp.
Inglewood, Calif.
Formerly at Jet Propulsion Lab.
Calif. Inst. Tech.
Pasadena, Calif.

On the Statistics of Filled Vessels*

An inductor with a ferromagnetic core stores energy $LI^2/2$ where inductance L is dependent upon current I as a consequence of the saturation characteristic; added increments of current yield continuously decreasing increments of stored energy. It would appear that an iron-cored inductor can be used as an electric analog in studies

* Received by the IRE, April 23, 1958. This note presents the results of one phase of research carried out at the Jet Propulsion Lab., Calif. Inst. Tech., under Contract No. DA-04-495-Ord 18, sponsored by the Dept. of the Army Ordnance Corps.

[1] R. M. Stewart, "Statistical design and evaluation of filters for the restoration of sampled data," PROC. IRE, vol. 44, pp. 253–257; February, 1956.

[2] R. J. Parks and R. M. Stewart, "The application of noise and filter theories to guidance problems," *Proc. AGARD (NATO) Symp. on Guidance and Control*, Venice, Italy, pp. 265–283; September 17, 1956.

[3] The effect of the approximation disappears as $T \to \infty$, as we shall do later.

* Received by the IRE, April 17, 1958.

pertaining to a class of statistical problems with important applications in commerce. In particular, it can aid in optimizing the mathematical equation for the sides of circularly symmetric containers which must be filled to within a certain distance of the top with relatively small standard deviation in this distance, in spite of a somewhat random distribution of filling charge. Use of an analog computer is indicated, because optimum configuration may be distinctly nonlinear.

In order to determine the proper analog, the (normalized) probability density function, and especially the variance, for the filling charge must be determined. As a rule, direct experimental observations for this are required; the usual Gaussian assumption is highly questionable. Unfortunately, certain problems in performing experimental observations are often encountered. Although it is assumed at the beginning of a sequence of tests that the filling charge process is ergodic, it is found to be distinctly nonstationary after only a few tests and, in fact, variance may become so large that experiments can not be continued. Strangely, the first two or three tests in any one experiment seem to indicate a stationary process, but thereafter, depending upon the experience of the observer, significance of statistical findings become highly questionable. This problem appears whenever statistical measures are obtained from sequential observations as a time series. It is evident that reliable data require performance of ensemble averages. Unfortunately, costs of performing ensemble averages restrict testing to large organizations working on defense contracts.

As in many optimization problems of practical value, hunch and experience over the years have yielded satisfactory solutions for container problems which may be fairly close to optimum. However, without a mathematical theory, it can not be stated categorically that appreciably better performance is not possible. Certainly, a statistical study would do well to start with containers with reasonably effective shapes such as the Martini glass. Without doubt, the successful theoretician, obtaining experimental data with strict adherence to ensemble averaging, will be able to obtain numerous design patents.

JOHN L. STEWART
Elec. Eng. Dept.
University of Southern California
Los Angeles, Calif.

Electron-Density Profiles in the Ionosphere During the IGY*

In many parts of the world during the last twenty years, regular measurements have been made of the maximum electron density (Nm) and the approximate true height (hm) of the various layers in the ionosphere. Both these parameters can be obtained fairly easily from the $h'(f)$ curves (ionograms), which are produced by automatic pulse-sounding equipment, and tabulated values of Nm and hm are generally available. On the other hand, only an extremely small amount of accurate information is available on $N(h)$ profiles, the distribution of electron density with height in the ionosphere, and how these profiles vary with time, season, and geographical location. It follows that very little is known about the variation of N with time at a constant true height [the $N(t)$ curve]. The ionograms contain all this information, but the mathematical procedure for deriving an $N(h)$ profile from an $H'(f)$ curve is very laborious, especially if the effect of the geomagnetic field is taken into account. Fortunately, electronic computers are now available, and they have opened up a new era in this field since they can readily be used to compute $N(h)$ profiles from ionograms.

TABLE I

Observatory	Location
Slough	51°29′N; 00°34′W
Ibadan	07°26′N; 03°54′E
Singapore	01°19′N; 103°49′E
Port Stanley	51°42′S; 57°51′W

The purpose of this note is to outline the scope of a program of such computations which has been organized by the Radio Research Station, Department of Scientific and Industrial Research, in Slough, England, and which forms part of the United Kingdom's program of observations during the International Geophysical Year. The $N(h)$ profiles are being produced by Ferranti, Ltd. on a "Pegasus" automatic digital computer using $h'(f)$ data obtained at the four observatories listed in Table I. For each observatory, profiles are being calculated for each hour of the day for about four days per month beginning in July, 1957. When the ionograms are suitable, "regular world days" are selected for analysis; when this is not practicable, over days are substituted. This program will be continued until December, 1958, when the possibility of extending the work will be considered.

The analysis is carried out according to a method which has recently been described[1] and which makes no *a priori* assumptions about the variation of electron density with height except that it increases monotonically. It can be applied to $h'(f)$ curves from any observatory merely by changing the geomagnetic dip angle and the gyro frequency, both of which are taken into account in the calculations. A fuller account of the use of a digital computer to carry out the calculations is in preparation and will be available later.[2]

The production of $N(h)$ profiles is now proceeding on a routine basis and the computer has been programmed to print out the data in the form shown in Table II, from which either the $N(h)$ or $N(t)$ variations can easily be extracted. It has also been found convenient to have the values of $hmF2$ and $NmF2$ computed and printed out at the bottom of the tables together with ho and No, the height and electron density at the base of the E ar F layer as appropriate.

TABLE II
$N(h)$ PROFILES (UNIT OF ELECTRON DENSITY 10^5 CM^{-3})

Port Stanley (Falkland Islands) July 27, 1957

	Local Mean Time							
h(km)	0000	0100	0200	0300	0400	0500	0600	0700
420	1.57							
410	1.53	1.68	1.76	1.65	1.78			
400	1.44	1.65	1.73	1.58	1.74			
390	1.28	1.61	1.70	1.46	1.69			
380	1.10	1.50	1.62	1.29	1.60			
370	0.85	1.36	1.50	1.10	1.45			
360	0.40	1.17	1.34	0.81	1.25	1.85		
350		0.82	1.13	0.28	1.03	1.80		
340			0.80		0.50	1.70		
330						1.56		
320						1.36		
310						1.11		
300						0.59	2.07	
290							2.01	
280							1.93	
270							1.77	
260							1.57	3.31
250							1.16	3.14
.								.
.								.
.								.
.								.
200								0.79
.								.
.								.
.								.
160								0.21
$hmF2$	429	415	418	419	412	366	302	263
$NmF2$	1.61	1.70	1.79	1.70	1.79	1.89	2.09	2.35
ho	360	345	335	350	340	295	245	160
No	0.40	0.28	0.36	0.28	0.50	0.12	0.28	0.21

Microfilm copies of the tables will be sent to the four IGY World Data Centers which collect ionospheric data at Boulder, Moscow, Slough, and Tokyo. A limited number of booklets containing the tables will also be available.

R. L. SMITH-ROSE
Radio Res. Station
Dept. of Sci. and Indus. Res.
Slough, Bucks, England

* Received by the IRE, May 5, 1958.

[1] J. O. Thomas, Haselgrove, and A. R. Robbins, "The electron distribution in the ionosphere over Slough; quiet days," *J. Atmos. Terr. Phys.*, vol. 13, pp. 46–56; 1958.

[2] J. O. Thomas and M. D. Vickers, "The reduction of $h'(f)$ records to $N(h)$ profiles using an electronic digital computer," to be published.

The Current Amplification of a Junction Transistor as a Function of Emitter Current and Junction Temperature*

A measurement of alpha as a function of emitter current in a typical germanium or silicon-junction transistor usually yields a dependence like the one shown in Fig. 1. The higher current range has been satisfactorily explained by Webster *et al.*,[1-4] but until recently no mechanism had been proposed to account for the drop in alpha at low-emitter currents. This now has been done by Sah *et al.*,[5] who calculated the effect of carrier generation and recombination inside the depletion layer of a *p-n* junction[6-9] on its characteristics. There are three processes, each dominant at a different current level, which account for the current dependence of alpha. At very low currents the recombination in the emitter-depletion layer is high compared to the diffusion current, and the emitter efficiency is low. With increasing total emitter current the useful diffusion current begins to dominate over the recombination current into the emitter junction and the emitter efficiency rises to the customary value given by the doping ratio in base and emitter regions, base width, and diffusion length in the emitter. For still higher emitter currents an aiding electric field develops across the base region and increases the effective diffusion length of the minority carriers. Thus alpha continues to rise. If the emitter current now is increased further, however, the injected carriers near the emitter junction decrease the base resistivity sufficiently to cause a drop in emitter efficiency. Thus alpha goes through a maximum and continues to fall for higher currents.

It is the purpose of this note to combine the above mentioned theories into a single approximate but useful expression for alpha as a function of emitter current. Adding (56) by Rittner[2] and (15) by Sah *et al.*[5] we find for the *p-n-p* transistor

$$I_E = K[2P - \ln(1+P) + \mathcal{E}P(1+P) + 2\,\mathcal{S}\sqrt{P}] \quad (1)$$

where the notation is explained in the list of symbols. The first two terms in the bracket describe the diffusion current, the third term describes the conventional emitter efficiency, and the last term takes the recombination in the emitter junction into account. Differentiating with respect to V_E and neglecting the voltage dependence of $\mathcal{S}$, we find for the new input admittance

$$y_{11} = (\partial I_E/\partial V_E) = (q/kT)KP[(1+2P)/(1+P) + \mathcal{E}(1+2P) + \mathcal{S}P^{-1/2}]. \quad (2)$$

From Rittner's[2] (65) and (72) one obtains the following expression for y_{21}

$$y_{21} = -K(q/kT)P[(1+2P)/(1+P) - \mathcal{R}] \quad (3)$$

where $\mathcal{R}$ describes the bulk and surface recombination in and around the base region. Combining (2) and (3) we finally find

$$1-\alpha = (y_{11}+y_{21})/y_{11} = \mathcal{R}a(I_E) + \mathcal{E}b(I_E) + c(I_E) \quad (4)$$

where

$$a(I_E) = \frac{(1+P)\sqrt{P}}{(1+2P)\sqrt{P} + \mathcal{S}(1+P)}, \quad (5)$$

$$b(I_E) = \frac{(1+P)(1+2P)\sqrt{P}}{(1+2P)\sqrt{P} + \mathcal{S}(1+P)}, \quad (6)$$

$$c(I_E) = \frac{\mathcal{S}(1+P)}{(1+2P)\sqrt{P} + \mathcal{S}(1+P)}. \quad (7)$$

These three factors which describe the current dependence of alpha are shown in Fig. 2(a)–2(c) as a function of the normalized emitter current, Z,

$$Z = I_E/K = 2P - \ln(1+P) + \mathcal{S}\sqrt{P}. \quad (8)$$

In (5) through (8) it has been assumed that the conventional emitter efficiency is high so that $\mathcal{E}$ is a small quantity.

If we apply these considerations to Fig. 1, we find that the curve can be fitted perfectly within the experimental accuracy if the following values of the parameters are assumed, which are very reasonable for the audio unit tested: $A = 1.25\times10^{-3}$ cm^2; $D_{pB} = 40$ cm^2/Vs; $n_{OB} = 5\times10^{14}$ cm^{-3}; $W = 10^{-2}$ cm; $K = 4\times10^{-4}$ amps; $\mathcal{S} = 0.08$; $\mathcal{E} = 5\times10^{-4}$; $\mathcal{R} = 1.3\times10^{-2}$.

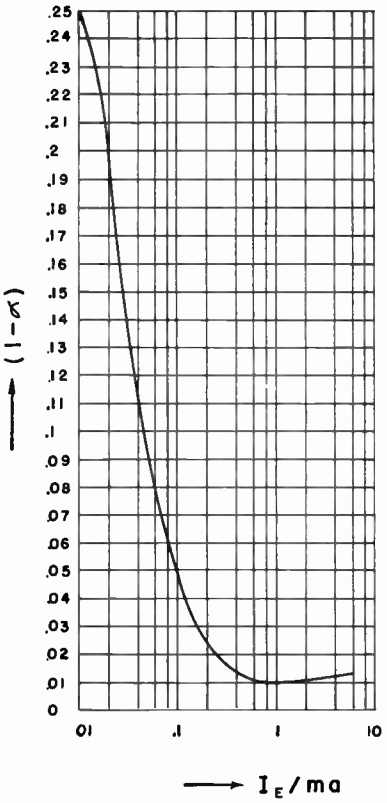

Fig. 1—(1—α) as a function of emitter current measured on a germanium *p-n-p* junction transistor.

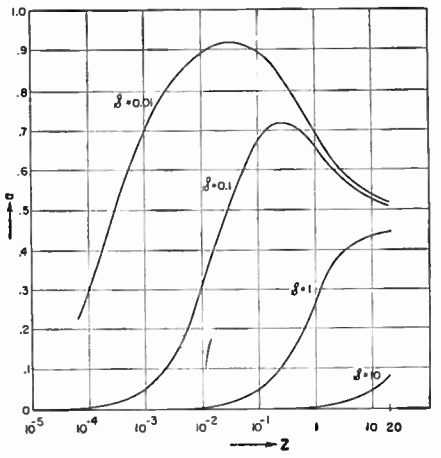

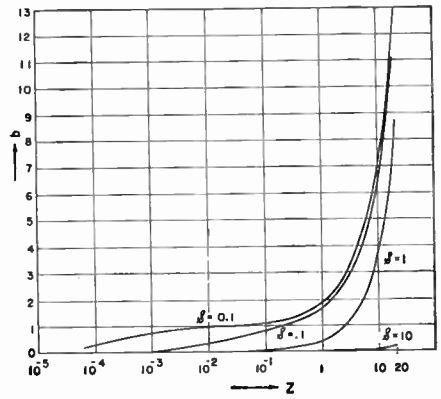

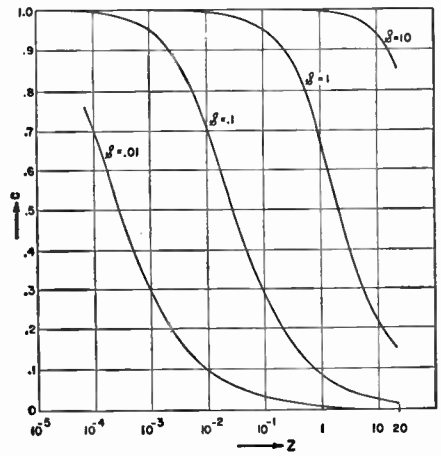

Fig. 2—(a) The function $a(I_E)$ plotted vs the normalized emitter current, Z. (b) The function $b(I_E)$ plotted vs the normalized emitter current, Z. (c) The function $c(I_E)$ plotted vs the normalized emitter current Z.

* Received by the IRE, April 30, 1958.

[1] W. M. Webster, "On the variation of junction-transistor current-amplification factor with emitter current," PROC. IRE, vol. 42, pp. 914–920; June, 1954.
[2] E. S. Rittner, "Extension of the theory of the junction transistor," *Phys. Rev.*, vol. 94, pp. 1161–1171; June, 1954.
[3] T. Misawa, "Emitter efficiency of junction transistor," *J. Phys. Soc., Japan*, vol. 10, pp. 362–367; May, 1955.
[4] L. D. Armstrong, C. L. Carlson, and M. Bentivegna. "*P-N-P* transistors using high-emitter-efficiency alloy materials," *RCA Rev.*, vol. 17, pp. 37–45; March, 1956.
[5] C. T. Sah, R. N. Noyce, and W. Shockley, "Carrier generation and recombination in *p-n* junctions and *p-n* junction characteristics," PROC. IRE, vol. 45, pp. 1228–1243; September, 1957.
[6] W. Shockley and W. T. Read, Jr., "Statistics of recombinations of holes and electrons," *Phys. Rev.*, vol. 87, pp. 835–842; September, 1952.
[7] H. Kleinknecht and K. Seiler, "Einkristalle und *pn* Schichtkristalle aus Silizium," *Z. Physik*, vol. 139, pp. 599–618; December 20, 1954.
[8] E. M. Pell and G. M. Roe, "Reverse current and carrier lifetime as a function of temperature in germanium junction diodes," *J. Appl. Phys.*, vol. 26, pp. 658–665; June, 1955.
[9] M. Bernard, "Mesures en fonction de la temperature du courant dans les junctions de germanium *n-p*," *J. Electronics*, vol. 2, pp. 579–596; May, 1957.

It will be noted that the drop in α at small currents is explained by recombination in the emitter junction (function c) and could not have been accounted for by the Webster-Rittner-Misawa theory alone.

If one measures the current-dependence of α as a function of operating temperature, one obtains curves like the ones shown in Fig. 3.

The room temperature curve in Fig. 3 can be fitted by the following values of the parameters which may be considered typical for a germanium p-n-p audio transistor: $A=2.5\times10^{-3}$ cm²; $D_{pB}=40$ cm²/√s; $n_{OB}=5\times10^{14}$ cm⁻³; $W=8\times10^{-3}$ cm; $K=10^{-3}$ amps; $\mathcal{S}=0.003$; $\mathcal{E}=1.1\times10^{-2}$; $\mathcal{R}=1.94\times10^{-4}$. To fit the curves at the other temperatures it is necessary to assume a temperature dependence of the various parameters as shown in Fig. 4. If these variations are compared with the temperature dependence of the material properties involved, using previously published data,[10] one finds that they follow completely the theoretical expectations. To obtain the proper variation of lifetime one has to assume a recombination level somewhat less than 0.2 ev above the valence band or below the conduction band. The proportionality constant, K, drops like the diffusion constant in high-resistivity material. The recombination term, $\mathcal{R}$, drops inversely proportional to the square of the diffusion length. According to the Hall[11]-Shockley-Read[12] mechanism of carrier recombination, the carrier lifetime increases as the material approaches the intrinsic range. This has also been experimentally verified.[13,14] Should the surface recombination be dominant in the recombination term, $\mathcal{R}$, one will still observe a similar behavior because surface recombination follows the same laws as volume recombination.[15] The term $\mathcal{E}$ describing the emitter efficiency increases with temperature proportional to the ratio of a diffusion constant in highly doped material[10] (impurity scattering) over a diffusion constant in pure material (lattice scattering). In short, one may say the variation with temperature of the current dependence of α is caused by both a decrease in recombination and in emitter efficiency. The maximum value of α is therefore higher and the falloff at high currents is more rapid at elevated temperatures. Theoretically, one expects that the parameter, $\mathcal{S}$, which specifies the relative importance of the recombination in the emitter-junction depletion layer, increases with temperature by approximately a factor of 2 from −20°C to 70°C. This does not seem to be fully borne out by the measurements, which may be due to the fact that (15) in the paper by Sah *et al.*[5] has been derived under the simplest possible assumptions. The recombination in junctions seems to require additional work and careful measurements of α as a function of emitter current may provide a valuable tool in such investigations.

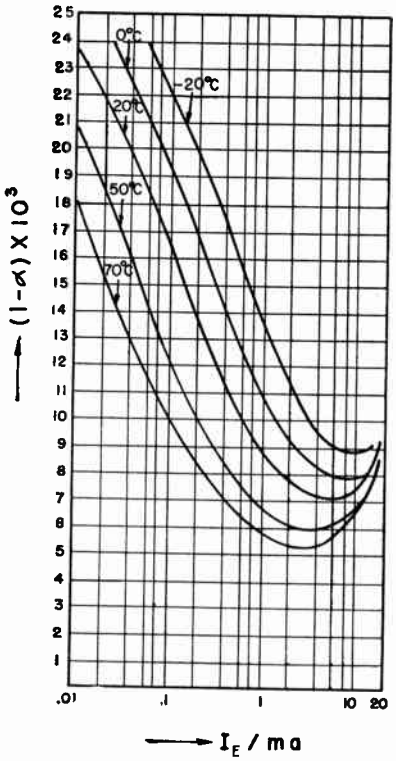

Fig. 3—$(1-\alpha)$ as a function of emitter current for various operating temperatures measured on a germanium p-n-p junction transistor.

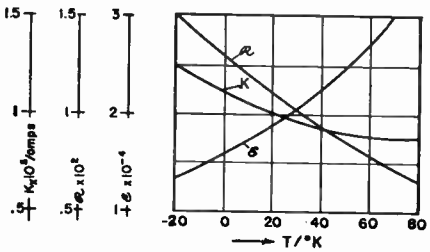

Fig. 4—Temperature dependence of parameters required to fit curves of Fig. 3.

In conclusion, by combining the Webster-Rittner theories with the effects of recombination in the emitter junction, the dependence of α on emitter current and temperature can be quantitatively explained over the whole operating range. It may also be deduced from the above considerations that the temperature effects may be minimized by high doping in the base region provided the emitter region is of still much lower resistivity to insure the necessary good emitter efficiency. Thin base width also acts in the same direction.

The refinements in the theory should also improve a previously described technique[16] to investigate changes in transistor surface conditions in an environmental reliability test. Similar measurements should yield information on what happens to transistors under nuclear irradiation.

The authors would like to thank Mrs. B. L. Yeamans for carrying out the numerical calculations.

List of Symbols

I_E = emitter current
$K=(qAD_{pB}n_{OB})/W$
$P=(p_{OB}/n_{OB})e^{qV_E/kT}$

$$\mathcal{E}=\frac{D_{nE}n_{OE}}{D_{pB}p_{OB}}\frac{W}{L_{nE}}$$

$$\mathcal{S}=\frac{1}{2}\frac{kT}{qE}\frac{W}{D_{pB}\tau_0}$$

q = electronic charge
A = conducting cross section
D_{pB} = diffusion constant of holes in the base
n_{OB} = equilibrium density of electrons in the base
W = base width
p_{OB} = equilibrium density of holes in the base
V_E = emitter voltage
k = Boltzmann's constant
T = absolute temperature
D_{nE} = diffusion constant of electrons in the emitter
L_{nE} = diffusion length of electrons in the emitter
E = average electric field strength in the depletion layer of the emitter junction
τ_0 = lifetime for carriers injected into the depletion layer of the emitter junction

$$\mathcal{R}=\frac{W'^2}{2D_{pB}\tau_{pB}}+\frac{A_s s_0 W}{2AD_{pB}}$$

τ_{pB} = lifetime of holes in the base region
A_s = surface area over which recombination takes place
s_0 = surface recombination velocity.

W. W. Gärtner
R. Hanel
R. Stampfl
F. Caruso
U. S. Army Signal Eng. Lab.
Fort Monmouth, N. J.

Alternative Detection of Co-Channel FM Signals*

The work of Granlund[1] and Baghdady[2,3] has demonstrated that the stronger of two co-channel FM signals can be freed of inter-

* Received by the IRE, April, 4, 1958.

[1] J. Granlund, "Interference in Frequency-Modulation Reception," Res. Lab. Electronics, M.I.T., Cambridge, Mass., Tech. Rep. No. 42; January 20, 1949.

[2] E. J. Baghdady, "Interference Rejection in FM Receivers," Res. Lab. Electronics, M.I.T., Cambridge Mass., Tech. Rep. No. 252; September 24, 1956.

[3] E. J. Baghdady, "Theory of feedback around the limiter," 1957 IRE National Convention Record pt. 8, pp. 176–202.

[10] W. W. Gärtner, "Temperature dependence of junction transistor parameters," Proc. IRE, vol. 45, pp. 662–680; May, 1957.

[11] R. N. Hall, "Electron-hole recombination in germanium," *Phys. Rev.*, vol. 87, p. 387; July, 1952.

[12] W. Shockley and W. T. Read, Jr., "Statistics of the recombination of holes and electrons," *Phys. Rev.*, vol. 87, pp. 835–842; September, 1952.

[13] G. Bemsky, "Lifetime of electrons in p-type silicon," *Phys. Rev.*, vol. 100, pp. 523–524; October, 1955.

[14] S. Goldstein, H. Mette, and W. W. Gärtner, "Temperature dependence of the PME effect in germanium," *Bull. Amer. Phys. Soc.*, ser. II, vol. 3, p. 104; March, 1958.

[15] D. T. Stevenson and R. J. Keyes, "Measurements of the recombination velocity at germanium surfaces," *Physica*, vol. 20, pp. 1041–1046; November, 1954.

[16] W. W. Gärtner and V. Boxer, "Beta-vs-I_E measurements as a tool in transistor reliability studies," *Proc. Transistor Reliability Symp.*, New York, N. Y., pp. 73–76; September, 1956.

ference due to the presence of the weaker signal for relative amplitudes approaching unity. Such a capability suggests a solution to the problem of reading the modulation of the weaker signal or, if desired, of reading the outputs due to both signals simultaneously. Wilmotte[1] proposed a means of accomplishing a similar task by working with the detected modulations themselves; indeed, it is interesting to note, in passing, that exact knowledge of the carrier frequency and relative amplitudes of the two signals in the absence of noise theoretically permits their complete separation after detection, but the attendant practical problems are considerable. These problems are not present if the necessary correlation between the stronger signal and the sum of the stronger and weaker signals is provided at the intermediate frequency of the receiver. A block diagram of such a receiver, indicating the principal stages required, is shown in Fig. 1.

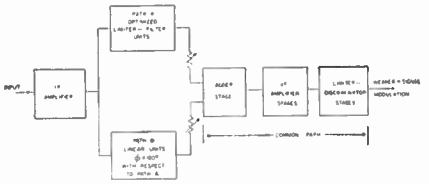

Fig. 1.

With linear operation through the first IF stage, the sum voltage available for excitation of the parallel paths, A and B, can be stated as

$$e(t) = e_1(t) + \alpha e_2(t),$$

where $0<\alpha<1$. Path A, operating as an optimized limiter-filter chain, is capable of producing an output, $e_1(t)$, as free of interference due to the presence of the weaker signal, $\alpha e_2(t)$, as desired. Path B, incorporating either one more or one less 180-degree phase reversal than Path A, delivers to an output attenuator an otherwise carefully preserved version of the summation signal. This signal is adjusted in amplitude to match the level of the limiter output in such a manner as to realize maximum common-mode rejection of the stronger signal, $e_1(t)$, in the output of the common-path adder. The roles of the two signals in the balance of the receiver are now interchanged, resulting in the residual signal, $\alpha e_2(t)$, being capable of capturing the common-path limiter amplifiers.

It can be readily appreciated that the stronger signal alone, $e_1(t)$, can be obtained by opening either Path A or Path B. However, if the two detected outputs are desired simultaneously, then the addition of the usual discriminator-detector and modulation amplifier units to Path A will permit such facility.

The advantages of the alternative scheme of co-channel reception in situations characterized by spectrum crowding are obvious, particularly in view of the relative simplicity of the receiver and the comparatively small number of components which must be incorporated into an existing quality receiver to achieve simultaneous or alternative detection.

The effective range of α which can be satisfactorily accommodated is determined by several circuit limitations: 1) the degree to which optimization of the limiter-filter path is economically feasible; 2) the amount of common-mode rejection which can be realized at the adder input; 3) the amount of incidental AM and noise present in the summation signal; and 4) the amplitude of the residual signal compared with the noise at the input to the common-path portion of the receiver. While these several factors restrict the effective range of operation, they do not nullify the potential usefulness of the proposed method of weak-signal or alternative-signal detection.

H. W. Farris
Eng. Res. Inst.
University of Michigan
Ann Arbor, Mich.

[1] R. M. Wilmotte, "Reception of an FM signal in the presence of a stronger signal in the same frequency band, and other associated results," *Proc. IEE*, vol. 101, pt. III, pp. 69–75; March, 1954.

A Series Expansion Method for Finding Approximate Laplace Transforms*

Gibbons' letter[1] represents the extension to Fourier analysis of a method known and used in the application of Laplace and Fourier transforms.[2,3]

The method is usually applied in finding the transform of a function which can be represented (or approximated) by a series of segments, the analytic expressions of which are simple polynomials in the variable t, and which are valid in an interval whose boundaries are given. By successive differentiation, the representation is reduced to a series of impulses appearing at the boundaries, which are then transformed in the usual manner. If the representation is well chosen, the impulses may be obtained almost by inspection. Though the formalism of the method seems to imply that the derivative of a simple discontinuity exists and is an impulse, the procedure can be justified by the use of the δ function.

It is the purpose of this letter to demonstrate a much less sophisticated approach which not only gives some insight into the impulse method, but is in its own right frequently as easy to apply. Moreover, this new method permits the inclusion of segments described by functions possessing an infinite number of nonzero derivatives, a situation which the impulse method does not permit.

* Received by the IRE, April 11, 1958.

[1] J. F. Gibbons, "A simplified procedure for finding Fourier coefficients," Proc. IRE, vol. 45, p. 243; February, 1957.

[2] J. G. Truxal, "Automatic Feedback Control System Synthesis," McGraw-Hill Book Co., Inc., New York, N. Y., p. 375; 1955.

[3] E. A. Guillemin, "Computational techniques which simplify the correlation between steady-state and transient response of filters and other networks," *Proc. Natl. Electronics Conf.*, vol. 9, pp. 513–532; 1953.

Suppose that it is desired to obtain the Laplace transform of the function $F(t)$ which has at most a finite number of simple discontinuities in the interval $0<t<\infty$. Suppose further that $F(t)$ may be represented by a finite number of segments [which we shall take for the moment as being simple polynomials in (t)] such that

$$\begin{aligned} F(t) &= f_0(t) \qquad 0 < t < t_1 \\ &= f_1(t) \qquad t_1 < t < t_2 \\ &= \cdots\cdots\cdots \\ &= f_i(t) \qquad t_i < t < t_{i+1} \\ &= \cdots\cdots\cdots \\ &= f_n(t) \qquad t_n < t < \infty. \end{aligned} \tag{1}$$

[$f_n(t)$ is required to be transformable.]

The transform of $F(t)$ is given by

$$\begin{aligned} \mathcal{L}[F(t)] = &\int_0^{t_1} f_0(t)e^{-st}dt \\ &+ \int_{t_1}^{t_2} f_1(t)e^{-st}dt + \cdots \\ &+ \int_{t_i}^{t_{i+1}} f_i(t)e^{-st}dt + \cdots \\ &+ \int_{t_n}^{\infty} f_n(t)e^{-st}dt. \end{aligned} \tag{2}$$

To evaluate the contribution of the ith segment, we integrate by parts

$$\begin{aligned} &\int_{t_i}^{t_{i+1}} f_i(t)e^{-st}dt \\ &= -\frac{1}{S}\left[f_i(t)e^{-st}\right]_{t_i}^{t_{i+1}} + \frac{1}{S}\int_{t_i}^{t_{i+1}} f_i^{(1)}(t)e^{-st}dt \end{aligned}$$

where $f_i^{(1)}$ is the first derivative of f_i. If this process is repeated, differentiating the derivative of f_i and integrating e^{-st} each time, the point will be reached when further differentiation of f_i yields zero. Hence, the result is obtained

$$\begin{aligned} \int_{t_i}^{t_{i+1}} f_i(t)e^{-st}dt = &\frac{1}{S}\sum_{K=0}^{K_i}\left[\frac{1}{S^K}f_i^{(K)}(t_i)e^{-st_i}\right] \\ &- \frac{1}{S}\sum_{K=0}^{K_i}\left[\frac{1}{S^K}f_i^{(K)}(t_{i+1})e^{-st_{i+1}}\right] \end{aligned} \tag{3}$$

where K_i is the number of nonzero derivatives of f_i.

Treating all the integrals in (2) in the same manner $\mathcal{L}(F)$ is found to be

$$\begin{aligned} \mathcal{L}[F(t)] = \sum_{e=0}^{n}\Bigg\{&\frac{1}{S}\sum_{K=0}^{K_e}\left[\frac{1}{S^K}f_e^{(K)}(t_e)e^{-st_e}\right] \\ &- \frac{1}{S}\sum_{K=0}^{K_e}\left[\frac{1}{S^K}f_e^{(K)}(t_{e+1})e^{-st_{e+1}}\right]\Bigg\} \end{aligned} \tag{4}$$

where $t_0=0$, and $t_{n+1}=\infty$.

For the purpose of delineation, suppose that $f_i(t)$ has just two nonzero derivatives and write (3) explicitly

$$\begin{aligned} &\int_{t_i}^{t_{i+1}} f_i(t)e^{-st}dt \\ &e^{-st_i}\left\{\frac{1}{S}f_i(t_i) + \frac{1}{S^2}f_i^{(1)}(t_i) + \frac{1}{S^3}f_i^{(2)}(t_i)\right\} \\ &-e^{-st_{i+1}}\left\{\frac{1}{S}f_i(t_{i+1}) + \frac{1}{S^2}f_i^{(1)}(t_{i+1})\right. \\ &\left.+\frac{1}{S^3}f_i^{(2)}(t_{i+1})\right\}. \end{aligned} \tag{5}$$

An examination of (5) shows that it could have been obtained in the usual formalism by a term-by-term transformation of the Taylor series expansions of f_i about the two points, t_i and t_{i+1}, the limits of its interval of validity. The quantities, $f_i(t_i)$, $f_i^{(2)}(t_{i+1})$, etc., are simply the constants in the Taylor expansion and are calculated in the usual way.

A better understanding of the impulse method may be obtained by writing explicitly the series obtained for the segment f_{i+1} at the lower limit of its interval of validity, t_{i+1}, and combining it with the series for f_i at its upper limit, which is also t_{i+1}. For convenience we assume that f_{i+1} has just one nonzero derivative. For the f_{i+1} series we have

$$e^{-st_{i+1}}\left\{\frac{1}{S}f_{i+1}(t_{i+1})+\frac{1}{S^2}f_{i+1}^{(1)}(t_{i+1})\right\}$$

and for the f_i series

$$-e^{-st_{i+1}}\left\{\frac{1}{S}f_i(t_{i+1})+\frac{1}{S^2}f_i^{(1)}(t_{i+1})+\frac{1}{S^3}f_i^{(2)}(t_{i+1})\right\}.$$

Combining them gives

$$e^{-st_{i+1}}\left\{\frac{1}{S}\left|f_{i+1}(t_{i+1})-f_i(t_{i+1})\right|+\frac{1}{S^2}\left|f_{i+1}^{(1)}(t_{i+1})-f_i^{(1)}(t_{i+1})\right|+\frac{1}{S^3}\left|0-f_i^{(2)}(t_{i+1})\right|\right\}. \quad (6)$$

If f_{i+1} and f_i are continuous at t_{i+1}, then $f_{i+1}(t_{i+1})=f_i(t_{i+1})$ and the first term in brackets would vanish. If their first derivatives are different at t_{i+1}, then the second term in brackets is seen to be precisely that which would be obtained by the impulse method, as is also the third term.

To illustrate, let us calculate the terms in the transform of $F(t)$ arising from the junction of $f_i(t)$ and $f_{i+1}(t)$ at t_{i+1}, if $f_i(t)=5-(t-3)^2$, $f_{i+1}(t)=20-4t$ and $t_{i+1}=4$.

The steps involved in the impulse method are shown in Fig. 1 and give

$$\frac{e^{-4S}}{S}\left[-\frac{2}{S}+\frac{2}{S^2}\right].$$

By the present Taylor series method we have

	t	$t=4$		t	$t=4$
f_i	$5-(t-3)^2$	4	f_{i+1}	$20-4t$	4
$f_i^{(1)}$	$-2(t-3)$	-2	$f_{i+1}^{(1)}$	-4	-4
$f_i^{(2)}$	-2	-2			

Combining as in (6) we have

$$e^{-4S}\left\{\frac{1}{S}\left|4-4\right|+\frac{1}{S^2}\left|-4-(-2)\right|+\frac{1}{S^3}\left|0-(-2)\right|\right\}$$

or

$$\frac{e^{-4S}}{S}\left[-\frac{2}{S}+\frac{2}{S^2}\right].$$

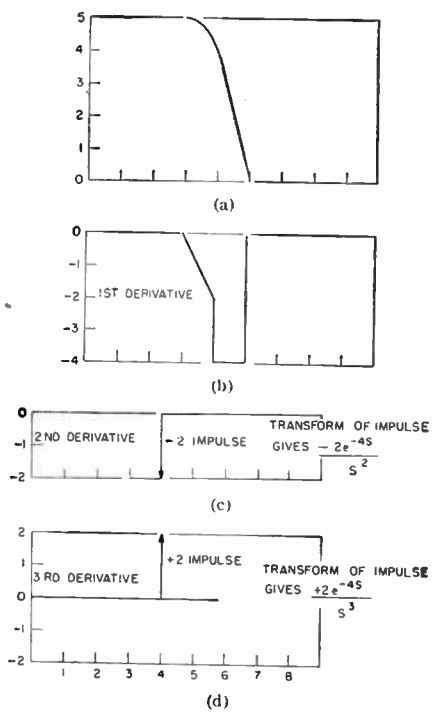

Fig. 1.

Thus, we see that the first term in the transform may be thought of either as arising from the transformation of the derivative of the negative step of 2 units in the first derivative at $t=4$, Fig. 1(b), or as the difference of the first derivative coefficients in the Taylor expansion of f_i and f_{i+1} at that point. A similar situation holds for the second term which comes from the difference of the second derivative.

It is frequently convenient to think of the series expansion method in terms of the contributions to the total transform arising from the interval boundaries. [If, for example, $f_{i+1}(t)=f_i(t)$, then all the brackets in (6) would be identically zero and there would be no contribution at the point $t=4$.] Except for the $t=0$ and $t=\infty$ points, these contributions would all have the form of expression (6). For $t=0$, all the negative bracketed terms vanish since $F(t)\triangleq 0$, for $t<0$. Evidently, all terms must vanish at $t=\infty$, hence, the requirement that the segment $f_n(t)$ which is valid in the interval ending at ∞ must be transformable.

If, on the other hand, the method is thought of in terms of the contribution arising from each analytic segment, functions more complicated than simple polynomials, *e.g.*, transcendental functions, may be used. In such a case, the transform of the function for the interval in which it is valid may be calculated by direct integration and the result simply added to the terms arising from the series expansion of the other segments. Such a combination of methods may save both time and labor.

It should be pointed out also that the use of the series expansion method in conjunction with the approximation of a function by a series of straight-line segments which are continuous at the boundaries of their intervals of validity and have at most one nonzero derivative is quite rapid and simple. Since the functions are continuous, the first brackets of expression (6) vanish, and only the second, involving first derivative differences, need be evaluated. Hence, the transform of the approximation depends primarily on the slopes of the approximating lines. This fact calls to mind Guillemin's argument[3] that a better approximation may be obtained by approximating a derivative than by approximating the function itself. In fact, if the nth derivative of a function is approximated by straight lines, continuous at the interval boundaries, none of the lower derivatives need be calculated since these will also be continuous at the boundaries. Therefore, only the nth and $(n+1)$th derivatives need be calculated.

W. H. Lucke
U. S. Naval Research Lab.
Washington 25, D.C.

Effective Collector Capacitance in Transistors*

The collector-to-base capacitance, C_{ob}, of a transistor biased in the usual manner, *i.e.*, collector-base voltage large compared to $kT/e=25$ mv (at room temperature) and negative for the p-n-p type here considered, is comprised of two terms,

$$C_{ob}=C_{sp}+C_{st}. \quad (1)$$

The first term arises from the change in number of electrons with the change of the width of the collector space-charge layer

$$C_{sp}=\frac{\partial Q_n}{\partial W}\cdot\frac{\partial W}{\partial V_c} \quad (2)$$

while the second term arises from the change in the number of holes stored in the base layer with a change in width of the collector space-charge layer:

$$C_{st}=\frac{\partial Q_{st}}{\partial W}\cdot\frac{\partial W}{\partial V_c}. \quad (3)$$

It is the purpose of this note to point out that the dependence of the storage capacitance, C_{st}, on the emitter current can be utilized to determine the base width of transistors with uniform impurity distribution in the base layer.

The following assumptions will be made: 1) an abrupt collector junction with much higher doping in the collector region than in the base region, 2) neglect of the spreading effects at the boundaries of the collector junction; *i.e.*, we consider a one-dimensional transistor model, 3) an emitter current carried practically entirely by holes, 4) a diffusion length of holes in the base region which is very large compared to the width of the base layer, and 5) a sufficiently low injection level of holes from the emitter that space charges arising from presence of holes in the base layer can be neglected.

For an abrupt junction with much higher doping in the collector region than in the

* Received by the IRE, April 11, 1958.

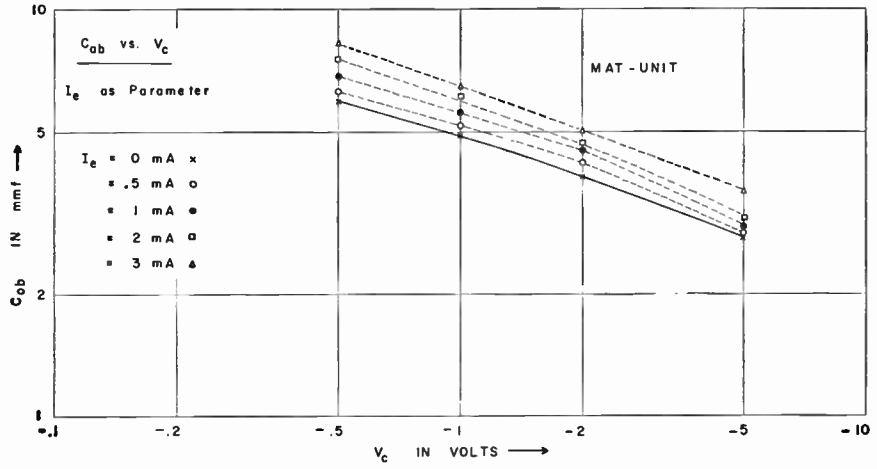

Fig. 1—Effective capacitance measurements on a microalloy transistor.

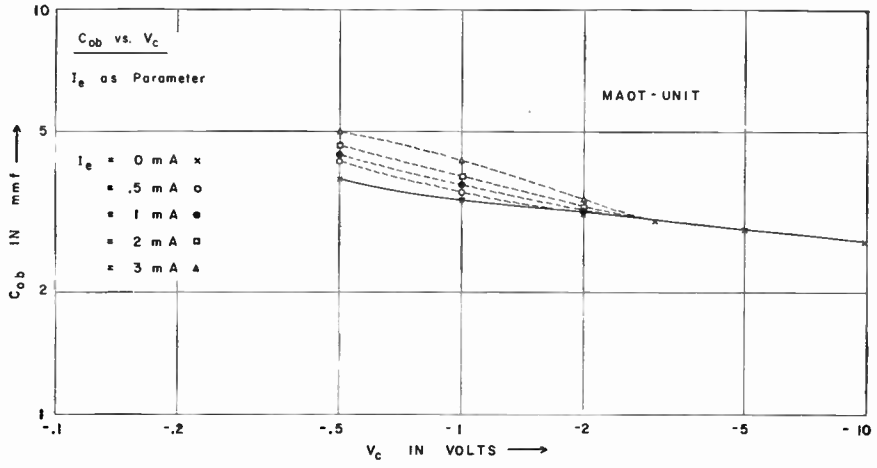

Fig. 2—Effective capacitance measurements on a microalloy-diffused transistor.

base region, one has[1]

$$\frac{\partial Q_n}{\partial W} = A \cdot N \cdot e \tag{4}$$

where A is the area of the collector junction, and N is the impurity concentration in the base layer, and[2]

$$\frac{\partial W}{\partial V_c} = \left[\frac{\epsilon\epsilon_0}{2V_c N e}\right]^{1/2}. \tag{5}$$

With the assumptions 2)–5), the hole distribution in the base layer decreases linearly from the emitter to the collector,[3] and

$$I_e \approx \frac{ep_0 D_p}{W}, \tag{6}$$

i.e.,

$$\frac{\partial Q_{si}}{\partial W} = \frac{e\partial(p_0 W/2)}{\partial W} = I_e W/D_p. \tag{7}$$

Since the space-charge capacitance does not depend on emitter current, one has from (1)–(4), and (7)

$$\frac{\partial C_{ob}}{\partial I_e} = W/D_p \cdot \frac{\partial W}{\partial V_c} = \frac{W}{D_p} \cdot \frac{C_{sp}}{ANe}. \tag{8}$$

The space-charge capacitance equals the collector-base capacitance at zero-emitter current, and (8) thus may be written also in the form

$$W = ANeD_p \cdot \frac{\partial C_{ob}}{\partial I_e} C_{ob}^{-1}\Big|_{I_e=0} \tag{9}$$

which lends itself to determination of W, since the quantities at the right side are either known or readily measurable.

Fig. 1 shows experimental results of a microalloyed transistor (MAT), for which $A = 2.4\times10^{-4}$ cm² and $N = 2.4\times10^{15}$ atoms/cm³, *i.e.*, a resistivity of 0.7 ohm-cm in the base region. Applying (9), one obtains a base width $W = 0.4\times10^{-3}$ cm which is of the correct order of magnitude. Collector-to-emitter distance determined by the processing method was 0.5×10^{-3} cm and subtracting the widths of the space-charge layers at the collector and emitter, which were estimated to 0.1×10^{-3} cm and $.05\times10^{-3}$ cm, respectively, yields $W = 0.35\times10^{-3}$ cm. Other effects such as the change in base-current distribution with a change in emitter current may have contributed to the observed dependence of C_{ob} on the emitter current; however, it is felt that the major contribution comes from the storage capacitance discussed in this note.

Fig. 2 shows the results of corresponding measurements on a graded-base microalloyed transistor (MADT). It appears that the storage capacitance vanishes at higher collector voltage. This is not unreasonable considering that the collector space-charge layer extends then into a base region of comparatively high impurity concentration, where $\partial W/\partial V_c$ becomes extremely small. Quantitative evaluation requires consideration of the drift field in the base layer when calculating the hole charge stored in the base layer.

The writer is grateful to C. Wrigley of this laboratory for measurements taken during this investigation.

R. Zuleeg
Sprague Electric Co.
North Adams, Mass.

[1] J. M. Early, "Design theory of junction transistors," *Bell Sys. Tech. J.*, vol. 32, pp. 1271–1312; November, 1953.

[2] It is assumed that V_c is much larger than the built-in potential which has been neglected.

[3] W. Shockley, "The theory of *p-n* junctions in semiconductors and *p-n* junction transistors," *Bell Sys. Tech. J.*, vol. 28, pp. 435–489; July, 1949.

Maximum Utility in Government Contract Reports*

In his short article, Herold[1] proposes four rules to promote effectiveness of R & D reports. In general, this theme is considered of great value. The topic is worthy of a full scale presentation in the Proceedings.

As to the rules themselves, however, several are subject to question. The first rule stated—to eliminate negative values altogether—is believed not appropriate to the intent of the contract report. Negative values or unsuccessful results frequently contain useful information. It is nearly axiomatic in scientific endeavor that all information obtained, even negative, is of potential value. Often the total result of a project is negative, *i.e.*, it does not achieve the desired or expected results, but the project proves ultimately useful. On any research project, the knowledge that someone else has been unsuccessful in a particular approach to a problem can, by obviating repetition, save considerable time and manpower. Knowledge of another's failures may well be all that is needed to at least expedite one's own successful conclusion of a project.

It is not suggested that any detailed description be made of unsuccessful or negative results, but sufficient data should be given so that any future researcher is warned away from previously explored paths.

In the same vein, the second rule—barely mentioning nearly valueless effort—is also doubtful. Marginal or submarginal effort should not necessarily be slighted to the extent suggested by Herold. A reasonable summary of accomplishment of this effort should be considered for the same reasons as for the purely negative results. Furthermore, since this low-grade result is not proved completely unfeasible, it has

* Received by the IRE, April 7, 1958.

[1] E. W. Herold, "A plea for maximum utility in governmen contract reports covering research and development," Proc. IRE, vol. 46, p. 360; January, 1958.

presumably not been fully discarded by the original researcher. If a fair description of this work is given, some other interested scientist may be able to pursue it further to an acceptable conclusion fitting his particular needs. If so, he will have benefited by another's labors, saving his time and the taxpayers' money. Presuming that in any one research task, the unsuccessful approaches numerically outnumber the obviously successful, it would appear that another researcher seeking a problem solution relating to but not identical with the original solution has a better chance of eventually using one of the unsuccessful.

In general, stating negative or marginal results in a report will effectively both warn another researcher away from the particular trend of investigation, and call his attention to it for further consideration. These two effects, although opposite, are not believed inconsistent.

Not to be discounted is the ever present opportunity for accidental discovery. A particular researcher, engrossed as he is in his own problem, vitally concerned with attaining a known end, is likely to ignore the possible alternate applications of his nominally unsuccessful endeavor. Only by recording this endeavor can anyone but the original worker pursue the alternates. It is noted that by so formally recording (in a contract report) these tribulations the original worker has effectively protected his future rights to credit, and in some circumstances to patents.

Consistent with the above thoughts, the first two rules of Herold's article could be reworked in the following manner:

1) Provide a brief statement of each negative or completely unsuccessful result, indicating simply what was done and why it was of no use in the particular application.

2) Severely summarize the description of all marginal activity providing, however, sufficient detail to allow evaluation by other interested scientists.

The remaining two rules are considered incapable of improvement. They state a primary duty of the reporter of a government R & D project. If the original researcher accents the important results of his work, his report will always be of maximum benefit to the government and industry.

This writer is a government employee whose responsibility it is to review a large number of R & D reports on many projects and in many scientific fields. He desires to add another rule to Herold's list. Most government agencies attempt to standardize and formalize contract reports by requesting adherence to specifications or contract requirements which dictate format, layout, content, etc. On a majority of projects, this is to the interest of the government and taxpayer and has no deleterious effect on the project or the report thereof. However, if these rigid requirements do not fit the special case at hand or will result in reduced value of the proposed report, it is strongly recommended that the reporter should not resignedly follow the government requirement. He can confer with the government agency preferably at the time of contract negotiation and request a change. In nearly every instance, the government technical personnel responsible for project performance will have no objection to waiving or modifying the requirements and will indeed welcome any suggestion that improves the quality of the project output, or in this instance, the contract reports. If the local government officer having cognizance of the contract is an engineer or a contract administrator fully aware of his responsibilities, he will recommend compliance with the improved report arrangement by endorsement or by separate correspondence with the government procuring agency. In special cases, the local government engineer will go even further in persuading the procuring agency to change its requirements or will even locally authorize deviations from a fixed requirement where the end result will benefit the scientific community. To this end, the following rule no. 5 is proposed:

5) Where conformance to the report-writing requirements of a specification or government contract will reduce the utility or value of a contract report, request the local cognizant government engineer and/or the procuring agency to modify the requirement.

It is suggested that Herold, or someone equally familiar with the need for more effective technical reports, be persuaded to expand on his theme in a paper in the PROCEEDINGS. Thus advertising the problem would undoubtedly aid in bettering the interchange of technical information between researchers and in giving the taxpayer a better, more effective job for his money.

FLETCHER H. WARREN
144 Cleveland Drive
Kenmore, N. Y.

Author's Comment

Warren's comments are valuable and pertinent in many respects, but in one instance he seems to have missed the point of my original letter. He states that the first rule, *i.e.*, to eliminate negative *values* altogether, is "not appropriate," and implies that the words "negative values" are synonymous with "negative results." It was clearly pointed out in the original letter that unsuccessful or negative results often have *positive* values.

My definition of "negative value" was supposed to have been made clear in the second paragraph of my original letter. One can hardly quarrel with the first rule if one understands my use of the words. By definition, a negative value impedes progress by others, rather than helping it. A result which goes far beyond having *no* value, and actually does harm, has negative value. An incorrect measurement, a lengthy computation with the wrong answer, or a completely misleading interpretation of an experiment, if any of these are recognized at the time, should not fill space in a contract report just to show how busy the investigator has been.

On the contrary, if a correctly done experiment is unsuccessful in achieving its objective, or a correct computation yields an undesired answer, or sound application of a technique fails to work, or an accidental discovery unrelated to the work is made, these may have *great value* and should then be reported in considerable detail.

In conclusion, it seems to me that Warren and I are in complete agreement concerning the requirements of a maximum-utility report, but we use somewhat different language in describing our views.

E. W. HEROLD
RCA Labs.
Princeton, N. J.

Proposal for a Maser-Amplifier System Without Nonreciprocal Elements*

A cavity-type solid-state maser[1,2] is intrinsically a regenerative device, so to take full advantage of its low-noise properties[3] one wishes to prevent noise from being fed back from its load; otherwise, the noise temperature of the system cannot be lower than that of the load (presumably a vacuum tube or crystal converter having an effective temperature greater than 290°K). A nonreciprocal device such as a ferrite circulator has been suggested[1] and appears to be the best solution, at least until means are found for using the gyromagnetic properties of the paramagnetic salt to make the maser itself nonreciprocal. However, as masers have been operated at frequencies such as 1380 mc[4,5] and even 300 mc[6] where satisfactory ferrite circulators are not yet available, and because this situation seems likely to continue for some time at low frequencies, a look into the possibility of using cavity masers without circulators seems worthwhile.

The most direct approach is to introduce attenuation between the maser and its load by some lossless power-dividing network such as a directional coupler. This reduces the noise fed back into the maser by sacrificing gain, but may be useful if enough gain remains (at the desired bandwidth) to overcome the noise from the next amplifier stage.

The system we wish to propose requires two matched masers but involves no loss of gain-bandwidth and is capable in principle of giving a system noise figure equal to that of the masers. As seen in Fig. 1, signal power entering arm 3 of a magic T (this may be coaxial or waveguide, or might be a side-

* Received by the IRE, May 16, 1958. The research in this document was supported jointly by the Army, Navy, and Air Force under contract with Mass. Inst. Tech.

[1] N. Bloembergen, "Proposal for a new solid state maser," *Phys. Rev.*, vol. 104, pp. 324–327; October 15, 1956.

[2] A. L. McWhorter and J. W. Meyer, "Solid-state maser amplifier," *Phys. Rev.*, vol. 109, pp. 312–318; January 15, 1958.

[3] A. L. McWhorter and F. R. Arams, "System-noise measurement of a solid-state maser," PROC. IRE, vol. 46, pp. 913–914; April, 1958.

[4] J. O. Artman, N. Bloembergen, and S. Shapiro, "Three-level solid-state maser at 21-cm," *Phys. Rev.*, vol. 109, pp. 1392–1393; February 15, 1958.

[5] S. H. Autler and N. McAvoy, "21-cm solid-state maser," *Phys. Rev.*, vol. 10, pp. 280–281; April 1, 1958.

[6] R. H. Kingston, "A uhf solid-state maser," PROC. IRE, vol. 46, p. 916; April, 1958.

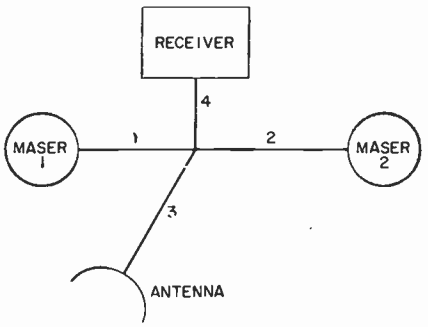

Fig. 1—Balanced amplifier using two one-port masers and a magic T. Arms 1 and 2 differ in length by λ/4. Variable phase-shifters and attenuators for balancing the bridge are not shown.

outlet T) divides equally between arms 1 and 2 and is amplified and reflected by the masers. If the masers and the lengths of arms 1 and 2 are adjusted so that the reflected waves are 180° out of phase at the junction, they will combine and go up arm 4 to the receiver. Noise from the receiver also divides between arms 1 and 2, but with 180° phase difference; therefore, the amplified noise returns to the junction in phase, goes up arm 3, and is radiated by the antenna. Ideally the gain, noise, and bandwidth are all the same as for a single maser with an ideal circulator.

Of course, for a number of reasons an actual system will fall short of this performance. Eq. (1) gives the noise temperature, T, of the system

$$T = T_1 + \frac{T_2}{G} + \frac{T_2'}{4}\left(\frac{\epsilon^2}{4} + \phi^2\right) + T_2'GR \quad (1)$$

where

T_1 = the noise temperature of the masers,
T_2 = the noise temperature of the receiver,
T_2' = the temperature of the noise emitted to the maser by the receiver at the signal frequency,
G = the maser gain,
R = the power-reflection coefficient in arm 3,
$\epsilon = G_2 - G_1/G_1$ is the fractional difference in gain between the two masers,
ϕ = the relative phase difference in radians for round trips in arms 1 and 2.

All terms are equivalent noise temperatures at the input of the system and are related to the usual noise figure, F, by $T = 290(F-1)$. The first term, the noise temperature of the masers, is of the order of 1°K.

The second term is the noise contributed by the receiver. If $G = 20$ db, a receiver noise figure of 6 db makes this term about 9°K.

The third term represents the part of the noise emitted by the receiver which is amplified by the masers and transmitted back to the receivers due to residual unbalance between arms 1 and 2. It is calculated in the Appendix. After the system has been balanced (using a variable phase-shifter and cold attenuator if necessary), any changes will introduce noise. If the maser gains fluctuate by less than ±1 per cent each, $\epsilon^2/4 < 10^{-4}$ and the noise contribution is less than 0.013°K. The phase unbalance, ϕ, contains contributions α due to variations in the electrical lengths of the arms and β due to phase shifts in the masers. Passive microwave bridges can be balanced to better than 80 db, corresponding to $\alpha^2 = 4 \times 10^{-8}$, so maintaining $\alpha^2 < 10^{-4}$ should not be difficult. Variations in β are about $2\Delta\nu/B$ where $\Delta\nu$ and B are the maser's frequency drift and bandwidth. If $B = 200$ kc, a maser drift of 1 kc will cause 10^{-2} radians phase shift equivalent to about 0.012°K input noise. It seems that this third term represents a (fluctuating) noise temperature which need not exceed a few hundredths of a degree.

The last term, which may be the most troublesome, is due to noise from the receiver, amplified by the maser but then reflected in arm 3 or at the antenna. With $G = 20$ db, a VSWR of 1.02 gives 4.5°K, while 1.05 gives 27°K, and 1.10 gives 104°K. As an untuned antenna may have a VSWR of 1.2 or greater it would probably be necessary to tune it; if the antenna is movable, variations of VSWR with position might complicate matters. The problem of matching the antenna might be eased by using a reasonably good ferrite isolator operating at room temperature; at a given frequency isolators will probably become available before circulators.[7] A perfect isolator inserted in arm 3 would emit no noise toward the junction but would absorb the high-temperature noise ($T_2'G$) traveling toward the antenna, reemitting only 290° noise. An actual isolator would contribute an additional input noise of about 7°K for each 0.1 db of forward attenuation, while imperfect isolation would allow some of the high-temperature noise to reach the antenna.

To summarize, a system noise temperature of 30°K or less (not including antenna noise) should be obtainable. For given values of T_2, T_2', and R there is an optimum gain given by $G_{opt} = T_2/T_2'R$. A low noise figure would be obtained only for the frequency band over which the masers are matched, so it would probably be desirable to make the receiver bandwidth less than that of the masers. We might remark that this type of balanced system could also be useful in connection with other types of low-noise amplifiers such as parametric amplifiers.

The author would like to express his appreciation for helpful discussions with a number of his colleagues, particularly R. H. Kingston, A. L. McWhorter, and J. W. Meyer.

Appendix

We wish to calculate the temperature, T_4, of the noise power reaching the receiver. V_4, the amplitude of the wave generated in arm 4, is proportional to the vector difference between the waves in arms 1 and 2 traveling toward the junction or

$$V_4^2 = \tfrac{1}{2}[V_1^2 + V_2^2 - 2V_1V_2\cos\phi]$$

where V_1 and V_2 are the amplitudes of the two incoming waves and will be assumed approximately equal; ϕ is their phase difference at the junction and assumed nearly zero.

Then

$$V_4^2 \approx \frac{V_1^2}{2}\left[\left(1 - \frac{V_2}{V_1}\right)^2 + \phi^2\right]$$

$$\left(\frac{V_2}{V_1}\right)^2 = \frac{G_2}{G_1}$$

where G_2 and G_1 are the power gains of the two masers and if

$$\epsilon = \frac{G_2 - G_1}{G_1}$$

$$\frac{V_2}{V_1} \approx 1 + \frac{\epsilon}{2}, \ \epsilon \text{ small},$$

so

$$V_4^2 \approx \frac{V_1^2}{2}\left(\frac{\epsilon^2}{4} + \phi^2\right).$$

Now,

$$V_1^2 \text{ is proportional to } \frac{G_1T_2'}{2},$$

so

$$\frac{T_4}{T_2'} = \frac{G_1}{4}\left(\frac{\epsilon^2}{4} + \phi^2\right)$$

where T_4 is the temperature of the noise power reaching the second stage. Its equivalent temperature at the input is

$$\frac{T_2'}{4}\left(\frac{\epsilon^2}{4} + \phi^2\right).$$

S. H. Autler
Lincoln Lab., M.I.T.
Lexington, Mass.

[7] G. S. Heller and G. W. Catuna, "Measurement of ferrite isolation at 1300 mc," IRE Trans. on Microwave Theory and Techniques, vol. MTT-6, pp. 97–100; January, 1958.

WWV Standard Frequency Transmissions*

Since October 9, 1957, the National Bureau of Standards radio stations WWV and WWVH have been maintained as constant as possible with respect to atomic frequency standards maintained and operated by the Boulder Laboratories, National Bureau of Standards. On October 9, 1957, the USA Frequency Standard was 1.4 parts in 10^9 high with respect to the frequency derived from the UT 2 second (provisional value) as determined by the U. S. Naval Observatory. The atomic frequency standards remain constant and are known to be constant to 1 part in 10^9 or better. The broadcast frequency can be further corrected with respect to the USA Frequency Standard as indicated in the table below. This correction is *not* with respect to the current value of frequency based on UT 2. A minus sign indicates that the broadcast frequency was low.

The WWV and WWVH time signals are synchronized; however, they may gradually depart from UT 2 (mean solar time corrected for polar variation and annual fluctuation in the rotation of the earth). Corrections are

* Received by the IRE, September 17, 1958.

determined and published by the U. S. Naval Observatory.

WWV and WWVH time signals are maintained in close agreement with UT 2 by making step adjustments in time of precisely plus or minus twenty milliseconds on Wednesdays at 1900 UT when necessary; no step adjustment was made at WWV and WWVH this month.

WWV FREQUENCY†

August, 1958 1500 UT	Parts in 10^9
1	−3.0
2	−3.0
3	−3.1
4	−3.1
5	−3.1
6	−3.2
7	−3.2
8	−3.2
9	−3.2
10	−3.2
11	−3.3
12	−3.3
13	−3.4
14	−3.4
15	−3.4
16	−3.3
17	−3.3
18	−3.3
19	−3.3
20	−3.3
21	−3.2
22	−3.1
23	−3.1
24	−3.0
25	−2.9
26	−2.8
27	−2.7
28	−2.7
29	−2.7
30	−2.6
31	−2.6

† WWVH frequency is synchronized with that of WWV.

D. M. KERNS
Radio Standards Lab.
Natl. Bur. of Standards
Boulder, Colo.

A Communication Technique for Multipath Channels*

The paper by Price and Green[1] has been examined with a great deal of interest. It would appear that a modification of the described apparatus would provide both increased usefulness and greater simplicity.

Price and Green provided a tapped transmission line of 3-msec delay to minimize errors for signals having multipath time differences of the same order of magnitude. If the time length of the transmission line in the receiving apparatus is extended appreciably beyond the multipath time difference, say to 30 msec, the multiplicity of cross-correlation multipliers are not needed. The entire transmission system (including the ionosphere) is then entirely linear, so that the theory of superposition can be applied and the transmission path is entirely suitable for all types of transmission including voice and analog information.

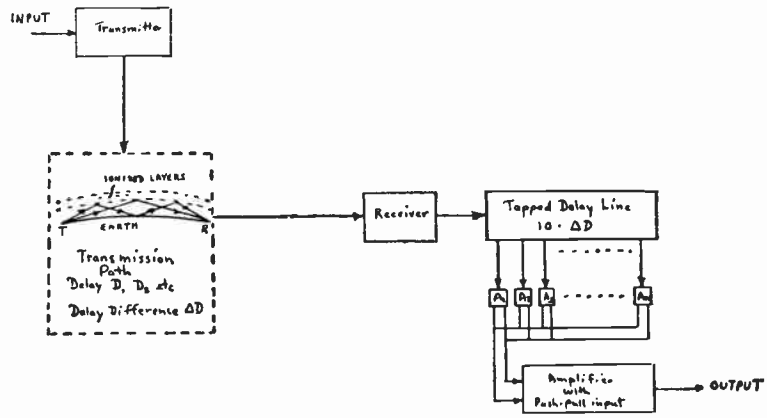

Fig. 1—Communication system using "inverse ionosphere."

The communication system so modified is shown in Fig. 1. A signal passes through a multipath channel containing a finite number of paths whose lengths do not differ from one another by more than 3 msec. Independent linear amplitude controls $A_1, A_2, \cdots, A_n$, connected to taps on the delay line, provide either positive or negative signals of individually controllable amplitudes to a linear mixer.

A convenient means for adjusting the controls is to transmit from time to time a signal of known shape such as a Morse dot or teletype synchronization signal. The controls $A_1, A_2, \cdots, A_n$ are manipulated to remove all multipath distortion from the known signal. Because the entire system is linear, all other forms of signals transmitted over the same path will also be undistorted. Multipath distortion will be removed.

In a given transmission system the adjustment of $A_1, A_2, \cdots, A_n$ can conveniently be made completely automatic and compatible to the requirements of the system and to the frequency of observed multipath changes, which usually are slow.

Equipment being developed at Federal Telecommunication Laboratories in accordance with this improvement can be identified by the name "inverse ionosphere."

GEORGE D. HULST
Federal Telecommunication Labs.
Nutley, N. J.

Magnetron Tuning Using a Ferrite Reciprocal Phase Shifter*

The type of reciprocal ferrite phase shifter described by Reggia and Spencer[1] has been previously used for frequency modulating an X-band spatial harmonic magnetron. A communication referring to this work has appeared elsewhere.[2]

In this communication it was stated that various types of ferrite phase shifter had been investigated. The most satisfactory configuration for X band considering phase shift per oersted per cm of ferrite, absorption loss, and VSWR, was a 0.25-inch diameter cylinder of a Mg-Mn ferrite located centrally in the waveguide (WG16—0.9×0.4 inch ID) and magnetized longitudinally. In the experiments performed here, cylindrical rods of diameter greater than 0.25 inch were not available, so the optimum diameter of 0.3 inch as shown by Reggia and Spencer was not realized.

For the magnetron tuning application, to obtain the maximum tuning range, it was required to change the electrical length of a short-circuited length of WG16 by 180°, the total length of this waveguide section being kept to a minimum and as loss-free as possible. A suitable configuration was found to consist of a cylinder of a Mg-Mn ferrite 2.0 inches long and 0.25 inch in diameter, located centrally in the waveguide using foamed plastic as a support. Conical tapers of a low-loss dielectric known as "Mycalex" (dielectric constant ~6), were attached to both ends of the ferrite to improve matching. A longitudinal magnetic field was applied using a solenoid, and at 9500 mc, 180° phase shift was produced by applying 200 oersteds, the absorption loss being less than 0.45 db, and VSWR > 0.63 throughout.

This phase shifter, when driven by a 50-cps modulating current, was used with a VX3238 magnetron. For a magnetic field variation of 120 oersteds about a steady biasing field of 60 oersteds, a frequency sweep of 120 mc was obtained, the output power being constant to within 1.1 db. The output level of the magnetron was approximately 1 watt, and little heating of the ferrite due to the absorption of microwaves or to hysteresis was experienced.

The author is indebted to the Admiralty for permission to publish this letter.

D. BUSH
The General Electric Co., Ltd.
Wembley, Middlesex, England

* Received by the IRE, April 21, 1958.
[1] R. Price and P. E. Green, "A communication technique for multipath channels," PROC. IRE, vol. 46, pp. 555–570; March, 1958.

* Received by the IRE, May 9, 1958.
[1] F. Reggia and E. G. Spencer, "A new technique in ferrite phase shifting for beam scanning of microwave antennas," PROC. IRE, vol. 45, pp. 1510–1517; November, 1957.

[2] D. Bush, "Contribution to discussion on 'microwave apparatus-I'," *Proc. IEE*, vol. 104, pt. B, supplement no. 6, pp. 267–398; 1957. See p. 368.

Contributors

George R. Briggs (A'55) was born in Ithaca, N. Y., on May 21, 1924. He received the A.B. degree in physics from Cornell University, Ithaca, in 1947, and the A.M. and Ph.D. degrees in physics from the University of Illinois, Urbana, in 1950 and 1953, respectively, doing research in nuclear particle scattering.

G. R. Briggs

In 1952, he joined the staff of the M.I.T. Lincoln Laboratory, Lexington, Mass., where he developed computer magnetic logic devices. In 1954, he joined the research staff of RCA Laboratories, Princeton, N. J. At RCA, he has made contributions in a wide field of computer problems, including electroluminescent display devices and magnetic and ferroelectric memory and logic systems. He aided also in the development of the transfluxor.

Dr. Briggs is a member of Phi Beta Kappa, Phi Kappa Phi, Sigma Xi, and the American Physical Society.

❖

Max P. Forrer (A'54–SM'57) was born on October 15, 1925, in St. Gallen, Switzerland. He received the Diploma in electrical engineering from the Federal Institute of Technology, Zurich, in 1950.

M. P. Forrer

From 1951 to 1952 Mr. Forrer was with the Standard Telephone and Radio Corporation (IT&T) in Zurich. After coming to the United States in 1952, he joined the Western Electric Company at Kearny, N. J. Since 1955, he has been a member of the technical staff of the General Electric Microwave Laboratory, Palo Alto, Calif., where he has been concerned with research in the microwave field.

❖

Frank J. Gaskins (A'53) was born on June 27, 1918 in Virginia. He attended George Washington University in Washington, D. C. He was employed by the Naval Research Laboratory at Bellevue, Md. from 1945 to 1947, where he was associated with the development of fire control radar.

F. J. Gaskins

In 1947 he joined the operating branch of NBC in Washington, and was transferred to the New York office in 1951 as a member of the operating team field testing the NTSC Color Television System. He was transferred to the Pacific division in 1956 where he is now employed as studio operations technical supervisor.

❖

William E. Gordon (A'46–M'49) was born in Paterson, N. J., on January 8, 1918. He received the B.A. degree in mathematics from Montclair State Teachers' College in 1939, the M.S. degree in meteorology from New York University in 1946, and the Ph.D. degree from Cornell University in 1953.

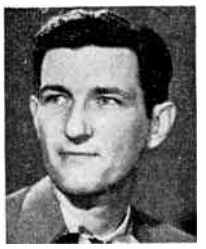

W. E. Gordon

Dr. Gordon was in the Air Force during the war, engaged in radio-meteorological studies in association with the Committee on Propagation of NDRC. At the close of the war he became associate director of the Electrical Engineering Research Laboratory, University of Texas. In 1948 he joined the staff of the School of Electrical Engineering, Cornell University, as research associate, becoming associate professor in 1953.

Dr. Gordon is Chairman of the USA National Committee, URSI, and a member of Tau Beta Pi, Sigma Xi, the American Meteorological Society, and the Joint Commission on Radio Meteorology, International Council of Scientific Unions.

❖

Keith W. Henderson (S'48–A'51–M'56) was born at Ogden, Utah, on December 25, 1921. He received the B.S. degree in engineering from the California Institute of Technology, Pasadena, in 1948, and the M.S. degree in electrical engineering from the University of Southern California, Los Angeles, in 1949. During 1949 and 1950 he pursued further graduate studies at the University of California at Los Angeles, where he was employed in the Engineering Research Department.

K. W. Henderson

From 1951 to 1953 he was employed by the Douglas Aircraft Co., Santa Monica, Calif., where he worked on the development of electrohydraulic controls for a guided missile. In 1953 he joined the Stanford Research Institute, Menlo Park, Calif., where he performed research on pulse transformers, magnetic components for digital computers, and electric filters, and participated in the development of a large special-purpose digital computer. Since 1957 he has been engaged in analog computer work at the Missile Systems Division of the Lockheed Aircraft Corp., Palo Alto, Calif.

Mr. Henderson is a member of the American Institute of Electrical Engineers and the National Society of Professional Engineers. He is a registered professional engineer in California.

❖

Ralph C. Kennedy was born in San Luis, Potosi, Mex. on August 30, 1912. He received the B.A. degree from San Jose State College, San Jose, Calif., in 1943, and the M.A. and E.E. degrees from Stanford University, Stanford, Calif., in 1945 and 1946, respectively.

R. C. Kennedy

In 1946, he transferred to the Development Group of the National Broadcasting Company in New York. Since that time, he has been engaged in various phases of RF broadcast relays, monochrome, and color television.

He was adjunct associate professor of physics in the graduate school at Hofstra College, Hempstead, N. Y., for six years and is now a lecturer in the graduate school of electrical engineering at the College of the City of New York. Mr. Kennedy is a member of Sigma Pi Sigma.

❖

Norman Lea was born in Coventry, Eng., on December 17, 1890. On leaving King Henry VIII School, Coventry, he served an apprenticeship in mechanical engineering. As Spencer Scholar, he went to Birmingham University and took the B.Sc. degree in mechanical engineering in 1913.

N. Lea

Having held an experimental radio licence from 1912, he was commissioned as Royal Navy Volunteer Reserve air observer in early 1915 and served overseas. From 1917 to 1919 he was engaged in air radio development at Cranwell and Biggin Hill. On demobilization he became chief engineer of Radio Communication Co., London, and specialized in the design of all kinds of radio gear for marine use. In 1929 he transferred to Marconi's Wireless Telegraph Co. Ltd., Chelmsford, where for four years he was chief of the testing division, with considerable freedom in developing measurement techniques. From 1934 onwards he has been with the research division of Marconi's, taking special interest in the de-

sign of auto alarm selectors, marine echometers, frequency measuring equipments, and oscillators of high stability.

Mr. Lea is a full member of both the Institution of Mechanical Engineers and the Institution of Electrical Engineers, London.

❖

A. W. Lo (S'48–A'50–SM'56) was born in Shanghai, China, on May 21, 1916. After receiving the B.S. degree in physics from Yenching University, Peiping, China, in 1938, he taught at West China Union University, Chengtu, and in Yenching University until he came to the United States in 1945. He received the M.S. degree in physics from Oberlin College, Oberlin, Ohio, in 1946, and the Ph.D. degree in electrical engineering from the University of Illinois, Urbana, in 1949, while serving as a research associate. He spent the following year as assistant professor in electrical engineering at Michigan College of Mining and Technology, Houghton, Mich., and the next as lecturer in electrical engineering at the College of the City of New York,

A. W. Lo

He joined RCA in 1951 as a member of the staff of the Advanced Development Engineering Section of the Engineering Products Department working on transistor circuitry. In 1952, he was transferred to the RCA Laboratories, Princeton, N. J., and is conducting research on the application of solid-state switching devices.

He is a co-author of "Transistor Electronics."

Dr. Lo is a member of Sigma Xi, Phi Kappa Phi, Pi Mu Epsilon, Eta Kappa Nu, and the American Association of University Professors.

❖

Thomas R. O'Meara was born in Kansas City, Missouri, on December 1, 1924. He received the B.S. degree in electrical engineering from the University of Illinois, Urbana, Ill., in 1948. From 1948 to 1955, he worked half time as a graduate research assistant in the Radio Direction Finding Laboratories of the University of Illinois while completing his graduate studies. He received his M.S. degree in electrical engineering in 1949 and accepted employment with the Ramo Wooldridge Corporation, Communications Division in 1955. He has been employed by the Hughes Aircraft Company, Culver City, Calif., since 1957, and completed the requirements for the Ph.D. degree in electrical engineering, in absentia, from the University of Illinois in June, 1957.

T. R. O'Meara

Dr. O'Meara is the author of publications in the areas of wide-band transformers, wide-band amplifiers, crystal filters, and phase-and-gain matched radio direction finding receivers.

He is a member of Sigma Xi.

❖

Jan A. Rajchman (SM'46–F'53) was born in London, England, on August 10, 1911. He received his diploma in electrical engineering in 1934 and the degree of Doctor in technical sciences in 1938 from the Swiss Institute of Technology, Zurich, Switzerland. He started in 1935 as a student engineer at RCA Manufacturing Co., Camden, N. J. In 1936 he joined the staff of RCA Manufacturing Co. as a research engineer and in 1942 he was transferred to the RCA Laboratories in Princeton where he is a member of the research staff.

J. A. Rajchman

At first Dr. Rajchman worked in electron optics. He is chiefly responsible for the development of the electron multiplier tube. During World War II he was among the first to apply electronics to computers. Later he worked on the betatron for which he became a co-recipient of the 1947 Levy Medal of the Franklin Institute. After the war he resumed work on computing devices. He developed the selective electrostatic storage tube. Turning to the new field of magnetics he developed the magnetic core memory, magnetic switching circuits, the transfluxor and the memory apertured plate. He is presently leading research in magnetics and other solid-state computing devices as well as digital systems. He holds more than 60 U. S. patents and is the author of many technical papers.

Dr. Rajchman is a member of the American Physical Society, the Council of the Association for Computing Machinery, and Sigma Xi.

❖

James W. Schwartz (S'52–A'53) was born in Elmira, N. Y. on February 11, 1927. He received the B.S. and M.S. degrees in engineering physics from Cornell University, Ithaca, N. Y., in 1951 and 1952, respectively. He has been employed in research at Corning Glass Works, Corning, N. Y., and at the Oak Ridge National Laboratories, Oak Ridge, Tenn. In 1952 he joined the technical staff of RCA Laboratories, Princeton, N. J.

J. W. Schwartz

He has done research work in electron optics, picture reproducers, servomechanisms, and systems engineering. In 1958, he joined the Kaiser Aircraft and Electronics Division of Kaiser Industries Corporation, Oakland, Calif.

Mr. Schwartz is a member of Sigma Xi.

❖

Richard L. Sydnor was born in Milan, Ill., on June 23, 1928. He received the B.S. degree in electrical engineering in 1952 and the M.S. degree in electrical engineering in 1953, both from the University of Illinois, Urbana, Ill. He is employed at present as a part-time graduate research associate in the Radio Direction Finding Laboratories of the University of Illinois while completing his graduate studies.

R. L. Sydnor

Mr. Sydnor is the author of publications in the fields of specialized computers for use in radio direction finding and computer components.

He is a member of Eta Kappa Mu, Tau Beta Pi, Pi Mu Epsilon and Sigma Xi.

❖

Alan T. Waterman, Jr. (S'51–A'53–SM'57) was born in Northampton, Mass., on July 8, 1918. He received the A.B. degree in physics in 1950 from Princeton University, the B.S. degree in meteorology in 1940 from the California Institute of Technology, and the A.M. degree in 1949 and the Ph.D. degree in 1952 in engineering sciences and applied physics from Harvard University.

A. T. Waterman, Jr.

He was employed by American Airlines as a meteorologist from 1940 to 1941, when he became an instructor in meteorology at the University of Minnesota. From 1942 to 1945 he did research on methods of weather forecasting at California Institute of Technology. He then engaged in research on radio meteorology at the University of Texas and Columbia University from 1945 to 1946. For the next six years, he was a research assistant at Harvard University in ionospheric radio-wave propagation.

Presently, he is associate professor of electrical engineering at Stanford University, where he is doing research in radio-wave propagation with particular emphasis on tropospheric scatter. He also is Associate Director of the Systems Techniques Laboratory at Stanford for a program of electronic countermeasures, and Consultant to Weapons Systems, Evaluation Group, Department of Defense.

Dr. Waterman is a member of the American Physical Society, the American Meteorological Society, the American Association for the Advancement of Science, and Sigma Xi.

Scanning the TRANSACTIONS

How efficiently do engineers use their time and abilities? A newly published study of manpower utilization and shortages comes up with this eye-opening conclusion: engineers and scientists are producing less than one-tenth as much as they are capable of, due to inefficient utilization of their abilities. This pronouncement is based in part on a detailed survey taken among members of the IRE and Institute of Aeronautical Sciences in Southern California. Two of the many interesting results of the study are shown in the accompanying table.

How Engineers Use Their Time and Abilities

Activity	Per cent of total time spent	Per cent of time spent usefully
Supervision	26.3	6.6
Conferences	14.0	3.5
Routine technical work	11.7	0
Nonroutine technical work	11.7	11.7
Report writing	10.3	2.6
Nonroutine designing	8.6	8.6
Routine designing	3.7	0
Drafting	3.3	0
Personal	2.0	0
Teaching	1.8	0.5
Misc. nontechnical	1.5	0
Routine laboratory work	0.9	0
Data searching	0.5	0.5
Others and uncertain	3.7	1.8
	100.0	35.8

The first column of numbers shows how the average engineer devotes his time. The second column gives the authors' estimates of how much time he spends "usefully," that is, time spent on tasks requiring full use of his engineering abilities. The total of the second column indicates that the average engineer utilizes his engineering capabilities with an efficiency of only 35.8 per cent. But this isn't the end of the story. Other causes of inefficiency enter the picture which reduce this figure still further. For example, the authors estimate that anywhere from 30 per cent to 85 per cent of the above "useful" engineering time is wasted in duplication of efforts, both within and between individual organizations. The result, they say, is a probable utilization efficiency of less than 10 per cent of ideal. Even if it were only possible to attain a maximum efficiency of 20 per cent or 30 per cent in practice, engineering and scientific output would be increased to two or three times their present level. Perhaps operations research can provide the key to better utilization of engineering manpower. (I. Hirsch, *et al.*, "The relation of utilization to the shortage of scientists," IRE Trans. on Engineering Management, September, 1958.)

Engineering writers will howl, a few with joy but most with intense pain, when they look closely at the table presented in the preceding item. First they will notice with some satisfaction that the average engineer spends 10.3 per cent of his time writing reports. Publications people have long maintained that report writing is a vital, yet somewhat neglected, part of an engineer's job and that an adequate amount of time must be provided for this important activity. But in the column to the right they will find to their horror that the authors of the table opine that only one-fourth of this time (2.6 per cent) represents efficient utilization of engineering manpower. The latter gentlemen point out that one of the more serious objections that engineers have toward report writing is having to provide the same information in a number of different reports (daily notebook, contractual reports, internal reports, etc.). They maintain that each engineer should have to write his story only once and without any necessary polish, and that a technical writer should be employed to generate from this source document all the additional reports required.

Publications-minded engineers are certainly going to bridle at this one (" . . . and without any necessary polish," *indeed!*). They hold a diametrically opposite opinion. Their viewpoint, as expressed in a recent PGEWS article, is: "Engineers must be required to write. They must be required to submit trip reports and task reports and reports upon reports. And they must be required to submit good ones." Improved writing is to them an all important goal, one that can best be attained only with more time for more writing.

Both sides of the argument sound irrefutable. As a friend of the court, may we suggest that the Professional Group on Engineering Writing and Speech invite a panel composed of efficiency experts, publications people, and engineers to debate the question of how much time should be devoted to report writing. A question which involves 10 per cent of every engineer's time is certainly worthy of the most earnest consideration. (T. Connors, "The double standard in engineering writing," IRE Trans. on Engineering Writing and Speech, August, 1958.)

$C = 3 \times 10^8$ meters per second—or does it? After 300 years, man is still trying to pin down precisely the speed of electromagnetic waves. It has long been recognized that although the foregoing familiar number is satisfactory for many practical cases, the exact value is somewhat lower. Twenty-five years ago Michelson, after performing nearly 3000 optical measurements with his remarkable mile-long 3-foot steel tube at the University of Chicago, narrowed down the value for the velocity of light to 299,774 km/sec with an average deviation of 11 km/sec. It is only in the last decade that substantially more accurate measurements have been made, both in the radio and visible light portions of the spectrum. As reported in the Proceedings last July, it was recommended at the Twelfth General Assembly of URSI, held last year in Boulder, Colorado, that in radio engineering problems the velocity of electromagnetic waves in a vacuum now be taken as 299,792.5 km/sec with a probable error of ± 0.4 km/sec, a higher and more certain figure than Michelson's.

When, as in most practical cases, the radio waves are transmitted through the atmosphere instead of a vacuum, the speed is reduced slightly to $1/n$ of this value, where n is the refractive index of the atmosphere. Due to variations in n, the velocity can change over the range 299,670 to 299,700 km/sec, and cannot be accurately specified in a practical situation without a detailed and precise knowledge of atmospheric conditions over the whole path and how they may vary with time.

It is interesting to note that the frequency of a wave can be specified much more accurately than either its velocity or wavelength. Frequency can be measured with a certainty of one part in 10^{10}. The velocity, as noted above, is less certain. And in deriving wavelength from frequency by means of the relationship $c = f\lambda$, these uncertainties are compounded. There is still room for improvement of our knowledge of this subject, particularly as some radio techniques, such as navigational aids, could with advantage make use of more precise determinations of the speed with which radio waves travel under the various conditions encountered in practice. (R. L. Smith-Rose, "The speed of light and radio waves," IRE Student Quarterly, September, 1958.)

English-German and German-English translations afford an interesting point of comparison of the relative efficiencies of the two languages. It turns out that although it takes more words to express oneself in English than in German, fewer alphabetic characters are required. It would seem from this that it is more economical to send telegrams in German and write letters in English. An intriguing sidelight is the fact that German requires 22 per cent more letters and spaces than English when translating from English to German, but only 7 per cent more when translating from German to English. A recent study concludes that the English language is somewhat more efficient than the German language in encoding semantic content into linguistic symbols to the extent that one bit of information in English carries as much semantic content as 1.15 bits of information in German. So the next time your secretary complains about all the typing she has to do, console her with the thought that she has roughly 15 per cent less than her German cousins. (B. S. Ramakrishna and R. Subramanian, "Relative efficiency of English and German languages for communication of semantic content," IRE TRANS. ON INFORMATION THEORY, September, 1958).

Megavolt electronics is making possible a group of devices which show considerable promise of extending the present frontier of the microwave spectrum. The devices make use of the rebatron, an electron bunching and accelerating system which produces a megavolt electron beam modulated at 2775 megacycles. Various types of coupling structures are being developed to extract energy from the beam at a high harmonic of the modulating frequency. Over 100 milliwatts of power have been produced at the twelfth harmonic and detectable power has been obtained at the thirty-fourth harmonic. A more recent model has been designed for operation at the 110th harmonic (0.982 millimeter wavelength) with an anticipated peak pulsed power output of tens of milliwatts. When this work is completed, attempts will be made to generate power in the submillimeter spectrum, with the expectation of eventually reaching an output level of one watt. (R. H. Pantell, *et al.*, "Dielectric slow-wave structures for the generation of power at millimeter and submillimeter wavelengths," IRE TRANS. ON ELECTRON DEVICES, July, 1958.)

Two famous papers are reviewed in an engaging guest editorial by Peter Elias, appearing in the IRE TRANSACTIONS ON INFORMATION THEORY. With tongue in cheek and an incisive wit, Professor Elias observes that these two papers have been written so often, by so many different authors, under so many titles that they have earned this editorial consideration. The two papers, "Information Theory, Photosynthesis and Religion" and "The Optimum Linear Mean Square Filter for Separating Sinusoidally Modulated Triangular Signals from Randomly Sampled Stationary Gaussian Noise with Applications to a Problem in Radar" are critically dissected and found insubstantive. He concludes that the two papers have been written—and even published—often enough by now, and suggests that we stop writing these papers and thereby release a large supply of manpower to work on the exciting and important problems which need investigation.

In the same issue a new sampling theorem is presented, introducing the concept of complex zeros to show that information related to the zeros of a signal occur at the Nyquist rate. This sampling theorem is of interest when considering the transmission of binary signals, such as facsimile and infinitely clipped speech, over a continuous band-limited channel. The various types of sampling discussed in the paper may be viewed as aspects of a generalized theory of sampling applicable to the various situations which arise in practice. Such a generalized theory has not yet been found. We need a major break-through comparable with the development of information theory itself. (F. E. Bond and C. R. Cahn, "On the sampling of zeros of bandwidth limited signals," IRE TRANS. ON INFORMATION THEORY, September, 1958.)

Books

Faisceaux Hertziens et Systèmes de Modulation, by L. J. Libois

Published (1958) by Editions Chiron, 40, rue de Seine, Paris 6, France. 494 pages+13 index pages. Illus. 9¾×6¼. 6200 fr.

The purpose of the author is to present in one book the basic principles connected with the modern design of radio link. L. J. Libois, professor at the Ecole Nationale Supérieure des Telécommunications, has taken an important part in the development of radio link techniques in France. He considers the classification of short-wave radio links to be more determined by the method of modulation than by the frequency assignment. That is the reason why modulation systems with their comparative merits and multiplexing in frequency and time division are considered extensively in this book.

The book is divided into ten chapters: Historic—Characteristics of audio and video signals—Information theory and amplitude modulation—Principles of frequency modulation—Linear and nonlinear distortion in frequency modulation—Theory of pulse modulation systems—Theory of time multiplex—Quantizing coding and delta modulation—Propagation, attenuation, choice of a site—Fundamental equation of a radio link system. The author's treatment is mainly theoretical.

One chapter is devoted to definitions of input signals, *i.e.*, telegraphy, telephony, multiplex telephony, normal broadcasting, high quality broadcasting, and television (819 lines). It contains complete definitions according to the norms published by the Comité Consultatif International de Telégraphie et Teléphonie (C.C.I.T.T.), and therein provides extremely useful material.

In chapters 4–8 distortions and signal-to-noise ratios peculiar to each system of modulation are fully analyzed in view of their application to the design of radio links.

After a classical chapter on propagation, the author shows with great clarity the influence of the fundamental parameters defined in the preceding chapters on the prediction of the performance of a radio link.

The text is very clear, concise, and easy to read. All lengthy demonstrations are reported in annex at the end of each chapter, which is followed by a succinct bibliography, mostly limited to recent publications.

J. B. LAIR
Federal Telecommun. Labs.
Nutley, N. J.

Programming for an Automatic Digital Calculator, by K. H. V. Booth

Published (1958) by Academic Press, Inc., 111 Fifth Ave., N. Y. 3, N. Y. 229 pages+1 bibliography page+4 appendix pages+2 index pages+vii pages. 8¼×5¾. $7.50.

On the cover of this book appears the following statement: "The technique of programming can be acquired by anyone with a capacity for accurate detailed thinking, and a talent for solving puzzles." It is unfortunate that study of this book confirms the impression that "a talent for solving puzzles" would indeed be helpful in becoming a successful programmer. The present trend is toward minimizing the value of that talent

by simplifying programming, but little mention is made of that trend or how it is being achieved.

This book creates the initial impression that it is designed to teach programming to the neophyte. In this reviewer's opinion it cannot be used for that. The machine described is the APEXC at Birkbeck College in London, England. In the preface the statement is made that "the code of the APEXC is extremely short and simple and is well adapted for learning the basic ideas of programming." Unfortunately, nearly the entire book is devoted to examples of actual programs, each discussed in considerable detail. There is a total of less than twenty pages devoted to discussions of programming in general, and even a fairly substantial portion of that is used to describe various features of the APEXC. Experienced programmers who have seen this book have commented that an understanding of the fifteen orders comprising the APEXC order code was far from easy. However, after careful study of some of the more simple programs, a fair amount of facility was gained in following various codes. There seems to be too little emphasis on the importance of flow charting. The author's usual approach to a problem is to write a "schematic program" as a vertical column of APEXC instructions with the paths of the jump instructions indicated by lines and arrows. The next step is to present a detailed APEXC code in the form in which it actually appears in the machine, using alphabetic operation codes and decimals and addresses and constants in binary notation.

The author presents many interesting and valuable techniques for computing various functions from square root and reciprocal on up through some elementary matrix routines. Some of the techniques have obviously been developed to take special advantage of the binary nature of the computer and appear to be fast and efficient. The reader interested in such matters will find them interesting, and usually the programs are clever and efficient. There is not enough emphasis on resetting before entering iterative loops. Many programmers regard this feature as essential, but in this book it is merely glossed over lightly. Interpretive floating point arithmetic is covered from the standpoint of writing the interpretive routine, but very little is said about the advantages and disadvantages of floating point computations. Some statements in the book reflect either a lack of appreciation of certain powerful features of modern digital computers, or the author's indulgence in English understatement. A prime example occurs on page 16, where it is stated, "since the orders forming a program are stored in the memory in numerical form, it is possible for the machine to perform arithmetic operations upon them and thereby modify them, and this property is of considerable use." Rather than being only of considerable use, this property is almost the key to the power of the modern digital computer.

It is difficult to say just what audience the author had in mind in writing this book. It is certainly too much for the beginner, and since so much of the book is devoted to detailed programs in the APEXC code, it would be of little use as a source of checked-out subroutines to most computer installations. Many of the programming tricks described in the book are of long standing in the programming profession. The book's greatest value seems to be in the presentation of a few highly specialized techniques for computing certain functions wherein full advantage is taken of the detailed binary nature of the computer. The book is definitely not a "must" for any computing installation, but it could prove at least occasionally interesting if not useful to the programmer interested in using refined techniques in certain applications. To a programmer who has been unable to learn detailed advanced techniques of coding, this book could serve to point out some of them which he may never learn otherwise. Careful study of the details of some of the programs presented would, in a sense, lift the curtain, and give him a glimpse of what may be described as graduate work in details of digital computer coding.

DONN COMBELIC
Ramo-Wooldridge Corp.
Los Angeles 45, Calif.

Switching Circuits and Logical Design, by S. H. Caldwell

Published (1958) by John Wiley and Sons, Inc., 440 Fourth Ave., N. Y. 16, N. Y. 662 pages+11 appendix pages+12 index pages+xvii pages. Illus. 9¼×6. $14.00.

This well-organized and well-written book is undoubtedly the best and most comprehensive publication to date in the rapidly growing field of switching circuits. The most recent prior efforts in this field, while not without merit, have been heavily slanted toward the application of switching circuits to digital computers. In this book, on the other hand, Professor Caldwell neatly achieves his stated intent of steering a median course between strict utility and pure mathematics.

Two introductory chapters on properties and applications of switching circuits, and switching components and their characteristics, are followed by an extremely lucid chapter on the fundamentals of switching algebra. Next is a chapter on the use of switching algebra in the analysis and synthesis of series-parallel contact networks. The next chapter deals with minimization methods other than algebraic manipulation, with principal emphasis on the Quine-McCluskey and Karnaugh-map methods. The following three chapters deal with multiterminal contact networks, symmetric functions, and non-series-parallel contact networks.

At this point, application of switching theory has been restricted to relay contact networks. This is definitely a wise restriction since the relay closely approximates an ideal switch, and the development of theory and application is consequently unencumbered by consideration of switch deficiencies. Chapter 9 is quite logically devoted to the adaptation of switching algebra to electronic and solid-state devices in combinational switching circuits. These nine chapters comprise over half the book and form a solid foundation in combinational switching circuit theory and application.

Chapter 10 is devoted to binary coding theory including computational and cyclic codes, and error detection and correction. Chapter 11 is an enlargement on the theory of iterative networks introduced previously. The remaining four chapters are a comprehensive treatment of sequential switching circuits, with basic emphasis on the Huffman flow-matrix technique. Included in these chapters are basic analysis-synthesis methods, electronic and solid-state sequential circuits, and pulsed sequential circuits.

At the end of suitable chapters, numerous representative problems are appended, together with bibliographies. Several useful appendixes have been added, including binary-decimal conversion, binary numbers, sum modulo two operations, numbers of functions of n variables, and classes of functions of three variables.

This book will be useful to a broad segment of the electrical engineering field, including the graduate engineer who knows nothing about switching circuits, but wishes to learn their theory and application, or who has a fundamental background but wishes to bring himself up to date on the rapid progress of recent years. It will find wide use as a student text and unquestionably make a strong bid to become the authoritative text in its field.

R. W. STUART
General Radio Co.
West Concord, Mass.

Missile Engineering Handbook, by C. W. Besserer (Principles of Guided Missile Design Series, Grayson Merrill, Ed.)

Published (1958) by D. Van Nostrand Co., Inc., 257 Fourth Ave., N. Y. 10, N. Y. 572 pages+27 index pages+xi pages. Illus. 10¼×7¼. $14.50.

The *Missile Engineering Handbook* is an excellent compilation of useful data for the missile design engineer. Its subject matter is well described by the section titles, viz. 1) General Data, 2) Properties of the Atmosphere, 3) Environmental Data and Reliability, 4) Properties of Materials Structures, 5) Aerodynamics, 6) Avionics, 7) Propulsion, 8) Space Flight Data, 9) Miscellaneous Data, and 10) Glossary.

Comprised of material filling six hundred pages, the book devotes only forty-eight pages to electronics (Avionics), but it thereby becomes an excellent vehicle for acquainting the electronics engineer engaged in missile work with the design problems in associated fields. The Avionics section itself is comprised of technical material well known to electronic engineers, but is carefully selected for application to missile programs and is conveniently located for maximum utility.

The volume is definitely a handbook in the true sense of the word and is not a text. It is packed with facts and figures in a well ordered arrangement for everyday use; included are liberal quantities of graphs and nomograms. Formulas displayed by the graphs and nomograms are given, but not their derivations. The handbook also abounds with numerous useful physical constants.

CONRAD H. HOEPPNER
Radiation, Inc.
Melbourne, Fla.

Abstracts of IRE TRANSACTIONS

The following issues of TRANSACTIONS have recently been published and are now available from the Institute of Radio Engineers, Inc., 1 East 79th Street, New York 21, N. Y. at the following prices. The contents of each issue and, where available, abstracts of technical papers are given below.

Sponsoring Group	Publication	Group Members	IRE Members	Non-Members*
Aeronautical & Navigational Electronics	Vol. ANE-5, No. 2	$1.50	$2.25	$4.50
Audio	Vol. AU-6, No. 3	0.55	0.80	1.65
Education	Vol. E-1, No. 3	1.10	1.65	3.30
Electron Devices	Vol. ED-5, No. 3	2.00	3.00	6.00
Engineering Management	Vol. EM-5, No. 3	0.70	1.05	2.10
Engineering Writing & Speech	Vol. EWS-1 No. 2	1.30	1.95	3.90
Information Theory	Vol. IT-4, No. 3	1.10	1.65	3.30

* Public libraries and colleges may purchase copies at IRE Member rates.

Aeronautical and Navigational Electronics

VOL. ANE-5, NO. 2, JUNE, 1958

1958 Pioneer Awards in Aeronautical and Navigational Electronics (p. 74)

The Air Traffic Control Paradox—P. C. Sandretto (p. 80)

ADF Interference Blanker Development—M. M. Newman, J. R. Stahmann, and J. D. Robb (p. 86)

Interference blankers have been developed to give improvement ratios of the order of 1000 in the presence of severe precipitation static of the order of 150,000 pulses per second. Recently the blanking technique has been applied to ADF receivers with the objectives of simplification, reduced size and weight, improved sensitivity in the presence of interference, reduced intermodulation distortion, maintenance of the relative phases of the sense and loop signals, and general compatibility with ADF receiver operation.

Improvements in Radar Data Presentation—K. V. Curtis and T. J. Kelly (p. 91)

This paper describes an application of the storage tube to marine radar, for providing an automatic plot of the equipped vessel as well as all other vessels within the radar's range. It further describes a new type of presentation which combines relative motion with true motion in a manner easily understood by the mariner and which requires no understanding by him, of new concepts. In addition to providing six different types of presentation, the system for the first time furnishes a means of directly determining the aspect, true course, and true speed of other vessels without auxiliary plotting and without calculations.

Characteristics and Stabilization of an Inertial Platform—T. Mitsutomi (p. 95)

In attempting to gain some insight into the synthesis and analysis of a stable platform system the simple assumption that the platform can be analyzed on a single-axis basis is adopted. The single-axis analysis is then made applicable to the three-axis case by introducing a coupling factor. Of course, the shortcomings of this assumption, such as the omission of mechanical interactions, must be recognized.

The inherently close association of the stability of the servosystem and the basis character of the input-output response will generally require that design requirements be compromised. The servosystem is essential to effect a suitable reduction in the influence of disturbances, and the factors involved in achieving stiffness must necessarily be considered.

Finally, in discussing the design and features of the servoamplifiers it should be realized that the conditionally stable character of the system and the large attenuation involved in securing adequate phase lead create a difficult circuitry problem. In this regard, active research and development programs are under way toward the development of improved transistorized amplifiers.

Stellar Inertial Navigation—R. B. Horsfall (p. 106)

Automatic navigation of aircraft may be accomplished in a number of ways. Where radiative contact with the ground is satisfactory, systems such as the conventional radio ranges and the more recently developed hyperbolic grid techniques are economical and normally reliable. However, in some regions of the earth and under certain atmospheric conditions, these types of radio aids may not be reliable. Other systems that involve radiative contact with the ground include radio mapping techniques and Doppler navigation; these generally require more expensive airborne equipment, although they are less subject to atmospheric disturbances. But since in military applications radiation from an aircraft furnishes a potential means of enemy detection, such techniques are relatively undesirable. At the present time, Doppler systems are the least subject to this objection.

Inertial navigation makes use of acceleration detection and integration for obtaining information on the progress of the aircraft over the surface of the earth. It is independent of radiative contacts, and therefore free from such detection. On the other hand, it is subject to errors resulting from instrumental imperfections. In particular, drift of the essential gyroscopes leads to cumulative errors in indicated position; consequently, pure inertial autonavigators are limited in the flight time over which their indications are satisfactorily accurate. Use of photoelectric telescopes (star trackers) in combination with an inertial system provides a tie to basic inertial space, such as to minimize or eliminate the cumulative effect of gyro drift. Such a combination is known as a stellar inertial autonavigator. The basic principles of these systems are essentially alike, although the methods of mechanizing the principles vary widely. Within security limitations, the fundamentals and some of the mechanization methods are discussed.

Comparative Evaluation of Several Azimuth Estimating Procedures Using Digital Processing and Search Radar Simulation—C. M. Walter, J. Atkin, and H. Bickel (p. 114)

In order to test and compare various azimuth estimating procedures, use was made of a search radar video simulator and a flexible high-speed digital video processor. The output of the video processor was recorded in digital form and analyzed on a general purpose digital computer.

The azimuths of approximately 30,000 simulated targets at signal-to-noise ratios of 3, 6, 10, and 15 db were estimated by several methods. A reliable indication was obtained of the detection efficiency, false alarm rate, and the obtainable azimuth accuracy under a variety of conditions. The data which have been processed so far indicate superior performance of the maximum likelihood method for azimuth estimation purposes. The experimental results are presented in graphical form.

Correspondence (p. 122)
Abstracts (p. 122)
PGANE News (p. 125)
Contributors (p. 128)
Roster of PGANE Members (p. 130)
Suggestions to Authors (p. 136)

Audio

VOL. AU-6, NO. 3, MAY–JUNE, 1958

From Our New Chairman—Frank H. Slaymaker (p. 47)
PGA News (p. 48)

Procedures for Loudspeaker Measurements—P. Chavasse and R. Lehmann, translated by Michel Copel (p. 56)

In this study the authors try to define the instrumentation and measurement procedures for the acoustic calibration of loudspeakers. They give some indication of the characteristics of the instrumentation and then specify the measurements to be taken in order to determine the acoustic (performance) quality of a loudspeaker.

They review successively the following problems: frequency response characteristic, directivity, harmonic and intermodulation distortion, impedance characteristic, efficiency, and transient response. For each they propose a method of measurement and give some practical examples of results obtained.

Design of Transistor RC Amplifiers—Ray P. Murray (p. 67)

Some of the basic factors involved in the design of transistor RC amplifiers are consid-

ered. Particular emphasis is placed on operating point stabilization and its relation to such factors as gain, battery drain, and distortion. The stabilization factor employed here is a measure (in terms of per cent) of the stabilization contributed by the stabilization circuitry. Only the fundamental common-emitter connection is discussed.

Correspondence (p. 76)
Contributors (p. 77)

Education

VOL. E-1, NO. 3, SEPTEMBER, 1958

"How to Do"—R. L. McFarlan (p. 65)

Electrical Machinery in an Electronics-Oriented Curriculum—John G. Truxal (p. 66)

Revision of the electrical machinery courses requires the selection of those concepts fundamental to the field and a studied organization and presentation of these concepts in a form which correlates with other courses in the curriculum (particularly in the method of approach to analysis) and which simultaneously provides motivation in the form of interesting examples and illustrations drawn from current technological frontiers. The paper describes briefly one such attempt, in which the emphasis is placed on electromechanical signal transducers and their description in terms of two-port network functions, linear incremental models, and transfer functions.

An Experiment in the Reduction of Physics Content—J. D. Ryder (p. 70)

An experiment has been conducted in which the conventional introductory physics course for engineers has been reduced, and the capabilities of two groups of students—one group having had certain physics topics and the second group without these—have been compared. The comparison was made in mixed classes in engineering statics. Insofar as the data can be analyzed, they seem to show no essential differences in the performance of the two groups. Certainly, preliminary work in physics did not give that group of students any major advantage.

A Student's View of Engineering—John E. Tirrell and Phillip Sidwell (p. 72)

The authors analyze the answers to 10 questions from 523 engineering students in three Michigan junior colleges, in an attempt to elicit the beginning student's view of engineering. The answers give information on the age of first interest in engineering, the age of decision on the field as a career, the influences that led to the choice of engineering, future aspirations, and six other related questions. The opening section briefly states the objectives of education in our society and indicates the contribution of the junior college. The conclusion suggests some specific assistance professional engineers can give to youth.

The Pros and Cons of Graduate Students Working Part-Time in Industry—Darrell E. Newell (p. 78)

To provide a method for graduate engineers to acquire advanced degrees, some industrial organizations have instituted a part-time employee program. The difficulties encountered by an industry, an employee and an educational institution which have been involved in such a program are indicated in this paper. Suggestions are made, which should improve the benefits derived from such a program.

Since programs of this type will provide a better qualified technical force for industry and the nation, they deserve the attention of educators at this time. Greater cooperation between industry and educational institutions will provide a benefit to all.

Education—The Foundation for Freedom and National Strength—Marion B. Folsom (p. 81)

One of the most pressing problems facing the nation today is the need to improve and enlarge our higher education system. Many of our college facilities and faculties are already overburdened, yet the number of students seeking higher education will double in the next decade. This paper points out the steps that must be taken to increase the number of potential teachers and to induce sufficient numbers of them to choose teaching as a career. A greater effort must also be made to see that more of our most able high school graduates have an opportunity to pursue a higher education; at present, one third of the top quarter of our high school graduates do not go on to college. A recent study of Russian education made by the U. S. Office of Education is reported and the relative emphasis which Russia and America are placing on education is discussed. The cost of meeting the increased educational needs in America will be immense by current standards, but the cost of not meeting these needs will be far greater.

Learning and Teaching Processes in Electrical Engineering Education—E. J. Angelo, Jr. (p. 84)

The modification of the various engineering curricula to permit adequate preparation of students in a four-year program for careers in a rapidly changing technology of ever increasing complexity is one of the chief concerns of the engineering educator. It is generally felt that a more scientifically oriented curriculum than has been customary in the past will provide a more efficient and more effective undergraduate program.

The actual realization of increased efficiency and effectiveness requires a great deal of careful thought and some bold experimentation with curricula. Some considerations in this connection are set forth. In particular, it is held that unification of subject matter, whenever possible, is of primary importance in realizing greater efficiency and effectiveness, and means whereby the scientific bases for engineering may be employed to achieve unity are suggested. In this connection certain tasks that belong uniquely to the teacher are pointed out.

Make Your Own Engineers—Howard J. Gresens (p. 88)

Can ability and exceptional experience be accepted as substitutes for formal education in engineering? This article tells how one company developed a program of qualifications and examinations through which its more talented technicians can achieve full engineer status. The program gives the aspiring technician a continuing incentive for work towards an advanced status that is accepted without reservation by every degr engineer in the company.

The Place of Languages in Scientific Education—L. A. Ware (p. 90)

Some of the weaknesses of the old method of handling the language requirements for Ph.D. candidates are pointed out. It is maintained that a considerable waste of time was involved and that the requirement was not satisfactory to all concerned. The author supports the proposal that a good training in *one* language is preferable.

Contributors (p. 91)

Electron Devices

VOL. ED-5, NO. 3, JULY, 1958

Germanium and Silicon Transistor Structures by the Diffused-Meltback Process Employing Two or Three Impurities—I. A. Lesk and R. E. Gonzalez (p. 121)

The diffused-meltback process for making transistor structures involves growing a crystal containing a donor and an acceptor impurity, cutting the crystal into pellets, melting and refreezing part of a pellet, and then diffusing. Two impurities may be used to produce high-frequency silicon structures. For best results with germanium, three impurities are required for practical reasons. The two- and three-impurity cases are analyzed, and illustrated by graphs and numerical examples. Some characteristic transistor parameters are given to show the applicability of the diffused-meltback process for high-frequency devices.

Characteristics, Structure, and Performance of a Diffused-Base Germanium Oscillator Transistor—R. M. Warner, Jr., J. M. Early, and G. T. Loman (p. 127)

The diffused-base transistor structure affords a degree of design flexibility not found in previous structures. This is true because it has a larger number of independently adjustable design parameters than the previous structures. Its flexibility has been exploited in an oscillator transistor for 200-mc service. Design analysis shows that low ohmic base resistance, low collector body resistance, and operation at about 0.3 of the collector breakdown voltage are desirable in the present application. The methods of Lee have been used in making this germanium p-n-p diffused-base unit. Alloyed emitter and base electrodes are parallel stripes approximately 0.5-mil apart, each measuring 1×6 mils. The collector is about 4.5×8 mils. Typical parameters at $V_C=-10$ volts and $I_E=10$ ma are: $f_\alpha=600$ mc, $r_b'=35$ ohms, and $C_C=1.0$ mmf. Median 200-mc oscillator efficiency of 50 per cent is obtained at the design bias point of -20 volts, 10 ma; this exceeds the performance objective. The unit withstands 20,000-g accelerations in any direction, an additional demand imposed by the specific application for which it was developed.

An Analysis of Base Resistance for Alloy Junction Transistors—A. J. Wahl (p. 131)

For the circular disk type of transistor geometry, as commonly used in alloy junction transistors, base resistance is determined by treating it as a boundary value problem. This treatment results from consideration of the over-all behavior of both minority and majority charge carriers in the base region and leads to an expression for base spreading resistance in terms of alpha, frequency, resistivity, and transistor dimensions. Further consideration of this over-all charge carrier behavior leads to a determination of the entire common-emitter short-circuit input impedance, which in general is complex. Comparison with measurement shows that this impedance, which includes the base resistance, can be calculated accurately over a wide frequency range in terms of physical constants, dimensions, frequency, dc emitter bias, and effective minority carrier lifetime in the base region for small-signal operation of low power alloy junction transistors. Application to other types, such as power transistors and diffused-base transistors, may require extension of the present analysis with a considerable increase in complexity. Limitations and extensions of the analysis in its present form are discussed.

Low-Voltage Operation of the Retarding-Field Oscillator at X Band and in the Millimeter Wavelength Region—C. J. Carter and W. H. Cornetet, Jr. (p. 139)

This paper concerns the partial development of two low-voltage designs of the retarding-field oscillator. These designs differ fundamentally in their power coupling system. The X-band model has coaxial-line coupling to a waveguide while the millimeter wavelength model has double-cavity coupling to a waveguide.

The design developed at X band allows

operation with the anode voltage as low as 200 volts and as high as 600 volts. Radio-frequency output power of 20 milliwatts at 200 volts and better than 1 watt at 600 volts is possible.

In the millimeter wavelength range, three double-cavity designs have been investigated. These tubes operate in the range of from 4.30 to 5.20 mm, 5.00 to 6.4 mm, and 5.80 to 6.8 mm, respectively. All of these oscillators have anode potentials of 800 volts or less. An output power of 175 milliwatts has been obtained at a wavelength of 6.00 mm.

A digest of characteristics possessed by important models of the retarding-field oscillator investigated as of November, 1957, also is included.

A Process for Making Clean Gas Discharge Tubes—J. M. Lafferty (p. 143)

Tube assemblies of forsterite ceramic and titanium are outgassed and then sealed together with reactive alloys in an atmosphere of the noble gas with which they are to be filled. The gettering action of the hot titanium results in a very pure gas filling. Examples of gas tubes constructed by this new process include voltage regulators, voltage reference tubes, thyratrons, and spark gaps. This method of making ceramic-metal seals in an inert atmosphere may be applied to the production of ceramic-metal subassemblies and tube types that do not require gas filling or evacuation at the time of assembly. The fact that a vacuum system is not required to make these seals, and that the cooling time is shorted by convection currents, results in simplification of equipment and reduction of expense and should extend the usefulness of this type of ceramic-metal sealing.

Physical Mechanisms Leading to Deterioration of Transistor Life—G. C. Messenger (p. 147)

Life tests on surface-barrier-type transistors have been conducted at various temperatures and power levels to identify and characterize the mechanisms which cause the transistor characteristics to deteriorate with time. Three mechanisms have been isolated: the formation of solution cavities in the base of the transistor, an increase in surface recombination velocity, and a decrease in surface resistance. In the normal surface-barrier transistor, the formation of solution cavities proceeds with an activation energy of about 20,000 cal. mole. This leads to an exponential dependence of life expectancy on temperature and dissipation. The formation of solution cavities is eliminated by the micro-alloy process, in which case the life expectancy is probably determined by the decrease in surface resistance or the increase in surface recombination velocity.

The increase in surface recombination velocity causes a well-correlated decrease in current gain and grounded-base output impedance. The decrease in surface resistance produces an increase in the collector "saturation" current and may contribute to a decrease in output resistance. The formation of solution cavities brings about a decrease in punch-through voltage and grounded-emitter output impedance.

A 20 to 40-KMC Backward-Wave Oscillator—R. W. Grow, D. A. Dunn, J. W. McLaughlin, and R. P. Lagerstrom (p. 152)

A 20 to 40-kmc backward-wave oscillator is described which employs a single-tape helix with a mean diameter of 0.039 inch and a length of 1.75 inches supported internally by a triangular sapphire rod. Physically, the helix is mounted in a hole drilled in the ridge of the output ridge waveguide, and a closely spaced hollow beam is located on the outside of the helix. The output from the helix passes through a short section of coaxial line to the ridge waveguide and then along this guide and through the vacuum envelope to an external mating ridge waveguide. The two sections of guide meet the envelope at an angle of 13 degrees. Output is obtained from the oscillator from 18 to 40 kmc with a voltage range of 300 to 2600 volts. The RF output varies relatively smoothly and exceeds 2 milliwatts with 5-ma collector current over the entire band from 21 to 37.5 kmc. The total variation of power over this band is 6 db. It is expected that this tube will be useful for signal-generator-type applications.

The Effect of an Initial Velocity Spread on Klystron Performance—L. A. Harris (p. 157)

The fundamental component of beam current in a klystron is calculated by integrating the contributions due to individual velocity classes. For relatively narrow velocity distributions and operation with optimum parameters, the ratio of fundamental current amplitude to that obtained for a uniform velocity beam is given by a simple ratio of Fourier transforms of the velocity distribution functions. Several examples are calculated and the results shown graphically.

For tubes with long transit angles, a moderate spread in velocity may result in appreciable decrease of the fundamental component of beam current. Considerable care in the focusing of beams therefore is warranted when efficiency is an important factor in tube performance.

A Hybrid-Type Traveling-Wave Tube for High-Power Pulsed Amplification—E. J. Nalos (p. 161)

A hybrid-type traveling-wave tube suitable for high gain amplification at pulsed high-power levels is described. The device utilizes a filter-type loaded waveguide slow-wave circuit, with interaction below the propagating range of the circuit. This gives rise to a broad-band inductive-wall type of amplification with high gain per unit length. The particular structure outlined employs a spatial-harmonic traveling-wave circuit to couple the energy to the input and to extract power at the output. The main interaction circuit is separated from the input and output section by short ceramic terminations. With proper design, performance at good efficiencies is obtained over a 10 per cent bandwidth to date. A special feature of the device is the possibility of adjusting the gain variation with frequency to suit the designer. This comes about from the fact that the gain per unit length decreases with frequency in the coupling sections, and increases with frequency in the center (nonpropagating) section. By proper selection of the relative lengths of the two circuits, it is possible to obtain either flat gain or peak gain at either end of the frequency range. The efficiency does not appear to be affected by the center section and is limited by the characteristics of the output section only. With the present configuration, it was possible to obtain both good stability and reasonable efficiency simultaneously.

Dielectric Slow-Wave Structures for the Generation of Power at Millimeter and Submillimeter Wavelengths—R. H. Pantell, P. D. Coleman, and R. C. Becker (p. 167)

Several new types of coupling structures, designed to extract energy from a megavolt electron beam at a harmonic of the frequency used to modulate the beam current, are considered. In particular, the advantages of a slow-wave device over a right cylindrical cavity are indicated. The slow-wave coupling device may be resonant or nonresonant; the latter corresponds to a Cerenkov radiator. Power measurements at the twelfth harmonic of the fundamental modulating frequency provide good correlation with the theoretical power output expected. The design of a submillimeter coupling device is described, and the theoretical pulsed power obtainable is shown to be at the milliwatt level for a harmonic current density of 74 ma/cm^2.

The Reflex Klystron as a Negative Resistance Type Amplifier—C. F. Quate, R. Kompfner, and D. A. Chisholm (p. 173)

A reflex klystron has been tested as a narrow-band amplifier at 11,000 mc. The performance is predicted rather accurately from simple theory and steady gain can now be obtained in the 30-db region with a bandwidth of the order of megacycles. A noise figure of 40 db was measured and the saturation power output was the same as the output of an oscillator. A circulator was used in these tests to separate input from output and we consider it important to use this component with any type of negative resistance type amplifier.

Temperature Sensitivity of Current Gain in Power Transistors—Bernard Reich (p. 180)

An analysis is made of the factors causing the variation of current gain as a function of operating temperature. As a result, conclusions are reached which indicate that the base resistivity is the major single factor contributing to these variations. Finally, the results of this investigation are directed toward possible applications.

Thermal Velocity Effects in Magnetically Confined Beams—A. Szabo (p. 183)

The spreading of magnetically confined electron beams caused by thermal velocities has been investigated theoretically and experimentally. An analysis of the spreading of confined beams of various geometries (strip, rectangular, and cylindrical) is presented.

The thermal spreading of a confined cylindrical beam was measured at the anode of a parallel-flow Pierce gun. A transparent fluorescent screen was used for the anode. The spot size at the anode was measured as a function of magnetic field and an attempt made to relate the results to the theory.

Characteristics of Traveling-Wave Tubes with Periodic Circuits—Roy W. Gould (p. 186)

An analysis of an electron beam which interacts with a chain of coupled resonators is presented. Several important characteristics of traveling-wave tubes which employ periodic slow-wave circuits are described. It is found that, even for a lossless circuit, the gain does not become large near either pass band edge although the interaction impedance does become very large. Furthermore, useful amplification is found to occur outside the normal circuit pass band, particularly when the frequency is below the low-frequency cutoff where the circuit presents an inductive reactance to the beam.

The problem of matching uniform transmission lines to the periodic circuit is discussed from the equivalent circuit point of view and it is shown that the terminating impedance which produces no reflection from the output end of the circuit when the beam is present may be appreciably different from that required when the beam is absent.

The method of analysis applies to spatial harmonic operation, including backward spatial harmonics, as well as to synchronously tuned multicavity klystrons.

A Barkhausen-Kurz Oscillator at Centimeter Wavelengths—E. M. Boone, M. Uenohara, and D. T. Davis (p. 196)

This paper describes a new device for the generation of high-frequency oscillations in the centimeter wavelength region with high efficiency and low starting currents.

The tube is fundamentally a Barkhausen-Kurz oscillator utilizing a resonant cavity and a magnetically focused electron beam, but with no accelerating grids. The important features of this tube are the use of a parabolic potential distribution to utilize multiple transit electron motion, and the use of the magnetic field to control coupling between the electron stream and the resonator field and to reduce to negligible value the current intercepted at the resonator gap. A preliminary theory of the electronic energy interchange of this oscillator is provided, and the background theory of the oscillator design is discussed. Both X-band and K-band tubes have been tested. In the X-band

ube, a maximum output power of 1.8 watts ınd a maximum efficiency of 13.5 per cent were ›btained. At K band, the maximum power ›utput was 430 milliwatts, and the maximum :fficiency was 12.2 per cent. Starting currents ›elow 0.1 ma have been observed at X band.

Experimental Notes and Techniques (p. !05)

Contributors (p. 206)

Engineering Management

Vol. EM-5, No. 3, September, 1958

Problems of Engineering Management—Merritt A. Williamson (p. 61)

All problems of management can ultimately be traced to human beings. The technical manager must have the respect of his people to be effective. They can best assess him through the common ground of technical ability. It is the obligation of the technical manager to convey his philosophy of management to his people and to train them in his methods of operation. The successful manager must constantly fight the desire to participate in the technical details of work. He must realize that it is wrong for him to make decisions which are not appropriate to his level in the organization where those decisions should be made by either those above or those below. He must permit people who work for him the freedom to make mistakes. Engineers have an underlying fear of criticism which makes supervising them often very difficult. This fear of criticism hinders their effective delegation of work. The aspirant to managerial status should seek out criticism and get used to receiving it. Reviews of work performance which have been requested of a supervisor will be invaluable in developing the recipient's managerial skills since it provides a greater awareness of the human problems that are involved in this phase of technical management.

Comprehensive Comparisons and Business Decisions—Roman Krzyczkowski (p. 65)

The paper sugests a method of quantitatively evaluating a managerial decision as a deliberate choice between different courses of action. The method, called the "Comprehensive Comparison Method," is demonstrated in application to two examples: the first describes the author's investigation of economic problems of submarine telephone cables. The second example presents a comprehensive comparison of radio and cable communication links.

In both cases the weighting system is evolved. Analysis of the total weighted scores for each choice gives a valuable guide when the final decision has to be made. This guide should not be mistaken, however, for the *decision* itself.

Training of Systems Engineers—Ralph I. Cole (p. 71)

This paper cites that, in the evolution of major systems, many new engineering responsibilities have been created. A critical analysis is made of the systems engineering task to be accomplished and recommendations for action are stated.

The basis of education of the systems engineer is also briefly discussed.

The Relation of Utilization to the Shortage of Scientists—I. Hirsch, W. Milwitt, W. J. Oakes, and R. A. Pelton (p. 73)

The present utilization of engineers and scientists by industry and its significance to the "shortage" of scientific manpower has been investigated. Based upon available data—a limited-sample survey of scientific manpower in the aviation and electronic industries—and analyses, a rough estimate indicates that the probable average effectiveness of these scientists is somewhat less than ten per cent of perfect utilization.

Various methods of increasing scientific productivity are examined. An operations research study is suggested. Improvements of communications, management techniques, and data processing methods are several recommendations.

A brief history of scientific manpower supply and demand is presented. Motivations of scientists are studied, as are motivations which lead students into science careers.

Estimates are made of the future supply of and demand for scientific manpower, assuming present utilization. These figures indicate the shortage will become a surplus by 1971.

PGEM News (p. 128)

Information Theory

Vol. IT-4, No. 3, September, 1958

Frontispiece—Peter Elias (p. 98)

Two Famous Papers—Peter Elias (p. 99)

An Experimental Investigation of Some Properties of Band-Pass Limited Gaussian Noise—Kjell Blötekjaer (p. 100)

The probability distribution of time intervals between successive zero crossings of bandpass limited Gaussian noise is determined experimentally for a number of different filters having nearly rectangular frequency characteristics. For one particular filter the distribution of time intervals between crossings of levels different from zero is also found.

Notes on the Penny-Weighing Problem, Lossless Symbol Coding with Non-Primes, Etc.—Marcel J. E. Golay (p. 103)

The method of construction of lossless symbol coding matrices for one-error correction is illustrated for the case when the prime symbol order is three, and the application of this matrix to the penny-weighing problem is described. This method is then extended to those cases in which the symbol order is 2^2, 2^3, 2^4, 2^6, 3^2, 3^3, 3^4, 3^5, 5^2, 5^3, 5^4, 7^2, 7^3, and p^2, where p is any higher prime. This extension is based on the concept of the master iterating matrix. These matrices are given for the first thirteen cases cited, and their existence is demonstrated for p^2.

This paper concludes with a short description of Zaremba's condition, and its application to various problems, and more particularly to the hypothetical one-error correcting close-packed code with the symbol order 6.

On Sampling the Zeros of Bandwidth Limited Signals—F. E. Bond and C. R. Cahn (p. 110)

The sampling theorem enables a band-limited signal to be expressed in terms of a set of sample point values, which occur at the Nyquist rate. The sampling theorem has been generalized to include nonuniform sampling and the use of derivatives of the signal. In the present paper, a sampling theorem has been developed which utilizes information related to the zeros of the signal. The concept of complex zeros is introduced to show that the zeros occur at the Nyquist rate. This sampling theorem can be of use for enabling the transmission of binary signals, such as facsimile and infinitely-clipped speech, over a continuous band-limited channel. The result indicates the desirability of developing a completely general theory of sampling applicable to the various situations which may arise in practice.

Enhancement of Pulse Train Signals by Comb Filters—Janis Galejs (p. 114)

The relative performance of different types of comb filters is investigated in conjunction with signal and noise types similar to those expected in radar applications. The filter types considered are idealized filters with zero transmission stop bands between their pass bands, optimum filters maximizing the peak signal-to-rms-noise ratio, cascaded delay line filters, feedback type filters, and storage tube filters. The pulse train signals consist of rectangular or sin x/x pulses with rectangular or sin x/x pulse envelope shapes. Power spectra of noise considered are rectangular and triangular. With a given number of signal pulses, the performances of the different filters vary from each other only by a few decibels in most cases analyzed. Storage tube filters exhibit lower signal-to-noise power ratios, but higher peak signal-to-rms-noise ratios, than the feed-back type filters. Inaccurate delay times of filter delay lines are shown to decrease the peak signal output more than the signal power output and to affect the cascaded delay line filter less than the feedback type filter. Correlation techniques are compared with comb filters. The crosscorrelator exhibits the same peak signal-to-rms-noise ratio as the optimum filter.

Non-Mean-Square Error Criteria—Seymour Sherman (p. 125)

While in the engineering literature non-mean-square error criteria for predictors are often presented as physically significant and then shunted aside because of mathematical unmanageability, it is shown here that in the case of Gaussian processes all such criteria given in three recent textbooks yield the same predictor as the linear minimum mean-square predictor of Wiener.

Correspondence (p. 127)

Contributors (p. 131)

Abstracts and References

Compiled by the Radio Research Organization of the Department of Scientific and Industrial Research, London, England, and Published by Arrangement with that Department and the *Electronic and Radio Engineer*, incorporating *Wireless Engineer*, London, England

NOTE: The Institute of Radio Engineers does not have available copies of the publications mentioned in these pages, nor does it have reprints of the articles abstracted. Correspondence regarding these articles and requests for their procurement should be addressed to the individual publications, not to the IRE.

Acoustics and Audio Frequencies..... 1892
Antennas and Transmission Lines..... 1892
Automatic Computers..... 1893
Circuits and Circuit Elements..... 1894
General Physics..... 1895
Geophysical and Extraterrestrial Phenomena..... 1897
Location and Aids to Navigation..... 1898
Materials and Subsidiary Techniques.. 1898
Mathematics..... 1902
Measurements and Test Gear..... 1902
Other Applications of Radio and Electronics..... 1902
Propagation of Waves..... 1903
Reception..... 1903
Stations and Communication Systems.. 1903
Subsidiary Apparatus..... 1904
Television and Phototelegraphy..... 1904
Transmission..... 1905
Tubes and Thermionics..... 1905
Miscellaneous..... 1906

The number in heavy type at the upper left of each Abstract is its Universal Decimal Classification number and is not to be confused with the Decimal Classification used by the United States National Bureau of Standards. The number in heavy type at the top right is the serial number of the Abstract. DC numbers marked with a dagger (†) must be regarded as provisional.

The Index to the Abstracts and References published in the PROC. IRE from February, 1957 through January, 1958 is published by the PROC. IRE, May, 1958, Part II. It is also published by *Electronic and Radio Engineer*, incorporating *Wireless Engineer*, and included in the March, 1957 issue of that journal. Included with the Index is a selected list of journals scanned for abstracting with publishers' addresses.

ACOUSTICS AND AUDIO FREQUENCIES

534.1-8-14:621.391.63 2944
Light Modulation by Standing Waves in Liquids—H. F. Reimann. (*Nachrtech. Z.*, vol. 7, pp. 515–518; November, 1957.) A light beam is modulated in passing through a liquid subjected to ultrasonic vibrations; a photomultiplier circuit is used for demodulation. Applications of the method may include communications and television projection.

534.2:621.395.623.52 2945
On the Attenuation of High-Amplitude Waves of Stable Sawtooth Form Propagated in Horns—I. Rudnick. (*J. Acoust. Soc. Amer.*, vol. 30, pp. 339–342; April, 1958.) A theoretical expression for the power loss for a generalized horn is obtained, and applied to horns of particular shape.

534.2-8-14 2946
Ultrasonic Dispersion in Oxygen—J. V. Connor. (*J. Acoust. Soc. Amer.*, vol. 30, pp. 297–300; April, 1958.)

534.21-8-13 2947
Sound Propagation in Gases at High Frequencies and Very Low Pressures—E. Meyer and G. Sessler. (*Z. Physik*, vol. 149, pp. 15–39; August 23, 1957.) Sound absorption and dispersion in argon, air and hydrogen is calculated and measured for frequency/pressure ratios of 10^7–10^{11} cps per atmosphere.

534.222.1 2948
Propagation of Sound Across a Boundary between Two Superfluid Phases—R. G. Arkhipov and I. M. Kholatnikov. (*Zh. Eksp. Teor. Fiz.*, vol. 33, pp. 758–764; September, 1957.) Theoretical treatment of the propagation of two different sound waves across a phase boundary showing that mode conversion can occur. Formulas are derived for the energy flux of the reflected, refracted and converted waves.

534.614-8-16 2949
On the Measurement of Ultrasonic Velocity in Solids—J. Williams and J. Lamb. (*J. Acoust. Soc., Amer.*, vol. 30, pp. 308–313; April, 1958.) The method is based on the cancellation of a traveling wave train after several reflections at the ends of the specimen by a second wave train from the same source. The velocity of propagation can be evaluated to within 1 part in 10^4 after taking account of phase shift.

534.78 2950
Frequency of Usage and the Perception of Words—M. R. Rosenzweig and L. Postman. (*Science*, vol. 127, pp. 263–266; February 7, 1958.) Conclusions drawn from tests on intelligibility and visual perception of words are summarized. More highly intelligible alphabetic equivalents may be obtained by selecting frequently used words which are longer than those in the current lists.

534.78 2951
Interaural Effects upon Speech Intelligibility at High Noise Levels—I. Pollack and J. M. Pickett. (*J. Acoust. Soc. Amer.*, vol. 30, pp. 293–296; April, 1958.) By presenting speech and noise to one ear and noise alone to the other, speech intelligibility was substantially decreased compared with either monaural or binaural listening conditions. See also 2286 of 1958.

534.78:621.391 2952
Construction and Investigation of a Transmission System for Synthetic Speech—E. Krocker. (*Nachrtech. Z.*, vol. 7, pp. 553–564; December, 1957.) Laboratory tests were carried out on a "vocoder" system [513 of 1949 (Molsey and Swaffield)] to investigate its performance and assess its practical value.

534.845 2953
The Effects of a Surface Covering on the Acoustic Absorption of Porous Materials—E. Brosio. (*Alta Frequenza*, vol. 26, pp. 632–638; December, 1957.) Covering absorbent panels by protective material, such as varnish, paper, etc. increases the absorptive power at low frequencies and diminishes it at high frequencies. Experimental results are in agreement with theoretical predictions.

621.395.623.7 2954
Investigations of Transients in Loudspeakers—G. Kaszynski. (*Hochfrequenztech. u. Electroakust.*, vol. 66, pp. 37–52; September, 1957.) The transients considered are those occurring at the beginning and end of each sound. Transient waveforms are derived theoretically from the characteristics of the loudspeaker, the source impedance and transmission coefficient, and are compared with experimentally obtained response curves and oscillograms.

621.395.623.8 2955
The Directivity of Acoustic Radiators Arranged in a Circular Arc—K. Feik. (*Hochfrequenztech. u. Elektroakust.*, vol. 66, pp. 29–37; September, 1957.) The radiation patterns of loudspeakers arranged in arcs subtending different angles up to 180 degrees are derived theoretically and by experiment for frequencies ranging from 0.9 to 11.4 kc. Approximately circular radiation patterns can be obtained with suitably proportioned arrays.

621.395.625.3 2956
High-Resolution Magnetic Recording Structures—A. S. Hoagland. (*IBM J. Res. Dev.*, vol. 2, pp. 91–104; April, 1958.) Design concepts are established and their application demonstrated. In addition to the conventional ring head two new devices are considered. These are a probe-type unit which lends itself to high-density vertical magnetic recording and a wire-grid array which yields high resolution.

621.395.625.3:621.317.616 2957
The Determination of Frequency Characteristics of Recording-Tape Magnetization—Schmidbauer. (See 3205.)

ANTENNAS AND TRANSMISSION LINES

621.315.212:[621.395.4+621.397.5 2958
Multichannel Systems along Coaxial Cables—J. Bauer. (*Bull. schweiz. elektrotech. Ver.*, vol. 49, pp. 412–416, 427; April 26, 1958.) The reference systems for telephony and television transmission via multichannel coaxial-cable links based on C.C.I.T.T. and C.C.I.R. recommendations are discussed. A 12-mc system is described which provides 2700 telephony channels, or one television and 1200 telephony channels.

621.315.212.4:621.315.513 2959
Multilayer Conductor having Low Resistance at High Frequencies—M. Sugi and K. Murai. (*Elect. Commun.*, vol. 34, pp. 332–336; December, 1957.) A cylindrical conductor consisting of layers of helically wound thin conducting tape each separated from the other by

insulation is considered. Skin effect is reduced by equalizing the effective inductance of all layers. The theory of the design and some experimental results are given.

621.372.2+621.396.11 2960
Surface Waves—Barlow. (See 3228.)

621.372.2:621.396.67:621.396.65 2961
Aerial Feeders for Multichannel Links—L. Lewin and J. Payne. (*Electronic Eng.*, vol. 30, pp. 414–419; July, 1958.) The reflections from coaxial-cable and waveguide feeders are investigated and the requirements for wide-band links given. The suitability of the various types of feeder for different frequency bands is outlined. In general, coaxial cables can meet most requirements up to 2000 mc, but above 3000 mc waveguides are to be preferred.

621.372.22:621.372.8 2962
Propagation in Coupled Transmission-Line Systems—J. Brown. (*Quart. J. Mech. Appl. Math.*, vol. 11, pp. 235–243; May, 1958.) A system of transmission lines coupled by reactive networks at regular intervals is examined.

621.372.3:621.318.134:537.226 2963
Theory of Nonreciprocal Ferrite Phase Shifters in Dielectric-Loaded Coaxial Line—K. J. Button. (*J. Appl. Phys.*, vol. 29, pp. 998–1000; June, 1958.) An antisymmetrically loaded line can produce a differential phase shift of 180 degrees per inch in the 2800-mc range. Such a line is described theoretically. See also *ibid.*, vol. 28, pp. 921–922; August, 1957 (Sucher and Corlin).

621.372.82 2964
Orthogonality Properties for Modes in Passive and Active Uniform Waveguides—A. D. Bresler, G. H. Joshi, and N. Marcuvitz. (*J. Appl. Phys.*, vol. 29, pp. 794–799; May, 1958.) Orthogonality relations are given for the four-vector guided modes of anisotropic uniform waveguides and for the six-vector guided modes in waveguides containing unidirectional electron beams with axially independent dc velocities.

621.372.831.4:621.318.134 2965
Coupling through an Aperture containing an Anisotropic Ferrite—D. C. Stinson. (IRE TRANS. ON MICROWAVE THEORY AND TECHNIQUES, vol. MTT-5, pp. 184–191; July, 1957. Abstract, PROC. IRE, vol. 45, p. 1312; September, 1957.)

621.372.837.3:621.318.134 2966
Two Short Low-Power Ferrite Duplexers—R. S. Cole and W. N. Honeyman. (*Electronic Radio Engr.*, vol. 35, pp. 282–286; August, 1958.) Two rotation-type duplexers, one of which uses a turnstile junction are described. Transmitter-receiver isolations of about 25 db are obtained over a bandwidth of 1.3 per cent at 3 cm λ.

621.372.85 2967
Application of Rayleigh-Ritz Method to Dielectric Steps in Waveguides—R. E. Collin and R. M. Vaillancourt. (IRE TRANS. ON MICROWAVE THEORY AND TECHNIQUES, vol. MTT-5, pp. 177–184; July, 1957. Abstract, PROC. IRE, vol. 45, p. 1312; September, 1957.)

621.372.85:538.221:621.318.134 2968
The Application of Ferrites in the Construction of Nonreciprocal Microwave Devices—W. H. Dörre. (*Nachrtech. Z.*, vol. 7, pp. 542–548; December, 1957.) Survey of applications including isolators, phase shifters and gyrators. Twenty-seven references.

621.372.852.2:621.372.832.6 2969
Errors in Magic-Tee Phase Changer—M. Vaillancourt. (IRE TRANS. ON MICROWAVE THEORY AND TECHNIQUES, vol. MTT-5, pp. 204–207; July, 1957. Abstract, PROC. IRE, vol. 45, p. 1312; September, 1957.)

621.372.852.323:621.318.134 2970
Field-Displacement Isolators at 4, 6, 11 and 24 kMc/s—S. Weisbaum and H. Boyet. (IRE TRANS. ON MICROWAVE THEORY AND TECHNIQUES, vol. MTT-5, pp. 194–198; July, 1957. Abstract, PROC. IRE, vol. 45, p. 1312; September, 1957.) See also 1628 of 1958.

621.372.852.4 2971
A Method of Producing Broad-Band Circular Polarization Employing an Anisotropic Dielectric—H. S. Kirschbaum and S. Chen. (IRE TRANS. ON MICROWAVE THEORY AND TECHNIQUES, vol. MTT-5, pp. 199–203; July, 1957. Abstract, PROC. IRE, vol. 45, p. 1312; September, 1957.)

621.372.853.1 2972
The Propagation of Constant Longitudinal Magnetic Waves in Dielectric-Filled Waveguides—L. G. Chambers. (*Quart. J. Mech. Appl. Math.*, vol. 11, pp. 244–252; May, 1958.) "The propagation of electromagnetic waves in an inhomogeneously filled waveguide is discussed and it is shown that, when the phase velocity of the wave down the guide is equal to the velocity of propagation in one of the dielectric media, then the longitudinal component of magnetic field is constant across that dielectric. Limits are also given for the propagation constants of TE and TM waves." See also 638 of 1955.

621.372.855 2973
An Adjustable Sliding Termination for Rectangular Waveguide—R. W. Beatty. (IRE TRANS. ON MICROWAVE THEORY AND TECHNIQUES vol. MTT-5, pp. 192–194; July, 1957. Abstract, PROC. IRE, vol. 45, p. 1312; September, 1957.)

621.396.67 2974
A New Method of Solving the Problem of Wide-Band Aerials—H. Meinke. (*Nachrtech. Z.*, vol. 10, pp. 594–601; December, 1957.) Considering the antenna to be an inhomogeneous transmission line with attenuation due to radiation, an explanation is derived for the dependence of antenna input impedance and radiation patterns on frequency. By means of a curvilinear coordinate system field equations of convenient form are derived which result in adequate approximations for wide-band antennas of simple shape.

621.396.674.1.029.51 2975
Loop Antennas for Long Waves—J. Wüstenhagen. (*Rundfunktech Mitt.*, vol. 1, pp. 237–243; December, 1957.) The suitability of loop antennas for transmission in the long-wave band is discussed with reference to input impedance, efficiency and bandwidth. A method of calculating input impedance over a wide frequency range is given; results of model tests confirm its accuracy. An advantage of loop antennas is that their input impedance can be varied within wide limits by appropriate structural changes.

621.396.674.3–41+621.396.677.3–41 2976
Investigations of Plane Surface Dipoles and Dipole Arrays—G. Arlt. (*Z. angew. Phys.*, vol. 9, pp. 379–388; August, 1957.) Radiation and impedance diagrams of surface antennas of different shape are examined to determine those with the best wide-band characteristics. A rhombus dipole with side links has good input impedance and directivity characteristics over a wide band of frequencies. A chequerboard array composed of such dipoles permits wide-band matching and radiation and reception with any type of polarization. Measurements were made on a two-element rhombus dipole whose directivity characteristics compare favorably with those of a tubular dipole. See also 2118 of 1952 (Wolter).

621.396.677:621.396.712.029.53 2977
The Medium-Wave Aerial at Hamburg for the Suppression of Sky-Wave Radiation towards Langenberg—E. Mohr and F. von Rautenfeld. (*Rundfunktech Mitt.*, vol. 1, pp. 209–220; December, 1957.) The design is described of the directive antenna system of the 971-kc, 100-kw transmitter at Hamburg which provides a minimum of sky-wave radiation at an elevation of about 30 degrees in the direction of Langenberg where a second 100-kw transmitter operating at the same frequency is situated. Details are given of model tests at 100 mc and of field plotting in a specially equipped aircraft. See also 592 of 1958 (von Rautenfeld and Thiessen).

621.396.677.029.6 2978
Considerations on the Plane Centre of Radiating Systems—C. Montebello and F. Serracchioli. (*Note Recensioni Notiz.*, vol. 7, pp. 57–66; January/February, 1958.) A simple criterion is derived for ascertaining the existence and location of a phase center defined with reference to equiphase surfaces. Some practical applications are discussed.

621.396.677.43:621.397.62 2979
Rhombic Antennas for TV—R. B. Cooper, Jr. (*Radio TV News*, vol. 59, pp. 64–65, 109; February, 1958.) Details of the electrical design suitable for reception in fringe areas are given and the practical construction is indicated.

621.396.677.832:537.226 2980
Field of a Dielectric-Loaded, Infinite Corner Reflector—A. W. Adey. (*Canad. J. Phys.*, vol. 36, pp. 438–445; April, 1958.) Calculations show that the radiation resistance and far-field amplitude are sensitive to the presence of the loading, particularly for small spacings between the feeding element and the apex. Unlike the no-dielectric case, there is no monotonic fall-off in amplitude with increasing element-apex spacing.

AUTOMATIC COMPUTERS

681.142 2981
The Logical Design of a Simple General-Purpose Computer—S. P. Frankel. (IRE TRANS. ON ELECTRONIC COMPUTERS, vol. EC-6, pp. 5–14; March, 1957.) "The logical design described here is used in MINAC, partially constructed at the California Institute of Technology, and LGP-30, manufactured by Librascope Inc. These serial binary digital computers make use of magnetic-drum bulk storage and use three circulating registers and fifteen flip-flops."

681.142 2982
Digital Computer Adding and Complementing Circuits—C. D. Florida. (*Electronic Eng.*, vol. 30, pp. 429–435; July, 1958.) Various direct-coupled transistor circuits are described, suitable for use with double-gate shifting registers. The performance of these circuits operating, with a digit spacing of 5 μsec, is illustrated with waveform photographs.

681.142 2983
An Algorithm for Determining Minimal Representations of a Logic Functions—B. Harris. (IRE TRANS. ON ELECTRONIC COMPUTERS, vol. EC-6, pp. 103–108; June, 1957. Abstract, PROC. IRE, vol. 45, p. 1311; September, 1957.)

681.142 2984
Computing Techniques for the Sampling Parametric Computer—C. J. Hirsch and F. C. Hallden. (IRE TRANS. ON ELECTRONIC COM-

PUTERS, vol. EC-6, pp. 108–119; June, 1957. Abstract, PROC. IRE, vol. 45, p. 1311; September, 1957.)

681.142 2985
Dynamic Accuracy as a Design Criterion of Linear Electronic Analogue Differential Analyzers—A. Nathan. (IRE TRANS. ON ELECTRONIC COMPUTERS, vol. EC-6, pp. 74–86; June, 1957. Abstract, PROC. IRE, vol. 45, p. 1311; September, 1957.

681.142 2986
Fine Graduation of the Timing-Pulse Generator Disk of an Electronic Computer—H. J. Dreyer, T. Gorr, and W. Schütte. (*VDI Zeitschrift*, vol. 100, pp. 329–331; March 11, 1958.) The construction is described of a disk providing the synchronizing pulses for the storage system of a digital computer. The nonferromagnetic disk of about 40 cm diameter carries a thin layer of nickel near the rim. The layer is cut by radial grooves of width 150 μ, and there are five concentric tracks with differing numbers of grooves. The outer track thus consists of 4200 ferromagnetic "teeth" which at 3000 rpm generate pulses at a repetition frequency of about 200 kc. Details of the dividing and engraving machinery are given.

681.142 2987
Nondestructive Memory employing a Domain-Oriented Steel Wire—U. F. Gianola. (*J. Appl. Phys.*, vol. 29, pp. 849–853; May, 1958.) A magnetic storage system using a steel wire under tension is described. A small solenoid is used to magnetize the wire locally and for observing the flux change produced by an interrogative current pulsed through the wire itself.

681.142 2988
An Electronic Analogue Multiplier using Carriers—E. S. Weibel. (IRE TRANS. ON ELECTRONIC COMPUTERS, vol. EC-6, pp. 30–34; March, 1957.) "An electronic analog multiplier is described, which is based on a modulation technique. No dc amplifiers are used, which makes the output entirely free of drifts. All distortions up to the fourth order are eliminated. The experimental model that has been built handles inputs from dc to 7 kc and gives an output from dc to 14 kc. The amplitude range of the output is 50 db."

681.142 2989
Trigonometric Resolution in Analogue Computers by means of Multiplier Elements—R. M. Howe and E. G. Gilbert. (IRE TRANS. ON ELECTRONIC COMPUTERS, vol. EC-6, pp. 86–92; June, 1957. Abstract, PROC. IRE, vol. 45, p. 1311; September, 1957.)

681.142 2990
Stability and Convergence Limitations on the Use of Analogue Computers with Resistance-Network Analogues—M. E. Fisher. (*Brit. J. Appl. Phys.*, vol. 9, pp. 288–291; July, 1958.) It is shown that the solution of equations such as $\nabla^2\Phi=f(\phi)$ breaks down if the gradient of $f(\phi)$ is negative and sufficiently large to cause the correct solution to be "wavelike." See also 673 of 1956 (Karplus) and 367 of 1958 (Hutcheon).

681.142 2991
Electronic Integrator with Immediate Digital Output—B. L. Hisey and E. R. Perl. (*Rev. Sci. Instr.*, vol. 29, pp. 355–359; May, 1958.) Details are given of a technique for obtaining an instantaneous numerical value proportional to the area of a recurring voltage transient. The basic principle is to summate the pulses from a generator whose repetition rate is a linear function of the instantaneous input voltage. The system has a a high order of linearity, approximately ± 0.1 per cent, and is used for roughly triangular pulses of 0.5–10 msec duration.

681.142 2992
An Improved Electromagnetic Integrator—A. J. Dyer. (*J. Sci. Instr.*, vol. 35, pp. 240–242; July, 1958.) Description of a permanent-magnet moving-coil system for integrating an electrical signal of varying polarity over integration times as long as one day.

681.142:061.3 2993
Symposium on Computers—(*Aust. J. Instrum. Tech.*, vol. 14, pp. 5–71; February, 1958.) The text is given of seven papers read at a symposium held at Mt. Eliza, Victoria, December 3–6, 1957.

681.142:538.652 2994
Magnetostrictive Delay Line—V. N. Kostić. (*Bull. Inst. Nuclear Sci. "Boris Kidrich,"* vol. 7, pp. 97–101; March, 1957.) "Equivalent electromechanical circuit for a magnetostrictive nickel delay line is given. The optimum matching at the input and output end is discussed."

681.142:621.318.134 2995
Magnetic-Core Memory Cell with Nondestructive Read-Out—T. Ž. Aleksić. (*Bull. Inst. Nuclear Sci. "Boris Kidrich,"* vol. 7, pp. 93–101; March, 1957.) Outline of a method of using different values of incremental permeability of a dc-biased magnetic core to obtain a binary storage cell. One of the possible applications is for visible indication of binary state in magnetic shift registers.

681.142:621.318.134:621.314.7 2996
A Transistor-Driven Magnetic-Core Memory—E. L. Younker. (IRE TRANS. ON ELECTRONIC COMPUTERS, vol. EC-6, pp. 14–20; March, 1957.) Description of a storage system, with a capacity of 1024 of 18-bit words designed for a transistor airborne digital computer TRADIC at Bell Telephone Laboratories. Both the read and write operations are based on a coincident-current technique.

681.142:621.318.134:621.318.57 2997
Current Steering in Magnetic Circuits—J. A. Rajchman and H. D. Crane. (IRE TRANS. ON ELECTRONIC COMPUTERS, vol. EC-6, pp. 21–30; March, 1957.) Magnetic switches are described in which the current from an energizing source is guided or steered through one out of many possible parallel branches; the conducting branch is selected by the presetting of appropriate magnetic elements.

681.142:621.374.32 2998
The Logic of Bidirectional Binary Counters—M. J. E. Golay. (IRE TRANS. ON ELECTRONIC COMPUTERS, vol. EC-6, pp. 1–4; March, 1957.) See also 42 of 1954 (Ware).

681.142:621.385.2 2999
A New Diode Function Generator—T. Miura, H. Amemiya, and T. Numakura. (IRE TRANS. ON ELECTRONIC COMPUTERS, vol. EC-6, pp. 95–100; June, 1957. Abstract, PROC. IRE, vol. 45, p. 1311; September, 1957.)

681.142:621.385.832 3000
A Cathode-Ray-Tube Analogue-to-Serial Digital Converter—J. Willis and M. G. Hartley. (*J. Sci. Instr.*, vol. 35, pp. 197–202; June, 1958.) Small fluctuations of the cathode ray tube screen equilibrium potential cause proportionate fluctuations in the steady secondary-emission current arriving at a collector anode. The parameters affecting changes in this current are investigated using an external electrode on the cathode ray tube face to modulate the screen potential. Experiments are described to determine minimum electrode width and spacing, consistent with the production of a discrete pulse output from each electrode when a pattern is scanned.

CIRCUITS AND CIRCUIT ELEMENTS

621.3.049.75 3001
Printed Circuits—N. Osifchin and S. J. Stockfleth. (*Bell Labs. Rec.*, vol. 36, pp. 117–121; April, 1958.) A review of printed circuit techniques suitable for modular equipment.

621.314.22:621.375.125 3002
Divided Output Transformers—R. Guelke. (*Wireless World*, vol. 64, pp. 384–385; August, 1958.) To overcome self-capacity in the primary winding of an AF output transformer at high frequencies, the output from the final stage may be fed to two transformers: one for the low-frequency and the other for the high-frequency range. This overcomes the necessity for a single high-quality transformer and the output can be fed directly to two separate loudspeakers.

621.314.67 3003
Contribution to the Study of a Rectifier in Series with an Inductive Resistance—G. Maizières (*Rev. gèn. Élect.*, vol. 66, pp. 565–568; November, 1957.) Different hypotheses are considered for expressing the voltage drop across the rectifier at low frequencies. Values of mean and maximum current are calculated according to each hypothesis and compared with values measured using a coil of inductance 0.99H and resistance 98Ω, in series with a valve rectifier. A circuit for measuring low peak voltages using a gas-filled tetrode is described.

621.316.727 3004
Capacitive Phase Shifters–B. Senf. (*Nachrtech. Z.*, vol. 7, pp. 507–511; November, 1957.) The design is described of a continuous phase shifter consisting of a variable capacitor with four groups of stator plates and one group of kidney-shaped rotor plates.

621.316.82:621.314.63 3005
A Field-Effect Varistor—(*Bell Lab. Rec.*, vol. 36, p. 150; April, 1958.) A two-terminal passive semiconductor is described in which the current can be held constant within 1 per cent in the voltage range 20–120 volts. Currents from 10 μa to 10 ma can be handled; the ac/dc resistance ratio in this region is of the order of 100.

621.372.4 3006
Elementary Proof of an Extended Reactance Theorem for Two-Terminal Networks—H. Wolter. (*Z. angew. Phys.*, vol. 9, pp. 340–347; July, 1957.) A proof is derived for Foster's reactance theorem which is also applicable to its extended form covering loss-free circuit elements and transmission lines.

621.372.412:549.514.51 3007
High-Q Quartz Crystals at Low Temperatures—D. L. White. (*J. Appl. Phys.*, vol. 29, pp. 856–857; May, 1958.) Q measurements over the range 4.2°K to over 100°K for several modes of vibration are described. In one case a value of 5.5×10^7 was obtained.

621.372.413 3008
Elimination of Unwanted Modes of Oscillation in Cylindrical Cavities—L. Grifone. (*Alta Frequenza*, vol. 26, pp. 580–602; December, 1957.) The possible modes in high-Q cylindrical cavity resonators are analyzed and the suppression of residual modes by special coupling systems or discontinuities inside the cavity is discussed. Measurements were made on ten tunable cavities of different size covering the frequency range 3.6–36 kmc. A frequency-modulated source was used to determine the permissible limits of the cavity tuning range and the dimensions of the discontinuities for obtaining the desired attenuation of unwanted modes without reducing Q by more than 5 per cent. The modes and their amplitudes are tabulated.

621.372.413:621.372.2 3009
Q Factors of a Transmission-Line Cavity—L. Young. (IRE TRANS. ON CIRCUIT THEORY, vol. CT-4, pp. 3–5; March, 1957. Abstract, PROC. IRE, vol. 45, p. 1034; July, 1957.)

621.372.414 3010
Exponential Transmission Lines as Resonators and Transformers—R. N. Ghose. (IRE TRANS. ON MICROWAVE THEORY AND TECHNIQUES, vol. MTT-5, pp. 213–217; July, 1957. Abstract, PROC. IRE, vol. 45, p. 1312; September, 1957.)

621.372.5 3011
General Method of Analyzing Bilateral, Two-Port Networks from Three Arbitrary Impedance Measurements—E. F. Bolinder. (*Ericsson Tech.*, vol. 14, no. 1, pp. 3–37; 1958.) The method consists in mapping stereographically on the surface of the Riemann unit sphere three given output quantities and their corresponding measured input quantities. The fixed points and the multiplier of the normal (canonic) form of the linear fractional transformation representing the network can be obtained by using Klein's three-dimensional generalization of the Pascal theorem. The different constructions of the geometric part can also be performed analytically. Simple numerical examples are worked out.

621.372.51 3012
Transformation Quadripoles according to the Insertion-Loss Theory—C. Kurth. (*Frequenz*, vol. 12, pp. 1–8; January, 1958.) The design of filter networks with prescribed attenuation characteristics and impedance transformation in the pass band is discussed. See also 2369 of 1957.

621.372.51 3013
Graphical Determination of Matching Sections—C. J. Vedin and P. O. Leine. (*Ericsson Tech.*, vol. 14, no. 1, pp. 91–99; 1958.) A description of graphical methods, using the Smith chart, for matching impedances by means of L, Π or T sections.

621.372.54 3014
Degenerate Solutions and an Algebraic Approach to the Multiple-Input Linear-Filter Design Problem—R. M. Stewart and R. J. Parks. (IRE TRANS. ON CIRCUIT THEORY, vol. CT-4, pp. 10–14; March, 1957. Abstract, PROC. IRE, vol. 45, p. 1035; July, 1957.)

621.372.54:621.391 3015
Optimum Filters for Independent Measurements of Two Related Perturbed Messages—J. S. Bendat. (IRE TRANS. ON CIRCUIT THEORY, vol. CT-4, pp. 14–19; March, 1957. Abstract, PROC. IRE, vol. 45, p. 1035; July, 1957.)

621.372.54:621.396.67 3016
Antenna Filters for a Military Radio System—M. D. Brill and R. M. Jensen. (*Bell Lab. Rec.*, vol. 36, pp. 142–145; April, 1958.) High-*Q* coaxial filters are described covering both transmission and reception over the range 50–600 mc in only 22 sub-bands.

621.372.55+621.375.4.126 3017
Bandwidth Limitations in Equalizers and Transistor Output Circuits—J. L. Stewart. (IRE TRANS. ON CIRCUIT THEORY, vol. CT-4, pp. 5–9; March, 1957. Abstract, PROC. IRE, vol. 45, pp. 1034–1035; July, 1957.)

621.373.421.13 3018
Temperature-Compensated Crystal Oscillators—(*Electronic Radio Engr.*, vol. 35, p. 314; August, 1958.) In the method described a passive network containing a thermistor is enclosed in the same envelope as the crystal.

621.373.431.1 3019
The Cathode-Coupled Multivibrator considered as a Coupled Pair of Two-Terminal Networks—P. Schiaffino. (*Alta Frequenza*, vol. 26, pp. 603–631; December, 1957.) The multivibrator is considered as an active two-terminal network with negative differential resistance, together with a passive two-terminal network. Formulas derived on this basis for determining the multivibrator operating characteristics give results in close agreement with experimental values.

621.373.44:621.317.755 3020
Sawtooth Generators with Commercial-Type Valves for Producing Deflection Voltages of High Amplitude and Extremely Short Duration—W. Kroebel and G. Olk. (*Z. angew. Phys.*, vol. 9, pp. 394–403; August, 1957.) The circuit of a special high-speed oscillograph with a time-base resolution of 4×10^{-9}s/mm is described which was used for examining the waveforms produced by various pulse generators investigated. Pulse amplitudes of 700 volts with rise time 3×10^{-8} seconds and 520 volts, 1.8×10^{-8} seconds have been obtained.

621.374.32:621.383.27 3021
Transistorized Photomultiplier has 0.1-μsec Resolution—G. S. Brunson. (*Nucleonics*, vol. 15, pp. 86–87; July, 1957.) Description of high-sensitivity photomultiplier circuit for use in a scintillation counter.

621.374.32:621.385.15 3022
Secondary-Emission Tubes in Coincidence Circuits—M. M. Vojinović. (*Bull. Inst. Nuclear Sci. "Boris Kidrich,"* vol. 7, pp. 103–108; March, 1957.) Switching waveforms of a trigger circuit based on a tube Type EFP60 are analyzed, and switching speed and operating conditions are discussed.

621.374.4 3023
Harmonic Amplifier for *X*-Band Local Oscillator—W. J. Dauksher. (*Electronics*, vol. 31, pp. 80–82; June 20, 1958.) The final frequency tripler in a harmonic-amplifier cascade uses an UHF triode with coaxial cathode input resonator and a waveguide output resonator giving about 3–5 mw output.

621.375.2.024 3024
A One-Valve D.C. Amplifier with High-Impedance Input—P. Belton. (*Electronic Eng.*, vol. 30, pp. 454–456; July, 1958.) A simple one-valve high-impedance probe circuit intended for direct connection to a dc amplifier is described. Drift is about 1 mv in the first half hour of use. A simple method of reducing the input time constant is also given.

621.375.2.029.6 3025
Low-Noise 30-Mc/s Amplifier—J. K. D. Verma. (*Rev. Sci. Instr.*, vol. 29, pp. 371–374; May, 1958.) Circuit details are given of a 30-mc cascode amplifier using disk-seal triodes, designed for the study of semiconductor noise at low temperatures. The theoretical noise figure of the amplifier is calculated and compared with the value obtained from radiometer measurements.

621.375.4 3026
Temperature Stability of Transistor Class-B Amplifiers—P. Tharma. (*Mullard Tech. Commun.*, vol. 3, pp. 265–277; March, 1958.) This is discussed generally and in relation to three types of circuit commonly used. Graphical design methods for achieving optimum stability are developed and comparative practical results are given.

621.375.9:538.569.4.029.6 3027
The Maser—W. H. Culver. (*Science*, vol. 126, pp. 810–814; October 25, 1957.) A review of development describing the principles of molecular-beam, "negative-temperature," "optically pumped" and solid-state masers.

621.375.9:538.569.4.029.6 3028
Maser Amplifier Characteristics for Transmission and Reflection Cavities—M. L. Stich. (*J. Appl. Phys.*, vol. 29, pp. 782–789; May, 1958.) The noise temperature, bandwidth and gain modulation for transmission and reflection-type masers are compared. The latter type is superior in most respects, although the same noise temperature may be obtained with the transmission type with some sacrifice in bandwidth and gain modulation. A figure of merit for both types is given.

621.375.9:538.569.4.029.64:621.372.632 3029
A Ferromagnetic-Resonance Frequency Converter—K. M. Poole and P. K. Tien. (PROC. IRE, vol. 46, pp. 1387–1396; July, 1958.) An experimental and theoretical study of a converter using a magnetized disk of single-crystal yttrium iron garnet. Inputs at 4.2 and 6.4 kmc are used to produce an output at 10.6 kmc in a cavity resonant at all three frequencies. The output power agrees with that expected theoretically, within experimental error. See also 3076 of 1957 (Suhl).

621.375.9:621.3.011.23 3030
A Parametric Amplifier using Lower-Frequency Pumping—K. K. N. Chang and S. Bloom. (PROC. IRE, vol. 46, pp. 1383–1386; July, 1958.) Experimental verification of the principle of parametric amplification using a pumping frequency lower than the signal frequency is described. Variable-inductance (ferrite-core) and variable-capacitance (semiconductor diode) elements have both been used, the former at 10 mc with pumping at 7 mc and the latter at 380 mc with pumping at 300 mc. Bandwidth and noise have been measured as functions of gain for the diode amplifier, and the results compared with theory. See also 1690 of 1958 and 2034 of 1958 (Bloom and Chang).

621.376.332 3031
Linear Frequency Discriminator for Subcarrier Frequencies—P. Kundu. (*Electronic Radio Engr.*, vol. 35, pp. 309–313; August, 1958.) The discriminator uses a heptode tube with out-of-phase signals on its two control grids. It is suitable for low-frequency FM signals having large deviations.

GENERAL PHYSICS

537/538 3032
The Electrodielectric Induction—P. de Belatini. (*Bull. Tech. Univ. Istanbul*, vol. 10, no. 1, pp. 81–111; 1957.) An analogy between magnetic and dielectric quantities discussed earlier (2581 of 1955) is developed with special reference to dynamic phenomena

537/538:519 3033
The Method of "Secondary Quantization" in Phase Space—Yu. L. Klimontovich. (*Zh. Eksp. Teor. Fiz.*, vol. 33, pp. 982–990; October, 1957.) A statistical analysis of systems of interacting particles in which use is made of the number of particles in various points of coordinate-momentum phase space, which at every point of phase space are random functions of time. This method can be used for considering particles and fields in electromagnetic interaction.

537/538].081 3034
Dimensions for a Unified Theory of Electromechanics—L. W. Allen. (*Elect. Eng.*, vol. 77, pp. 134–140; February, 1958.) A dimensional relation between voltage and mechanical force is derived, and a set of three dimensions, length, time and the square root of force, is proposed for a unified theory.

537.226 3035
Interaction of Charged Particles in a Dielectric—W. Kohn. (*Phys. Rev.*, vol. 110, pp. 857–864; May 15, 1958.) Analytical results may be

summarized by the statement that, if sufficiently distant, external charges in a dielectric interact with each other and with the charge of an extra electron or hole as if all charges were renormalized according to the expression $Q \rightarrow Q/\kappa^{1/2}$.

537.226:538.569.4 3036
Absorption in a Dielectric Slab—M. P. Bachynski. (*Canad. J. Phys.*, vol. 36, pp. 456–461; April, 1958.) Energy incident on a parallel slab of high-loss material with high dielectric constant is considered. At angles of incidence greater than 60°, the reflected energy is smaller the more lossy the material. The absorbed energy is a maximum at certain angles of incidence depending on the polarization and dielectric constant.

537.533:538.63 3037
Magnetic Forces and Relativistic Speeds in Stationary Electron Beams—B. Meltzer. (*J. Electronics Control*, vol. 4, pp. 350–354; April, 1958.) In non-relativistic electron beams magnetic forces may have to be considered; they are still more important in relativistic beams. Care must be taken in using the results of calculations in which these forces are neglected.

537.533:621.385.029.6 3038
Note on Positive-Ion Effects in Pulsed Electron Beams—J. T. Senise. (*J. Appl. Phys.*, vol. 29, pp. 839–841; May, 1958.) Experimental results are given for electron beams of 0.5–5 μsec duration under conditions normally encountered in high-power microwave tubes.

537.533.7 3039
Energy Spectrum of an Electron Beam after Passing through a Thin Metallic Film—C. Fert and F. Pradal. (*C.R. Acad. Sci., Paris*, vol. 246, pp. 252–255; January 13, 1958.) The energy loss is determined for films of Al, Cr, Bi, Au, Ag, and Cu.

537.533.73 3040
Very-High-Voltage Electron Diffraction—R. Papoular. (*Cah. Phys.*, vol. 11, pp. 202–216; May, 1957.) Description of a diffractograph operating at voltages up to 1.2 mev.

537.533.73:621.317.42 3041
The Use of Electron Diffraction for Magnetic Analysis—S. Yamaguchi. (*Naturwissenschaften*, vol. 45, pp. 7–8; January, 1958.) Brief note on a method of evaluating magnetic field strength from the eccentricity of superposed diffraction rings.

537.533.74 3042
Electron Scattering Phenomena—L. Marton. (*J. Sci. Indus. Res.*, vol. 16A, pp. 221–230; June, 1957.) New methods of investigation are reviewed.

537.56 3043
Diffusion and Elastic Collision Losses of the "Fast Electrons" in Plasmas—G. Medicus. (*J. Appl. Phys.*, vol. 29, pp. 903–908; June, 1958.) When the energy spectrum in Ne at 1 mm Hg pressure can be separated into a primary high-energy and a secondary low-energy Maxwellian group, then the mean free path l of the fast electrons can be evaluated by use of the diffusion laws; l is found to be independent of the plasma density. It is remarkable that there is little interaction between fast and slow groups even when the density of the slow one becomes comparable to or even higher than that of the fast group.

537.56 3044
Electron Energy Distributions in Uniform Electric Fields and the Townsend Ionization Coefficient—T. J. Lewis. (*Proc. Roy. Soc. A*, vol. 244, pp. 166–185; March 11, 1958.) The second-order differential equation which expresses the equilibrium conditions of an electron swarm in a uniform electric field in a gas, the electrons suffering both elastic and inelastic collisions with the gas molecules, is solved using the Jeffreys or WKB method of approximation. The theory is illustrated by a comparison of calculated and observed results for hydrogen.

537.56 3045
Experimental Examination of Holtsmark's Theory of Line Broadening—P. Bogen. (*Z. Physik.*, vol. 149, pp. 62–72; August 23, 1957.)

537.56 3046
Deviation from the Holtsmark Shape of the Balmer Lines in Plasma—G. Ecker. (*Z. Physik*, vol. 149, pp. 254–266; October 2, 1957.) See also 2695 of 1958.

537.56:538.56 3047
Scattering of Electromagnetic Waves in a Plasma—A. I. Akhiezer, I. G. Prokhoda, and A. G. Sitenko. (*Zh. Eksp. Teor. Fiz.*, vol. 33, pp. 750–757; September, 1957.) The intensity of combination scattering due to plasma density oscillations is determined with and without a constant uniform magnetic field.

537.56:538.56 3048
Suppression of Plasma Oscillations—D. W. Mahaffey and K. G. Emeleus. (*J. Electronics Control*, vol. 4, pp. 301–304; April 1958.) In a hot-cathode discharge tube containing gas at low pressure, oscillations of frequency 10^3–10^4 mc can be generated. The oscillations can be suppressed by mounting a plane anode and cathode sufficiently close together; the discharge can still be maintained.

537.56:538.6 3049
On the Propagation of Hydromagnetic Waves in Compressible Ionized Fluid—T. Taniuti. (*Prog. Theor. Phys.*, vol. 19, pp. 69–76; January, 1958.) Mathematical treatment based on a method of characteristics.

537.56:538.63 3050
The Behaviour of a Completely Ionized Plasma in a Strong Magnetic Field—S. I. Braginskiĭ. (*Zh. Eksp. Teor. Fiz.*, vol. 33, pp. 645–654; September, 1957.)

537.563:535.336.2 3051
Mass-Spectroscopy Investigations of Photoionization in Gases—E. Schönheit. (*Z. Physik*, vol. 149, pp. 153–179; October, 1957.) Experimental equipment is described and eighty-eight references are given.

538.221:538.569.4 3052
The Theory of Ferromagnetic Resonance at High Signal Powers—H. Suhl. (*Phys. Chem. Solids*, vol. 1, pp. 209–227; January, 1957.) It is shown that two anomalous effects in the microwave absorption of ferromagnets are connected with two kinds of instability of the uniform precessional motion of the total magnetization against certain spin-wave disturbances. The susceptibilities are calculated for the final state attained by the medium with high signal levels, and are shown to agree with experiment.

538.3:52 3053
Reflection and Refraction in Magnetohydrodynamics—C. Totaro. (*R. C. Acad. naz. Lincei*, vol. 24, pp. 310–316; March, 1958.) Fluids of finite conductivity are considered on the basis of the Euler-Minkowski system, for hydromagnetic waves propagated in a direction differing from that of the external magnetic field.

538.311:621.318.3 3054
Investigation of and Compensation for the Inhomogeneity of the Magnetic Field of an Electromagnet—H. Benoit and M. Sauzade. (*C.R. Acad. Sci., Paris*, vol. 246, pp. 579–582; January 27, 1958.)

538.311:621.318.3:538.569.4 3055
Stabilization and Control of an Electromagnet by Means of Magnetic Proton Resonance—H. Andresen. (*Z. angew. Phys.*, vol. 9, pp. 326–333; July, 1957.) Long-term magnetic field stability $\Delta H/H$ of the order of 10^{-6} is obtained by means of a proton-resonance system incorporating a field discriminator circuit and a variable-frequency transitron circuit.

538.566 3056
On the Reflection of Electromagnetic Waves on a Rough Surface—M. A. Biot. (*J. Appl. Phys.*, vol. 29, p. 998; June, 1958.) Note of correction to 1392 of 1958.

538.566 3057
Propagation of Plane Electromagnetic Waves in a Directional Conductor with Variable Direction of Conductivity—C. Banfi. (*R.C. Acad. naz. Lincei*, vol. 24, pp. 306–310; March, 1958.) Propagation through a series of directional screens is considered, each screen being rotated by the same angle with respect to the adjacent screen. See also 3705 of 1956 (Toraldo di Francia).

538.566 3058
The Theory of Electromagnetic Waves in a Crystal in which Excitons are Produced—S. I. Pekar. (*Zh. Eksp. Teor. Fiz.*, vol. 33, pp. 1022–1036; October, 1957.) It is shown that in a crystal several waves of the same frequency, polarization and propagation direction exist, but with different indexes of refraction. This phenomenon differs from double refraction of light and occurs even in isotropically polarizing (cubic) crystals.

538.566:535.42 3059
Diffraction Patterns at the Plane of a Slit in a Reflecting Screen—R. K. Hadlock. (*J. Appl. Phys.*, vol. 29, pp. 918–920; June, 1958.) Measurements were made of the diffraction pattern in slits ranging in width from 0.2 to 2.5 λ. Microwave radiation of 10.4 and 16 cm λ was used. Ratios of intensity in the slit to intensity of the unperturbed beam were determined for plane-polarized radiation incident on the conducting screen.

538.566:535.42 3060
Diffraction by a Perfectly Absorbing Thin Screen—C. C. Derwin. (*J. Appl. Phys.*, vol. 29, pp. 921–922; June, 1958.) Comparative measurements of the diffraction patterns in and near slits of perfectly absorbing and reflecting thin screens show that the reflected diffraction patterns of the slits are the same for distances greater than λ/2.

538.566:535.42 3061
The Edge Conditions and Field Representation Theorems in the Theory of Electromagnetic Diffraction—A. E. Heins and S. Silver. *Proc. Camb. Phil. Soc.*, vol. 54, pp. 131–133; January, 1958.) Addendum to 1959 of 1955.

538.566:535.43–15 3062
Wavelength Dependence of Scattering Coefficient for Infrared Radiation in Natural Haze—M. G. Gibbons. (*J. Opt. Soc. Amer.*, vol. 48, pp. 173–176; March, 1958.) A formula consistent with the Mie scattering coefficient is given for 0.61–11.48 μ. See 1705 of 1958 (Penndorf).

538.566.2 3063
Propagation in a Gyrational Medium—L. G. Chambers. (*Quart. J. Mech. Appl. Math.*, vol. 11, pp. 253–255; May, 1958.) Addendum to 1731 of 1957.

538.569.4:530.145 3064
Cooperative Phenomena in Quantum

Theory of Radiation—A. Gamba. (*Phys. Rev.*, vol. 110, pp. 601–603; May 1, 1958.) Cooperative effects in systems, having dimensions small relative to the wavelength are investigated in relation to the quantum-mechanical identity principle. The application of this effect to a gas maser is mentioned.

GEOPHYSICAL AND EXTRATERRESTRIAL PHENOMENA

523.164.3 3065

The Radio Source in the Direction of the Galactic Centre—F. G. Smith, P. A. O'Brien, and J. E. Baldwin. (*Mon. Not. R. Astr. Soc.*, vol. 116, no. 3, pp. 282–287; 1956.) Observations of radio flux densities at frequencies from 38–500 mc show that the radiation could originate from a nonthermal source lying behind ionized hydrogen.

523.164.3:523.3 3066

Radio Observations of a Lunar Occultation of the Crab Nebula—C. H. Costain, B. Elsmore, and G. R. Whitfield. (*Mon. Not. R. Astr. Soc.*, vol. 116, no. 4, pp. 380–385; 1956.) Comparison of brightness distributions at 3.7 and 7.9 m λ shows a difference in apparent size of the radio source. Details of the lunar atmosphere are also obtained (see 3067 below).

523.164.3:523.3 3067

Radio Observations of the Lunar Atmosphere—B. Elsmore. (*Phil. Mag.*, vol. 2, pp. 1040–1046; August, 1957.) The refraction occurring in the lunar atmosphere is estimated from observations at 3.7 m λ of the lunar occultation of the Crab Nebula on January 24, 1956. The electron density at the moon's surface is derived for an atmosphere in hydrostatic equilibrium and for a continuously escaping atmosphere.

523.164.32 3068

The Distribution of Brightness at Metre Wavelengths across the Sun's Disk—R. G. Conway and P. A. O'Brien. (*Mon. Not. R. Astr. Soc.*, vol. 116, no. 4, pp. 386–394; 1956.)

532.72:621.317.794 3069

Apparent Temperatures of some Terrestrial Materials and the Sun at 4.3-Millimetre Wavelengths—A. W. Straiton, C. W. Tolbert, and C. O. Britt. (*J. Appl. Phys.*, vol. 29, pp. 776–782; May, 1958.) Report of measurements made using a Dicke-type radiometer. The apparent temperature of the sun was between 10^4 °K and 1.2×10^4 °K. At vertical angles the sky temperature was 90°K under clear conditions, but cumulus-rimbus cloud raised this to a value nearly equal to that for ground-level air.

523.755:523.164.32 3070

Magnetohydrodynamic Shock Waves in the Solar Corona, with Applications to Bursts of Radio-Frequency Radiation—K. C. Westfold. (*Phil. Mag.*, vol. 2, pp. 1287–1302; November, 1957.) Shock fronts ahead of corpuscular streams may account for Type II and Type III bursts. Detailed calculations are given, based on a set of transport equations previously derived for an ionized gas (115 of 1954).

525.35:529.786:621.3.018.41(083.74) 3071

Variation in the Speed of Rotation of the Earth since June 1955—Essen, Parry, Markowitz, and Hall. (See 3195.)

550.371:551.594 3072

The General Expression of the Diurnal Variation of the Atmospheric Electric Field considering the Influence of the Eddy Diffusion near the Ground—M. Kawano. (*J. Geomag. Geoelect.*, vol. 9, no. 3, pp. 123–132; 1957.)

550.371:551.594:621.317.792 3073

Simultaneous Measurement of Air-Earth Current and the Atmospheric Electric Potential Gradient—M. Goto. (*J. Geomag. Geoelect.*, vol. 9, no. 3, pp. 133–139; 1957.)

550.38:538.3 3074

Oscillations of a System of Disk Dynamos—T. Rikitake. (*Proc. Camb. Phil. Soc.*, vol. 54, pp. 89–105; January, 1958.) "The behavior of two disk dynamos coupled to one another is examined in relation to the earth's magnetic field. It is found that reversals of electric current and magnetic field occur, unlike the case of a single disk dynamo." See also 1401 of 1956 (Bullard).

550.382.4 3075

The Earth's Magnetic Field above WSPG, New Mexico, from Rocket Measurements—J. P. Heppner, J. D. Stolarick and L. H. Meredith. (*J. Geophys. Res.*, vol. 63, pp. 277–288; June, 1958.) The absolute magnetic field was measured from ground level to 163 km with a proton precessional magnetometer. The typically quiet field differed significantly from that of a dipole, but no ionospheric discontinuity was found.

550.385 3076

Some Observations of Geomagnetic Micropulsations—H. J. Duffus and J. A. Shand. (*Canad. J. Phys.*, vol. 36, pp. 508–526; April, 1958.) These new observations of diurnal variation, direction and frequency spectrum are viewed in comparison with published data and it is suggested that they have a solar time dependence and may occur locally. At two stations 60 degrees in longitude apart, related signals are only occasionally observed; however the phase relationship of the few which are related, together with differences in direction characteristics reported by other observatories, are not in agreement with recent theories of the origin of micropulsations.

550.385 3077

The Propagation Velocity of World-Wide Sudden Commencements of Magnetic Storms—A. J. Dessler. (*J. Geophys. Res.*, vol. 63, pp. 405–408; June, 1958.) A model is presented in which a longitudinal hydromagnetic wave, generated by impact between a plasma cloud from the sun and the earth's field, travels east and west round the geomagnetic equator. The wave will be stable at 400 km altitude and travel at about 130 km/s.

550.385.523.72:523.165 3078

The Magnetic-Storm Effects and the Interplanetary Electromagnetic State—D. Venkatesan. (*Tellus*, vol. 9, pp. 209–219; May, 1957.) Alfvén's theory (see 2620 of 1955) that a beam of rarefied ionized gas is ejected from the sun can be applied to explain terrestrial cosmic-ray observations and magnetic-storm effects.

550.389.2:629.19 3079

Visual Thresholds for Detecting an Earth Satellite—I. S. Gulledge, M. J. Koomen, D. M. Packer, and R. Tousey. (*Science*, vol. 127, pp. 1242–1243; May 23, 1958.)

550.389.2:629.19 3080

Effect of Length of Observing Time on the Visual Threshold for Detecting a Faint Satellite—W. D. Garvey, I. S. Gulledge, and J. B. Henson. (*Science*, vol. 127, pp. 1243–1244; May 23, 1958.)

550.389.2:629.19 3081

Formula for Inferring Atmospheric Density from the Motion of Artificial Earth Satellites—T. E. Sterne. (*Science*, vol. 127, p. 1245; May 23, 1958.)

550.389.2:629.19 3082

Effect of the Earth's Equatorial Bulge on the Lifetime of Artificial Satellites and its Use in Determining Atmospheric Scale-Heights—G. V. Groves. (*Nature, London*, vol. 181, p. 1055; April 12, 1958.)

550.389.2:629.19 3083

Calculation of the Lifetime of a Satellite—D. G. Parkyn. (*Nature, London*, vol. 181, pp. 1156–1157; April 19, 1958.)

550.389.2:629.19 3084

Explorer (Satellite 1958α) over Africa—D. S. Evans. (*Nature, London*, vol. 181, pp. 1173–1174; April 26, 1958.) Records of visual observations made in South Africa.

550.389.2:629.19 3085

Determination of Radio-Propagation Elements due to an Artificial Earth Satellite—E. Woyk-Chvojková. (*Nature, London*, vol. 181, pp. 1195–1196; April 26, 1958.) A simple formula is given expressing path length for determining the virtual position of a radiating source.

550.389.2(54) 3086

The International Geophysical Year—Indian Programme—(*J. Sci. Indus. Res.*, vol. 16A, pp. 231–233; June, 1957.)

551.510.5:535.334.08 3087

High-Altitude Infrared Studies of the Atmosphere—D. Murcray, J. Brooks, F. Murcray and C. Shaw. (*J. Geophys. Res.*, vol. 63, pp. 289–299; June, 1958.) A balloon flight with a Littrow spectrometer gave spectra from ground level to 65,000 feet. Water vapor bands (1.4 and 1.9μ) had completely disappeared above 46,000 feet.

551.510.535 3088

Calculation of True Heights of Electron Density in the Ionosphere—N. Ganesan. (*Tijdschr. ned. Radiogenoot.*, vol. 22, pp. 277–291; September, 1957. In English.) By assuming that the electron density distribution can be approximated by taking linear sections of variable length, $h'(f)$ records may be manually converted to true-height/electron-density profiles. The method takes into account the earth's magnetic field and is similar to that used by Jackson (2381 of 1956). Results are compared with actual electron density profiles derived from rocket observations.

551.510.535 3089

The Analysis of Rocket Experiments in Terms of Electron-Density Distributions—W. Pfister and J. C. Ulwick. (*J. Geophys. Res.*, vol. 63, pp. 315–333; June, 1958.) The relative delay of a pulsed signal as a function of rocket position (USAF Aerobee No. 38) is used to deduce the electron-density distribution to heights of about 135 km. The data are analyzed for ascent and descent, at frequencies of 4.05 and 4.87 mc; peaks are shown at 106, 111, 117, and 128 km, and an intense irregularity on ascent at 98 km. Good agreement with a simultaneous $P'(f)$ record is obtained.

551.510.535:621.396.11 3090

Solar Activity and Radio Communication—R. Naismith. (*Nature, London*, vol. 181, pp. 954–956; April 5, 1958.) The monthly median value of the F_2 critical frequency for noon during December, 1957 was 15.2 mc, the highest December average value ever recorded at Slough. This gives a value close to 50 mc for the "demarcation" frequency used for planning radio communication in temperate latitudes.

551.594.2:621.396.969.36 3091

Correlation of the Initial Electric Field and the Radar Echo in Thunderstorms—S. E. Reynolds and M. Brook. (*J. Met.*, vol. 13, pp. 376–380; August, 1957.) Precipitation, as detected with 3-cm radar, is a necessary, but not

sufficient, condition for significant cloud electrification. The presence of detectable precipitation does not lead to thunderstorm electrification unless the precipitation echo shows rapid vertical development.

551.594.21 3092
The Development and Masking of Charges in Thunderstorms—J. Kuettner. (*J. Met.*, vol. 13, pp. 456–470; October, 1956.)

551.594.5:523.164 3093
Auroral Absorption of 18-Mc/s Cosmic Radio Waves on February 11th 1958—R. Fleischer. (*Nature, London*, vol. 181, p. 1156; April 19, 1958.) A relative absorption of approximately 11 db was recorded near Troy, N. Y., during a spectacular auroral display.

551.594.5:621.396.11:551.510.535 3094
The Role of *F*-Layer Tilts in Detection of Auroral Ionization—S. Stein. (*J. Geophys. Res.*, vol. 63, pp. 391–404; June, 1958.) Back-scatter echoes received at Stanford, Calif., from the auroral *E* region are shown to be propagated by way of a tilted *F* layer. The rays returned from the *E*-region scattering source proceed to the F layer without intermediate earth reflection. The *F* layer is so tilted that the rays are then returned to the receiver. A tilted mirror model of the *F* layer demonstrates the effect. This explanation is shown to be more probable than that in which the echoes are presumed to be returned from auroral ionization at great heights, although this latter explanation may occasionally be true.

551.594.6 3095
Natural Electrical Oscillations in the Earth-Air-Ionosphere Cavity Excited by Lightning Discharges—W. O. Schumann. (*Z. angew. Phys.*, vol. 9, pp. 373–378; August, 1957.) The theory underlying the experimentally observed resonance effects [2948 of 1954 (Schumann and König)] is discussed. See also 2195 of 1954 and back references.

LOCATION AND AIDS TO NAVIGATION

621.396.933:621.396.676 3096
TACAN Data Link—(*Elect. Commun.*, vol. 34, pp. 150–275; September, 1957.) A symposium comprising the following papers:

1) **Electronic Systems in Air-Traffic Control**—P. C. Sandretto. (pp. 153–159.)

2) **Background and Principles of Tacan Data Link**—B. Alexander and R. C. Renick. (pp. 160–178.)

3) **History of Tacan Data Link**—R. I. Colin. (pp. 179–185.)

4) **Tacan Data Link for Common-System Air-Traffic Control**—M. Block. (pp. 186–191.)

5) **Vortac Data Link**—R. C. Renick. (pp. 192–197.)

6) **Operation of AN/URN-6 Data-Link Surface Equipment**—J. F. Sullivan. (pp. 198–208.)

7) **Input and Output Facilities of Data-Link Surface Equipment**—G. W. Reich, Jr. and H. J. Mills. (pp. 209–218.)

8) **Standardization of Circuits for Data-Link Surface Equipment**—H. J. Mills and F. L. Van Steen. (pp. 219–227.)

9) **Airborne Tacan Data-Link Equipment AN/ARN-26**—E. R. Altonji. (pp. 228–242.)

10) **Techniques Developed for Airborne Tacan Data Link**—E. R. Altonji, E. A. Kunkel, H. G. Whitehead, and R. Mead. (pp. 243–263.)

11) **Data-Link Airborne Instrumentation**—M. A. Argentieri and F. E. Lind. (pp. 264–270.)

12) **Evaluator and Trainer for Tacan Data Link**—W. B. Sudduth and J. F. Sullivan. (pp. 271–275.)

See also 3386 of 1956.

621.396.933.1:621.396.962.23 3097
Doppler Navigation—(*J. Inst. Nav.*, vol. 11, pp. 117–145; April, 1958. Discussion, pp. 146–149.)

1) **Airborne Doppler Equipment**—G. E. Beck. (pp. 117–124.) An account of the basic principles of Doppler navigation, including antenna patterns, presentation of data and various sources of error.

2) **The Navigational Applications of Doppler Equipments**—C. N. Moorhen. (pp. 125–130.) A description of operational procedures and the accuracy achieved in military aircraft.

3) **The Future Development of Doppler Navigation**—P. A. Houghton. (pp. 130–137.) Various possible improvements in equipment are described. These mainly concern the use of automatic computers to simplify the presentation of data. Experimental models of units are discussed.

4) **Doppler and Civil Aviation**—D. O. Fraser. (pp. 138–143.) A discussion of accuracy requirements, and integration with other navigational aids.

5) **The Sea Surface and Doppler**—C. S. Durst. (pp. 143–145.) Data on the frequency of occurrence of calm conditions in various sea areas, and of the dependence of the sea roughness on wind speed.

621.396.933.23 3098
The Power Level Controls in the Transmitters of the Instrument Landing System (ILS)—K. May. (*Nachrtech. Z.*, vol. 10, pp. 612–617; December, 1957.) Bridge-type power control circuits are described which are used for ensuring the correct balance of the power radiated by the two transmitters of the system. A detailed analysis of the operation of the controls indicates that undesirable phase shifts can occur in the approach-course transmitter; these can be cancelled by compensation.

621.396.963 3099
Radar Plotting Errors—H. Topley. (*J. Inst. Nav.*, vol. 11, pp. 167–171; April, 1958.) A discussion of methods of plotting and errors in the derived course and speed of an observed vessel.

621.396.963.3:551.576/.578 3100
Interpretation of the Height-versus-Time Presentation of Radar Echoes—V. G. Miles. (*J. Met.*, vol. 13, pp. 362–368; August, 1956.) Discussion of meteorological factors affecting the echo trace on a 1.25-cm radar used for detection of precipitation and clouds. See 2749 of 1956 (Plank, *et al.*).

621.396.969.33 3101
The Accuracy of Radar Plotting in Estimating Course and Speed—S. Holmström. (*J. Inst. Nav.*, vol. 11, pp. 157–166; April, 1958.) A statistical assessment of errors and their influence on the accuracy of the measurement from one ship of the movements of another.

MATERIALS AND SUBSIDIARY TECHNIQUES

535.215 3102
Analysis of Photoconductivity Applied to Cadmium-Sulphide-Type Photoconductors—R. H. Bube. (*Phys. Chem. Solids*, vol. 1, pp. 234–248; January, 1957.) A model of a photoconductor having two different types of recombination center is used to describe phenomena such as supralinearity, temperature dependence, infrared quenching and variations in speed of response. When applied to experimental data a ratio 8×10^5 is given for the capture cross section of the sensitizing centers for holes, to that for electrons, and a value 0.64 ev for the energy difference between the level corresponding to this type of center and the top of the valence band.

35.215:546.482.21 3103
Observation of the Photovoltaic Effect in a Film of Cadmium Sulphide—F. Cabannes. (*C.R. Acad. Sci., Paris*, vol. 246, pp. 257–260; January 13, 1958.) Report of measurements made on a CdS film betewen Cu (or Ag) and In electrodes.

535.37:546.472.21 3104
The Luminescence of Self-Coactivated ZnS:Cu—M. H. Aven and R. M. Potter. (*J. Electrochem. Soc.*, vol. 105, pp. 134–140; March, 1958.) Phosphors prepared by firing ZnS with Cu in purified H_2S show a simple orange emission band, with no other bands in evidence even at 90°K. Possible models for the orange center are discussed.

537.37+535.215]:546.482.21 3105
Fluorescence and Photoconduction of Silver-Activated Cadmium Sulphide—W. van Gool. (*Philips Res. Rep.*, vol. 13, pp. 157–166; April, 1958.) With Ga or Cl as coactivator, the fluorescence at low temperature shows two bands with maxima at 6200 Å and 7300 Å. The proportion of each emission can be varied by altering the concentrations of activator and coactivator. Previous conclusions regarding the impurity level responsible for the 6200 Å Ag emission in CdS cannot be applied to the normal blue Ag emission in ZnS-Ag and this has led to an improvement in the properties of a red color-television phosphor.

535.37:546.482.21 3106
The Nature of the Edge Emission in CdS—G. Diemer, G. J. van Gurp and H. J. G. Meyer. (*Physica*, vol. 23, pp. 987–988; October, 1957.) Experiments on relatively pure crystals give support to the views of Lambe, *et al.* (797 of 1957) and Smith (2467 of 1957).

535.376:537.311.33:546.26–1 3107
Electroluminescence of Diamonds—A. Fischer. (*Z. Physik.*, vol. 149, pp. 107–110; August 23, 1957.) Preliminary report and interpretation of test results. See also 2468 of 1957 (Wolfe and Woods).

537.226/.228.2:546.431.824–31 3108
Electrostriction in Barium Titanate above the Curie Point—G. Schmidt. (*Naturwissenschaften*, vol. 45, pp. 8–9; January, 1958.) Preliminary report of tests on single-crystal specimens. See also 2754 of 1958.

537.226/.227 3109
Structural and Electrical Properties of Silver Niobate and Silver Tantalate—M. H. Francombe and B. Lewis. (*Acta cryst.* vol. 11, pp. 175–178; March 10, 1958.) At room temperature both $AgNbO_3$ and $AgTaO_3$ possess orthorhombic multiple-cell perovskite-type structures and are isomorphous with $NaNbO_3$. In $AgNbO_3$, the structure changes sharply to near-tetragonal at 325°C, while in $AgTaO_3$ a similar change occurs, more smoothly, at about 375°C. The permittivity of $AgNbO_3$ shows a peak at the orthorhombic-tetragonal transitoin. Weak hysteresis and pyroelectric effects indicate a low value of spontaneous polarization. With $AgTaO_3$ the nature of its structure transitions and the permittivity data obtained for the solid solution $AgNb_{0.75}Ta_{0.25}O_3$ suggest the absence of ferroelectricity. See 1783 of 1957.

537.226/.227:546.431.824–31 3110
Examination of the Surface and Domain Structure in Ceramic Barium Titanate—V. J. Tennery and F. R. Anderson. (*J. Appl. Phys.*, vol. 29, pp. 755–758; May, 1958.) Polished, etched and free surfaces are examined by the direct carbon replica technique. Domain configurations are studied at a higher magnification than that obtained in optical methods.

537.227 3111
Growing of Ferroelectric $PbTiO_3$ Crystals—J. Kobayashi. (*J. Appl. Phys.*, vol. 29, pp. 866–867; May, 1958.)

537.227:537.533.8 3112
Interaction of Low-Energy Electrons with Ferroelectric Materials—R. C. Miller and R. D. Heidenreich. (*J. Appl. Phys.*, vol. 29, pp. 957–963; June, 1958.) An investigation of the effects of low-energy electron bombardment on $BaTiO_3$ and triglycine sulphate.

537.227:546.431.824–31 3113
Free Energy, Internal Fields and Ionic Polarizibilities in $BaTiO_3$—S. Triebwasser. (*Phys. Chem. Solids*, vol. 3, nos. 1-2, pp. 53–62; 1957.) Calculations are made allowing for the atomic displacements found from neutron diffraction data.

537.227:547.476.3 3114
Theory of Rochelle Salt—A. F. Devonshire. (*Phil. Mag.*, vol. 2, pp. 1027–1039; August, 1957.) An attempt is made to explain the results of Bancroft's high-pressure measurements of dielectric constant (*Phys. Rev.*, vol. 53, pp. 587–590; April 1, 1938.) by a modification of Mason's theory (*Phys. Rev.*, vol. 72, pp. 854–865; November 1, 1947.)

537.311.31:539.234:538.63 3115
Magneto-electric Properties of Thin Films of Nickel Magnetized to Saturation—T. Rappeneau. (*C.R. Acad. Sci., Paris*, vol. 246, pp. 571–574; January 27, 1958.) Investigation of the variation of resistance as a function of magnetic field strength and direction for field strengths of 4000–8000 oersteds. For earlier experiments see 1107 of 1957.

537.311.32:546.212–16 3116
Conduction of Electricity through Ice and Snow—R. Siksna and A. Metnieks. (*Ark. Fys.*, vol. 11, pt. 6, pp. 495–528, 567–585; 1957.) The article, which is in four parts, describes a series of measurements of the conductivity of ice and snow designed to serve as a basis for investigations of more general problems in that field.

537.311.33 3117
On the Statistical Mechanics of Impurity Conduction in Semiconductors—P. J. Price. (*IBM J. Res. Dev.*, vol. 2, pp. 123–129; April, 1958.) The case of low donor density with partial acceptor compensation is analyzed on the basis of the Mott model. An expression for the thermoelectric power is obtained. The special case of mixed donors in disparate proportions is also considered.

537.311.33 3118
Scattering of Carriers by Ionized Impurities in Semiconductors—F. J. Blatt. (*Phys. Chem. Solids*, vol. 1, pp. 262–269; January, 1957.) The scattering cross section due to ionized impurities has been calculated assuming the surfaces of constant energy in **k** space to be spheres. The results have been compared with the Born approximation. This gives incorrect results at low temperatures. Calculation of Hall and drift mobilities have been made. This shows that the $T^{3/2}$ law for scattering is not followed accurately.

537.311.33 3119
On Impact Ionization in Semiconductors—H. L. Armstrong. (*J. Electronics Control*, vol. 4, pp. 355–357; April, 1958.) An alternative treatment to that of Rose (624 of 1958) giving somewhat different results.

537.311.33 3120
New Semiconducting Ternary Compounds—J. H. Wernick and K. E. Benson. (*Phys. Chem. Solids*, vol. 3, nos. 1–2, pp. 157–159; 1957.) Preliminary resistivity/temperature data on impure polycrystalline specimens of synthesized sulpharsenates of copper and silver and analogous compounds indicate that the intrinsic energy gaps lie in the range 0.2–1.0 ev.

537.311.33 3121
Infrared Measurements of the Temperature Dependence of the Electron Activation Energy in Trivalent Tellurides—G. Harbeke and G. Lautz (*Optik, Stuttgart*, vol. 14, pp. 547–554; December, 1957.) Report on measurements of infrared transmission through crystals of Ga_2Te_3 and In_2Te_3 in the temperature range 20–650 degrees Kelvin. The temperature dependence of the forbidden band is found to be -7.7×10^{-4} ev/degree for Ga_2Te_3 and -5.59×10^{-4} ev/degree for In_2Te_3. Results obtained by optical and by electrical methods are compared.

537.311.33:537.29 3122
The Behaviour of Nonmetallic Crystals in Strong Electric Fields—L. V. Keldysh. (*Zh. Eksp. Teor. Fiz.*, vol. 33, pp. 994–1003; October, 1957.) Expressions are derived for the number of electron-hole pairs generated in a semiconductor by a uniform electric field. In the absence of electron-phonon collisions and collisions between electrons themselves, the magnitude of the effective potential barrier is determined not by the width of the forbidden band, but by the lower edge of optical absorption.

537.311.33:537.32 3123
Theory of Thermoelectric Effects in Semiconductors—O. Madelung. (*Z. Naturf.*, vol. 13a, pp. 22–25; January, 1958.) Some inconsistencies in the relevant literature are critically discussed. See, *e.g.*, 3771 of 1956 (ter Haar and Neaves).

537.311.33:[546.28+546.289 3124
On Spiral Etch Pits in Germanium and Silicon—S. G. Ellis. (*Phil. Mag.*, vol. 2, p. 1285; October, 1957.) The author's earlier theories (see 466 of 1956) are reconsidered in the light of subsequent work by others.

537.311.33:546.28 3125
Solubility of Lithium in Silicon—E. M. Pell. (*Phys. Chem. Solids*, vol. 3, nos. 1–2, pp. 77–81; 1957.) Measurements from 529 to 1382 degrees Centigrade show a maximum impurity atom function of 1.3×10^{-3} at about 1200 degrees Centigrade. A Li-Si eutectic point at 58 ± 5 atom per cent of Li was found at 590 ± 10 degrees Centigrade.

537.311.33:546.28 3126
Electrolysis of Copper in Solid Silicon—C. J. Gallagher. (*Phys. Chem. Solids*, vol. 3, nos. 1–2, pp. 82–86; 1957.) Transport measurements indicate that a large fraction, possibly 50 per cent, of the Cu in solution is positively charged, interstitial, and diffuses rapidly at 1100 degrees Centigrade. Cu also diffuses in Ge with a positive charge at 700 degrees Centigrade.

537.311.33:546.28 3127
Lifetime and Nickel Precipitation in Silicon—W. J. Shattes and H. A. R. Wegener. (*J. Appl. Phys.*, vol. 29, p. 866; May, 1958.)

537.311.33:546.28 3128
Two Chemical Stains for Marking *p-n* Junctions in Silicon—P. J. Whoriskey. (*J. Appl. Phys.*, vol. 29, pp. 867–868; May, 1958.)

537.311.33:546.28 3129
Junction Delineation in Silicon by Gold Chemiplating—S. J. Silverman and D. R. Benn. (*J. Electrochem. Soc.*, vol. 105, pp. 170–172; March, 1958.) The method described is based on the preferential plating of gold on *n*-type material in the presence of light.

537.311.33:546.28 3130
Energy of Ionization by Electrons in Silicon Crystals—V. M. Patskevich, V. S. Vavilov, and L. S. Smirnov. (*Zh. Eksp. Teor. Fiz.*, vol. 33, pp. 804–805; September, 1957.) The mean ionization energy ϵ for primary electron energies up to 30 kev was determined from the excess carrier current through a *p-n* junction located about 20μ beneath the irradiated surface. The value of ϵ obtained was 4.2 ± 0.6ev. See 2502 of 1957 (Vavilov, *et al.*).

537.311.33:546.28 3131
Breakdown in Silicon—B. Senitzky and J. L. Moll. (*Phys. Rev.*, vol. 110, pp. 612–620; May 1, 1958.) The characteristics of Si junctions in the breakdown region are investigated for uniform diffused junctions and an alloyed junction having only one small breakdown region (microplasma). The V/I characteristic of a single-microplasma junction is compared with a previous theoretical prediction of Rose (2183 of 1957). The behavior of a uniform junction is explained in terms of the results obtained for the single microplasma junction.

537.311.33:546.28 3132
Birefringence Caused by Edge Dislocations in Silicon—R. Bullough. (*Phys. Rev.*, vol. 110, pp. 620–623; May 1, 1958.) The intensity distribution of a beam of infrared light transmitted by a Si crystal containing a dislocation is calculated. The difference between an edge dislocation and an inclusion is noted. See also 2438 of 1956 (Bond and Andrus).

537.311.33:546.28:621.314.63 3133
Crack-Free Alloyed Junctions in Silicon using Pure Aluminium—T. C. Taylor. (*J. Appl. Phys.*, vol. 29, pp. 865–866; May, 1958.) The technique involves removing the molten-phase Al-Si alloy from the fusion cavity after sufficient cooling but before total solidification. A gold wire or ribbon plunged into the molten alloy forms solid reaction products which are readily lifted or blown out.

537.311.33:546.28:621.314.7 3134
Improved Diffusion Boundary Junctions in Silicon due to Scratch-Free Polishing—F. Keywell. (*J. Appl. Phys.*, vol. 29, pp. 871–872; May, 1958.) A surface preparation is discussed which permits fabrication of diffused silicon *p-n-i-p* transistors of 10^{-2}-cm^2 emitter area with 1.5 μ base layer.

537.311.33:546.281.26 3135
Electrical Properties of Silicon Carbide—R. Goffaux. (*Rev. gén. Élect.*, vol. 66, pp. 569–576; November, 1957.) It is suggested that the boundaries of SiC grains are covered with a semiconducting layer, probably SiO_2, and that the interior acts as a conductor. Experimental results are found to be consistent with this theory. See also 2786 of 1958.

537.311.33:546.281.26:621.314.63 3136
Electrical Contacts to Silicon Carbide—R. N. Hall. (*J. Appl. Phys.*, vol. 29, pp. 914–917; June, 1958.) Rectifying junctions may be made by heating Si-Al or Si-B alloys in contact with *n*-type SiC. Visible radiation is emitted uniformly over the rectifying junctions when current is passed in the forward direction, with a quantum efficiency of the order of 10^{-6}.

537.311.33:546.289 3137
Solubility of Lithium in Germanium—E. M. Pell. (*Phys. Chem. Solids*, vol. 3, nos. 1–2, pp. 74–76; 1957.) Measurements from 593 to 899 degrees Centigrade show a maximum impurity atom fraction of 1.7×10^{-4} at about 800 degrees Centigrade. A Li-Ge eutectic point at 49 ± 5 atom per cent of Li was found at 525 ± 10 degrees Centigrade.

537.311.33:546.289 3138
Variation of Contact Potential with Crystal for Germanium—F. G. Allen and A. B. Fowler. (*Phys. Chem. Solids*, vol. 3, nos. 1/2, pp. 107–114; 1957.) The areal average work functions

of the different crystal faces for Ge are measured and found to give a reproducible pattern of values correlated with crystallographic directions. Results are insensitive to bulk doping.

537.311.33:546.289 3139
Characteristics of Junctions in Germanium—N. J. Harrick. (*J. Appl. Phys.*, vol. 29, pp. 764–770; May, 1958.) Junction theory is tested by measuring the current/carrier-density characteristics by an infrared technique. The results agree with existing theories in the case of highly doped Ge regions and low injection levels, but an extended theory is necessary for other conditions.

537.311.33:546.289 3140
Thermal Restoration of Oxygenated Germanium Surfaces—A. J. Rosenberg, P. H. Robinson, and H. C. Gatos. (*J. Appl. Phys.*, vol. 29, pp. 771–775; May, 1958.) The oxygen-adsorbing capacity of cleaved Ge surfaces was restored by heating in vacuo above 575 degrees Centigrade; this effect was absent below 425 degrees Centigrade.

537.311.33:546.289 3141
Majority-Carrier Lifetime in Copper-Doped Germanium at 20°K—D. A. H. Brown. (*J. Electronics Control*, vol. 4, pp. 341–349; April, 1958.) The time constant for recombination of a hole with a negatively charged Cu impurity center in Ge at 20 degrees Kelvin has been derived experimentally by two independent methods. The values obtained agree in order of magnitude, but are several orders of magnitude less then the theoretical ones; this confirms previous results. The recombination time constants did not decrease as the impurity concentration rose; this too is not in accordance with theory. See 3641 of 1955 (Sclar and Burstein).

537.311.33:546.289 3142
Isotopic and Other Types of Thermal Resistance in Germanium—T. H. Geballe and G. W. Hull. (*Phys. Rev.*, vol. 110, pp. 773–775; May 1, 1958.) The occurrence of isotopes in a crystal disturbs the periodicity of the lattice and produces thermal resistance. This effect has been shown to occur in crystals of Ge.

537.311.33:546.289 3143
Rate Processes and Low-Temperature Electrical Conduction in *n*-Type Germanium—S. H. Koenig. (*Phys. Rev.*, vol. 110, pp. 986–988; May 15, 1958.) Discussion of experimental results and their theoretical implications.

537.311.33:546.289 3144
Recombination of Thermal Electrons in *n*-Type Germanium below 10°K—S. H. Koenig. (*Phys. Rev.*, vol. 110, pp. 988–990; May 15, 1958.) The thermal recombination coefficient is derived from measurements of the current decay time constant using very rapidly changing voltage steps.

537.311.33:546.289 3145
Chill Casting of Thin Plates of Single-Crystal Germanium—W. Bösenberg. (*Z. angew. Phys.*, vol. 9, pp. 347–349; July, 1957.) Germanium is cast in water-cooled graphite or quartz moulds; the thickness of the plate is of the order of 0.5 mm.

537.311.33:546.289 3146
Solid-State Dissolution of Germanium by Indium in Semiconductor Devices—J. Roschen and C. G. Thornton. (*J. Appl. Phys.*, vol. 29, 928; June, 1958.) Small cavities have been observed to develop in Ge semiconductor devices with In metal contacts. These occur below the melting point of In and are due to a solid-state dissolution of Ge by In with a subsequent more rapid diffusion of Ge in In. This is limited by a 0.01–0.011 per cent solubility of the one in the other.

537.311.33:546.289 3147
Germanium Arsenide as Diffusion Surface Compound—W. Waring, D. T. Pitman, and S. R. Steele. (*J. Appl. Phys.*, vol. 29, pp. 1002–1003; June, 1958.) On doping Ge with arsenic, GeAs and $GeAs_2$ are formed on the surface of the Ge. X-ray spectrometer data on lattice spacings and relative intensities are given.

537.311.33:546.289:537.533.8 3148
Investigation of Characteristic Energy Losses of Electrons and the Secondary Electron Emission from GeOi—N. B. Gornyi and A. Yu. Reitsakas. (*Zh. Eksp. Teor. Fiz.*, vol. 33, pp. 571–575; September, 1957.) The energy loss of reflected electrons has been determined from measurements on GeO_2-coated plates of *n*- and *p*-type Ge. Characteristics for both types are similar. The secondary-electron yield from GeO_2 is almost twice that from Ge.

537.311.33:546.289:539.32.08 3149
Elastic Moduli of Single-Crystal Germanium as a Function of Hydrostatic Pressure—H. J. McSkimin. (*J. Acoust. Soc. Amer.*, vol. 30, pp. 314–318; April, 1958.) Report of measurements made at 62.5 and 125 mc using a quartz crystal transducer and a phase comparison technique.

537.311.33:546.289:539.433 3150
Temperature Dependence of Internal Friction in Germanium—P. D. Southgate. (*Phys. Rev.*, vol. 110, pp. 855–857; May 15, 1958.) The friction has been measured as a function of temperature at 100 kc. All crystals showed a peak at 420 degrees Centigrade. A specimen strained in tension showed a rapid rise with temperature above 500 degrees Centigrade. A small peak at 770 degrees Centigrade is attributed to the presence of oxygen. See also 3540 and 3541 of 1957 (Kessler).

537.311.33:546.47–31 3151
Concentration of Hydrogen and Semiconductivity in ZnO under Hydrogen-Ion Bombardment—J. J. Lander. (*Phys. Chem. Solids*, vol. 3, nos. 1/2, pp. 87–94; 1957.)

537.311.33:546.561–31 3152
Discussion of some Optical and Electrical Properties of Cu_2O—J. Bloem. (*Philips Res. Rep.*, vol. 13, pp. 167–193; April, 1958.) From known data a band scheme is constructed for this semiconductor, and equilibrium conditions for solid constituents at high temperatures with an applied partial pressure of oxygen are calculated. An evaluation of conductivity and the concentrations of defect centers is in good agreement with experiment. The change in properties observed after quenching is attributed to association between defects and the chemisorption of oxygen.

537.311.33:546.621.86 3153
Single Crystals and *p*-*n*-Layer Crystals of Aluminium Antimonide—H. A. Schell. (*Z. Metallkde*, vol. 49, pp. 140–144; March, 1958.) Techniques of crystal pulling and zone refining are described. AlSb of *n* type can be produced by adding Te or Se. The barrier voltage of junction-type rectifiers may be raised above 30 volts, with a reverse current of less than 300 μa and a forward current greater than 500 ma/cm² at 2 volts.

537.311.33:546.682.19:538.63 3154
Magnetoresistance Oscillations in Single-Crystal and Polycrystalline Indium Arsenide—R. J. Sladek. (*Phys. Rev.*, vol. 110, pp. 817–826; May 15, 1958.) Resistivity measurements were made on both crystal forms of *n*-type InAs with magnetic fields up to 29,000 g and temperatures between 1.25 and 20.2 degrees Kelvin. In both crystals oscillations in resistivity occur as the field strength is varied. Very good agreement is obtained between the calculated and observed periods. The phase and temperature dependence of the oscillations is discussed.

537.311.33:546.682.19:538.63 3155
Oscillatory Galvanomagnetic Effects in *n*-Type Indium Arsenide—H. P. R. Frederikse and W. R. Hosler. (*Phys. Rev.*, vol. 110, pp. 880–883; May 15, 1958.) The period of the de Haas-van Alphen oscillations was found to be in good agreement with theoretical predictions.

537.311.33:546.682.86 3156
Band Structure of Indium Antimonide—E. O. Kane. (*Phys. Chem. Solids*, vol. 1, pp. 249–261; January, 1957.) The band structure of InSb has been calculated using perturbation theory. The small band gap requires an accurate treatment of conduction and valence-band interactions. A nonparabolic conduction band is found, while the valence band is similar to Ge. An absolute calculation of optical absorption is made for *n*-type InSb, which agrees with experimental results. See 2468 of 1958 (Ehrenreich).

537.311.33:546.682.86 3157
On the Mechanical Properties of Indium Antimonide—J. W. Allen. (*Phil. Mag.*, vol. 2, pp. 1475–1481; December, 1957. Plate.)

537.311.33:546.682.86 3158
Distribution Coefficients for Solute Elements in Single-Crystal Indium Antimonide—J. B. Mullin. (*J. Electronics Control*, vol. 4, pp. 358–359; April, 1958.)

537.311.33:546.682.86:538.63 3159
Hall Effect and Magnetoresistance in Indium Antimonide—G. Fischer and D. K. C. MacDonald. (*Phil. Mag.*, vol. 2, pp. 1393–1395; November, 1957.) Note of measurements made at field strengths up to 40 k oersteds at −12, −4 and 0 degrees Centigrade. See also 1468 and 1469 of 1958 (Frederikse and Hosler).

537.311.33:548.0 3160
Crystal Structure of Ternary Compounds of Type $A^{II}B^{IV}C^{V}$—H. Pfister. (*Acta Cryst.*, vol. 11, pp. 221–224; March 10, 1958. In German.)

537.583 3161
Thermionic and Related Properties of Calcium Oxide—B. J. Hopkins and F. A. Vick. (*Brit. J. Appl. Phys.*, vol. 9, pp. 257–264; July, 1958.) Changes in thermionic emission and conductivity of cathodes of CaO on Ni during activation and positioning are described. The mean nominal thermionic work function is 1.69 ev for the fully activated cathode. A linear relation was found between the logarithms of emission and conductivity during activation, and gives a mean value of 0.7 ev for the surface work function.

537.583:621.385.032.213.13 3162
Diffusion of Tungsten in Nickel and Reaction at Interface with SrO—H. W. Allison and G. E. Moore. (*J. Appl. Phys.*, vol. 29, pp. 842–848; May, 1958.)

538.22 3163
Antiferromagnetism of $CuF_2.2H_2O$ and MnF_3—R. M. Bozorth and J. W. Nielsen. (*Phys. Rev.*, vol. 110, pp. 879–880; May 15, 1958.) Measurements of the molar susceptibility were made at temperatures between 1.3 and 260 degrees Kelvin.

538.22:538.569.4.029.65 3164
Paramagnetic Resonance Absorption in Two Copper Salts at Wavelengths of 5.4 mm and 6.6 mm—K. Ôno and M. Ohtsuka. (*J. Phys. Soc. Japan*, vol. 13, pp. 206–209; February, 1958.) The shape of the absorption lines varies considerably with the orientation of the crystal in the magnetic field. The variation is

interpreted in terms of the exchange interaction between copper ions.

538.221 3165
The Remanent Magnetization of Single-Domain Ferromagnetic Particles—E. P. Wohlfarth and D. G. Tonge. (*Phil. Mag.*, vol. 2, pp. 1333–1344; November, 1957.) The remanent magnetization is calculated for particles with a number of equivalent easy directions of magnetization, and also for particles with mixed uniaxial anisotropies. Application is made to a variety of materials, such as Co and αFe_2O_3.

538.221 3166
Determination of the Magnetic Anisotropy Constant K_2 of Cubic Ferromagnetic Substances—H. Sato and B. S. Chandrasekhar. (*Phys. Chem. Solids*, vol. 1, pp. 228–233; January, 1957.)

538.221 3167
The Anhysteretic Magnetization of Permanent-Magnet Alloys—E. P. Wohlfarth. (*Phil. Mag.*, vol. 2, pp. 719–725; June, 1957.)

538.221 3168
Investigation of the Magnetic Properties of a Series of Nickel-Copper Alloys—A. J. P. Meyer and C. Wolff. (*C.R. Acad. Sci., Paris*, vol. 246, pp. 576–579; January 27, 1958.) Results of measurements of Curie point and magnetization are in agreement with those of Ahern and Sucksmith (1156 of 1957).

538.221 3169
The Magnetization of Cobalt-Manganese and Cobalt-Chromium Alloys—J. Crangle. (*Phil. Mag.*, vol. 2, pp. 659–668; May, 1957.)

538.221 3170
Observations on the Magnetic Transition in Haematite at −15°C—G. Haigh. (*Phil. Mag.*, vol. 2, pp. 877–890; July, 1957.) The effects of cooling and reheating on a magnetized specimen of αFe_2O_3 are described, and observations are discussed with reference to the two-component magnetic structure suggested by Néel. (*Rev. Mod. Phys.*, vol. 25, pp. 58–63; January, 1953.)

538.221 3171
The Electric and Magnetic Spectra of γ-Fe_2O_3 Oxides—J. C. Bluet, I. Epelboin, and D. Quivy. (*C.R. Acad. Sci., paris*, vol. 246, pp. 246–249; January 13, 1958.) Report of measurements made at frequencies from 10 kc to 23 kmc to determine the complex permittivity and permeability of powder specimens.

538.221:[538.63+538.66 3172
Relations between the Coefficients of Transverse Galvanomagnetic and Thermomagnetic Effects in Ferromagnets—G. Busch, F. Hulliger, and R. Jaggi. (*Helv. phys. Acta*, vol. 31, pp. 3–16; February 15, 1958. In German.) Calculation and comparison of parameters based on the investigations of various authors. Forty-one references.

538.221:538.632 3173
On the Hall Effect in Ferromagnetics—N. V. Bazhanova. (*Zh. Eksp. Teor. Fiz.*, vol. 33, pp. 567–570; September, 1957.) An investigation of Fe-Ni alloys of the invar group near the Curie temperature.

538.221:538.632 3174
The Spontaneous Hall Effect in Ferromagnetics: Part 2—J. Smit. (*Physica*, vol. 24, pp. 39–51; January, 1958.) "It is shown that the spontaneous part of the Hall effect arising from the spontaneous magnetization is caused by skew scattering of the magnetized conduction electrons (in this case the 3*d*-electrons) due to their transverse polarization induced by spin-orbit interaction, which acts as an impact parameter in the collision process." Part 1: 1465 of 1956.

538.221:621.318.134 3175
Microwave Ferrites—B. Josephson and P. E. Ljung. (*Ericsson Tech.*, vol. 14, no. 1, pp. 39–70; 1958.) A general description of the structure of ferrites, their electrical properties, and the physical phenomena underlying their use at microwave frequencies. Details are given of the optimum composition of ferrites for Faraday rotation at wavelengths of 3, 6 and 10 cm.

538.221:621.318.134 3176
Low-Frequency Rotational Hysteresis Losses in Ferrites—H. Seiwatz. (*J. Appl. Phys.*, vol. 29, pp. 994–995; June, 1958.) The frequency range covered in 5–55 cps using magnetic field strengths up to 11,000 oersteds. For sufficiently strong magnetic fields the losses are found to be independent of field strength, and in some ferrites there is essentially no frequency dependence.

538.221:621.318.134 3177
Effect of Magnetic Viscosity on the Frequency Characteristics of Ferrites—R. V. Telesin and A. G. Shishkov. (*Zh. Eksp. Teor. Fiz.*, vol. 33, pp. 839–844; October, 1957.) Investigation of a series of Ni-Zn ferrites under conditions of free (aperiodic) and forced (sinusoidal) variations of magnetization. Viscosity characteristics obtained from measurements on the same sample by both methods are compared and an estimate is made of the viscous friction constant.

538.221:621.318.134 3178
Low-Temperature Heat Capacity and Thermodynamic Properties of Zinc Ferrite—E. F. Westrum, Jr. and D. M. Grimes. (*Phys. Chem. Solids*, vol. 3, nos. 1/2, pp. 44–49; 1957.)

538.221:621.318.134 3179
Time-Dependent Constricted Hysteresis Loops in a Single Crystal of Manganese Ferrous Ferrite—U. Enz. (*Physica*, vol. 24, pp. 68–70; January, 1958.) The initial permeability of a crystal of composition $Mn_{0.84}Fe_{2.14}O_4$ is approximately 2000 at room temperature and shows a very strong disaccommodation or time-dependent decrease of permeability after demagnetization.

538.221:621.318.134 3180
The Crystal Structure and Ferrimagnetism of Yttrium-Iron Garnet, $Y_2Ge_2(FeO_4)_3$—S. Geller and M. A. Gilleo. (*Phys. Chem. Solids*, vol. 3, nos. 1/2, pp. 30–36; 1957.) A refinement of the crystal structure of Y-Fe garnet, obtained by application of the least-squares method to single-crystal X-ray data. Interionic distances and angles which are important to the interaction between magnetic ions are calculated.

538.221:621.318.134 3181
Interpretation of Magnetic Properties of Yttrium Garnet in which the Ions Al^{3+} Ga^{3+} and Gr^{3+} have been Substituted for Fe^{+3} Ions—G. Villers and J. Loriers. (*C.R. Acad. Sci., Paris*, vol. 245, pp. 2033–2036; December 4, 1957.)

538.221:621.318.134 3182
Lattice Changes in Spinel-Type Iron Chromites—M. H. Francombe. (*Phys. Chem. Solids*, vol. 3, nos. 1/2, pp. 37–43; 1957.)

538.221:621.318.134:537.311.33 3183
Electrical Conductivity of Ferromagnetic Semiconductors (Ferrites)—A. A. Yudin. (*Zh. Eksp. Teor. Fiz.*, vol. 33, pp. 873–876; October, 1957.) Treatment of conduction in a ferrite, considered as a lattice of classical magnetic dipoles submerged in a dielectric continuum, shows that the conductivity/temperature characteristic must have a break at the Curie point, which is in agreement with experiment and with decreasing activation energy in the ferromagnetic region.

538.221:621.318.134:538.569.4 3184
Magnetic Spectra of Manganese Ferrites—S. E. Harrison, C. J. Kriessman, and S. R. Pollack. (*Phys. Rev.*, vol. 110, pp. 844–849; May 15, 1958.) The complex initial permeability of polycrystalline ferrites of the type $Mn_{1+x}Fe_{2-x}O_3$ has been measured between 20 and 2000 mc. Two resonances occur below 200 mc and are associated with domain wall motion. A resonance which occurs between 300 and 600 mc, depending on the composition, allows the calculation of an effective polycrystalline anisotropy constant.

538.221:621.318.134:621.372.85 3185
Mixed Garnets for Nonreciprocal Devices at Low Microwave Frequencies—B. Ancker-Johnson and J. J. Rowley. (PROC. IRE, vol. 46, pp. 1421–1422; July, 1958.) Report on the properties of 2:1 and 5:1 mixtures of Y-Gd iron garnet and their application in S-band and L-band isolators.

538.221:621.318.134:621.372.85 3186
The Application of Ferrites in the Construction of Nonreciprocal Microwave Devices—Dörre (See 2968.)

538.222 3187
The Thermal and Magnetic Properties of Ytterbium Ethyl Sulphate between 20°K and 1°K—A. H. Cooke, F. R. McKim, H. Mayer, and W. P. Wolf. (*Phil. Mag.*, vol. 2, pp. 929–935; July, 1957.) Report of measurements of susceptibility, magnetic specific heat and spin-lattice relaxation time.

539.2:537.311.31 3188
The Band Structure of the Transition Metals—N. F. Mott and K. W. H. Stevens. (*Phil. Mag.*, vol. 2, pp. 1364–1386; November, 1957.)

539.2:537.311.33 3189
Electronic Properties of Transition-Metal Oxides: Part 1.—Distortions from Cubic Symmetry—J. D. Dunitz and L. E. Orgel. (*Phys. Chem. Solids*, vol. 3, nos. 1/2, pp. 20–29; 1957.) It is shown that much of the data on distortions from cubic symmetry in transition-metal oxides, and particularly in spinels, can be understood in terms of crystal (ligand) field theory. Many such distortions are simply related to the electronic configuration of the metal ion and may be considered to arise as a consequence of a Jahn-Teller type of distortion. Forty-five references.

621.791.9:621.3.049.7:537.311.33 3190
Electrical Contact with Thermo-compression Bonds—H. Christensen. (*Bell Lab. Rec.*, vol. 36, pp. 127–130; April, 1958.) By application of heat and pressure, a bond can be formed either with or without the formation of a liquid phase; the appropriate techniques can produce either an ohmic or a rectifying bond between a wire and a semiconductor.

666:621.3.032.53 3191
Vacuum-Tight Metal-Ceramic Seals—K. Müller. (*Elektrotech. Z., Ed. B*, vol. 10, pp. 69–71; March 21, 1958.) Ag-Ti alloys are particularly suitable for use as solders.

537.311.33 3192
Progress in Semiconductors, Vol. 2 [Book Review]—A. F. Gibson, R. E. Burgess, and P. Aigrain (eds). Publishers: Heywood, London, Eng., 280 pp.; 1957. (*Nature, London*, vol. 181, p. 1168; April 26, 1958.) An annual publication containing eight contributions on semiconduc-

tor alloys and compounds, effects of irradiation, carrier lifetime, impurities, and effects of electric fields. See also 215 of 1957.

MATHEMATICS

513.81:621.3 3193

A Survey of the Use of Non-Euclidean Geometry in Electrical Engineering—E. F. Bolinder. (*J. Franklin Inst.*, vol. 265, pp. 169–186; March, 1958.) Forty-eight references.

516.2:517.522.5 3194

Analytical Representation of Angular Distribution Data—S. C. Snowdon, L. Eisenbad, and J. F. Marshall. (*J. Appl. Phys.*, vol. 29, pp. 950–953; June, 1958.) A quick approximate method of curve fitting, using a Legendre polynomial series, is described. It is useful for curves where the experimental points do not justify great accuracy. Eleven equally spaced points are used.

MEASUREMENTS AND TEST GEAR

621.3.018.41(083.74):529.786:525.35 3195

Variation in the Speed of Rotation of the Earth since June 1955—L. Essen, J. V. L. Parry, W. Markowitz, and R. G. Hall. (*Nature, London*, vol. 181, p. 1054; April 12, 1958.) The rate of rotation of the earth is measured in U.S.A. and compared with the frequency of the Cs standard in England by means of GBR and WWV time signals. Since September, 1955, this rate shows a constant deceleration of 5 parts in 10^9 per year.

621.317.31 (083.74) 3196

Measurement of Current with a Pellat-Type Electrodynamometer—R. L. Driscoll. (*J. Res. Natl. Bur. Stand.*, vol. 60, RP 2845, pp. 287–296; April, 1958.) Detailed description of an absolute determination of the ampere using a Pellat-type electrodynamometer with a fused-silica balance beam and single-layer helical coils. See 2182 of 1958.

621.317.31(083.74) 3197

Measurement of Current with the National Bureau of Standards Current Balance—R. L. Driscoll and R. D. Cutkosky. (*J. Res. Natl. Bur. Stand.*, vol. 60, RP 2846, pp. 297–305; April, 1958.) The weighted mean of recent measurements made with the National Bureau of Standards current balance and with a Pellat-type balance (see 3196 above) is 1 NBS ampere $= 1.000010 \pm 0.000005$ absolute amperes.

621.317.34:621.372.413 3198

Measurement of Shunt Impedance of a Cavity—K. B. Mallory. (*J. Appl. Phys.*, vol. 29, pp. 790–793; May, 1958.) A simple graphical method is given for the analysis of transmission measurements.

621.317.361:621.384.7 3199

Frequency Measurements in Microwave Spectroscopy—G. Erlandsson and H. Selén. (*Ark. Fys.*, vol. 11, pt. 4, pp. 391–393; 1957.) A variable-frequency oscillator in combination with a crystal calibrator may be used to measure line frequencies to within ± 2 mc.

621.317.373 3200

An Accurate Phase Meter for Four-Terminal Networks—B. Chatterjee. (*Indian J. Phys.*, vol. 31, pp. 541–552; November, 1957.) Details of AF and RF measurements made with the phase meter described in 3479 of 1956. A small phase change can be measured within about 0.1 degree.

621.317.382.029.6:538.632:537.311.33 3201

The Hall Effect and its Application to Microwave Power Measurement—H. M. Barlow. (PROC. IRE, vol. 46, pp. 1411–1413; July, 1958.) The basic theory of the Hall effect is given and its relation to radiation pressure is shown. A microwave wattmeter depending on the Hall effect for its operation is described. See 2552 of 1957.

621.317.382.029.6:621.396.61–181.4 3202

Power Measurements on Miniature Transmitters—K. H. Fischer and C. Fink. (*Elektrotech. Z., Ed. A*, vol. 79, pp. 150–153; March 1, 1958.) Methods are reviewed which are suitable for measuring the output of low-power high-frequency transmitters used for radiosondes or medical applications. Results obtained for a 400-mc radiosonde transmitter are given as example.

621.317.4 3203

Methods of Deriving the Heterodyne Frequency of a Receiver from the Measurement Frequency of a Transmitter—R. Kersten. (*Frequenz*, vol. 11, pp. 370–379; December, 1957, and vol. 12, pp. 15–25; January, 1958.) Methods are discussed for ensuring a constant relation between generator frequency and receiver heterodyne frequency for the measurement of transmission characteristics of filters with sharp cut-off or networks with high cross-talk attenuation. In one method signal generator and receiver are combined in a single unit which incorporates an auxiliary oscillator controlled by the generator frequency; in others the heterodyne frequency is equal to the unmodulated generator frequency.

621.317.616:621.317.755 3204

Video-Frequency Response Testing—R. G. Middleton. (*Radio TV News*, vol. 59, pp. 59–61; February, 1958.) Describes the technique of testing the response of video-frequency amplifiers, using a sweep-frequency generator and a CRO.

621.317.616:621.395.625.3 3205

The Determination of Frequency Characteristics of Recording-Tape Magnetization—O. Schmidbauer. (*Elektronische Rundschau*, vol. 11, pp. 373–375; December, 1957.) See also 2505 of 1958.

621.317.7:621.373.42 3206

A Wide-Range Sine-Wave Generator—L. H. Dülberger and H. T. Sterling. (*Electronic Eng.*, vol. 30, pp. 424–428; July, 1958.) Full details of a Wien-bridge oscillator circuit are given for the frequency range 0.9 cps–510 kc, with 0.15 per cent distortion for an output of 2 watts into 600 Ω. Frequency stability is within 0.5 per cent for a wide range of temperature and line-voltage variations.

621.317.715.5.087.5 3207

Ten-Channel Miniature Galvanometer Recorder—I. A. W. Halliday and A. L. N. Stephens. (*Instrum. Practice*, vol. 12, pp. 242–246; March, 1958.) Description of a compact instrument for recording on 35-mm film the movement of ten "pencil" galvanometer elements.

621.317.729.1 3208

The Electrolytic Tank Analogue—K. F. Sander. (*Beama J.*, vol. 65, pp. 17–23; February, 1958.) Outline of the problems involved in designing and setting up electrolyte-tank equipment. Various types of errors are enumerated and conditions for obtaining accurate and reproducible measurements are formulated. A system for measuring field gradients to 0.1 per cent is briefly described.

621.317.73.012.11:518.5 3209

A Mechanical Version of the Smith Chart—J. E. Knowles. (*J. Sci. Instrum.*, vol. 35, pp. 233–237; July, 1958.) For computing the transmission characteristics of optical or electrical filters, the chart has been replaced by a system of mechanical linkages and a computing element.

621.317.73.012.11:621.317.755 3210

Two Automatic Impedance Plotters—R. S. Cole and W. N. Honeyman. (*Electronic Eng.*, vol. 30, pp. 442–446; July, 1958.) Description and comparison of two methods of automatic impedance plotting at microwave frequencies based on a) a four-probe detector and frequency-swept klystron, and b) a three-slot waveguide coupler together with a rotating-crystal head. The single-crystal method is inherently more accurate, although both methods facilitate production testing.

621.317.733:681.142 3211

A High-Sensitivity D.C. Null Indicator with Automatic Reduction of Sensitivity for Large Inputs—R. Thorn. (*J. Sci. Instr.*, vol. 35, pp. 265–266; July, 1958.) The instrument can be used in bridge measurements which cover large voltage and source resistance ranges, *e.g.*, in the solution of problems by resistance-network analog methods.

612.317.742 3212

Voltage Standing-Wave Ratio Measurement—E. W. Collings. (*Electronic Radio Engr.*, vol. 35, pp. 287–290; August, 1958.) A substitution method is described in which a short-circuited attenuator replaces the equipment under test. Various errors inherent in the normal method are eliminated.

621.317.755 3213

Wide-Band Oscilloscope—G. H. Leonard. (*Wireless World*, vol. 64, pp. 395–398; August, 1958.) A commercial model can be modified to have a bandwidth of 30 mc without using a distributed amplifier. A circuit is described which uses tubes having high figures of merit, with low anode loads and as cathode followers to reduce the effects of input capacitance; ac coupling must be used.

621.317.794:621.396.822 3214

L.F. Random-Signal Generator—J. L. Douce and J. M. Shackleton. (*Electronic Radio Engr.*) vol. 35, pp. 295–297; August, 1958.) A simple noise generator having a power spectrum uniform from zero up to about 15 cps.

621.317.799:621.314.7 3215

The Measurement of Transistor Voltage /Current Characteristics using Pulse Techniques—B. J. Cooper. (*Electronic Eng.*, vol. 30, pp. 440–441; July, 1958.) The effects of junction heating and thermal runaway effects are reduced, which enables the ambient temperature characteristics to be read from meters or displayed on an external cathode ray tube.

621.317.799:621.314.7 3216

Transistor Test Set—J. N. Prewett. (*Wireless World*, vol. 64, pp. 369–372; August, 1958.) An inexpensive test set is described which will measure the collector leakage current and current amplification factor of transistors, with up to 200 mw collector dissipation, with an accuracy sufficient to determine their suitability for a particular circuit.

621.317.799:621.385.1 3217

New Portable Electron-Tube Tester—A. A. Heberlein. (*Bell Lab. Rec.*, vol. 36, pp. 179–181; May, 1958.) The equipment is designed for testing most tubes including cold-cathode and subminiature types.

OTHER APPLICATIONS OF RADIO AND ELECTRONICS

531.787:621.383.4 3218

A Sensitive Defocusing Photoelectric Pressure Transducer—J. R. Greer. (*Electronic Eng.*, vol. 30, pp. 436–439; July, 1958.) The instrument depends on the pressure difference existing across an extremely thin aluminized terylene foil diaphragm to focus or defocus the

beams of light falling on Ge-type photocells. The frequency response extends to 500 cps and the maximum sensitivity obtained is approximately 8 volts for a pressure change of 1 cm of water.

535.33-15:621.383.4 3219
A Design for a Multichannel Infrared Spectrometer using Transistor Electronics—D. G. Avery and R. C. Bowes. (*J. Sci. Instr.*, vol. 35, pp. 212–216; June, 1958.) A demonstration instrument in which InSb photoconductive cells from the detectors, each acting as its own "exit slit." The fast response of the detectors makes possible the use of low-noise transistor amplifiers.

535.822.5:621.397.6:535.623 3220
Ultraviolet Television Colour-Translating Microscope—V. K. Zworykin and F. L. Hatke. (*Science*, vol. 126, pp. 805–810; October 25, 1957.) A microscope projects the image on to the photosensitive targets of a television camera, the video signal from which is used for the reproduction of the image on the screen of a trichromatic receiver. Illumination is so arranged that radiation of the three selected ultraviolet wavelengths falls on the specimen in successive pulses.

621.365.52 3221
Frequency and Phase Relations in a Transmitter for R.F. Heating—K. H. Kerber. (*Nachrtech. Z.*, vol. 7, pp. 512–514; November, 1957.) Design criteria for maximum efficiency are derived.

621.374.33:77 3222
Inexpensive Photographic Timer—J. H. Jowett. (*Wireless World*, vol. 64, pp. 385–387; August, 1958.) Description of a simple system, based on a "bootstrap" circuit, for compensating variations in enlarger-lamp supply voltage.

621.384.622.2 3223
New Method of Control of Ultra-High-Frequency Circuits for a Linear Electron Accelerator—M. Pillon. (*C.R. Acad. Sci., Paris*, vol. 246, pp. 582–586; January 27, 1958.) By controlling the output of a carcinotron by a suitable circuit it is possible to obtain a power constant within ±2 db at any frequency from 2 to 4 kmc.

621.385.833 3224
Chromatic Aberration and Resolving Power of Electron Microscopes—W. E. Meyer. (*Optik, Stuttgart*, vol. 15, pp. 43–46; January, 1958.) The resolution limit for very large chromatic aberration is found to exceed the one for vanishing aberration by a factor of only 1.4.

621.385.833 3225
Correction of the Aperture Aberrations of a System of Two Four-Pole Magnetic Lenses—A. Septier. (*C.R. Acad. Sci., Paris*, vol. 245, pp. 2036–2039; December 4, 1957.)

621.387.424 3226
Measurements of the Discharge Propagation Time in Geiger-Müller Counter Tubes and their Use in Portraying Fields of Radioactive Radiation—P. Kienle. (*Z. Naturf.*, vol. 13a, pp. 37–47; January, 1958.)

621.398:621.396.934 3227
Guided Weapon Techniques—P. Cave. (*Wireless World*, vol. 64, pp. 354–359; August, 1958.) Systems are classified in two main groups: a) continuous-data systems in which data relating to the position of the target are analyzed while the missile is in flight; this system is necessary for interception of moving targets; b) systems of preset trajectory suitable for long-range missiles, in which the missile is programmed to locate its position in flight by terrestrial, inertial, celestial or radio measurements and to adjust its own course to the preset one. The principles of different guidance techniques are described.

PROPAGATION OF WAVES

621.396.11+621.372.2 3228
Surface Waves—H. M. Barlow. (Proc. IRE, vol. 46, pp. 1413–1417; July, 1958.) Qualitative discussion of the important characteristics of surface waves, including the launching problem and the effect of surface curvature.

621.396.11 3229
The Calculation of the Coefficients of Reflection from the Ground—C. Rudilosso. (*Note Recensioni Notiz.*, vol. 6, pp. 848–860; November/December, 1957.) Summary of formulas for various types of surface, and description of the use of a Smith chart instead of Burrows' field strength curves for obtaining the coefficients.

621.396.11 3230
Transient Radio-Frequency Ground Waves over the Surface of a Finitely Conducting Plane Earth—J. R. Johler. (*J. Res. Natl. Bur. Stand.*, vol. 60, RP 2844, pp. 281–285; April, 1958.) Displacement currents in the conducting earth are neglected. The results of an analysis using Laplace transformations indicate that current sources with sinusoidal form in the time domain can be used to simulate atmospherics and to reconstruct propagated signals of pulsed radio-navigation systems.

621.396.11:551.510.535 3231
Solar Activity and Radio Communication—Naismith. (See 3090.)

621.396.11:551.510.535 3232
Limiting Polarization Curves for Radio Wave Propagation in the Ionosphere—R. N. Singh and Y. S. N. Murty. (*Curr. Sci.*, vol. 27, pp. 161–162; May, 1958.) Application of Bailey's method of conformal representation to conditions at Banaras, India.

621.396.11:551.510.535 3233
Ray-Tracing Technique in a Horizontally Stratified Ionosphere using Vector Representations—R. J. Marcou, W. Pfister, and J. C. Ulwick. (*J. Geophys. Res.*, vol. 63, pp. 301–313; June, 1958.) "Vector expressions are derived for tracing oblique ray paths, taking into account the full effect of the earth's magnetic field. The method is an extended analytical treatment of Poeverlein's two dimensional case based upon crystal optics (718 of 1950). A method for high-speed computers is described for ray tracing in a horizontally stratified ionosphere, for determining by an iteration process the index of refraction and wave normal direction, and for determining electron-density distributions from rocket data."

621.396.11.029.55:551.510.535 3234
The Use of Sweep-Frequency Back-Scatter Data for Determining Oblique-Incidence Ionospheric Characteristics—R. Silberstein. (*J. Geophys. Res.*, vol. 63, pp. 335–351; June, 1958.) Data from further back-scatter experiments (see 3019 of 1954) at Boulder, Colo., with antennas beamed on Sterling, Va. (2370 km), are compared with a) frequency-sweep point-to-point recorder data for the Boulder-Sterling path, and b) mid-point vertical-incidence data. The difference between MUFs deduced by skilled personnel from frequency-sweep back-scatter data and actual MUFs determined by means of a) is shown to be small, provided proper antennas are used. Many records are illustrated.

621.396.11.029.6 3235
The Mechanism of Long-Distance Propagation of Ultra Short Waves—R. Schünemann. (*Hochfrequenztech. u. Elektroakust.*, vol. 66, pp. 52–61; September, 1957.) Theoretical investigations indicate that in addition to scattering processes partial reflections by inversion layers may contribute significantly to the propagation of ultra short waves over long distances. Results of field-strength measurements of signals propagated over distances of 195, 360 and 450 km at 88.2, 88.5 and 92.1 mc, respectively, are of the same order of magnitude as those derived theoretically assuming partial reflections.

621.396.11.029.6:[621.396.41+621.397.26] (489) 3236
Television and Telephone Radio Links in Denmark—B. Nielsen, P. Christensen, P. Sterndorff, and P. Gudmandsen. (*Teleteknik, Copenhagen*, English Ed., vol. 1, no. 2, pp. 131–174, 194; 1957.) English version of 1908 of 1957.

621.396.11.029.62 3237
Long-Distance Radio Propagation above 30 Mc/s—J. A. Saxton. (*Nature, London*, vol. 181, pp. 1184–1187; April 26, 1958.) Report of an I.E.E. symposium held in London, January 28, 1958. More than 20 papers were read.

621.396.11.029.63 3238
Investigation of Long-Distance Overwater Tropospheric Propagation at 400 Mc/s—H. E. Dinger, W. E. Garner, D. H. Hamilton, Jr. and A. E. Teachman. (Proc. IRE, vol. 46, pp. 1401–1410; July, 1958.) Experimental results of signal strength measurements for oversea paths up to 630 nautical miles are presented. For signals believed to be unaffected by super-refractive conditions, a cyclic variation of attenuation rate with distance was found, but this did not differ substantially from a linear rate of 0.16–0.18 db per nautical mile.

RECEPTION

621.372.632.029.64:538.632 3239
A New Microwave Mixer—H. M. Barlow, J. Brown, and K. V. G. Krishna. (*Nature, London*, vol. 181, p. 1008; April 5, 1958.) Equipment based on the Hall effect for measuring power at microwave frequencies using a semiconductor in a resonant cavity [see 1217 of 1958 (Barlow and Kataoka)], may be modified for use as a mixer. The conversion loss is about 60 db for InAs with a local-oscillator power of 100 watts at 8 cm λ.

621.376.23 3240
The Calculation of the Performance of A.M. Detectors with Characteristics represented by Angled Straight Lines—H. Schneider and G. Petrich. (*Nachrtech. Z.*, vol. 7, pp. 549–551; December, 1957.) An investigation of harmonic distortion in AM detectors shows that freedom from distortion and increased sensitivity are obtained if the operating point moves in accordance with the fluctuations of the modulation. See also 2893 of 1957.

621.396.82:621.397.62](083.74) 3241
Supplement to "I.R.E. Standards on Receivers: Methods of Measurement of Interference Output of Television Receivers in the Range of 300–1,000 kc/s, 1954" (Standard 54 I.R.E. 17.S1)—Proc. IRE, vol. 46, pp. 1418–1420; July, 1958.) Standard 48 IRE 27.S1.

621.396.828 3242
The Problem of Eliminating Radio Interference Originating from High-Frequency Heating Installations—H. Stier and E. Rosemann. (*Nachrtech. Z.*, vol. 7, pp. 523–525; November, 1957.) Comment on 1250 of 1958 and author's reply.

STATIONS AND COMMUNICATION SYSTEMS

621.391:519.21 3243
On Measures of Information—A. J. Stam.

(*Proc. kon. ned. Akad. Wetensch., B.*, vol. 60, no. 3, pp. 201–211; 1957. In English.) Generalization of Schutzenberger's definition (1769 of 1951).

534.78:621.391 3244
Construction and Investigation of a Transmission System for Synthetic Speech—Krocker. (See 2952.)

621.395.4+621.397.5]:621.314.212 3245
Multichannel Systems along Coaxial Cables—Bauer. (See 2958.)

621.396.3:621.396.43:523.5 3246
On the Transmission Error Function for Meteor-Burst Communication—C. F. Montgomery. (PROC. IRE, vol. 46, pp. 1423–1424; July, 1958.) Addendum and note of correction to 911 of 1958 (Montgomery and Sugar).

621.396.41 3247
A Mathematical Analysis of the Kahn Compatible Single-Sideband System—J. P. Costas. (PROC. IRE, vol. 46, pp. 1396–1401; July, 1958.) Analysis of a system proposed for generating a single side-band signal for reception by a conventional AM receiver. Computations are made of the signal spectra for various input signal conditions. The theoretical results are used to predict certain system operating characteristics. A comment by Kahn (*ibid.*, pp. 1429–1430) refers to improved systems in operation.

621.396.41+621.397.26](489):621.396.11.029.6 3248
Television and Telephone Radio Links in Denmark—B. Nielsen, P. Christensen, P. Sterndorff, and P. Gudmandsen. (*Teleteknik, Copenhagen*, English Ed., vol. 1, no. 2, pp. 131–174, 194; 1957.) English version of 1908 of 1957

621.396.43:621.396.65 3249
Some Problems in Radio Link Equipment for a Small Number of Channels—I. Wigdorovits. (*Elektrotech. Z., Ed. A*, vol. 79, pp. 86–89; February 1, 1958.) Constructional requirements and the relation between quality of transmission and bandwidth are considered for equipment with two to six telephony channels.

621.396.65+621.397.7 3250
The NARCOM Plan for Transatlantic Television and other Wide-Band Telecommunication Services—W. S. Halstead. (*J. Soc. Mot. Pict. Telev. Engrs.*, vol. 67, pp. 134–138; March, 1958.) A proposed North Atlantic Relay Communication System (NARCOM) is discussed in detail. The system is based on propagation by tropospheric scatter between a chain of UHF relay stations located at suitable land sites across the North Atlantic. The longest link would be some 290 miles.

621.396.74.029.62:621.376.3 3251
The Offset Operation of U.S.W. F.M. Broadcast Transmitters—P. Klarm. (*Frequenz*, vol. 11, pp. 351–360; November, 1957.) The conditions are determined for ensuring minimum mutual interference in operating transmitters with offset carrier frequencies. An arrangement using carrier spacings between 50 and 100 kc combined with suitable program allocation and regional distribution of the transmitters is discussed. Improvements in receiver performance are necessary to exploit to the fullest extent the possible advantages of the system. See also 275 of 1958 (Belger, *et al.*).

621.396.931 3252
Signal Transmission between Underground Cables and Vehicles—H. Fricke and H. Rummert. (*Frequenz*, vol. 11, pp. 380–385; December, 1957, and vol. 12, pp. 9–15; January, 1958.) Investigation of the transmission of signals for traffic supervision and control between a fixed station and trains of road vehicles by means of cables buried along the track or under the road surface. Field strength is calculated and measured for systems operating at 100 mc and 30 kc. A comparison of the systems shows that the frequency range 10–100 kc is the most advantageous for this purpose.

SUBSIDIARY APPARATUS

621.311.6:537.324 3253
Thermoelements and Thermoelectric D.C. Generators—K. Peschke. (*Arch. Elektrotech.*, vol. 43, pp. 328–354; November 29, 1957.) Detailed theoretical investigation of thermodynamic efficiency taking account of the various thermoelectric effects, and changes in resistivity and thermal conductivity. Higher efficiencies should be obtainable [see also 3655 of 1957 (Käch)] than those indicated by other authors. Problems of construction and mechanical strength are also considered.

621.311.62:621.314.7 3254
A Mains-Operated D.C. Stabilized Transistor Power Supply for Laboratory Use—W. L. Stephenson. (*Mullard Tech. Commun.*, vol. 3, pp. 282–284; March, 1958.) Modification of a unit described earlier [281 of 1958 (Brown and Stephenson)] with operating range 0–30 volts, 0–100 ma.

621.311.69 3255
Investigation of the Utilization of Solar Energy for the Production of Electrical Energy—G. Réméniéras. (*Rév. gén. Élect.*, vol. 66, pp. 593–626; December, 1957.) A description of a Si *p-n*-junction photoelectric generator made in 1954 is included in a comprehensive summary of the meteorological, engineering and economic aspects of the subject.

621.316.722.1:621.314.63 3256
Zener-Diode Voltage Stabilizer—S. Welldon. (*Wireless World*, vol. 64, pp. 381–383; August, 1958.) The breakdown voltage of a Zener diode is suitable for use in stabilizing the voltage supplied to motors operated from small batteries.

621.316.92:621.314.7 3257
Transistor Power Supply has Overload Protection—H. D. Ervin. (*Electronics*, vol. 31, pp. 74–75; June 20, 1958.) The current limiting circuit described has an instantaneous response.

621.396.679.1 3258
Low-Resistance Earth Electrodes—their Achievement and Accurate Measurement—A. N. Richter. (*Trans. S. Afr. Inst. Elect. Engrs.*, vol. 48, pp. 333–347; November, 1957.) The electrical characteristics of various soils and the effects of moisture content, temperature, and additives as well as electrode shape and spacing are discussed.

TELEVISION AND PHOTOTELEGRAPHY

621.397.5:061.6 3259
The Television Allocations Study Organization—G. R. Town. (*Elect. Eng.*, vol. 77, pp. 126–128; February, 1958.) The structure and general objectives of the organization are discussed.

621.397.5:535.623 3260
Colour Distortion in the N.T.S.C. Colour Television System due to Chrominance Signal Limiting and Vestigial-Side-Band Operation—G. Emmrich. (*Nachrtech. Z.*, vol. 7, pp. 538–542; December, 1957.) Distortion effects are calculated and compared.

621.397.5:778.5 3261
Anamorphic Television Circuit Requirements—M. Cawein. (*J. Soc. Mot. Pict. Telev. Engrs.*, vol. 67, pp. 257–259; April, 1958.) Theoretical circuit requirements for the production of a wide-screen television image are discussed. The frequency bandwidth required is determined from a consideration of the relation between aspect ratio and pictorial information, defined in terms of contrast and resolution. The anamorphic compression and subsequent decompression of the image are described.

621.397.5:621.317](083.74) 3262
I.R.E. Standards on Television: Measurement of Luminance Signals Levels, 1958—(PROC. IRE, vol. 46, p. 1417; July, 1958.) Correction to 1567 of 1958.

621.397.6:535.623:621.396.664 3263
A Stabilized Monitor for Colour-Television Picture Quality Control—E. E. Gloystein and N. P. Kellaway. (*J. Soc. Mot. Pict. Telev. Engrs.*, vol. 67, pp. 157–162; March, 1958.)

621.397.6:621.317.7 3264
Testing of Television Measuring Demodulators and Television Relay Receivers—H. Thielcke. (*Rundfunktech Mitt.*, vol. 1, pp. 221–231; December, 1957.) The design of test equipment for monitoring and receiving units is discussed. Methods of measuring receiver characteristics are described and details are given of rack-mounted test equipment.

621.397.61:621.316.729 3265
Some Aspects of the Performance of Television Mains-Hold Circuits—R. D. A. Maurice. (*Electronic Eng.*, vol. 30, pp. 447–454; July, 1958.) Phase instability of the electricity supply to a television studio causes transient changes in the repetition frequency of the field synchronizing pulses. This causes the received image to move vertically, particularly during the transmission of film. The effects of film-traction mechanical filters on these transients is examined in detail and recommendations are made on specifying "mains-hold" performance to avoid excessive vertical movement of the picture.

621.397.61:535.316/.319].001.4 3266
An Optical Method of obtaining the Frequency Response of a Lens—K. Hacking. (*Nature, London*, vol. 181, pp. 1158–1159; April 19, 1958.) Description of a method used to test lenses for television equipment.

621.397.611.2 3267
The Modern Camera Tube and its Limitations—A. E. Jennings. (*Brit. Commun. Electronics*, vol. 5, pp. 250–255; April, 1958.) Comparative survey of the various types of storage tube with particular reference to signal/noise ratio.

621.397.611.2 3268
Beam-Landing Errors and Signal-Output Uniformity of Vidicons—R. G. Neuhauser and L. D. Miller. (*J. Soc. Mot. Pict. Telev. Engrs.*, vol. 67, pp. 149–153; March, 1958.) The uniformity of signal output is markedly affected by the beam-landing characteristics that result when the vidicon is operated in present deflecting and focusing systems. A comparison of various types of vidicon tube is made.

621.397.611.2 3269
Improved Developmental One-Inch Vidicon for Television Cameras—L. D. Miller and B. H. Vine. (*J. Soc. Mot. Pict. Telev. Engrs.*, vol. 67, pp. 154–156; March, 1958.) Tentative performance data are given and compared with those for present vidicon-type camera tubes. Methods of compensating for beam-landing errors are explained.

621.397.62:621.396.677.43 3270
Rhombic Antennas for TV—Cooper. (See 2979.)

621.397.62:621.396.82](083.74) 3271
Supplement to "I.R.E. Standards on Receivers: Methods of Measurement of Interference Output of Television Receivers in the Range of 300–10,000 kc/s, 1954" (Standard 54 I.R.E. 17.S1)—(Proc. IRE, vol. 46, pp. 1418–1420; July, 1958.) Standard 58 IRE 27.S1.

621.397.62.001.4:621.397.8 3272
An Aircraft Simulator for Television Signals—M. C. Gander and P. L. Mothersole. (*Electronic Eng.*, vol. 30, pp. 408–413; July, 1958.) The circuit enables a delayed signal to be combined with the RF source used to test TV receivers. The delay, amplitude and rate of change of phase of the delayed signal are variable and enable the effects of signals reflected from fixed or moving objects to be tested under laboratory conditions.

621.397.7+621.396.65 3273
The NARCOM Plan for Transatlantic Television and other Wide-Band Telecommunication Services—Halstead. (See 3250.)

621.397.7 3274
Problems of International Television Broadcasting—T. H. Bridgewater. (*J. Soc. Mot. Pict. Telev. Engrs.*, vol. 67, pp. 129–133; March, 1958.) The difficulties encountered in the Eurovision system of international television broadcasting are discussed. The main problems are noncompatible line structure and frame rate, relay time and language differences.

621.397.7:535.623:621.396.65 3275
Relay System Diplexes Audio and Colour Video—T. G. Custin and J. Smith. (*Electronics*, vol. 31, pp. 64–67; June 20, 1958.) Modulated klystrons, locked to a crystal reference oscillator, are used in a wide-band FM system at a frequency near 2 kmc. Hybrid rings are used to combine sound and vision carriers at the transmitting antennas and to give balanced mixing in the receiver.

621.397.7:621.317.799 3276
Signal Generator for Tests on Long-Distance Television Links—E. Guva. (*Note Recensioni Notiz.*, vol. 7, pp. 67–78; January/February, 1958.) The generator described is capable of producing bursts of 3–7-mc sine waves repeated at line frequency, and is intended to detect ringing in a television link system.

621.397.8 3277
Systems Approach to Determination of Television Coverage—R. M. Bowie. (*Elect. Eng.*, vol. 77, pp. 129–132; February, 1958.) Description of methods adopted by T.A.S.O. (see 3259 above) for assessing the over-all performance of a television system.

TRANSMISSION

621.396.61.029.62:621–523 3278
Supervision of Unattended Transmitters with Passive Stand-By—P. G. Zehnel. (*Frequenz*, vol. 11, pp. 365–370; December, 1957.) Methods of safeguarding the continuity of service by means of active or inactive stand-by transmitters are outlined and automatic switching systems are described with brief details of modern USW automatic transmitters. See also 1576 of 1958 (Zehnel and Brose).

TUBES AND THERMIONICS

621.314.63+621.314.7 3279
Progress in the Development of Semiconductors—W. Taeger. (*Frequenz*, vol. 11, pp. 333–342; November, 1957.) The characteristics of various semiconductor devices such as Ge and Si junction diodes and transistors, including recent high-frequency and high-power types, are reviewed.

621.314.63:621.318.57 3280
The Forward Switching Transient in Semiconductor Diodes at Large Currents—F. S. Barnes. (Proc. IRE, vol. 46, pp. 1427–1428; July, 1958.) The phenomenon is explained in terms of the current modulation of the resistance of the bulk of the semiconductor diode. Methods of reducing the voltage transient are noted.

621.314.63.029.6:621.374.4:621.396.822 3281
Excess Noise in Microwave Crystal Diodes used as Rectifiers and Harmonic Generators—J. M. Richardson and J. J. Faris. (IRE Trans. on Microwave Theory and Techniques, vol. MTT-5, pp. 208–212; Abstract, Proc. IRE, vol. 45, p. 1312; September, 1957.)

621.314.632:621.316.722.1 3282
The Characteristics of Zener Diodes and their Application as Voltage Standards—G. Meyer-Brötz. (*Elektronische Rundschau*, vol. 11, pp. 376–377; December, 1957.) Note on applications of Si reference diodes, particularly for voltage stabilization in transistor circuits. See also 3684 of 1957 (Dobrinski, *et al.*).

621.314.632.1:546.321.31 3283
Rectifying Effects of Sodium Chloride Crystals—S. Császár. (*Nature, London*, vol. 181, p. 1158; April 19, 1958.) Note of I/V characteristics obtained using NaCl crystals at 250 degrees Centigrade with point contacts of platinum or tungsten wire. The crystals were grown from the melt and some were colored electrolytically.

621.314.7 3284
The Transistor, 1948–1958—(*Bell Labs. Rec.*, vol. 36, pp. 192–233; June, 1958.) Nine papers, listed below, review progress in selected areas of research and development. Transistors with functional properties of a sufficiently wide range are now available for application in most communication systems. Significant progress has been made in realizing the reliability and long life required for telephone service. Transmission and switching systems, signaling and station facilities employing transistors and other solid-state devices, are being developed. Titles of the papers are as follows:

1) **Semiconductor Research**—M. Sparks. (pp. 193–197.)

2) **Research in Circuits and Systems**—R. L. Wallace, Jr. (pp. 198–201.)

3) **Transistor Designs: The First Decade**—W. J. Pietenpol. (pp. 202–206.)

4) **Transmission Applications**—M. B. McDavitt. (pp. 207–211.)

5) **Applications in Telephone Switching**—A. E. Ritchie. (p. 212–215.)

6) **Station Apparatus, Power and Special Systems**—W. A. Depp and L. A. Meacham. (pp. 216–220.)

7) **Military Applications**—J. A. Baird. (pp. 221–225.)

8) **Transistor Manufacture**—J. E. Genther. (pp. 226–228.)

9) **Systems Planning**—D. F. Hoth. (pp. 229–233.)

621.314.7 3285
On the Variation of Transistor Small-Signal Parameters with Emitter Current and Collector Voltage—N. I. Meyer. (*J. Electronics Control*, vol. 4, p. 305–334; April, 1958.) Experimentally determined variations of the low-frequency hybrid parameters are in agreement with calculations, apart from the variation of h_{12} with emitter current, which shows a quantitative disagreement with theory. Misawa's theoretical expression for α cut-off frequency (see 597 of 1958) is compared with experimental results and is found to lead to a wrong dependence on emitter current.

621.314.7 3286
Design Theory for Depletion-Layer Transistors—J. E. Rosenthal and W. W. Gärtner. (Proc. IRE, vol. 46, pp. 1422–1423; July, 1958.) Comment on 306 of 1958 and author's reply.

621.314.7:621.317.799 3287
The Measurement of Transistor Voltage/Current Characteristics using Pulse Techniques—Cooper. (See 3215.)

621.317.799:621.314.7 3288
Transistor Test Set—Prewett. (See 3216.)

621.383.2 3289
The Temperature Dependence of the Photoeffect of Sb-Cs Photocathodes in the Temperature Range —170°C to +20°C—Zs. Náray. (*Ann. Phys., Lpz.*, vol. 20, pp. 386–389; November 30, 1957.)

621.383.4:537.531 3290
The Measurement of X-Ray Interference by means of Cadmium Sulphide Photocells—H. Simon and M. v. Heimendahl. (*Ann. Phys., Lpz.*, vol. 20, pp. 355–367; November 30, 1957.) Description of apparatus and details of some of its applications.

621.383.42 3291
Spontaneous Appearance of an Electromotive Force in Selenium Photocells at Low Temperatures—G. Blet. (*C.R. Acad. Sci., Paris*, vol. 245, pp. 2044–2047; December 4, 1957.)

621.383.5+621.314.63]:537.533.9 3292
Current Amplification by Electron Bombardment in the Semiconductor Barrier Layer—K. Takeya and K. Nakamura. (*J. Phys. Soc. Japan*, vol. 13, p. 223; February, 1958.) Current gain is defined as the ratio of excess current to bombarding current. Experimental curves of current gain vs bias voltage, for various bombarding energies, are given for Se, Ge (alloyed), Si (diffused), and Si (grown). See also 2303 of 1951 (Ehrenberg, *et al.*).

621.385:537.533 3293
Transverse Instability of Electron Beams—B. Epsztein. (*C.R. Acad. Sci., Paris*, vol. 246, pp. 586–588; January 27, 1958.) The existence of this instability in thin beams is explained. See also 2568 of 1956.

621.385.001.4 3294
The Life Test Contribution to the Improvement of Valve Reliability—R. Brewer. (*Brit. Commun. Electronics*, vol. 5, pp. 258–263; April, 1958.) The results are analyzed of vibration and electrical life tests made on four types of tubes of the CV4000 series intended for highly reliable performance in military applications.

621.385.029.6 3295
Beam Focusing in Microwave Amplifiers—P. P. Cioffi. (*Bell Lab. Rec.*, vol. 36, pp. 172–175; May, 1958.) The methods by which the magnetic field may be accurately aligned with the tube axis are discussed. The best adjustments enable 99.9 per cent of the emitted electrons to be delivered to the collector.

621.385.029.6 3296
Pumping to Extend Travelling-Wave-Tube Frequency Range—L. D. Buchmiller and G. Wade. (Proc. IRE, vol. 46, pp. 1420–1421; July, 1958.) Using an S-band traveling-wave tube the small-signal gain for an L-band signal (1 kmc) was increased by 35 db by adding at the input a high-level signal at 3.2 kmc. Without readjustment a similar gain enhancement was measured for signals at frequencies well above the S band. An explanation is given in terms of mixing effects associated with electron beams [see 3073 of 1957 (DeGrasse and Wade)].

621.385.032.21:537.29:621.374.4 3297
Harmonic Generation at Microwave Frequencies using Field-Emission Cathodes—J. R. Fontana and H. J. Shaw. (PROC. IRE, vol. 46, pp. 1424–1425; July, 1958.) An expression for the harmonic amplitudes in the emission current is obtained, from which the performance of any field emitter whose basic properties are known can be calculated.

621.385.032.213.13 3298
The High-Temperature Conductivity–Mechanism of Oxides with Thermal Electron Emission—A. Paulisch. (*Z. angew. Phys.*, vol. 9, pp. 412–426; August, 1957.) The results of conductivity and emission measurements on a number of oxides confirm the more general applicability of the pore conduction mechanism previously defined for (Ba,Sr)O cathodes [see, *e.g.*, Loosjes and Vink (2934 of 1950)].

621.385.032.213.13:537.583.08 3299
Measurement of Instantaneous Absolute Barium Evaporation Rates from Dispenser Cathodes—W. C. Rutledge, A. Milch, and E. S. Rittner. (*J. Appl. Phys.*, vol. 29, pp. 834–839; May, 1958.) The evaporation rate and the BaO content of the evaporant are determined by exposing a clean tungsten wire to a stream of Ba and noting the time required to reach maximum emission. Typical results are given for a wide range of Ba-BaO compositions.

621.385.1:621.317.799 3300
New Portable Electron-Tube Tester—Heberlein. (See 3217.)

621.385.1:621.372.622:621.396.822 3301
Noise in Mixer Tubes—A. van der Ziel and R. L. Watters. (PROC. IRE, vol. 46, pp. 1426–1427; July, 1958.) It is proved that the theorem for calculating mixer tube noise by averaging over a complete local-oscillator cycle is valid for noise with a white spectrum. The theorem is incorrect if the spectrum is not white.

621.385.1(083):681.18 3302
Automatically Recording Tube-Life Data—A. T. Ross. (*Bell Lab. Rec.*, vol. 36, pp. 176–178; May, 1958.) A system for recording aging data automatically on business-machine cards is described.

621.385.14-713 3303
The Utilization of the Waste Heat of Transmitter Valves with Evaporation Cooling—W. Voigt. (*VDI Z.*, vol. 100, pp. 564–565; May 1, 1958.) In the transmitting station Jülich most of the heat extracted from the tubes is used for station heating purposes, resulting in considerable fuel economy. See, *e.g.*, 1982 of 1957 (Protze).

621.385.2 3304
Transit Time and Space Charge in the Spherical Diode—L. Gold. (*J. Electronics Control*, vol. 4, pp. 335–340; April, 1958.) The transit time and current/voltage relation for a spherical diode have been determined using a time-dependent Poisson equation as applied in the case of a cylindrical diode (1931 of 1958). The effect of cathode-anode inversion is also examined.

621.385.4:621.395.64 3305
Electron Tubes for Super Wide-Band Coaxial-Cable Systems—M. Kuwata, K. Sato, T. Kojima, and H. Hara. (*Rep. Elect. Commun. Lab., Japan*, vol. 6, pp. 35–39; February, 1958.) Characteristics of tetrodes Type ECL 1084 and ECL 1144 are discussed.

MISCELLANEOUS

061.3:621.37/.39 3306
Twelfth General Assembly of International Scientific Radio Union—F. H. Dickson. (PROC. IRE, vol. 46, pp. 1350–1383; July, 1958.) The program of the assembly at Boulder, Colo., August 22–September 5, 1957, is given together with summaries of the principal discussions of the seven commissions.

378.962:[621.397.5+534.6 3307
The Training of Sound and Television Technicians for the Broadcasting Organizations of the German Federal Republic—K. Hoffmann. (*Rundfunktech Mitt.*, vol. 1, pp. 232–236; December, 1957.)